

AMRL-TDR-63-100

STUDY OF REQUIREMENTS FOR THE SIMULATION OF RENDEZVOUS AND DOCKING OF SPACE VEHICLES

O. T. S.

425499 \$3.50

U. S. DEPT. OF COMMERCE
WASHINGTON 25, D. C.

TECHNICAL DOCUMENTARY REPORT No. AMRL-TDR-63-100

OCTOBER 1963

BEHAVIORAL SCIENCES LABORATORY
6570th AEROSPACE MEDICAL RESEARCH LABORATORIES,
AEROSPACE MEDICAL DIVISION
AIR FORCE SYSTEMS COMMAND
WRIGHT-PATTERSON AIR FORCE BASE, OHIO

PROPERTY OF

LTV VOUGHT AERONAUTICS DIVISION

Contract Monitor William L. Foley
Project No. 6114, Task No. 611402

MAR 17 1965

(Prepared under Contract No. AF 33(657)-8620 by
John M. Ryken, Jerome E. Emerson
George T. Onega, James L. Bilz
Bell Aerosystems Company, Buffalo, New York)

69,628

NOTICES

When US Government drawings, specifications, or other data are used for any purpose other than a definitely related government procurement operation, the government thereby incurs no responsibility nor any obligation whatsoever; and the fact that the government may have formulated, furnished, or in any way supplied the said drawings, specifications, or other data is not to be regarded by implication or otherwise, as in any manner licensing the holder or any other person or corporation, or conveying any rights or permission to manufacture, use, or sell any patented invention that may in any way be related thereto.

Qualified requesters may obtain copies from the Defense Documentation Center (DDC), Cameron Station, Alexandria, Virginia. Orders will be expedited if placed through the librarian or other person designated to request documents from DDC formerly ASTIA).

Do not return this copy. Retain or destroy.

Stock quantities available at Office of Technical Services, Department of Commerce, Washington 25, D. C. Price per copy is \$3.50.

Change of Address

Organizations receiving reports via the 6570th Aerospace Medical Research Laboratories automatic mailing lists should submit the addressograph plate stamp on the report envelope or refer to the code number when corresponding about change of address.

800 - December 1963 - 162-19-294

FOREWORD

This research was conducted under Contract AF33(657)-8620, Project No. 6114, "Simulation Techniques for Aerospace Crew Training", and Task No. 611402, "Energy Management Simulation", by Bell Aerosystems Company, Buffalo, New York. This program, sponsored by the Simulation Techniques Branch, Training Research Division, Behavioral Sciences Laboratory, 6570th Aerospace Medical Research Laboratories, was initiated in April 1962 and was completed in July 1963. Mr. W.L. Foley was contract monitor for the 6570th Aerospace Medical Research Laboratories. The principal investigators at Bell Aerosystems Company were Mr. John M. Ryken and Mr. Jerome Emerson of the Systems Analysis and Integration Section of the Aerospace Department.



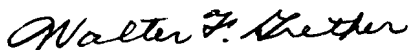
ABSTRACT

This report presents results of a study to establish computer requirements for the simulation of rendezvous and docking systems in space vehicles. A literature search was made to establish rendezvous and docking systems which have been proposed. A complete simulation of a representative automatically controlled rendezvous and docking system was formulated and programmed on an IBM-7090 digital computer. Sufficient flexibility was incorporated into this simulation so that the proposed rendezvous and docking techniques could be studied. This program was used to determine digital computer requirements for the simulation of rendezvous and docking systems. Mission runs were made covering terminal guidance, docking, departure, retro, and deorbit to the earth's atmosphere.

A simplified simulation of rendezvous and docking was programmed on analog computers and coupled with a cockpit simulator. This simulation included an electronic image generation of a target vehicle as viewed by an astronaut through a window in the interceptor vehicle. Information on accuracy of this simulation, pilot control capabilities, and control techniques was obtained.

PUBLICATION REVIEW

This technical documentary report is approved.



WALTER F. GREETHER
Technical Director
Behavioral Sciences Laboratory

CONTENTS

Section		Page
I	INTRODUCTION.	1
II	VEHICLES AND MISSIONS.	3
	A. Vehicles.	3
	B. Missions.	6
III	RENDEZVOUS AND DOCKING TECHNIQUES AND SYSTEMS	11
	A. General	11
	B. Discussion of the Rendezvous Problem	11
	C. Discussion of Techniques.	22
	1. Orbital Mechanics Techniques	22
	2. Proportional Navigation Techniques.	22
	D. System Descriptions	23
	1. Proportional Navigation Systems	23
	2. Orbital Mechanics Systems	37
	3. Docking Phase.	40
IV	SIMULATOR ELEMENTS AND ASSOCIATED EQUATIONS.	43
	A. General	43
	B. Description of Simulator Elements	43
	1. Vehicle Equations of Motion.	43
	2. Thruster Forces, Vehicle Mass, and ΔV Calculations	54
	3. Interceptor Attitude Control System.	57
	4. Input/Output Transformations Associated with Rendezvous and Docking Systems	62
	5. Deorbit System	72
	6. Visual Scene and Pilot Displays	74
V	DIGITAL SIMULATION	85
	A. General	85
	B. Equations and Flow Diagrams.	85
	C. Simulated Interceptor	88
	D. Data Inputs, Gain Selections, and Mission Runs	89
	1. Attitude Control System.	89
	2. Docking Translational System.	91
	3. Rendezvous - Selection of Gains and Constants	94
	E. Requirements for a Digital Computer Simulation	122
	1. Accuracy Requirements.	122
	2. Cycling Time.	124
	3. Digital Requirements	130
VI	ANALOG SIMULATION	135
	A. General	135
	B. Simulation Description	135
	1. Analog Computer Program.	135
	2. Cockpit Simulator Description	142

CONTENTS (CONT)

C.	Pilot Control Techniques for Rendezvous	147
1.	Rendezvous	147
2.	Docking	148
D.	Computer Mechanization	149
1.	Simplifications.	149
2.	Accuracy	149
E.	Mission Runs and Results	152
1.	General	152
2.	Mission Runs.	153
3.	Pilot Capabilities.	159
4.	Computational Task for the Analog Computer	159
VII	SUMMARY AND CONCLUSIONS	161
REFERENCES	163

ILLUSTRATIONS

Figure		Page
1	Rendezvous and Docking Missions	4
2	Velocity Required to Place a Vehicle in 450 n. mi. and 2000 n. mi. Orbits with 0° or 10° Changes in Inclination	7
3	Injection Velocities Required for Rendezvous at Altitudes of 450 n. mi. and 2000 n. mi.	8
4	Total ΔV Required to Change Altitude of Circular Orbit	9
5	Relative Positions During Ascent Trajectories (Closing Velocities = 600 ft/sec)	12
6	Typical Ascent Paths	13
7	Closing Velocities During Ascent Trajectories Shown in Figure 5 (Closing Velocities = 600 ft/sec)	14
8	Relative Positions During Ascent Trajectories (Closing Velocities = 10 ft/sec)	15
9	Ranges at Which Braking Maneuvers Must Start	16
10	Closing Velocity versus Range During Typical Manually Controlled Rendezvous	17
11	Effect of Rendezvous Time on ΔV Required	18
12	Variation of Velocity Change for Intercept and Rendezvous	19
13	Effect of Elevation Angle on ΔV Required for Rendezvous	20
14	ΔV Required for Change of Orbit Inclination	21
15	ΔV Required for Rendezvous of Vehicles in Noncoplanar Orbits	21
16	Summary of Coordinate Systems	24
17	Guidance Command System of Reference 13	27
18	Variation of Range Rate with Range During Braking Maneuver	30
19	Guidance Command System of Reference 14	31
20	Typical Range Rate and Normal Velocity versus Range	32
21	Guidance Command System of Reference 10	34
22	Variation of the Ratio β_{L_0} / δ_0 with τ_f	35
23	Variation of Thrust Angle with Time for Various Conditions	35
24	Guidance Command System of Reference 15	36
25	Guidance Command System of References 9 and 11	38
26	Guidance Command System of Reference 12	39
27	Docking Guidance Command System of Reference 12	42
28	Major Elements of Rendezvous Simulator	44
29	Sketch Illustrating Relative Motion Parameters	47
30	Equations of Interceptor and Target Relative Motion	48
31	Transformation from Body Axes to Inertial Axes	48
32	Target Equations of Motion	50
33	Interceptor Flight Conditions Relative to the Earth	51
34	Sketch Illustrating Earth Reference Parameters	52
35	Simplified Interceptor Flight Condition	53
36	Velocity of the Interceptor Relative to the Earth	54
37	Interceptor Rockets for Maneuvering	55
38	Vehicle Mass and ΔV Equations	58
39	Interceptor Body Axes	59

ILLUSTRATIONS (CONT)

Figure		Page
40	Interceptor Attitude Dynamics	60
41	Schematic Diagram of Attitude Control System	61
42	Interceptor Attitude Control System.	63
43	Thrust Misalignment Moments	64
44	Inputs and Outputs of the Rendezvous and Docking Command Systems	66
45	Input Transformation Coordinate Systems.	68
46	Output Transformation Coordinate Systems.	70
47	Deorbit Maneuver.	72
48	Deorbit Mode Equations.	73
49	Euler Angles of the Target Vehicle	75
50	Digital Flow Chart	86
51	Attitude Loop Cycle Time Studies - Case 1.	90
52	Attitude Loop Cycle Time Studies - Case 2.	91
53	Command Lines for Range and Range Rate Control.	92
54	Command Lines for $R \dot{\alpha}$ and $R \dot{\beta} \cos \alpha$	93
55	Mission Run No. 1 - Range Rate versus Range.	95
56	Mission Run No. 1 - $R \dot{\alpha}$ and $R \dot{\beta} \cos \alpha$ versus Range.	96
57	Mission Run No. 1 - Time History.	97
58	Acceleration Capabilities.	98
59	Mission Run No. 2 - Time History of Braking Phase.	100
60	Mission Run No. 3 - Range Rate, $R \dot{\alpha}$, and $R \dot{\beta} \cos \alpha$ versus Range for Braking Phase.	103
61	Mission Run No. 3 - Angles, Thrust and ΔV_{cap} versus Range (Braking Phase)	104
62	Docking Phase, Mission Run No. 3.	105
63	Mission Run No. 4 - Range Rate, $R \dot{\alpha}$, and $R \dot{\beta} \cos \alpha$ versus Range for Braking Phase	106
64	Mission Run No. 4 - Angles, Thrust and ΔV_{cap} versus Range (Braking Phase)	107
65	Mission Run No. 5 - Alignment and Braking Phases	108
66	Mission Run No. 5 - Docking Phase.	109
67	Mission Run No. 6 - Alignment and Braking Phases	110
68	Mission Run No. 7 - Alignment and Braking Phases	111
69	Mission Run No. 8 - Alignment and Braking Phases	114
70	Mission Run No. 9 - Braking Phase.	116
71	Complete Mission Phase Involving Departure and Deorbit - Alignment and Braking.	119
72	Complete Mission Phase Involving Departure and Deorbit - Docking Phase	120
73	Complete Mission Phase Involving Departure and Deorbit - Departure.	120
74	Complete Mission Phase Involving Departure and Deorbit - Deorbit	121
75	Miss Distance Per Degree Aiming Error	123
76	Allowable Velocity Error Normal to the Line of Sight.	124
77	Allowable Cycling Time.	126
78	Range Rate versus Range for Several (T/W) Values	128
79	Accuracy Studies, Case 1.	131
80	Accuracy Studies, Case 2.	132
81	Interior of the Rendezvous and Docking Simulator Cockpit.	136
82	Block Diagram of the Analog Simulation.	137

ILLUSTRATIONS (CONT)

83	Miss Distance Due to the Effects of Differential Gravity	139
84	Simulator Cockpit Displays	143
85	Schematic of the Analog Computer Mechanization of the Rendezvous and Docking Simulation	150
86	Velocity Trajectories of Mission Run No. 3.	154
87	Time Histories of Mission Run No. 3.	155
88	Velocity Trajectories of Mission Run No. 8.	156
89	Time Histories of Mission Run No. 8.	157
90	Time Histories of a Manually Controlled Docking Maneuver.	158
91	Initial Conditions Within the Pilot's Capabilities	160

TABLES

Number		Page
I	Vehicle Configurations	5
II	Input and Output Transformation Requirements	65
III	Summary of Display Requirements	80
IV	Simulated Vehicle Parameters	88
V	Orbital Conditions	118
VI	Computer Variables, Ranges, Accuracies and Resolutions	125
VII	Summary of Mathematical Operations	133
VIII	Estimated Computing Time for the IBM-7090	134
IX	Display Quantities - Alignment and Braking	140
X	Display Quantities - Docking	142
XI	Cockpit Controls for Rendezvous and Docking	144
XII	Parameter Accuracy and Range	152

LIST OF SYMBOLS

<u>Symbol</u>	<u>Description</u>	<u>Units</u>
A_1, A_2	Acceleration switching limit gains	
A^*	Nondimensional required acceleration = a_{req}/a_{avail}	
a	Acceleration	ft/sec ²
a_{LOS}	Desired rate of change of the closing velocity	ft/sec ²
a_{req}	Acceleration required to reduce range rate to zero at a desired range	ft/sec ²
a_T	Minimum longitudinal acceleration capability required for docking	ft/sec ²
C_s	Constant of angular momentum per unit mass	ft ² /sec or mi. ² /sec
c_1	Proportional control gain	
d	Distance from the pilot's eye to the interceptor window	ft
d_x, d_y, d_z	Moment arms of the reaction control jets along the interceptor X_B, Y_B, Z_B axes, respectively	ft
$\bar{e}_R, \bar{e}_\theta$	Unit vectors along the line of sight and normal to the line of sight, respectively	
F_{XI}, F_{YI}, F_{ZI}	Components of the thrust being applied to the interceptor along the $X_I, Y_I,$ and Z_I axes, respectively	lb
$(F_X)_M, (F_Y)_M, (F_Z)_M$	Forces in the interceptor body axes directions due to the moments created by firing the reaction control jets	lb
$(F_{total})_M$	Total force due to moments created by firing the reaction control jets	lb

LIST OF SYMBOLS (CONT)

<u>Symbol</u>	<u>Description</u>	<u>Units</u>
f_1, f_2, f_3	Limiting functions included in the attitude control system so that attitude rates can be limited to any desired values	
G	The universal gravitational constant	lb ft ² /slug ²
g	Acceleration due to gravity	ft/sec ²
g_e, g_o	Acceleration of gravity at the surface of the earth	ft/sec ²
h	Altitude	ft or n. mi.
h_h	Specified altitude for second retro firing in the deorbit maneuver	ft or n. mi.
h_R	Constant range controller parameter	ft or n. mi.
h_1	Initial orbit altitude	ft or n. mi.
Δh	Increment of altitude	ft or n. mi.
I_{sp}	Specific impulse	sec
I_x, I_y, I_z	Moments of inertia of the interceptor about the $X_B, Y_B,$ and Z_B interceptor body axes, respectively	slug-ft ²
i	Inclination of the launch site from the orbit plane	deg
K, k	Denotes use of constant in an equation	
K_T'	Gain constant in the equation for the thrust-on boundary of the docking guidance command system of Reference 12	ft/sec
K_Y	Gain constant used in the equation to determine the desired out of plane velocity in the guidance command system of Reference 12	1/sec
K_3, K_2, K_1	Gain constants in p, q, and r, respectively	
K_6, K_5, K_4	Gain constants in p, q, and r, respectively, relating $p_\xi, q_\xi,$ and r_ξ to $M_{XB}, M_{YB},$ and M_{ZB}	

LIST OF SYMBOLS (CONT)

<u>Symbol</u>	<u>Description</u>	<u>Units</u>
K_ϕ, K_θ, K_ψ	Position gain constants in ϕ , θ , and ψ , respectively	
k_x, k_y, k_z	Gain constants defining response speeds along the X_R , Y_R , and Z_R axes, respectively	
LOS	Line of sight	
M_{XB}, M_{YB}, M_{ZB}	Moments about the X_B , Y_B , and Z_B interceptor body axes, respectively, produced by the attitude controls	ft-lb
$M_{X_{total}}, M_{Y_{total}}, M_{Z_{total}}$	Total moments about the X_B , Y_B , and Z_B interceptor body axes, respectively, produced by the attitude controls and misalignment of the translational thrusters	ft-lb
m	Mass	slugs
m_e	Mass of the earth	slugs
m_{empty}	Mass of the interceptor without fuel	slugs
p, q, r	Rates of rotation about the X_B , Y_B , Z_B interceptor body axes, respectively	deg/sec
R	Distance along the line of sight from the target to the interceptor	ft or n. mi.
R_A or R_a	Minimum range at which R is to be zero	ft or n. mi.
R_c	Crossrange	ft or n. mi.
R_E and r_e	Radius of the earth	ft or n. mi.
R_{TG}	Range-to-go	ft or n.mi.
R_{TG}^h	Range-to-go to deorbit point	ft or n.mi.
R_{TG}^o	Range-to-go to entry into the atmosphere	ft or n.mi.
R_ξ	Distance the interceptor will miss target	ft or n.mi.

LIST OF SYMBOLS (CONT)

<u>Symbol</u>	<u>Description</u>	<u>Units</u>
\dot{R}_d	The desired velocity to rendezvous in a specified time (t_d)	ft/sec
$\dot{R}_{MAX}, \dot{R}_{MIN}$	On-off switching criteria for the longitudinal rocket engine	ft/sec
\dot{R}_R	A residual velocity (0.1 ft/sec) defined as a servo compensating factor	ft/sec
S'	Reentry criticality factor	
T	Thrust	lb
T^*	Fictitious intercept time	sec
T'	Predetermined docking time	sec
T_E	Constant range controller parameter	sec
T_{MAX}, T_{MIN}	Maximum and minimum levels of interceptor longitudinal variable thrust engine	lb
$T_{X_c}, T_{Y_c}, T_{Z_c}$	Thrust commands along $X_B, Y_B,$ and Z_B interceptor body axes, respectively, generated by rendezvous and docking guidance command systems	lb
T_{XB}, T_{YB}, T_{ZB}	Thrusts along $X_B, Y_B,$ and Z_B interceptor body axes, respectively	lb
$T_{V_{XB}}$	Thrust along X_B axis from variable thruster	lb
T/W	Thrust to weight ratio	
ΔT	Integration interval of the overall digital simulation program	milliseconds
t	Time	sec
t_b	Burning time	sec
t_c	Cycle time, or elapsed time between solutions in the computer	milliseconds
t_d	Specified time to rendezvous	sec

LIST OF SYMBOLS (CONT)

<u>Symbol</u>	<u>Description</u>	<u>Units</u>
t_{req}	Time to be used for rendezvous	sec
t_1	Integration interval used in the attitude loop in the digital simulation program	milliseconds
t_2	Integration interval for the relative equations of motion in the digital simulation program	milliseconds
V, v	Velocity	ft/sec
V_a	The amount of ΔV to be used for rendezvous	ft/sec
V_a, V_d	Thrust-on and thrust-off boundaries used in the guidance command system of Reference 12	ft/sec
V_{H_h}	Horizontal component of velocity at point of second retro firing	ft/sec
$V_{H_h}^d$	Desired horizontal component of velocity at point of second retro firing	ft/sec
$V_{I_{XY}}$	The component of inertial velocity of the interceptor in the target's local horizontal plane	ft/sec
V_N	Total velocity component normal to the line of sight	ft/sec
V_R	Velocity of the interceptor relative to the rotating earth	ft/sec
V_T	Velocity of the target vehicle	ft/sec
V_{V_h}	Vertical component of velocity at point of second retro firing	ft/sec
$V_{V_h}^d$	Desired vertical component of velocity at point of second retro firing	ft/sec
ΔV	Velocity increment between the target and interceptor	ft/sec
$\Delta V_{available}$ or ΔV_{avail}	Available ΔV	ft/sec

LIST OF SYMBOLS (CONT)

<u>Symbol</u>	<u>Description</u>	<u>Units</u>
ΔV^h	Impulse required for the first retro firing	ft/sec
ΔV_c	Computed velocity change required for interception	ft/sec
$\Delta V_{\text{capability or}} \Delta V_{\text{cap}}$	The amount of ΔV the interceptor has for maneuvering	ft/sec
ΔV_h^r	Impulse that will be required during the second retro firing	ft/sec
$\Delta V_{H_h}^r$	Required horizontal component of retro ΔV for second firing	ft/sec
ΔV_H^*	Desired horizontal velocity increment between vehicle velocity for reentry and circular speed	ft/sec
ΔV_i^r	Impulse that will be required during the first retro firing	ft/sec
ΔV_{tot}	Total velocity increment	ft/sec
$\Delta V_{V_h}^r$	Required vertical component of retro ΔV for second firing	ft/sec
ΔV_v^*	Desired vertical velocity of vehicle required for reentry	ft/sec
$\Delta V_1, \Delta V_2$	First and second velocity changes required for a two impulse rendezvous	ft/sec
$\dot{W}_{F_{XB}}, \dot{W}_{F_{YB}}, \dot{W}_{F_{ZB}}$	Rate of propellant consumption for fixed thrust engines aligned along the interceptor body axes, X_B , Y_B , and Z_B , respectively	lb/sec
\dot{W}_{V_X}	Rate of propellant consumption for variable thrust engine aligned along the interceptor longitudinal body axis, X_B	lb/sec
X, Y, Z	Coordinate system with axes inertially fixed in direction and with origin at earth's center. The X and Z axes lie in the target orbit plane	

LIST OF SYMBOLS (CONT)

<u>Symbol</u>	<u>Description</u>	<u>Units</u>
X_B, Y_B, Z_B	Interceptor body axes. Origin at the interceptor centroid. X_B, Z_B plane coincident with plane of symmetry of the interceptor. X_B axis positive forward, Y_B axis positive to the right, Z_B axis positive down	
X_I, Y_I, Z_I	Coordinate system with axes inertially fixed in direction and centered in the interceptor. $X_I, Y_I,$ and Z_I are parallel to $X, Y,$ and Z	
X_R, Y_R, Z_R	Coordinate system with origin in the target vehicle. The X_R and Z_R axes lie in the plane of the target's orbit. The X_R and Z_R axes rotate about the Y_R axis such that the Z_R axis always points away from the center of the earth	
X_T, Y_T, Z_T	Coordinate system with axes inertially fixed in direction and centered in the target vehicle. $X_T, Y_T,$ and Z_T are parallel to $X, Y,$ and Z	
X_{TB}, Y_{TB}, Z_{TB}	Target vehicle body axes. Origin at the target centroid. X_{TB}, Z_{TB} plane coincident with plane of symmetry of the target. X_{TB} axis positive forward, Y_{TB} axis positive to the right, Z_{TB} axis positive down	
X_I', Y_I', Z_I'	Coordinate system with axes inertially fixed in direction and centered in the interceptor. $X_I', Y_I',$ and Z_I' are parallel to $X_T', Y_T',$ and Z_T'	
X_T', Y_T', Z_T'	Coordinate system with axes inertially fixed in direction and centered in the target. Initially the X_T' axis passes through the interceptor	

LIST OF SYMBOLS (CONT)

<u>Symbol</u>	<u>Description</u>	<u>Units</u>
x, y, z	The relative distances from the target to the interceptor measured in the $X_T, Y_T,$ and Z_T coordinate system. Note: In Section III-B, $x, y,$ and z are relative distances from the target to the interceptor measured in a coordinate system with origin in the target and where the X and Y axes lie in the plane of the target orbit and the Y axes always point away from the center of the earth	
x_R, y_R, z_R	The relative distances from the target to the interceptor measured in the $X_R, Y_R,$ Z_R coordinate system	
y_w, z_w	Coordinates of the target image projection on the interceptor window y_w is positive to the right; z_w is positive up	
α	Angle subtended by the line of sight between the target and the interceptor and its projection on the $X_T Y_T$ plane	deg
α_R	Angle subtended by the line of sight and its projection on the $X_R Y_R$ plane	deg
α_{TB}	Angle subtended by the interceptor thrust vector and its projection on the $X_I Y_I$ plane	deg
α_o	Angle subtended by the X_T' axis and its projection on the $X_T Y_T$ plane	deg
α'	Angle subtended by the line of sight and its projection on the $X_T' Y_T'$ plane	deg
β	Angle between the X_T axis and the projection of the line of sight on the $X_T Y_T$ plane	deg
β_L	Angle between the interceptor velocity vector and the line of sight measured in the plane defined by the velocity vector and the line of sight	deg
β_R	Angle between the X_R axis and the projection of the line of sight on the $X_R Y_R$ plane	deg

LIST OF SYMBOLS (CONT)

<u>Symbol</u>	<u>Description</u>	<u>Units</u>
β_{TB}	Angle between the X_I axis and the projection of the interceptor thrust vector on the $X_I Y_I$ plane	deg
β_o	Angle between the X_T axis and the projection of the X_T' axis on the $X_T Y_T$ plane	deg
β'	Angle between the X_T' axis and the projection of the line of sight on the $X_T' Y_T'$ plane	deg
γ	Angle between the line of sight and an inertial reference in the interceptor (see Reference 10)	deg
δ	Angle subtended by the thrust vector and the line of sight	deg
ϵ_v	Total expected deviation in resultant velocity	ft/sec
ϵ_{ij}	(i = X, Y, Z; j = X, Y, Z) Offset in the j direction of the body thrust vector in the i direction from the c.g.	ft
$\epsilon_x, \epsilon_y, \epsilon_g$	Error signals used to generate M_{XB} , M_{YB} , and M_{ZB} control moments, respectively	
θ_I	The angle the projection of the interceptor on the XZ plane has made since crossing the Z axis	deg
θ_T	The angle the target vehicle has travelled since crossing the Z axis	deg
θ	Elevation angle in Figure 13. In all other cases, θ represents Euler pitch angle in the sequence ψ, θ, ϕ	deg
$\theta_{c_1}, \theta_{c_2}$	The desired vehicle pitch attitudes during the first and second retro firings, respectively	deg
λ_I	Colatitude of the interceptor	deg
λ_T	Colatitude of the target	deg

LIST OF SYMBOLS (CONT)

<u>Symbol</u>	<u>Description</u>	<u>Units</u>
λ_{IT}	Colatitude of the projection of the interceptor position on the orbit plane of the target	deg
μ_0	Longitude of the target orbit at the equator	deg
μ_I	Longitude of the interceptor	deg
μ_T	Longitude of the target	deg
μ_{IT}	Longitude of the projection of the interceptor position on the orbit plane of the target	deg
\mathcal{N}_I	The angle measured from the origin of the XYZ coordinate system, between the radial lines to the interceptor and to the projection of the interceptor position in the XZ plane	deg
ξ_0	Heading angle of the target orbit at the equator with respect to East	deg
ξ_I	Heading angle of the interceptor with respect to East	deg
ξ_{IT}	Heading angle of the projection of the interceptor position on the orbit plane of the target with respect to East	deg
σ_I	The radial distance from the center of the earth to the interceptor	ft or n. mi.
σ_T	The radial distance from the center of the earth to the target	ft or n. mi.
σ_{XI} σ_{ZI}	The X and Z coordinates, respectively, of the interceptor in the XYZ coordinate system	ft or n. mi.
σ_{XT} σ_{ZT}	The X and Z coordinates, respectively, of the target in the XYZ coordinate system	ft or n. mi.
τ	Time until rendezvous	sec
τ	Time constant or lag in the transfer function for the rocket engines for maneuvering	milliseconds
$\tau = t/t_b$	Fraction of mass used (Reference 10)	
τ_1	Time until $x_R = y_R = 0$	sec
τ_2	Time until $z_R = 0$	sec

LIST OF SYMBOLS (CONT)

<u>Symbol</u>	<u>Description</u>	<u>Units</u>
$(\tau_1)_L$	Approximate time to intercept at time of launch	sec
$\tau_\psi, \tau_\theta, \tau_\phi$	Lags associated with thrust buildups in the attitude jets	milliseconds
ϕ_V	Angle between the velocity component normal to the line of sight, $R\dot{\alpha}$, and the total component of velocity normal to the line of sight, V_N (see Section IV-B-8)	deg
ϕ'	Roll angle required in the transformation T_{3C} from the spherical coordinate system associated with the $X_T, Y_T,$ and Z_T coordinate system to the spherical coordinate system associated with the $X_{T'}, Y_{T'},$ and $Z_{T'}$ coordinate system (see Section IV-B-8)	deg
ψ, θ, ϕ	Euler yaw, pitch and roll angles, respectively	deg
ψ actual, θ actual, ϕ actual	Actual Euler yaw, pitch and roll angles of the $X_B, Y_B,$ and Z_B interceptor body axes with respect to the $X_I, Y_I,$ and Z_I axes	deg
ψ_c, θ_c, ϕ_c	Command Euler yaw, pitch, and roll angles of the $X_B, Y_B,$ and Z_B interceptor body axes with respect to the $X_I, Y_I,$ and Z_I axes	deg
$\psi_{R'}, \theta_{R'}, \phi_{R'}$	Euler yaw, pitch and roll angles of the $X_B, Y_B,$ and Z_B interceptor body axes with respect to the $X_R, Y_R,$ and Z_R axes	deg
$\psi_{R_c}, \theta_{R_c}, \phi_{R_c}$	Command Euler yaw, pitch and roll angles of the $X_B, Y_B,$ and Z_B interceptor body axes with respect to the $X_R, Y_R,$ and Z_R axes	deg
ψ_T, θ_T, ϕ_T	Euler yaw, pitch and roll angles of the $X_{TB}, Y_{TB},$ and Z_{TB} target vehicle body axes with respect to the $X_T, Y_T,$ and Z_T axes	deg
ψ_1, θ_1, ϕ_1	Yaw, pitch and roll angles describing the target orientation relative to the line of sight	deg
$\psi_c', \theta_c', \phi_c'$	Command Euler yaw, pitch, and roll angles of the $X_B, Y_B,$ and Z_B interceptor body axes with respect to the $X_{T'}, Y_{T'},$ and $Z_{T'}$ axes	deg

LIST OF SYMBOLS (CONT)

<u>Symbol</u>	<u>Description</u>	<u>Units</u>
ψ_I, θ_I, ϕ_I	Euler yaw, pitch and roll angles of the X_B , Y_B , and Z_B interceptor body axes with respect to the X_I , Y_I , and Z_I axes	deg
Ω	Rotational velocity of the earth	rad/sec
ω	Angular velocity of the target about the earth	rad/sec

SUBSCRIPTS

avail	Available
c	Command
cap	Capability
D	Desired
f	Final condition
I	Interceptor
o	Initial condition
T	Target
ϵ	Error

A dot over a quantity denotes first derivative with respect to time; two dots denote second derivative with respect to time.

A bar over a quantity denotes a vector.

I. INTRODUCTION

The results of a study to establish equations, techniques, and desirable characteristics of computers for the simulation of energy management in rendezvous and docking of earth orbiting vehicles is presented. An important goal was to determine requirements applicable to a general class of simulators suitable for pilot training, for maintaining pilot proficiency, or for evaluation and/or development of rendezvous techniques in which a pilot plays at least a monitoring role. Thus, the simulators must be capable of operating in real time and must include the equations needed for driving cockpit displays including a visual scene.

The study included a survey of rendezvous and docking systems from the literature and considered the effects of various representative rendezvous and docking systems and various vehicles. Included were systems required for rendezvous in minimum time, with minimum energy, or along "optimum" trajectories. Vehicles with single and multiple rocket engines, and with either fixed or variable thrust were considered.

Specific objectives of the study were to establish:

- (a) The equations required for simulation of rendezvous and docking.
- (b) All required computer inputs and outputs, their accuracy, resolution, and range of operation. Also, estimates of the ranges of problem variables that are within the pilot's control capabilities.
- (c) The nature and amount of data to be stored in the computer.
- (d) The nature, number, and type of mathematical operations required.
- (e) The flow chart functional diagrams required for mechanization on a digital or analog computer.
- (f) Whether the computer shall be digital or analog.
- (g) The required computation cycle time if the computer is digital.
- (h) Whether or not the equations should be mechanized in the same computing equipment that is used for simulation of energy management during reentry and flight in the atmosphere*.

The program has involved both analog and digital computer simulations of rendezvous and docking. For the digital simulation using an IBM-7090 computer, representative techniques for automatically controlled rendezvous and docking were programmed. Also programmed were six-degree-of-freedom flight path equations of a represented vehicle with a hypothetical automatic flight path and reaction control system. The flight phases simulated included rendezvous, docking, departure, and reentry. The digital simulation was used to obtain data to establish the required computer characteristics and to confirm the adequacy of the equations and techniques for the simulation of rendezvous and docking missions.

The analog simulation involved the rendezvous and docking phases and included an electronic target image generation device which generated a view of a toroidal shaped space

* Reference 1 and 29 define the simulator requirements for these energy management systems.

station as it would be seen from a window in the interceptor vehicle. In addition to the visual scene, the simulation was coupled to cockpit simulator equipment with operating controls, displays, and instrumentation, giving the pilot the capability of controlling the rendezvous and docking maneuvers. The analog simulation provided the simplest means for conducting studies of pilot capabilities. Further, it permitted comparisons with the digital simulation which provided a great deal of information for determining whether analog or digital equipment is more suitable for the problem of simulation of rendezvous and docking missions.

The effects of particular applications on the rendezvous and docking simulation have been considered. For some applications it will be desirable to have a simulator which can readily be reprogrammed so that various rendezvous and docking systems and techniques can be evaluated and compared. Therefore, the problems encountered in changing from the simulation of one system to another have been studied. Because of the many possible coordinate systems, transformations likely to be required between them are also presented.

In some cases a rendezvous simulator will be part of a full mission simulator. Therefore, compatibility with the equations and equipment required for simulation of other mission phases was considered to be important. A set of equations that could be used for simulating undocking, retro, and descent to the atmosphere phases are also presented. In the present study, efforts were made to keep simplifying assumptions and limitations to a minimum. Allowable simplifications for specific applications either are obvious, or are suggested in this report.

This report has been divided into seven sections. Section II presents a brief description of the types of vehicles and missions that were considered in this study. Section III discusses the rendezvous and docking problems, and describes techniques used for specific rendezvous and docking systems. Section IV describes major elements of a rendezvous and docking simulator, and presents the equations that must be solved by the simulator computer. Section V is devoted to the digital simulation, its setup, flow charts, a description of the vehicle chosen, and data inputs. In addition, a series of mission runs and study results leading to a definition of computer requirements are included in this section. Section VI presents a complete description of the analog simulation, the visual display and simulator cockpit, and typical mission runs conducted using both the automatic rendezvous and docking control modes, and corresponding runs with a pilot controlling the vehicle manually. Conclusions are presented in Section VII.

II. VEHICLES AND MISSIONS

A complete rendezvous mission, as illustrated in Figure 1, consists of the following phases:

Launch and Ascent

Terminal Guidance

Docking

Undocking

Retro

Descent

Flight within the Atmosphere

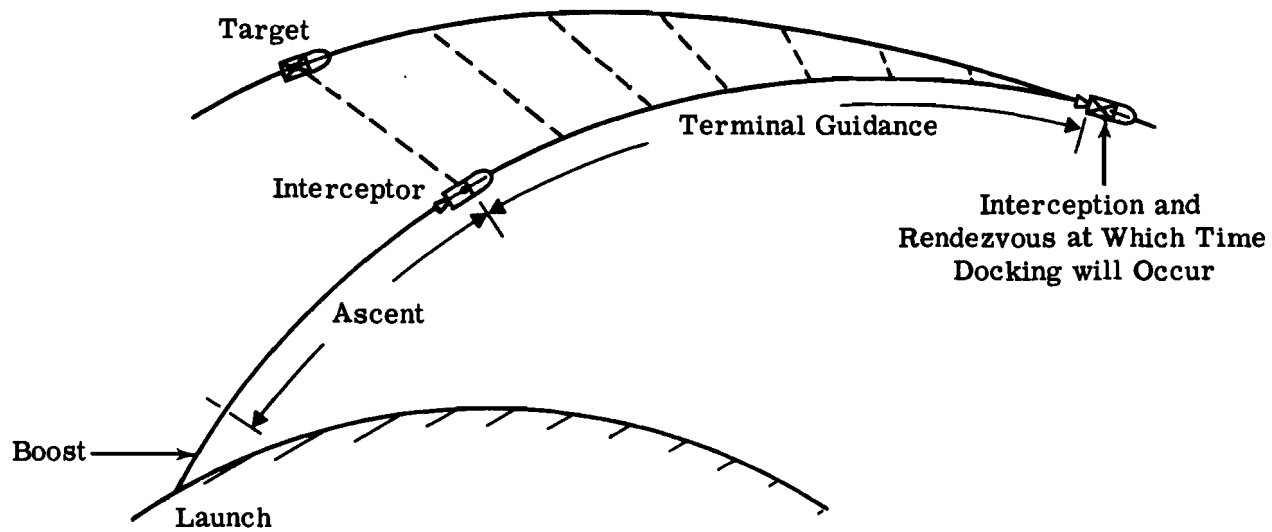
The rendezvous portion of this complete mission is generally considered to include the terminal guidance and docking phases. In this report these two phases are referred to as the rendezvous and docking phases. In addition to considering the simulation aspects of these two phases, the subject program has considered the problems of simulation of undocking, retro, and descent to the atmosphere. The simulation of retro and descent, as well as flight within the atmosphere, has been studied previously in Reference 1; hence, retro and descent have been considered in the current program only to the degree necessary to ensure compatibility of the rendezvous and undocking simulation with the simulation of the in-atmosphere phases.

The launch and ascent phases are considered to the degree necessary to indicate realistic initial conditions for the terminal guidance and docking phases.

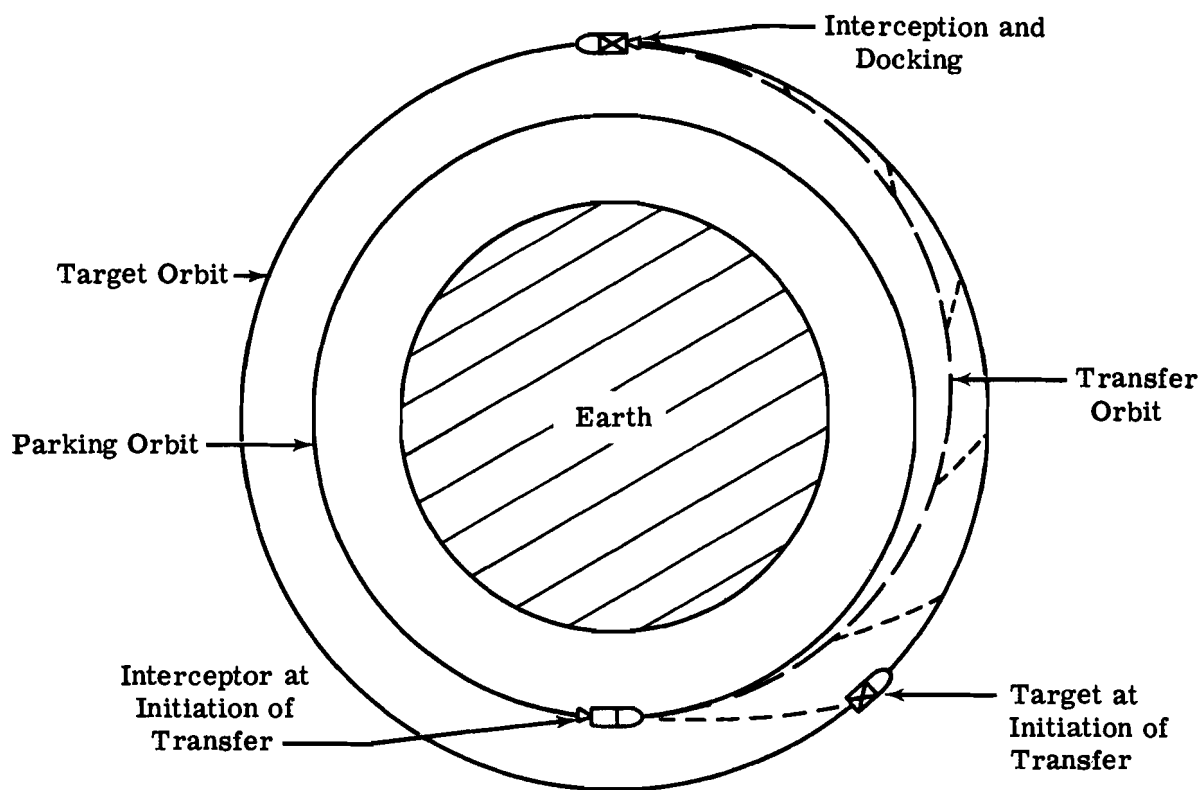
Throughout this report, the two vehicles involved in the rendezvous maneuver will be designated as the target and the interceptor. The target is a nonmaneuverable vehicle in a fixed orbit, either circular or elliptical. The interceptor is the vehicle which will maneuver with the objective to rendezvous and dock with the target. The characteristics of vehicles have been considered to the extent necessary to indicate how the various configurations affect computing requirements for the rendezvous and docking simulator.

A. VEHICLES

Since rendezvous takes place outside the appreciable atmosphere where aerodynamic forces are essentially zero, the shapes of the vehicles involved will only influence the implementation of simulated visual scenes. For example, the shapes, sizes, and location of windows, periscopes, or TV systems that are used to provide the pilot of the actual interceptor with a view may determine techniques and physical details of systems that are used in generating the simulated visual presentation. Discussions of these factors and alternate techniques for providing the simulated visual scene have been presented in Reference 30. These discussions will not be repeated here; however, it appears that the equations and the computer requirements for the rendezvous and docking simulator may be significantly affected by the choice of technique for generating and presenting the visual scene. For example, the choice of coordinate systems, the Euler angle sequence, and the overall complexity of the computations involved for a given application may be determined by the hardware to which the



a. Ground Launch



b. Orbital Transfer

Figure 1. Rendezvous and Docking Missions

simulator computer is to be connected. Coordinate systems and inputs likely to be required by devices used to simulate the visual scene and cockpit displays will be discussed in later sections of the report.

If the target vehicle has one or more planes of symmetry, some of the equations that determine the attitude of the target relative to the line of sight from the maneuvering vehicle may be simplified. Similarly, if the target is stabilized with respect to the earth or inertial space, certain expressions or equations can be eliminated.

For the purposes of this study, it was assumed that rockets will be used for maneuvering and for attitude control. These rockets may have single fixed thrust levels, multiple fixed thrust levels, or they may be throttleable. Most rendezvous studies to date have assumed that the rockets are all fixed relative to the vehicle and that attitude changes are obtained by firing pairs of rockets. However, a gimballed thruster which could be used for simultaneously controlling vehicle velocity and attitude during initial phases of rendezvous is also a reasonable configuration. Table I lists three possible arrangements of rockets for maneuvering and attitude control. The equations and computer requirements presented in this report have been derived with the assumption that it may be necessary to simulate these and other similar combinations of rockets.

The thrust to weight ratios (g's) that will be used for rendezvous and docking may range from values of the order of 0.001 to values of the order of 2. The high values often will be used when ΔV 's of several hundred or even thousands of ft/sec must be added in order to match the speed of the interceptor with that of the target. These situations are discussed further in Section III.

TABLE I
VEHICLE CONFIGURATIONS

Configuration Number	Attitude Control	Translational Control
1.	12 reaction jets controlling pitch, roll, yaw	6 fixed thrust translation rockets for $\pm X_B, Y_B, Z_B$ thrusting. (One direction possibly variable thrust.)
2.	12 reaction jets for controlling pitch, roll, yaw	One fixed or variable translation rocket. The vehicle must be pitched or yawed to obtain thrust in a prescribed direction. Attitude reaction jets synchronized for translation forces needed for station keeping and docking.
3.	12 reaction jets for controlling pitch, roll, yaw. Attitude control may be supplemented or accomplished by the gimballed thruster during the time the main thruster is active.	One fixed or variable translation rocket. The vehicle must be pitched or yawed to obtain thrust in a prescribed direction. Attitude reaction jets synchronized for translation forces needed for station keeping and docking.

When the relative velocities are of the order of a few hundred ft/sec, it is generally desirable to have available a T/W considerably less than one. These thrust levels may be obtained from fixed thrust engines or by throttling engines with higher maximum thrust.

B. MISSIONS

Techniques of rendezvous have been proposed for missions such as supply or repair of large space stations, assembly of space stations or boost systems, rescue, and inspection of friendly or unfriendly vehicles. With the exception of the case of inspection of unfriendly or unknown vehicles which may have an evasive maneuvering capability, the purpose of a rendezvous mission will not directly affect the simulator computer requirements. Because the present study has been limited to rendezvous with vehicles in fixed orbits about the earth, the missions of interest only influence the simulator insofar as they establish the target vehicle orbit altitudes, ellipticity, and inclination.

In order to ensure that atmospheric drag is not significant, these orbits will be at least 100 miles above the earth. Avoidance of the radiation belts will generally limit target orbit altitudes to less than 300 miles. Therefore, in formulating simulator requirements, such orbits have been considered to be the ones of most interest. However, the possibility of rendezvous with target vehicles at higher altitudes has been considered.

The launch and ascent phase may either place the maneuvering vehicle in the immediate vicinity of the target vehicle (direct ascent) or it may place it in a parking orbit. Parking orbits will probably be used for at least the early attempts to rendezvous manned vehicles because they ease the problem of launching at a very precise time. These orbits are selected so that, even though the maneuvering vehicle is launched when the target vehicle is in a non-optimum position, the difference in orbital periods of the two vehicles will result in their coming within a specified terminal guidance range of each other after a period of time that may range from a few minutes to several hours.

Figure 2 shows the velocity increments required to place a maneuvering vehicle in an orbit with an altitude of 450 or 2000 miles with a direct ascent. The ΔV requirement increases as the rendezvous point is moved closer to the launch site (small θ_R) for the cases where the launch site is essentially beneath the orbit plane ($i = 0^\circ$). However, if the launch site is displaced 10 degrees from the orbit plane, the minimum ΔV requirement will occur when the vehicle is injected about 60 or 110 degrees downrange for the 450 mile and 2000 mile orbits, respectively.

Figure 3 shows the closing velocities just before the start of the terminal rendezvous phase for the cases presented in Figure 2. Therefore, this figure indicates typical initial closing velocities for the terminal phase of rendezvous.

The largest lateral displacement of the launch site from the final orbit plane will probably occur if a vehicle is launched from Cape Canaveral (latitude 28.46 degrees) into an equatorial orbit. Mission considerations suggest that equatorial orbits will probably be used primarily for synchronous or 24-hour satellites at altitudes of about 19,350 miles. It seems rather unlikely that rendezvous of manned vehicles with such satellites will be required in the near future. Because of the large ΔV penalties associated with out-of-plane launches (Figure 2), it is to be expected that in the foreseeable future we need only concern ourselves with simulation of missions in which the launch site is within 10 degrees from the target orbit plane. Generally, the launch trajectory and final orbit plane will be nearly coplanar so that inclination changes of less than 1 degree will be much more common than changes of 10 degrees.

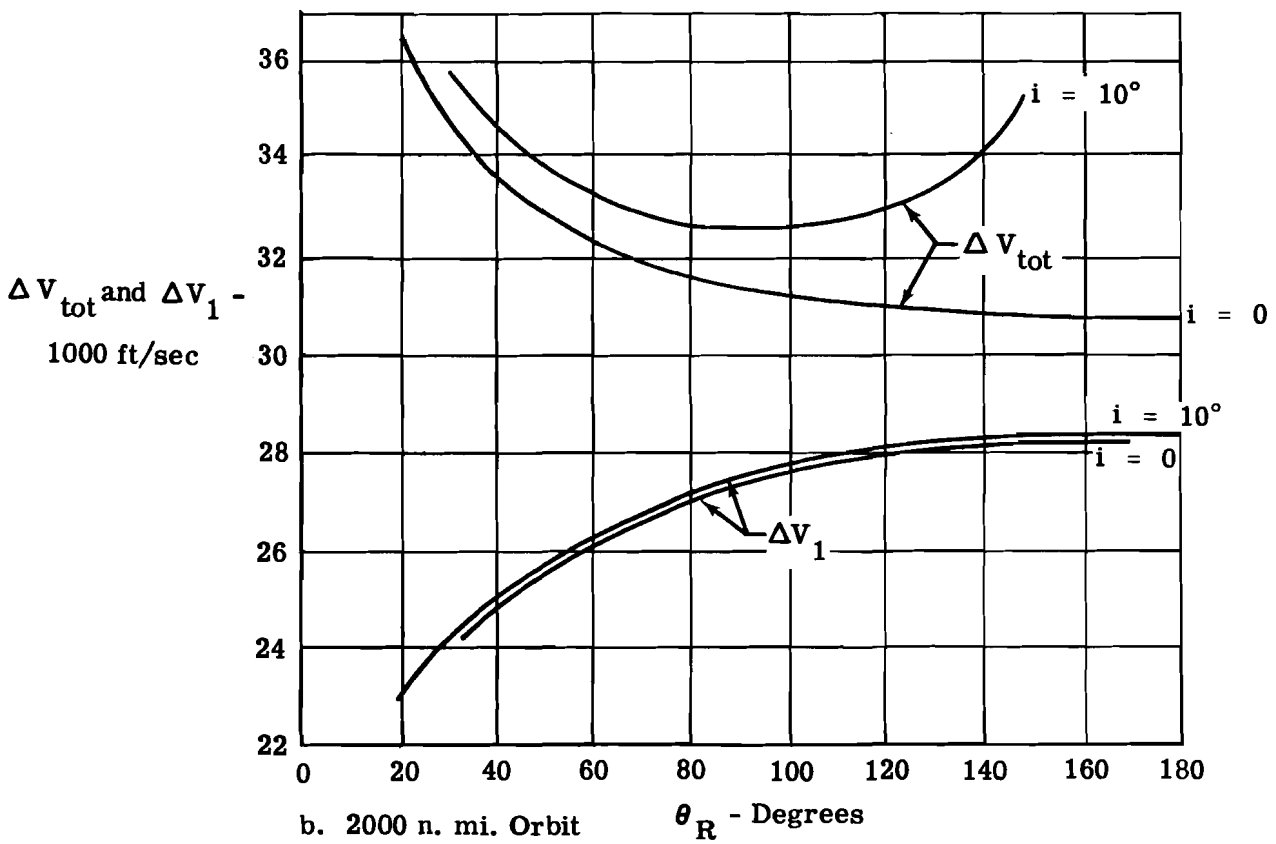
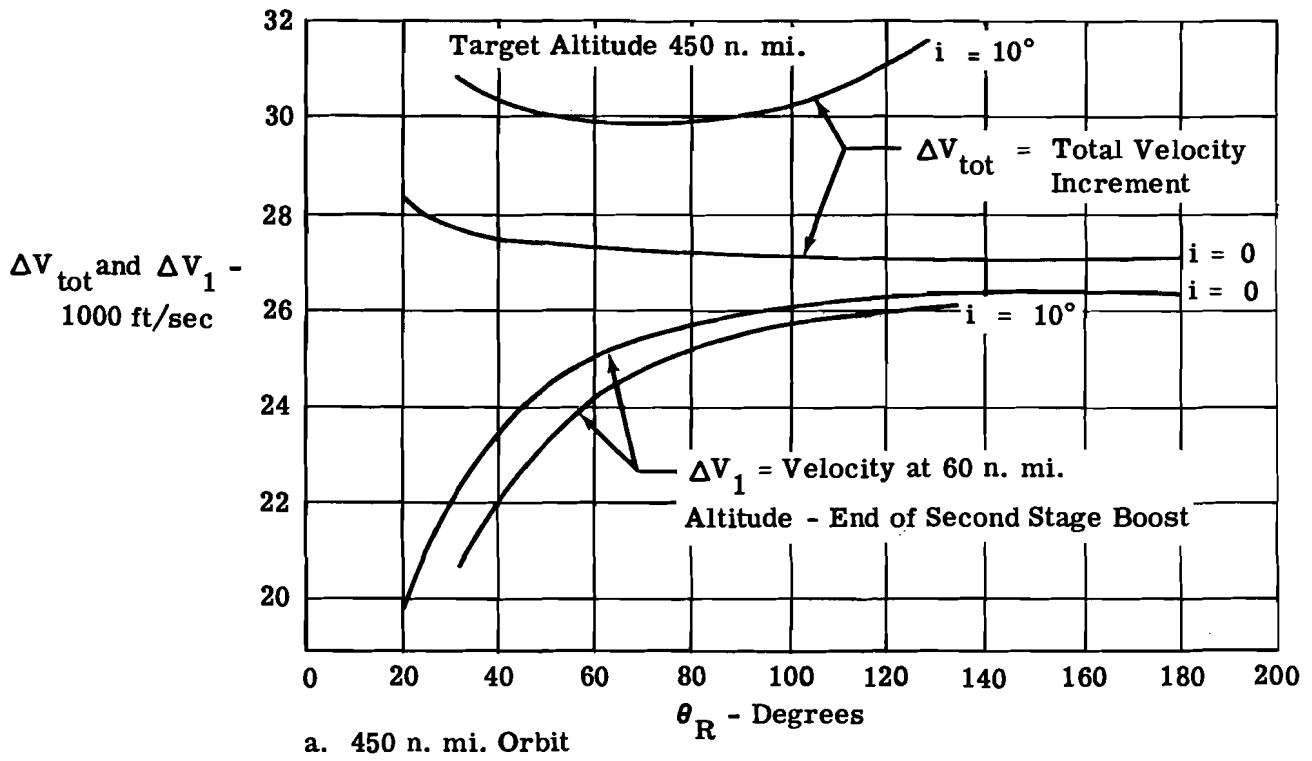


Figure 2. Velocity Required to Place a Vehicle in 450 n. mi. and 2000 n. mi. Orbits with 0° or 10° Changes in Inclination

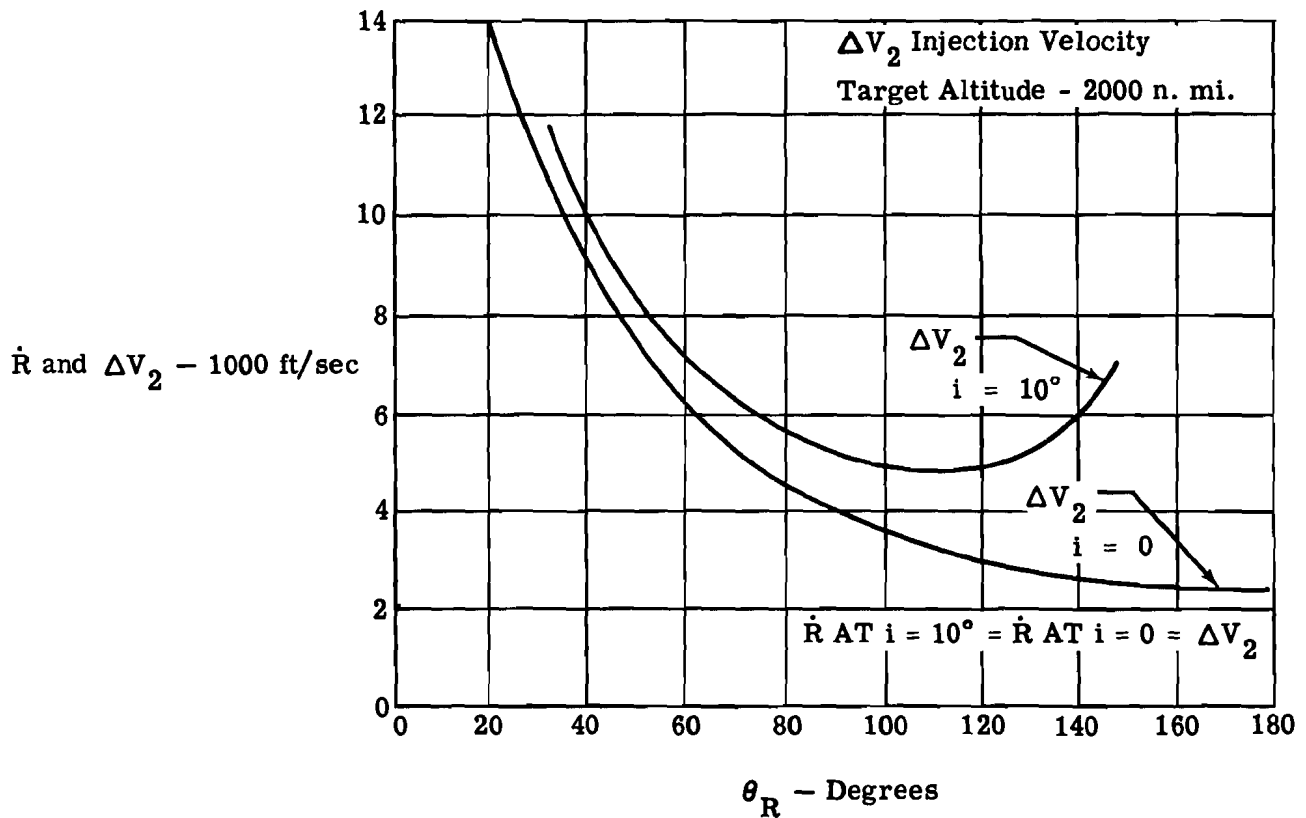
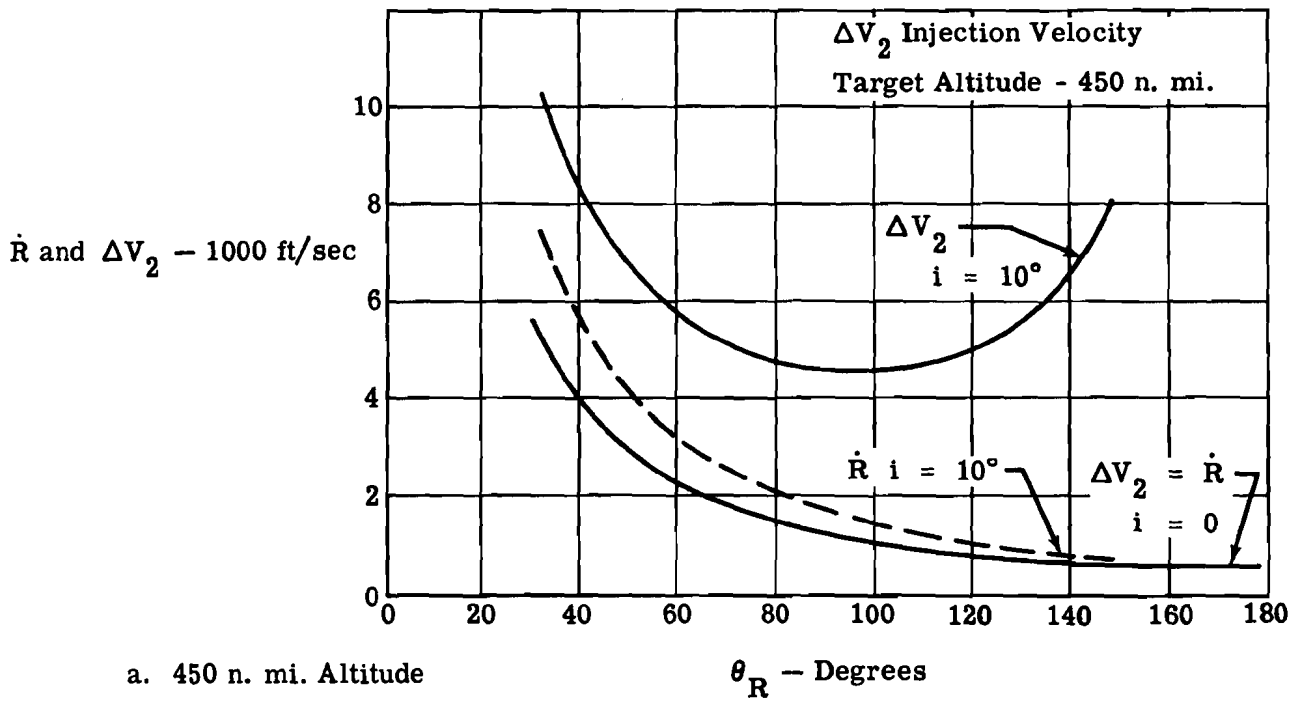


Figure 3. Injection Velocities Required for Rendezvous at Altitudes of 450 n. mi. and 2000 n. mi.

Figure 4 shows the minimum total velocity increment required to change altitude of circular orbits. Approximately half of this amount would be used to initiate the transfer, the second half to inject into the new orbit. Thus, if rendezvous is initiated by transferring from one orbit to another, typical closing velocities at the start of the terminal rendezvous phase would be one-half the ΔV values shown in Figure 4.

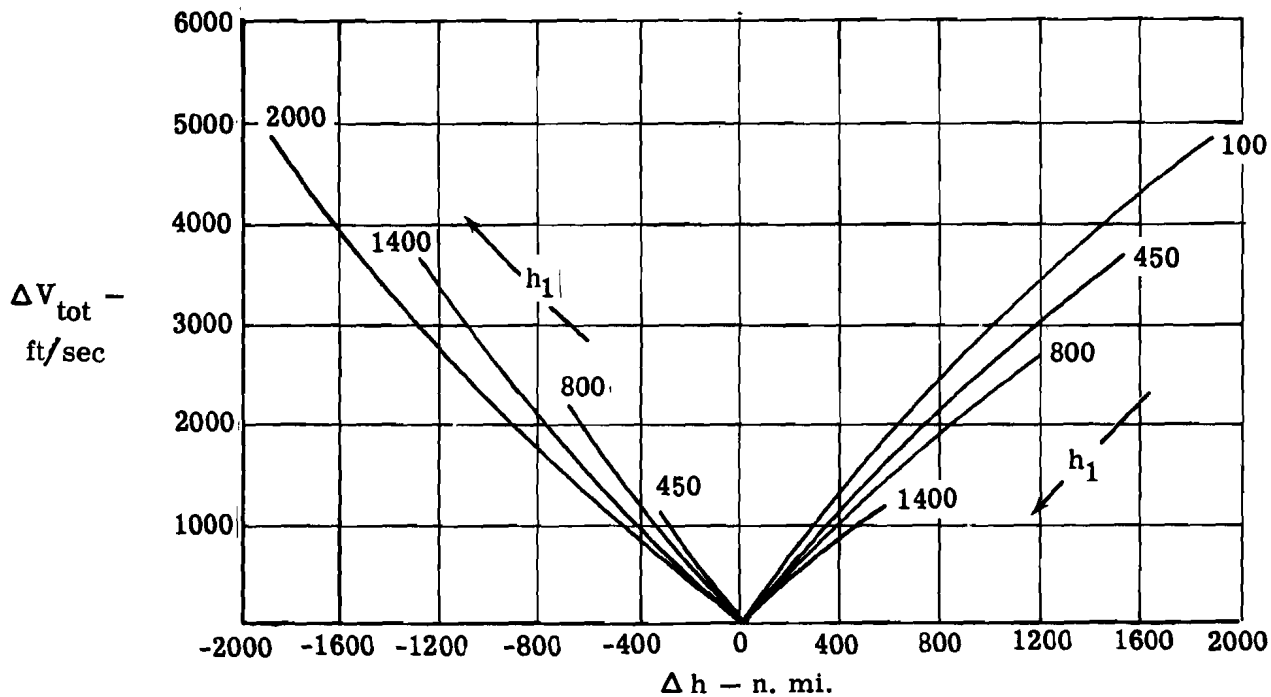
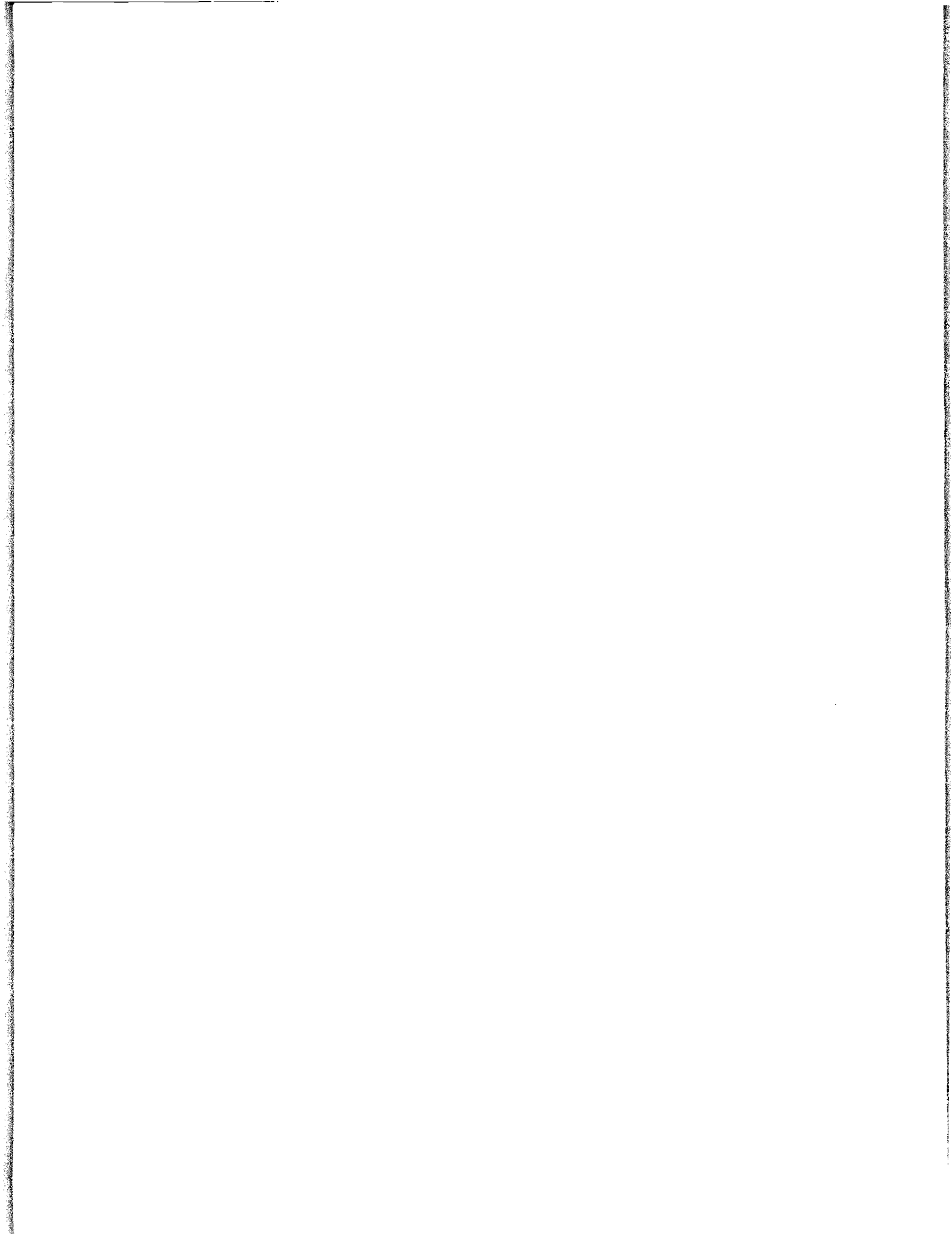


Figure 4. Total ΔV Required to Change Altitude of Circular Orbit



III. RENDEZVOUS AND DOCKING TECHNIQUES AND SYSTEMS

A. GENERAL

Since the primary objective of the subject program was to determine techniques and requirements for the simulation of rendezvous and docking, the first important task was to review the literature and establish what techniques and systems had been proposed and were practical for accomplishing the rendezvous and docking functions. This literature review has revealed many excellent reports on this subject describing various approaches and systems of equations. The reader who is interested in extensive background information on the rendezvous problem is referred to Reference 5 which discusses many of the important facets of this problem such as launch trajectories, launch times, guidance schemes, fuel consumption, axes systems, and equations of motion. This reference is essentially a summary of most of the NASA reports that are listed in the References. The April 1962 issue of *Astronautics* (Reference 6), which was devoted almost entirely to discussions of rendezvous, also provides a good cross section of rendezvous problems and techniques. Reference 7 describes the Gemini rendezvous plan.

The following paragraphs present a discussion of typical rendezvous trajectories, ΔV and acceleration requirements, and other associated factors in the terminal guidance and docking phases of rendezvous. This discussion emphasizes those aspects of rendezvous and docking pertinent to the simulation problem, and in particular to the determination of simulator computer requirements.

B. DISCUSSION OF THE RENDEZVOUS PROBLEM

The terminal guidance phase is generally defined as beginning when radar or other sensors in the interceptor vehicle first acquire or begin searching for the target. In some cases a rendezvous without the aid of electronic or optical sensors may be possible. In such cases, the terminal phase would begin when the pilot begins his visual search for the target.

A review of systems that might be used in the maneuvering vehicle to obtain range, relative velocity, and other data required for rendezvous indicates that these systems may have range capabilities of as much as 400 miles (Reference 2). However, ranges of the order of 50 miles or less are more typical of the capabilities of hardware and initial ranges assumed in most studies of the terminal guidance that have been reported in the literature.

Information to indicate the range at which a pilot can control rendezvous on the basis of visually derived data is quite limited. Reference 3 concludes that for completely unaided visual rendezvous, estimates of range and closing velocity will be very inaccurate except at ranges of less than 100 feet. Reference 4 states that stadiometric ranging, in which an observer uses a scale to measure the angle subtended by a target, would be of little use for ranges greater than 1 mile unless an optical aid such as a surveyor's transit is used. Such aids could increase the useful range by several orders of magnitude. Reference 4 also indicates that search and target detection by visual means is feasible up to fairly long ranges unless relative positions of the sun, target, and interceptor are very unfavorable.

Closing velocities at the beginning of the terminal guidance phase can range from the neighborhood of 100 ft/sec to several thousand ft/sec. The lower values will generally be

encountered if the launch and ascent phases involve large range angles or if parking orbits are employed. The higher velocities may result if a direct ascent is made.

Eggleston, Reference 8, has presented results of a study of rendezvous ascent. Figure 5 presents typical results from that reference. It shows the motion of the interceptor vehicle relative to an axis system fixed in the target and with the x-axis always locally horizontal. In each case, the interceptor is on an exact collision course with the target vehicle. Further thrusting after the initial conditions have been established is unnecessary. These results are all for cases where the trajectories start at the end of boost occurring at an altitude of 60 miles.

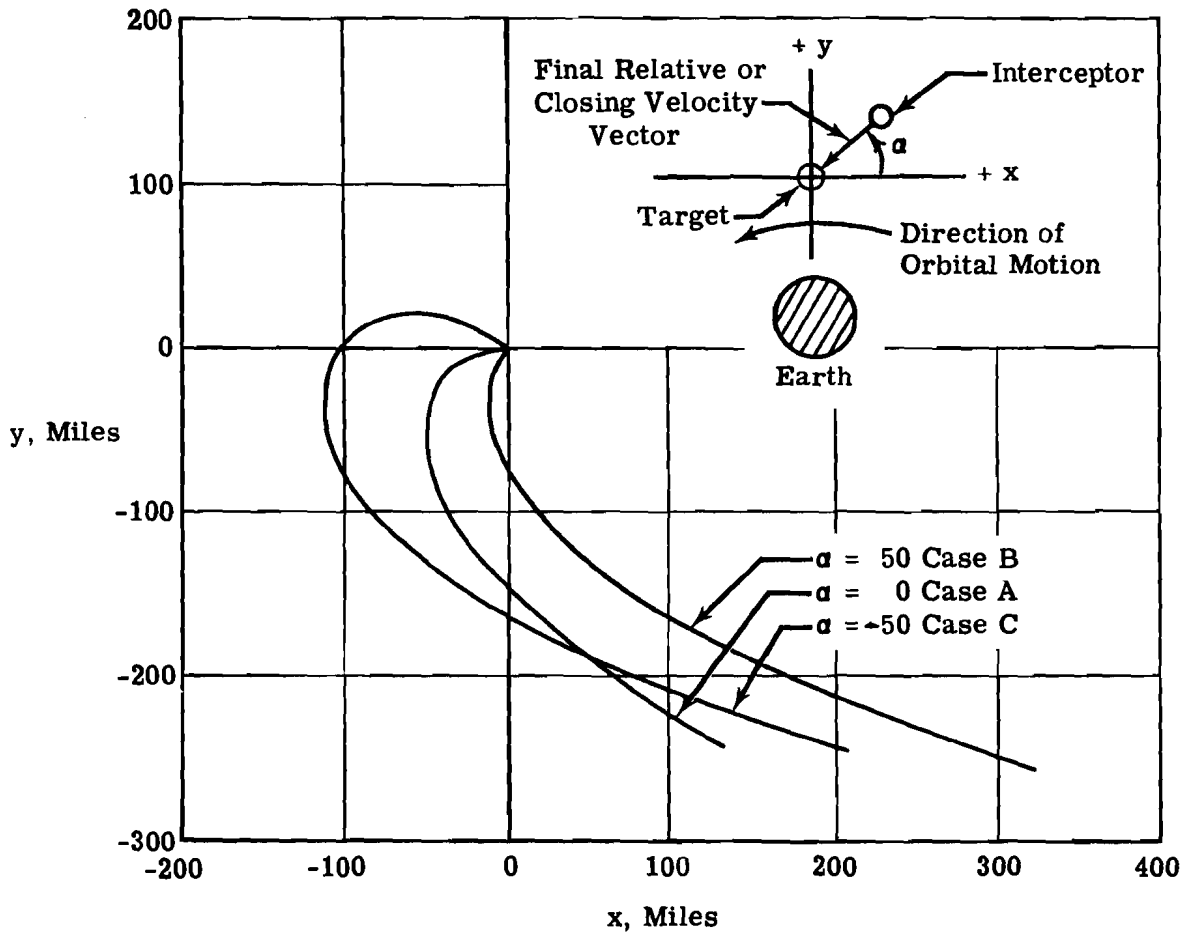


Figure 5. Relative Positions During Ascent Trajectories
(Closing Velocities = 600 ft/sec)

It will be noted that in all cases presented, the interceptor vehicle will approach the target from one of the quadrants which is ahead of the target. The final closing angle that the relative velocity makes with the target total velocity vector is primarily determined by the range along the ground from the end of boost to the rendezvous point. If the rendezvous occurs approximately 180 degrees from the launch site (Case A of Figures 5 and 6), the ascending vehicle will approach the target from almost directly ahead of the target. The ascending vehicle must then fire a rocket in the horizontal direction to accelerate it to avoid collision from the rear by the target. If rendezvous is made at less than 180 degrees from the launch site, the maneuvering vehicle will generally approach the vehicle from below (Case B of Figures 5 and 6). This generally has the disadvantage of requiring more fuel than the preceding case because the interceptor approaches its target with a vertical component of velocity that must be removed in order to match the orbit of the target.

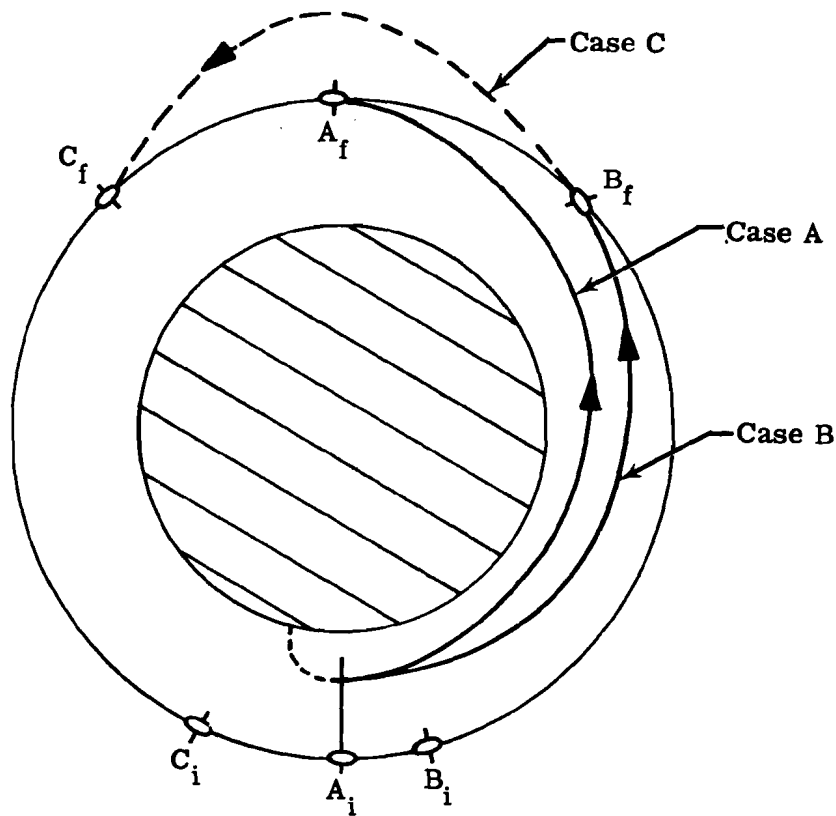


Figure 6. Typical Ascent Paths

The third case (Case C of Figures 5 and 6) consists of an approach from ahead of and above the target and generally occurs if rendezvous is made more than 180 degrees from the launch site. A similar closing situation could occur at shorter downrange distances from the launch site if the interceptor is launched at a steep angle. If the launch site is near the orbital plane, this technique is costly in fuel because of gravity losses during the ascent. However, for certain cases where the launch site is displaced from the orbit plane and the ascent trajectory reaches an apogee altitude far above the target altitude, this approach can be efficient. The saving in this case results because the change in heading can be made at the apogee of the ascent trajectory where the vehicle's velocity is lower than at the lower altitude of the final orbit.

Figure 5 indicates that if the rendezvous is initiated from the ground, the interceptor will, for a most efficient rendezvous, approach its target from one of the quadrants ahead of the target. If rendezvous is initiated from an orbit above the target, the approach will normally be from one of the quadrants behind the target. In such cases the relative motion will be essentially what one would obtain by reflecting Figure 5, first about the x-axis, and then about the y-axis. Thus, if all possible situations are considered, the maneuvering vehicle may approach its target from any quadrant in or near the plane of the orbit.

Figure 7 (taken from Reference 8) illustrates another significant feature of the rendezvous problem; namely, that over a considerable portion of the trajectory in the terminal guidance phase in which thrust is not being applied, the relative velocity will for all practical purposes be constant. During this final portion of the approach, if the interceptor is on a collision course, the rotation of the line-of-sight angle between the two vehicles will also be nearly zero. In other words, the interceptor will be approaching its target in almost a straight line and at a constant velocity. This is further illustrated by noting that the final portions of the previously discussed relative motion plots of Figure 5 are almost straight lines.

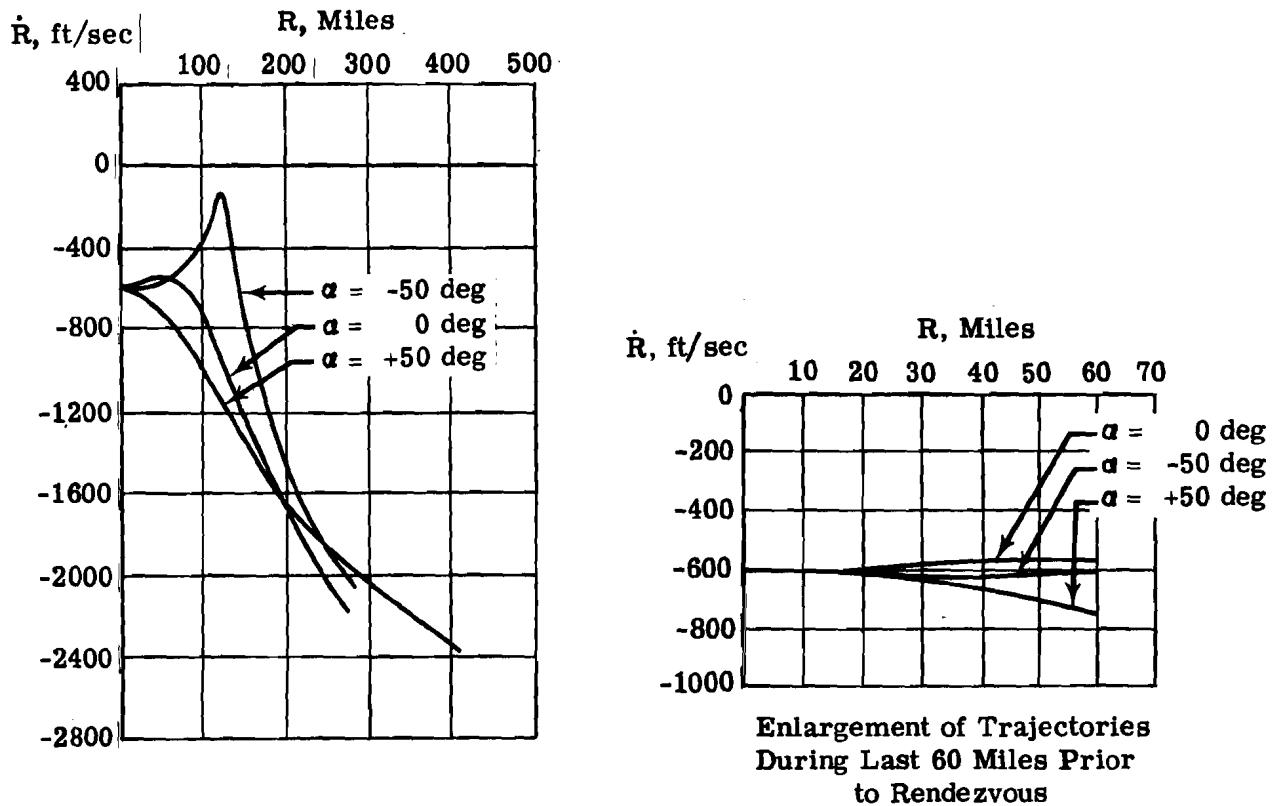


Figure 7. Closing Velocities During Ascent Trajectories Shown in Figure 5
(Closing Velocities = 600 ft/sec)

Figure 8 shows the relative motion of two vehicles for several cases in which the final closing velocity is only 10 ft/sec. A comparison with Figure 5, where closing velocity is 600 ft/sec, shows a striking similarity of the trajectories with final closing velocities of 10 and 600 ft/sec. However, with a final closing velocity of only 10 ft/sec, the straight-in approach and constant velocity portion of the trajectory does not begin until the two vehicles are about one-half mile from one another while for the 600 ft/sec case, the straight-in approach is about 30 nautical miles.

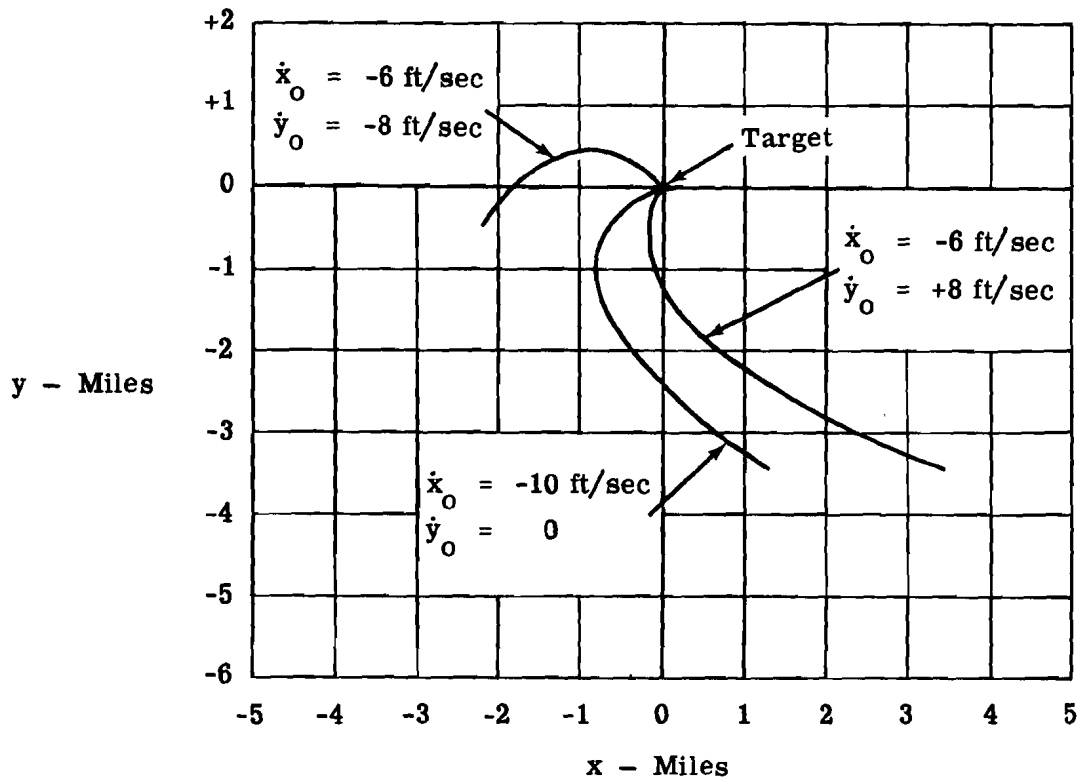


Figure 8. Relative Positions During Ascent Trajectories
(Closing Velocities = 10 ft/sec)

Figure 9 indicates the distances at which the closing velocity becomes essentially constant and the line-of-sight rotation nearly zero. This figure also indicates, for several maximum T/W's, the distances at which an astronaut must fire his rockets to match the target velocity if rendezvous is to occur without overshoot or danger of collision. It will be seen that in theory, this final firing can be delayed until the two vehicles are quite close to one another. However, in practice, most rendezvous systems will reduce the closing velocity in a series of steps or in a more gradual manner as indicated by Curves A and B of Figure 10.

Figure 11 illustrates the importance of time allowed for terminal rendezvous or docking. Data presented in this curve were computed with the assumption that two vehicles were both in the same circular orbit but one was a specified distance ahead of the other. Thus, the chase vehicle must first increase speed to catch its target, then it must slow down to accomplish rendezvous. Two rendezvous techniques are indicated; two-impulse and constant bearing techniques. With the two-impulse technique, the chase vehicle fires a high thrust rocket in the direction that would result in rendezvous in the specified time with only one further thrusting to bring the relative velocity back to zero at the end of the transfer. With the constant bearing technique which was selected to illustrate the other extreme in fuel economy, the rocket was fired horizontally and then a constant downward thrust was used to counteract the increase in centrifugal force and, hence, to maintain a constant altitude.

Figure 12, which is reproduced from Reference 11, illustrates the fact that if the interceptor initially has a velocity component toward the target, ΔV requirements will generally be less than indicated by Figure 11. Initial components of velocity normal to the line of sight will add linearly to the ΔV requirements unless they are removed concurrently with additions or subtractions to the velocity along the line of sight. In the latter case, some economy of fuel will result from vector additions of the two components of velocity corrections.

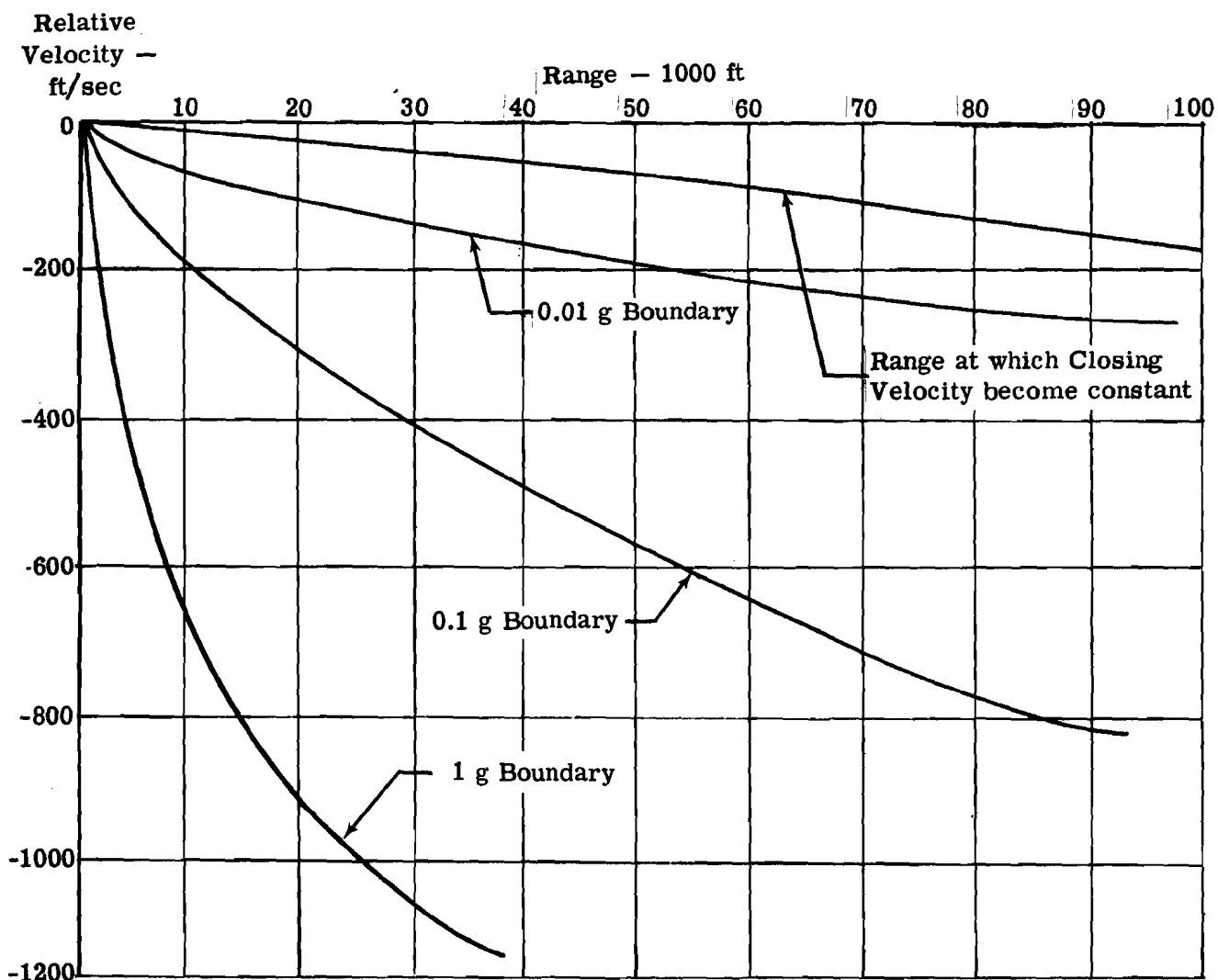


Figure 9. Ranges at which Braking Maneuvers Must Start

By comparison, the constant bearing technique has the advantage of simplicity. For example, in an ideal situation, an astronaut might be able to detect any rotation of his line of sight to the target by simply observing the apparent motion of the target relative to a reference such as the horizon or the stars. He would then fire a rocket perpendicular to the line of sight to bring this rotation to zero. By contrast, it seems certain that a true two-impulse technique, or even a multi-impulse technique based on orbital mechanics concepts, would require accurate data and a computer.

Figure 13 shows the ΔV required for rendezvous with the two-impulse method if the target is at a given distance from the maneuvering vehicle, but at various elevation angles. It can be seen that as the elevation angle is changed, the ΔV requirements only change a few percent. If the time allowed for rendezvous is changed from 10 minutes to 5 minutes, the required ΔV increases and the effect of the elevation angle decreases.

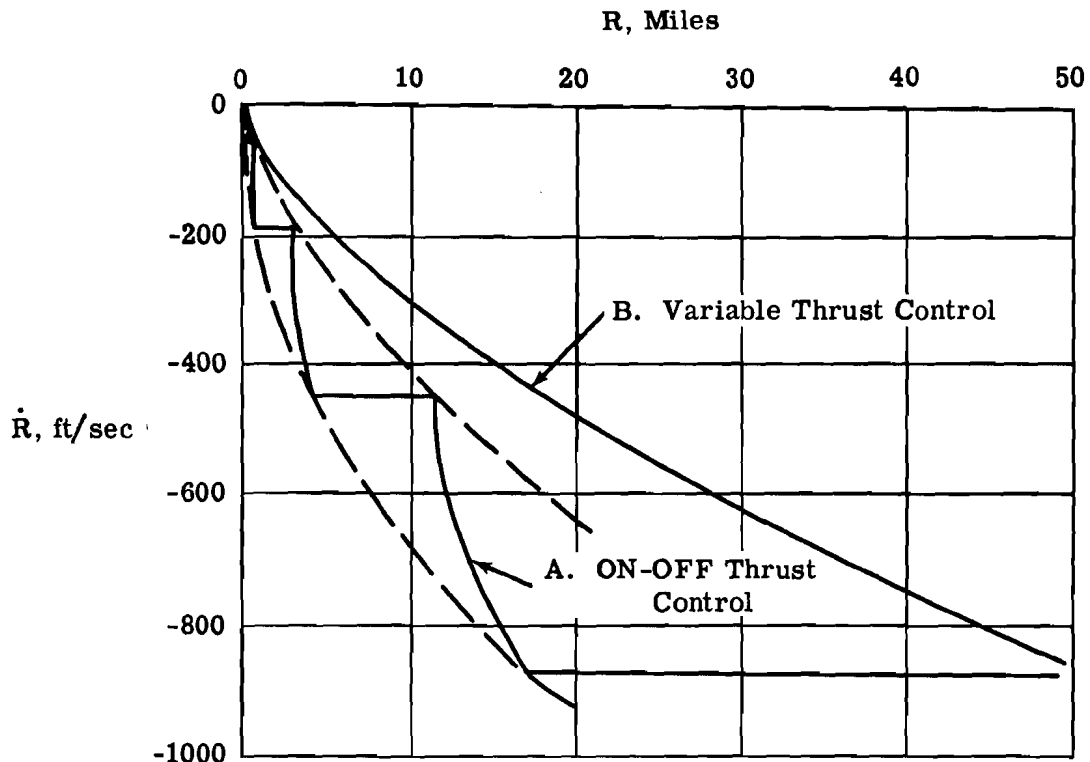


Figure 10. Closing Velocity versus Range During Typical Manually Controlled Rendezvous

This figure also applies to other ranges if the range, R , and required ΔV are both increased or decreased by the same factor. For example, if the initial range is 500 feet, rather than 5000, the ΔV required for rendezvous in 10 minutes is approximately 2 ft/sec, rather than 20 ft/sec.

Figure 14 shows the ΔV required to align two orbits if the correction is made as the two orbits cross. Figure 15 shows that if the time allowed for a rendezvous maneuver is specified, a maneuver to correct the misalignment will be considerably more expensive if it is made at a time other than when the maneuvering vehicle is crossing the orbit of the other vehicle.

A "short-time" maneuver near a point 90 degrees from the point of intersection of two orbits would correspond to lateral motion relative to the orbital planes. It can be easily seen by comparing Figures 11 and 15 that a lateral maneuver to rendezvous in a given time when in such a position in orbit takes essentially the same ΔV as if the two vehicles were separated the same distance, but one was chasing the other in the same orbit. In fact, for times and distances considered here, the ΔV required is dependent primarily on the line-of-sight distance between the two vehicles and their relative velocities. If the initial relative velocities are zero, the ΔV required is almost independent of whether the target is ahead of, behind, above, below, or beside the maneuvering vehicle.

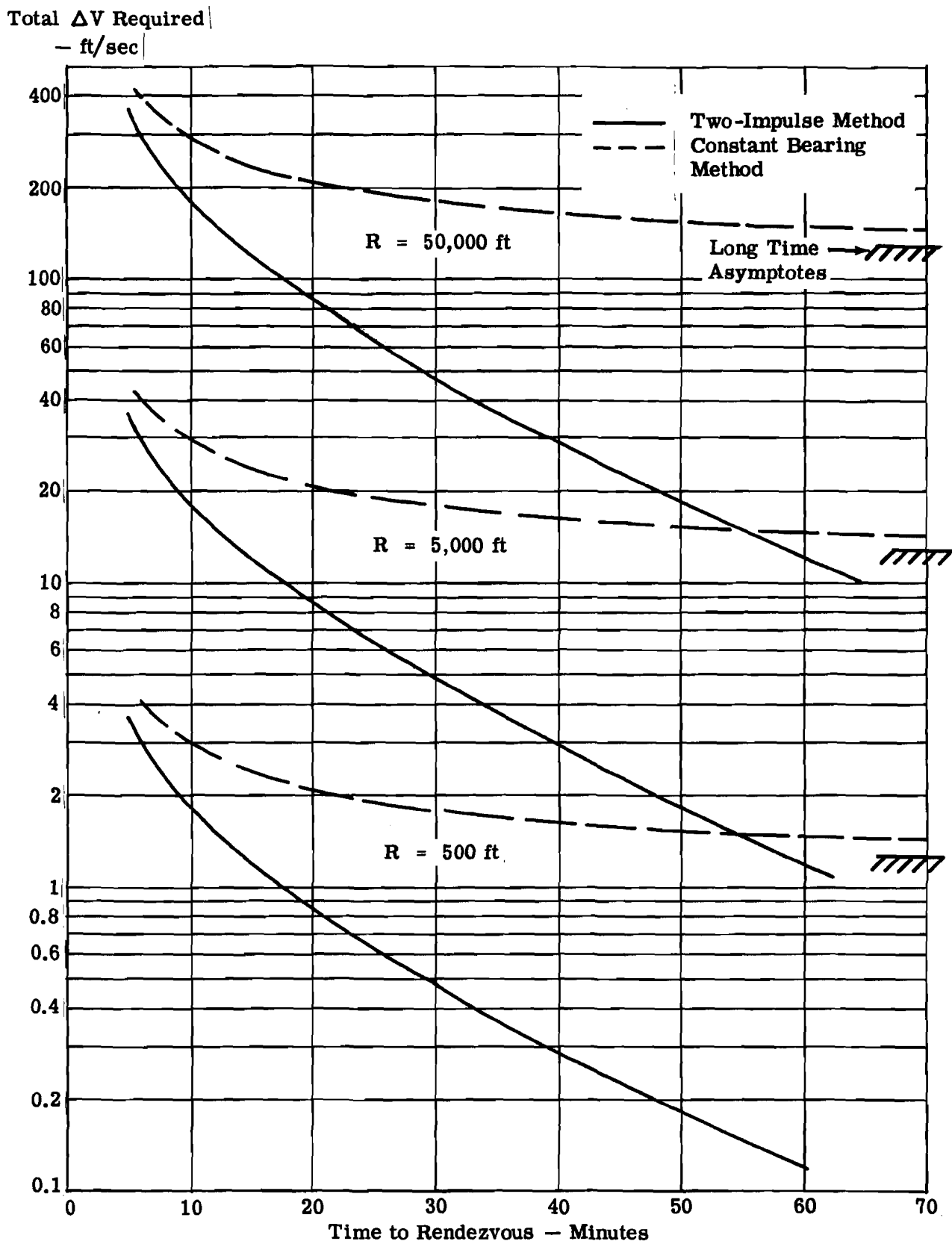


Figure 11. Effect of Rendezvous Time on ΔV Required

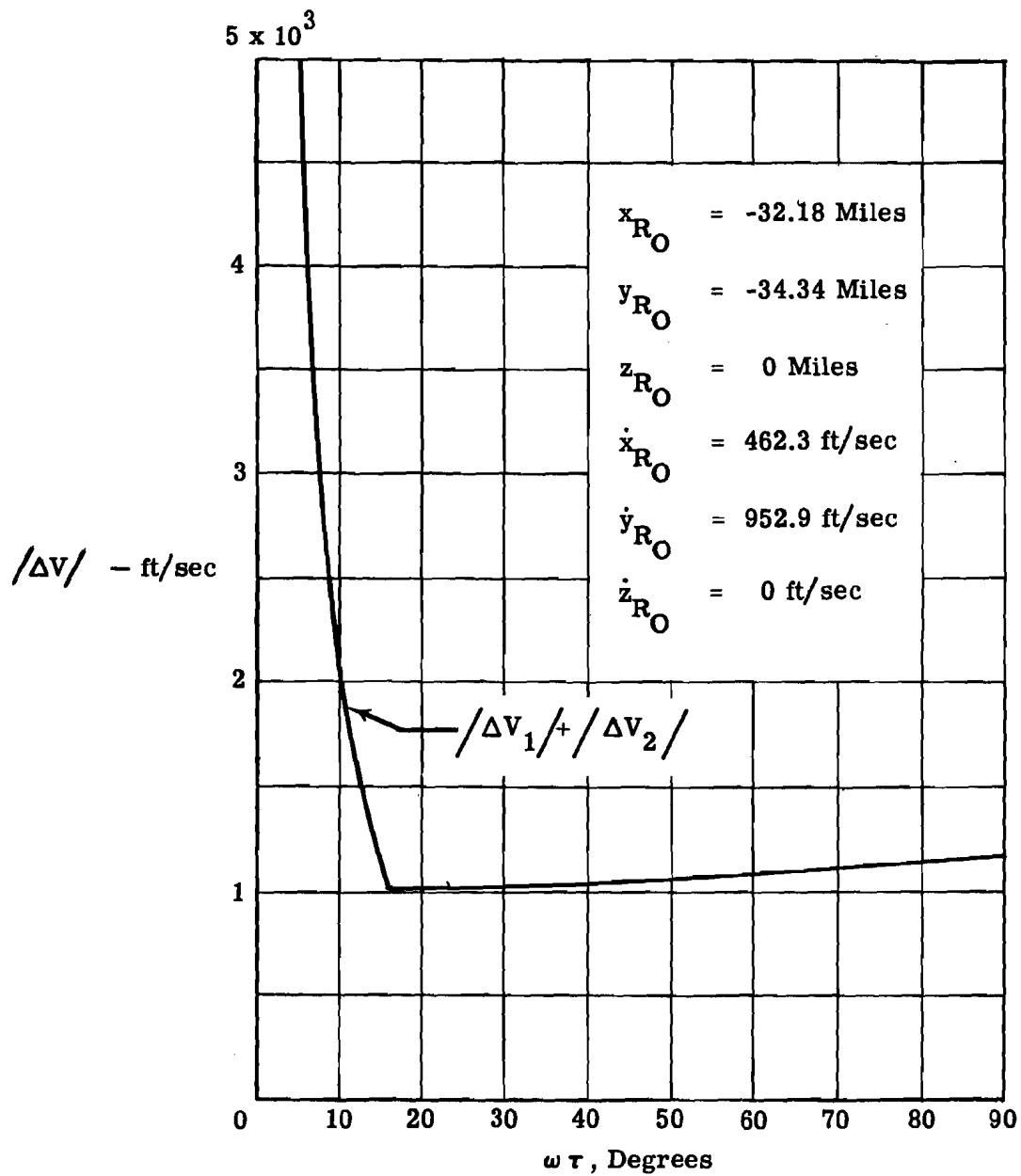
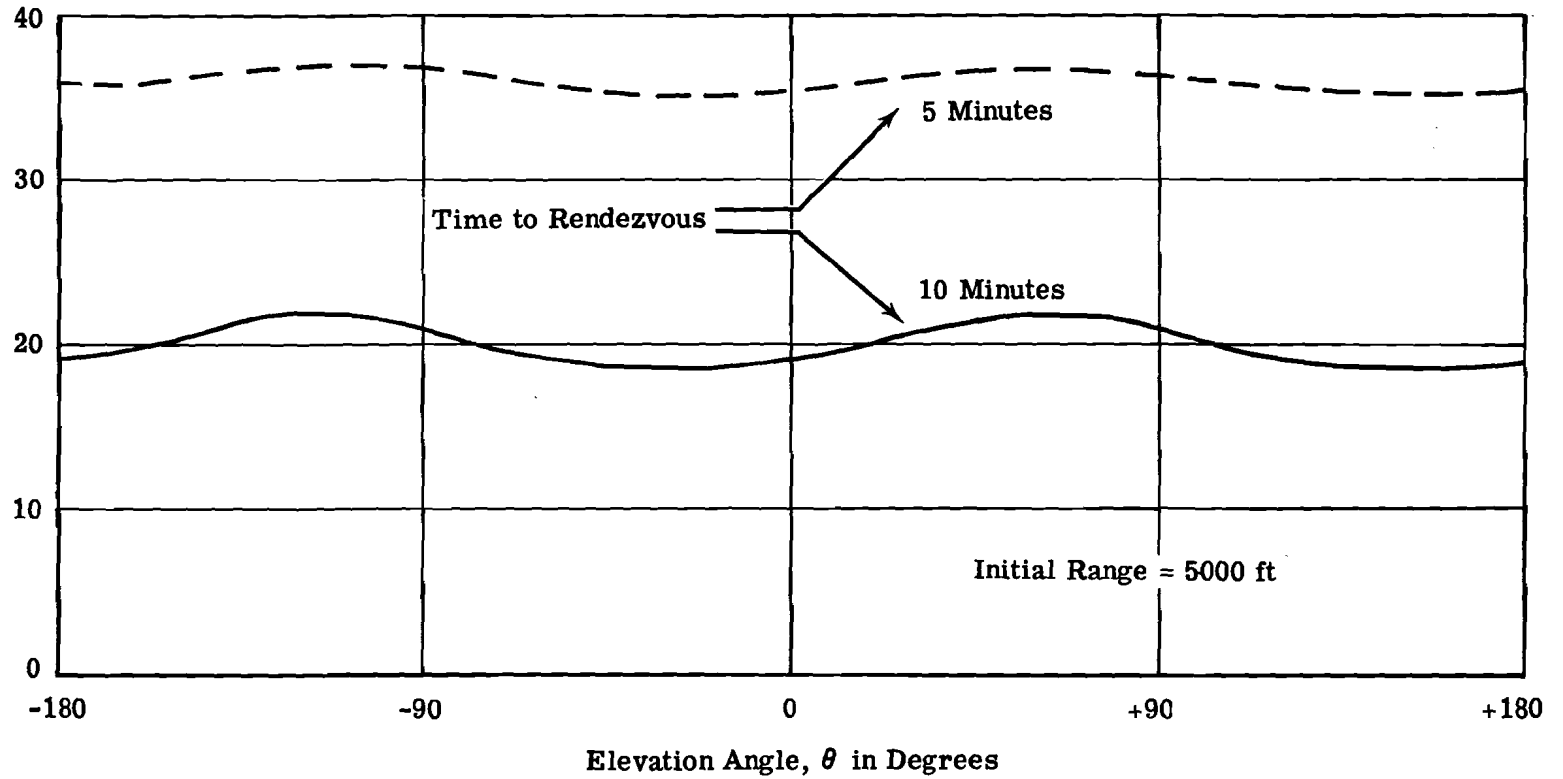


Figure 12. Variation of Velocity Change for Intercept and Rendezvous

Total ΔV Required -- ft/secFigure 13. Effect of Elevation Angle on ΔV Required for Rendezvous

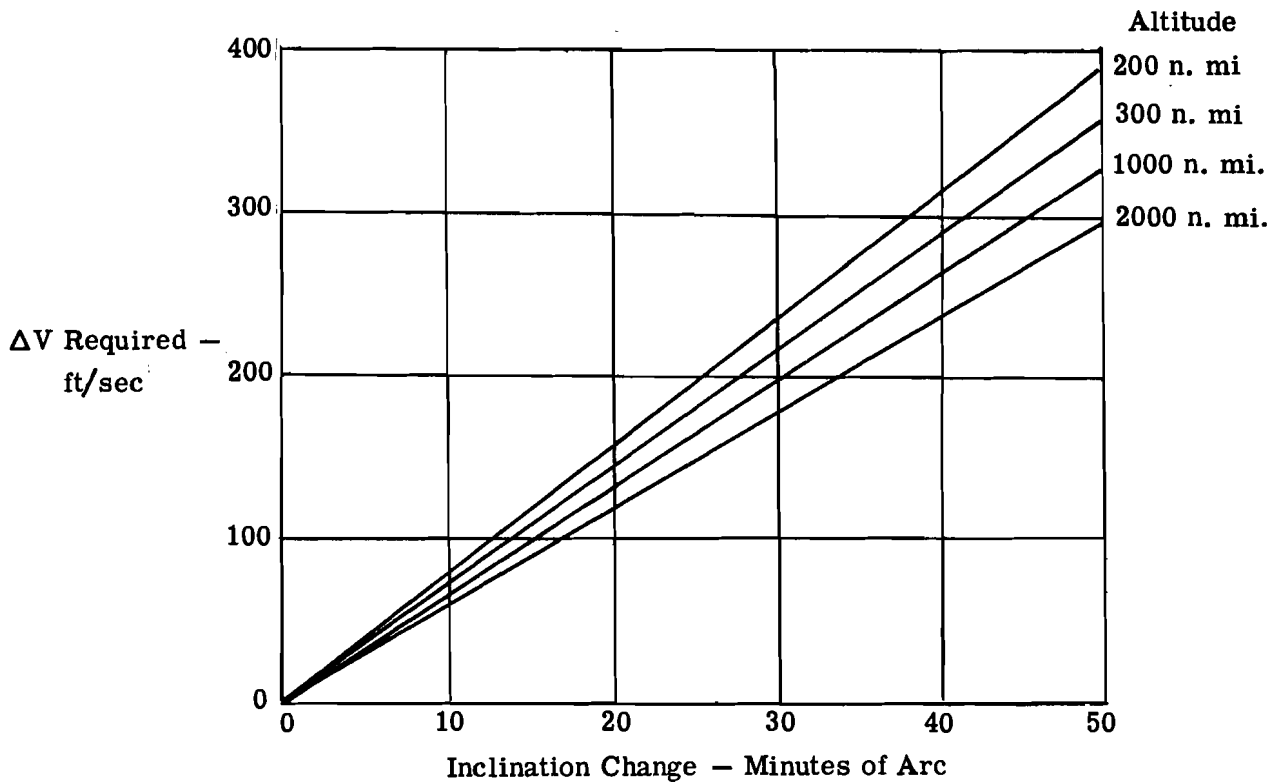


Figure 14. ΔV Required for Change of Orbit Inclination

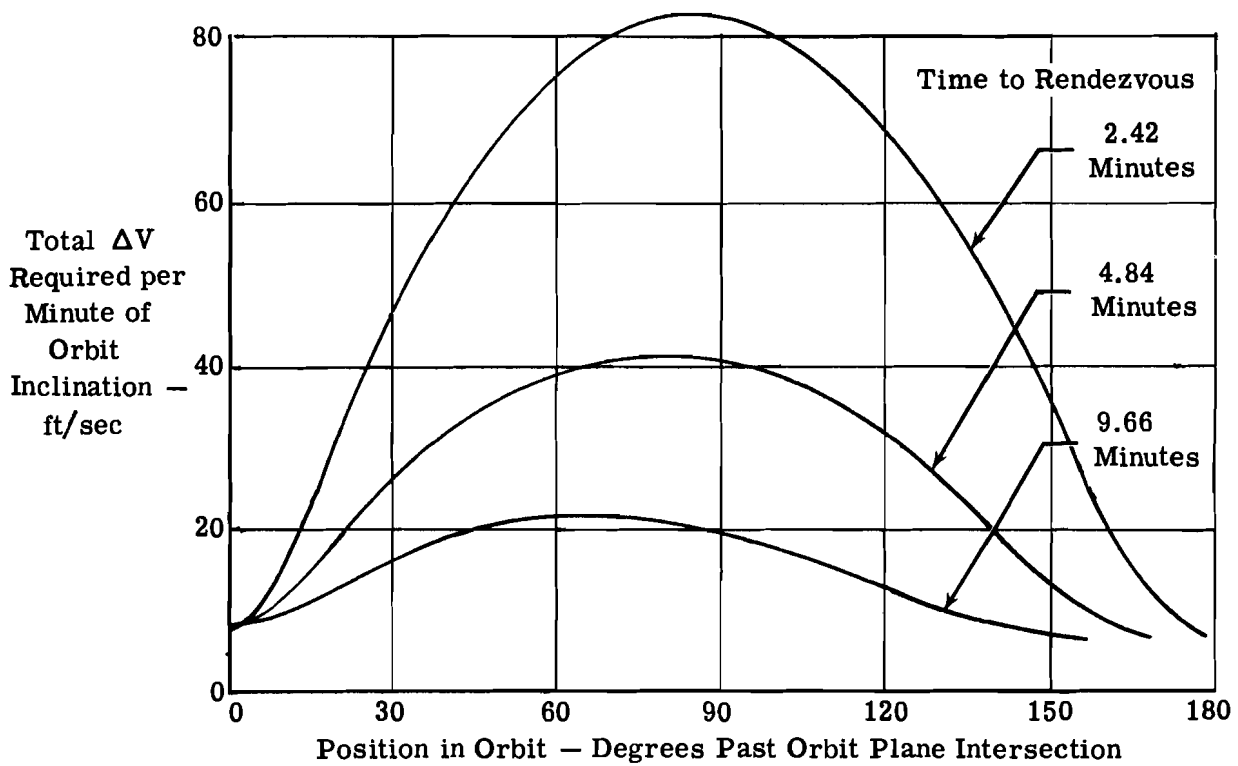


Figure 15. ΔV Required for Rendezvous of Vehicles in Noncoplanar Orbits

C. DISCUSSION OF TECHNIQUES

A technique, as referred to in this report, is any method that predicts the magnitude, direction, and duration of thrust which should be applied to the interceptor vehicle to accomplish rendezvous and docking. As suggested from material presented in the previous section, someplace in the total rendezvous mission, guidance techniques based on exact equations involving a full set of orbital mechanics expressions can be replaced by simplified methods for aiming and thrusting. Where this division occurs, is dependent largely on time to rendezvous and relative velocity. That is, if closing speeds are large such that the time to interception is short, the relative motions of the two vehicles are similar to their motions as if they were in free space. This similarity can be verified analytically and, in fact, has been studied and indicated in References 13, 15 and 18 among others, as well as in Section VI of this report. As a result, techniques which have been proposed for control in the terminal phase of rendezvous have been of two types: (1) "Orbital Mechanics Techniques" which do not make use of the simplified dynamics and, as a result, are based upon the exact equations of orbital mechanics; and (2) "Proportional Navigation Techniques" which do make use of it to obtain a simplified set of commands or rules based upon the relative motion between interceptor and target.

1. Orbital Mechanics Techniques

In many idealized cases, orbital mechanics systems utilize some form of the two-impulse orbital transfer technique where the first impulse is used to place the vehicle in a transfer orbit that will intercept the target at a given point in space. The second impulse is used to match the magnitude and direction of the target when the interceptor has entered the near vicinity of the target. Since a two-impulse transfer requires very accurate input data and the solution of complex equations of motion, most of the orbital mechanics techniques use either an n-impulse or a continuous thrust transfer. For these cases, velocity corrections are made continuously or at a number of times during the rendezvous maneuver from updated solutions of the equations of motion. Generally, some simplifying assumptions are made and equations having a closed form solution are employed.

The two-impulse maneuver represents the most efficient case for the orbital mechanics techniques. Because of the complexity of solving exact equations of relative motion and of possible errors inherent in any sensor system, most orbit mechanics techniques use updated solutions to make periodic velocity corrections. This results in a multi-impulse maneuver and ΔV requirements are somewhat larger than for the minimum two-impulse transfer shown in Figure 11.

2. Proportional Navigation Techniques

In the proportional navigation technique, output commands are based on solutions of equations of only the relative dynamics of the two vehicles, involving such variables as line-of-sight range, closing speed, and line-of-sight rotation rate. Although in some cases, time or position of intercept and fuel usage may play a part in generating the commands (viz., Reference 13), these techniques disregard the orbital mechanics portion of the relative equations of motion. As a result, the long range effects (the accumulated effects of differential gravity between the two vehicles) are neglected and the control laws have either been generated empirically or derived from simplified equations of motion. The procedures used in most proportional systems can be reduced to a common pattern, varying from one another in minor details only. In the general pattern, thrust, or a component of thrust, is applied normal to the line of sight to control the rate of rotation of the line of sight, either with respect to inertial space or the local earth horizontal, and along the line of sight to achieve the desired closing velocity.

The simplest version of proportional navigation technique applies the initial thrust perpendicular to the line of sight to reduce the rate of rotation of the line of sight to zero. More sophisticated versions take advantage of the cosine effect and orient the thrust so that the closing velocity is controlled at the same time that rotation of the line of sight is brought to zero. Unless a precise closing velocity is desired, this technique requires less accurate orientation of the thrust than does a two-impulse (orbital mechanics) transfer.

The word "proportional" in the term "proportional navigation" does not imply a requirement for a variable thrust engine. As it is used here, "on-off" systems in which fixed thrust levels are commanded whenever error signals exceed specified values or fall outside a specified band are also included in the proportional navigation category. In such systems, the error signals are generally proportional to deviations of problem variables from desired values. Thus, there is some basis for classifying such systems as proportional systems instead of defining a special classification for them. The principal reason for not using separate classifications is that in several instances the same basic rendezvous and docking systems have been studied with both true proportional and with on-off modes. The error signals generated are the same in both cases. Thus, the two modes differ only in a final step where the error signals are converted to thrust commands.

Several representative systems that have been proposed in the literature for terminal rendezvous are summarized in the following section.

D. SYSTEM DESCRIPTIONS

In this section, summaries and block diagrams of a number of systems that have been proposed in the literature for terminal rendezvous are presented. These systems fall either into the category of the proportional or orbital mechanics systems as described in the previous section. In general, the conditions within which these systems operate are:

$$\begin{array}{ll}
 R \approx & 50 \text{ n. mi.} \\
 \dot{R} \approx & -1000 \text{ ft/sec} \\
 R\dot{\alpha} \approx & \pm 500 \text{ ft/sec} \\
 R\dot{\beta} \approx & \pm 500 \text{ ft/sec}
 \end{array}$$

However, the system of Reference 9 has been demonstrated for ranges in excess of 450 miles and the system of Reference 10 for relative velocities up to 6000 ft/sec. Many of the other systems could probably also operate satisfactorily from similar initial conditions, even though this has not yet been demonstrated. Each of the rendezvous systems which have been reviewed in the literature are described separately in the following paragraphs under headings of proportional navigation and orbital mechanics systems. Each system employs its own uniquely defined coordinate system which is summarized in the first two columns of Figure 16. Some changes in the symbols and notation have been made to effect more uniformity between system descriptions. These are described in the last two columns of Figure 16. No loss in the generality of the methods has been caused by these changes in notation.

1. Proportional Navigation Systems

a. NASA TR R-128, Lineberry, Jr. and Foudriat (Reference 13)

This report presents a fully automated system utilizing the proportional navigation technique. Figure 17 shows the equations which this system employs. Rendezvous is accomplished by first establishing a collision course by removing the velocity component normal to the line of sight. The second step is a braking maneuver for reducing the range rate to zero at zero range. Both modulated thrust control and on-off thrust control were investigated for the braking maneuver and system performance was found to be satisfactory.

As given in Referenced Report		As used in this Report	
Description	Diagram	Description	Diagram
<p>NASA TN D-747 Brissenden, Burton, Foudriat, Whitten (Reference 15)</p> <p>A rectangular coordinate system with origin at the center of the earth and the axes directions fixed with respect to the stars. The X_I and Z_I axes lie in the plane of the target's orbit. Also defined is a coordinate system, x_I, y_I, z_I, with center in the target vehicle and whose axes are parallel to the X_I, Y_I, Z_I axes.</p>	<p>Interceptor Z_I</p> <p>Target</p> <p>x_I y_I z_I</p> <p>X_I Y_I</p> <p>Projection of \bar{R} on $X_T Y_T$ plane</p>	<p>The coordinate system as given in Reference 15 has been used. However, the X_I, Y_I, Z_I and x_I, y_I, z_I axes have been designated X, Y, Z and X_T, Y_T, Z_T, respectively. A coordinate system X_I, Y_I, Z_I with origin in the interceptor and whose axes are parallel to X, Y, Z axes has been defined. Vector $\bar{\sigma}$ and $\bar{\rho}$ are designated $\bar{\sigma}_I$ and $\bar{\sigma}_T$, respectively.</p>	<p>Projection of X_B Axis on $X_I Y_I$ Plane</p> <p>Interceptor Z_I</p> <p>Target Z_T</p> <p>X_I Y_I X_T Y_T Z</p> <p>θ_I ϕ_I α β</p> <p>Projection of \bar{R} on $X_T Y_T$ Plane</p>
<p>NASA TR R-128, Lineberry Jr. and Foudriat (Reference 13)</p> <p>At system lock-on a non-rotating set of reference axes is established with the origin in the target vehicle. The X_i axis passes through the interceptor and the Y_i axis (direction arbitrary) and Z_i axis complete a right-handed orthogonal frame.</p>	<p>Target</p> <p>Interceptor</p> <p>X_i Y_i Z_i</p> <p>a. Initial Position of Interceptor</p> <p>Interceptor Y_i</p> <p>Target Z_i</p> <p>X_i α β</p> <p>Projection of R on $X_i Y_i$ plane</p> <p>b. Future Position of Interceptor</p>	<p>The X_i, Y_i, Z_i axes have been replaced by X_T', Y_T', Z_T', and α and β have been replaced by α' and β'. The X_T', Y_T', Z_T' axes have been oriented such that positive α' corresponds to negative α of the original system. The X_T', Y_T', Z_T' axes are related to the X_T, Y_T, Z_T axes described above for Reference 15 by the angles α_0 and β_0 (see Figure 45c).</p>	<p>Interceptor Z_T'</p> <p>Target</p> <p>X_T' Y_T'</p> <p>a. Initial Position of Interceptor</p> <p>Interceptor Z_T'</p> <p>Target</p> <p>X_T' α' $-\beta'$</p> <p>Projection of R on $X_T' Y_T'$ Plane</p> <p>b. Future Position of Interceptor</p>

Figure 16a. Summary of Coordinate Systems

As given in Referenced Report		As used in this Report	
Description	Diagram	Description	Diagram
<p>AAS Preprint 62-10, Stapleford (Reference 14)</p> <p>A rectangular coordinate system, RNT, with origin in the target vehicle. The R axis is along the line of sight from the target to the interceptor. The N axis is in the direction $\bar{\Omega}_{LOS} \times R$, where $\bar{\Omega}_{LOS}$ is the angular velocity vector of the line of sight. The T-axis is normal to the other two and together they form a right-handed coordinate system. $\bar{\Omega}_{LOS}$ lies along the T axis.</p>		<p>The interceptor body axes, X_B, Y_B, Z_B are aligned such that the X_B axis is in the direction of the velocity component along the line of sight, R, and Y_B and Z_B axes are in the directions of the components of velocity normal to the line of sight, $R \dot{\beta} \cos \alpha$ and $R \dot{\alpha}$, respectively. This is accomplished by the attitude commands:</p> $\psi_c = -\beta$ $\theta_c = \alpha$ $\phi_c = 0$	
<p>IAS Paper 61-206, Kidd and Soule (Reference 10)</p> <p>The target and interceptor are viewed in a coordinate system centered on the target and in the plane of the relative position and velocity vectors (\bar{R} and \bar{v}, respectively).</p>	<p>(Note \bar{e}_R and \bar{e}_θ are unit vectors along and normal to the LOS)</p>	<p>Angles β and ϵ have been designated β_L and δ, respectively. The inertial axes X_T, Y_T, Z_T have been used to establish the inertial reference.</p>	

Figure 16b. Summary of Coordinate Systems

As given in Referenced Report		As used in this Report	
Description	Diagram	Description	Diagram
<p>NASA TN D-883, Eggleston and Dunning (Ref. 9) and NASA TN D-1029, Eggleston (Ref. 11)</p> <p>A rectangular coordinate system with its center in the target vehicle. The X and Y axes lie in the plane of the target orbit, while the Z axis is perpendicular to this plane. The X and Y axes rotate about the Z axis at the same angular velocity, $\dot{\theta}_S$, as the angular velocity of the target in its orbit about the earth so that the Y axis always points away from the center of the earth.</p>		<p>A rectangular coordinate system with its origin in the target vehicle. The X_R and Z_R axes lie in the plane of the target's orbit, and the Y_R axis is perpendicular to this plane. The X_R and Z_R axes rotate about the Y_R axis at the same angular velocity, $\dot{\theta}_T = \omega$, as the angular velocity of the target in its orbit about the earth so that the Z_R axis always points away from the center of the earth.</p>	
<p>ARS Paper 62-155-1849, Shapiro (Reference 12)</p> <p>A rectangular coordinate system with origin in the target vehicle. The Z axis denotes the local vertical, the X axis the local horizon and the Y axis completes a right-hand set ($\bar{Y} = \bar{Z} \times \bar{X}$).</p>		<p>The X_R, Y_R, Z_R coordinate system described above for Reference 9 and 11, was also used for this system.</p>	

Figure 16c. Summary of Coordinate Systems

Two techniques are available for determining attitude command angles for orienting the interceptor. The component of velocity normal to the line of sight is then reduced to a near zero threshold by applying a constant thrust, T_{XB_c} .

Technique 1

$$(1) \quad \psi_c = - \left(\beta + \tan^{-1} \frac{R \dot{\alpha} \sin \alpha}{R \dot{\beta} \cos \alpha} - \frac{R \dot{\beta}}{R \dot{\beta}} 90^\circ \right)$$

$$(2) \quad \theta_c = -\tan^{-1} \frac{R \dot{\alpha} \cos \alpha}{\left[(R \dot{\beta} \cos \alpha)^2 + (R \dot{\alpha} \sin \alpha)^2 \right]^{1/2}}$$

Equations (1) and (2) can be used with α' and β' of the X_T' , Y_T' , Z_T' coordinate system (Figure 16) to provide ψ_c' and θ_c' commands. However, this will require additional transformations (see Section IV-B-8) when used in the complete simulation.

In the X_T' , Y_T' , Z_T' coordinate system α' and β' will be small angles. Thus, equations (1) and (2) can be simplified.

$$(1s) \quad \psi_c' \approx \frac{R \dot{\beta}'}{R \dot{\beta}'} 90^\circ$$

$$\theta_c' \approx -\tan^{-1} \frac{R \dot{\alpha}'}{R \dot{\beta}'}$$

Technique 2

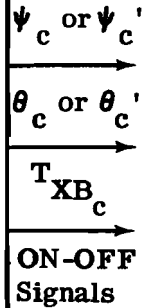
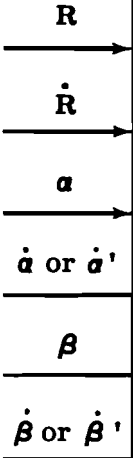
$$(3) \quad \psi_c' = - \left\{ \left(\tan^{-1} \left[\frac{V_N \cot \delta}{R \dot{\beta}'} \right] \right) - \frac{R \dot{\beta}'}{R \dot{\beta}'} 90^\circ \right\}$$

$$(4) \quad \theta_c' = \left\{ \tan^{-1} \left[\frac{R \dot{\alpha}'}{R \dot{\beta}'} \right] - \tan^{-1} \left[\frac{R \dot{\alpha}'}{\left[(R \dot{\beta}')^2 + (V_N \cot \delta)^2 \right]^{1/2}} \right] \right\} - \tan^{-1} \frac{R \dot{\alpha}'}{R \dot{\beta}'}$$

where

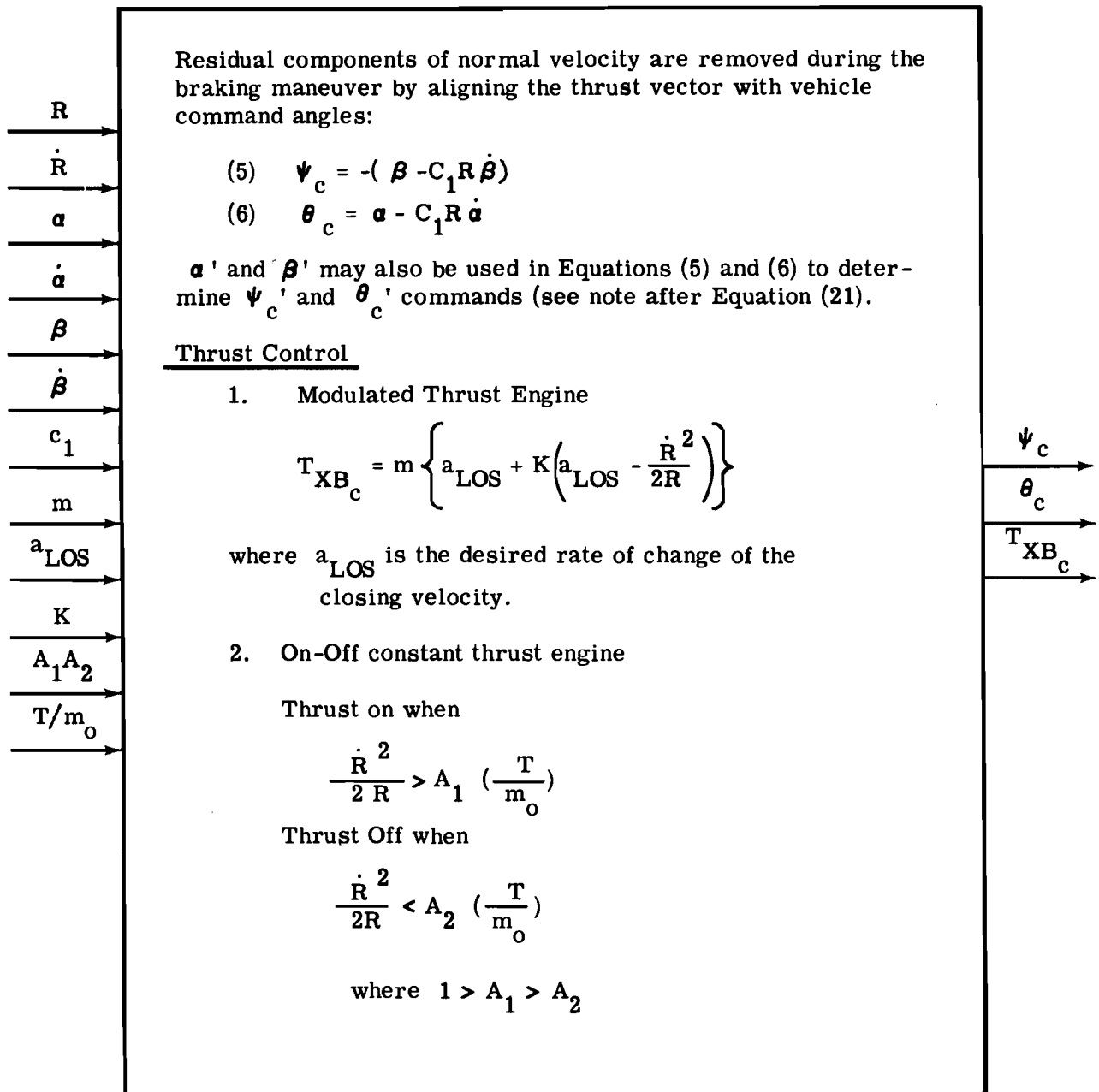
$$\delta = 2 \tan^{-1} \left[\frac{V_a - \dot{R}}{V_N} \right] \quad \text{if } V_a, \text{ the amount of } \Delta V \text{ to be used for rendezvous is specified}$$

$$\text{or } \delta = \tan^{-1} \left\{ \left[\frac{V_N}{\dot{R}} \right] \left[\frac{1}{1 - \frac{(R/\dot{R})}{t_{req}}} \right] \right\} \quad \text{if } t_{req}, \text{ the time to be used for rendezvous is specified.}$$



a. Normal Velocity Control

Figure 17. Guidance Command System of Reference 13



b) Braking Maneuver

Figure 17. Guidance Command System of Reference 13

Two techniques for eliminating the component of velocity normal to the line of sight, thereby establishing a collision course, are presented. In the first technique, attitude command angles are determined to orient the interceptor vehicle normal to the line of sight. Constant thrust is then applied to reduce the normal velocity to a near zero threshold value. Residual components of normal velocity are removed during the subsequent braking maneuver.

The second technique for establishing a collision course is based on energy management considerations. With this technique, either the total velocity increment to be used, or the time allowed for rendezvous, can be specified. In each of these techniques the

system computes the thruster angle, δ , in the plane of the relative motion which will produce the required closing velocity at the same time that the normal velocity component is reduced to a specified small threshold value. The desired thruster angle, δ (the angle between the thrust vector and the line of sight), is then used to determine the required interceptor attitude commands, θ_c and ψ_c .

It is to be noted that in the first technique, the ΔV required is equal to the sum $|V_{N_o}| + |\dot{R}_o|$ (see the dashed line on Figure 11). In the second technique for establishing a collision course, the ΔV required is equal to $|\sqrt{V_{N_o}^2 + \dot{R}_1^2}| + |\dot{R}_2|$ where $\dot{R}_1 + \dot{R}_2 = \dot{R}_o$ and \dot{R}_1 is the amount the range rate is reduced at the same time that V_N is removed.

In addition to the equations shown in Figure 17a, a complete system description requires that certain switching logic be defined. Thus, the system must detect when the angular velocities of the line of sight have been reduced sufficiently to allow transition to the braking phase. To accomplish this, switching logic is used in the system to compare the values of $R\dot{\alpha}$ and $R\dot{\beta}$ with preselected threshold values. If the magnitude of the velocity components is greater than the threshold values, the system switches to the thrusting mode and commands the attitude angles given by Equations (1) and (2) or (3) and (4) of Figure 17a. The yaw and pitch attitude errors are summed and compared with the threshold value in a switching logic which prevents thrusting until the vehicle is in an attitude close to that commanded. When the normal velocity components have been reduced to the threshold level, the system switches to the nonthrusting mode and commands the vehicle attitude angles given by Equations (5) and (6) of Figure 17b. This procedure insures that the vehicle will be properly oriented for the braking phase of the rendezvous maneuver.

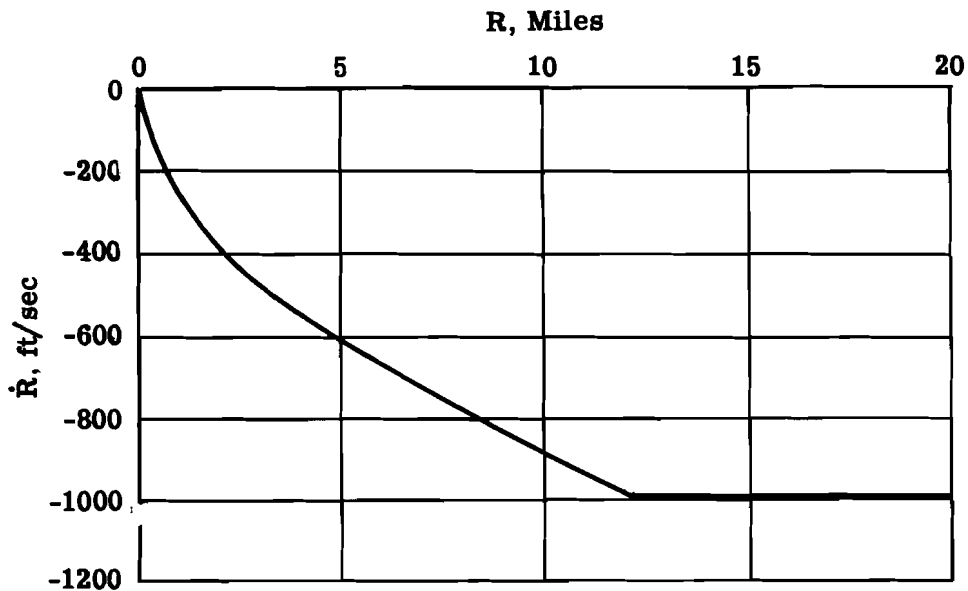
The braking maneuvers consists of either throttling the engine so that the velocity along the line of sight is reduced at a specified rate (a typical example is shown in Figure 18a) or a constant thrust engine is operated in an on-off manner to keep the closing velocity between the limits $\dot{R}^2 = 2RA_1 \frac{T}{m_o}$ and $\dot{R}^2 = 2RA_2 \frac{T}{m_o}$ (Figure 18b). Here, A_1 and A_2 are constants which must be less than one in magnitude, and T/m_o is the thrust-to-weight capability of the engine at the start of the braking maneuver.

In an analog simulation study reported in Reference 13, these systems were found to be effective over a wide range of initial lock-on conditions. The cases studied included the following range of initial conditions.

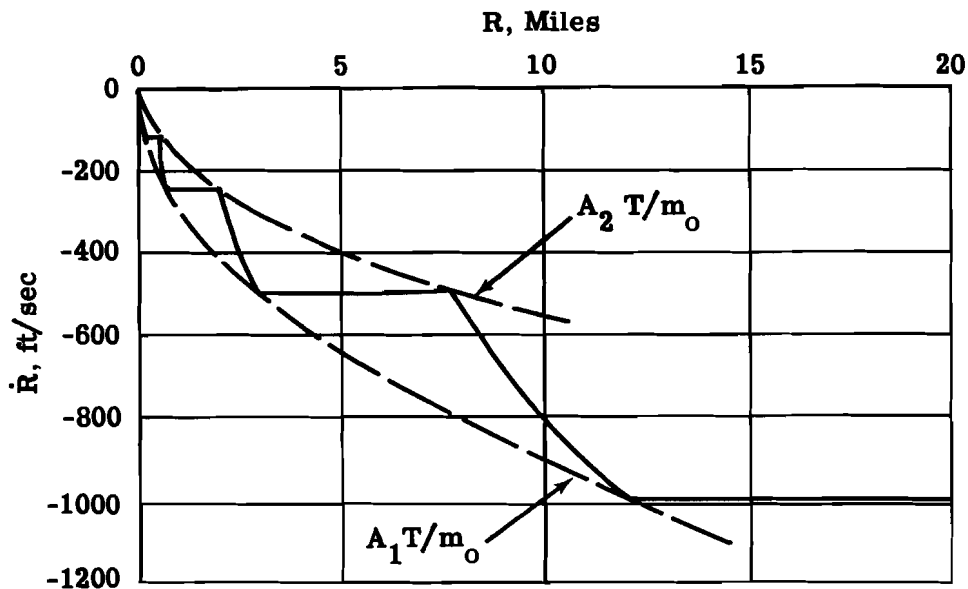
Range	R	to 50 n. mi.
Range rate	\dot{R}	to -1000 ft/sec
Normal velocity components	$\begin{cases} R\dot{\alpha} \\ R\dot{\beta} \end{cases}$	to ± 500 ft/sec
		to ± 500 ft/sec

In these simulation studies, the normal velocity components were initially controlled to 0.2 ft/sec, then the threshold or dead zone was increased to 200 ft/sec to prevent further correction until the braking phase was initiated. Thrust turn-on and turn-off delay times of 200 milliseconds were used. Pitch and yaw rates were limited to about 4 deg/sec.

It was found that the quantity $\dot{R}^2/2R$, used for controlling thrust modulation, became quite sensitive to noise at ranges less than one mile. Therefore, thrust modulation was ceased at that range and thrust became constant for the remainder of the braking maneuver. With this type of control, the final separation distance varied from 100 to 150 feet when range rate had been reduced to -0.5 ft/sec.



a) Modulated Thrust Control



b) ON-OFF Thrust Control

Figure 18. Variation of Range Rate with Range During Braking Maneuver

b. AAS Preprint 62-10, R. L. Stapleford (Reference 14)

This automatic flight path control system takes a minimum complexity approach where reliability and low cost rather than fuel economy are stressed. Figure 19 presents the equations which are employed by this system. It is composed of two main elements; a range controller and a line of sight (LOS) controller. Simplicity is obtained by using nonmovable fixed thrust rockets along each vehicle axis. The attitude system utilizes four transverse rockets to maintain the vehicle longitudinal axis along the line of sight between the interceptor and the target, and limits roll rate to prevent excessive gyroscopic crosscoupling between pitch and yaw. Attitude control system dynamics were not considered in this paper.

The range controller employs a switching criteria to operate, in an on-off manner, a single fixed thrust engine aligned along the interceptor vehicle's longitudinal axis. Thus, the closing velocity is kept within prescribed limits as indicated in Figure 20a. In an example in which it was desired to limit the final range rate to less than 10 ft/sec, the range controller parameters shown in Figure 19 were set at $T_E = 56$ sec and $h_R = 283$. A rocket that provided an acceleration of 5 ft/sec^2 was used.

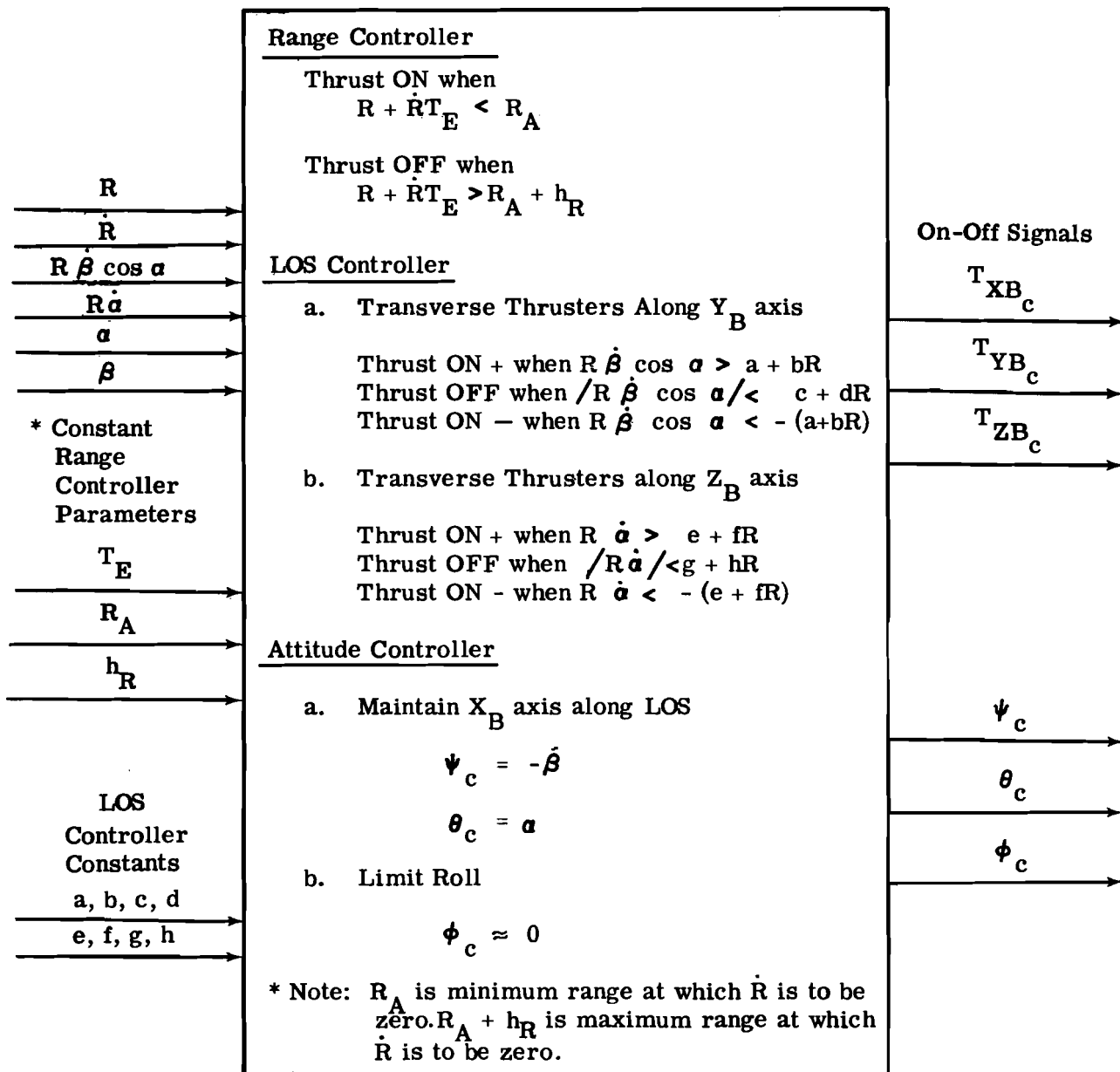


Figure 19. Guidance Command System of Reference 14

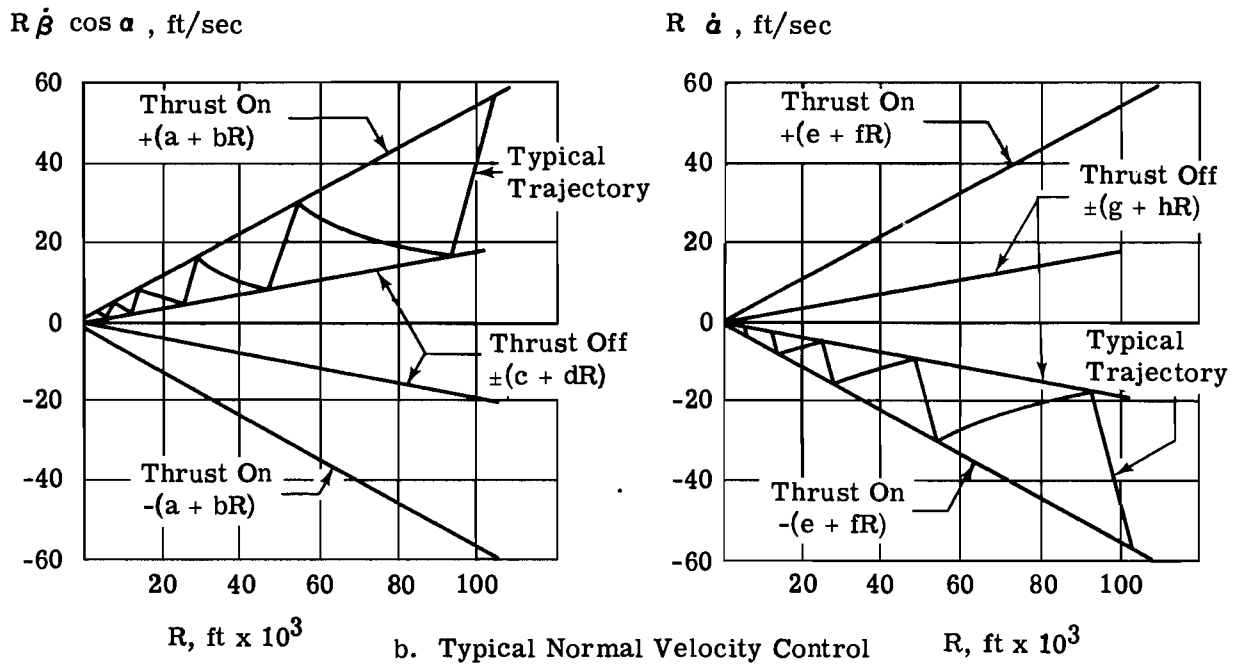
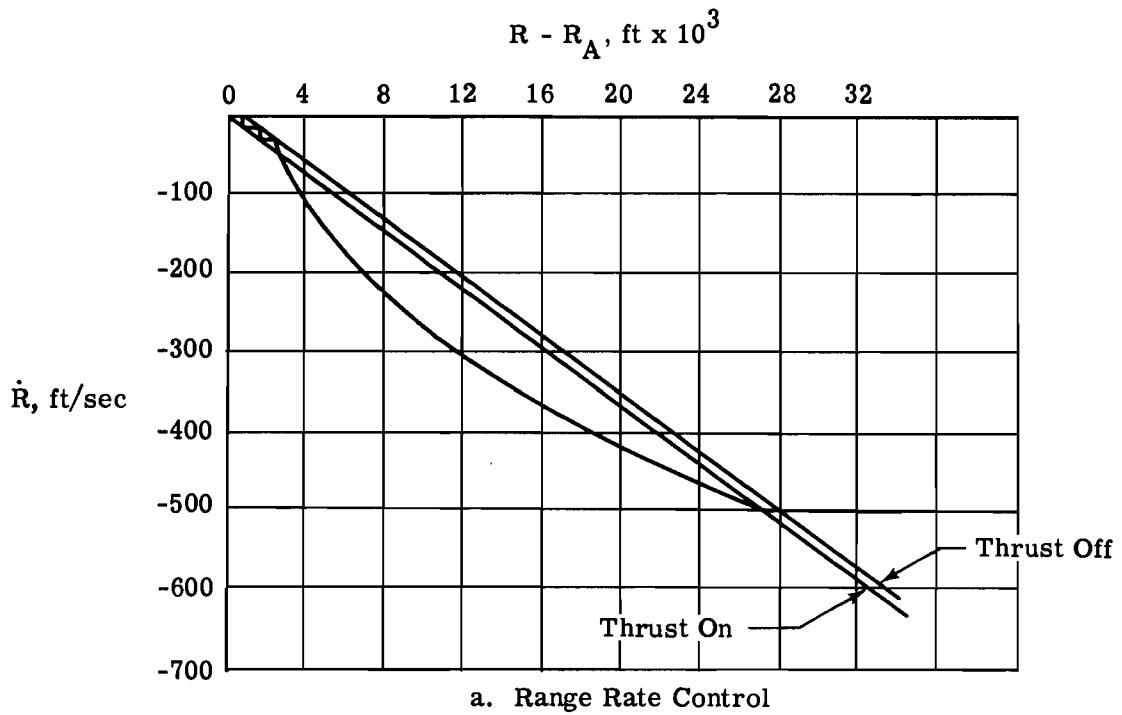


Figure 20. Typical Range Rate and Normal Velocity versus Range

The LOS controller employs a switching criteria to operate the four transverse rockets (the same rockets as used for attitude control) which are mounted normal to the longitudinal axis. The LOS controller has two identical channels, each of which control two diagonally opposite rockets. Figure 20b shows an illustrative example of system operation in controlling the components of velocity normal to the line of sight. A transverse acceleration capability of 2 ft/sec^2 was used in this run.

c. IAS Paper 61-206, Kidd and Soule (Reference 10)

Figure 21 summarizes the control equations employed by this system, which assumes that a single firing of a relatively large fixed thrust rocket will be accomplished either automatically or manually to accelerate the interceptor until the closing velocity is reduced to a small value, of the order of 50 ft/sec . At this point, the authors assume that a smaller thrust engine can then be employed for fine control of range rate versus range. The system determines the time to initiate the initial firing, and the desired variation of vehicle attitude during the firing. The attitude commands result in the components of velocity normal to the line of sight being removed, while the closing velocity and range between the vehicles are being reduced to small values.

The system is fully automated and assumes a thruster of sizeable magnitude ($T/W \leq 2$) along the vehicle longitudinal axis. This type of thrust is necessary for accomplishing rendezvous for initial relative velocities up to 6000 ft/sec , with an acquisition range up to 50 n.mi . These initial conditions are typical of those which will be encountered in a ground launch, direct ascent mission. However, the system is also applicable for rendezvous with initial conditions resulting from orbital transfer.

In actual operation, the system does not have to be as complex as the equations of Figure 21 infer. For example, the computer would determine the angle β_L as the vehicle approaches the thrust initiation point. At initiation of thrust this will be the quantity β_{L_0} . Once β_{L_0} is determined, the scale factor δ_0 / β_{L_0} can be computed from the integral equation of Figure 21, or taken from a design curve as shown in Figure 22. (If the range, R_f , at which the closing velocity is to be zero is specified, only a single curve of β_{L_0} / δ_0 versus τ_f needs to be stored or generated in the computer.) Thus, δ_0 , the initial angle that the thrust is to make with the line of sight, is determined. The variation of the thrust angle, $\delta(t)$, can then be computed from the equations of Figure 21 or taken from stored design curves such as those shown in Figure 23.

d. NASA TN D-747; Brissenden, Burton, Foudriat, Whitten (Reference 15)

This report presents a proportional type system for pilot controlled rendezvous. Figure 24 presents the equations required for the implementation of this system. The pilot's task can be divided into two parts:

- (1) Effect a collision course by driving the rotation rate of the line of sight to zero.
- (2) Brake to drive range and range rate to zero simultaneously.

The interceptor vehicles studied had a single main thruster fixed along the longitudinal axis. The engine had four fixed thrust levels that produced accelerations of 0.1 , 0.2 , 0.3 , and $0.4g$. Intermittent or continuous operation was possible. The attitude control system provided maximum angular acceleration in yaw, pitch and roll of 2.8 , 2.3 , and 4.5 deg/sec^2 , respectively. Proportional and on-off attitude controls were provided.

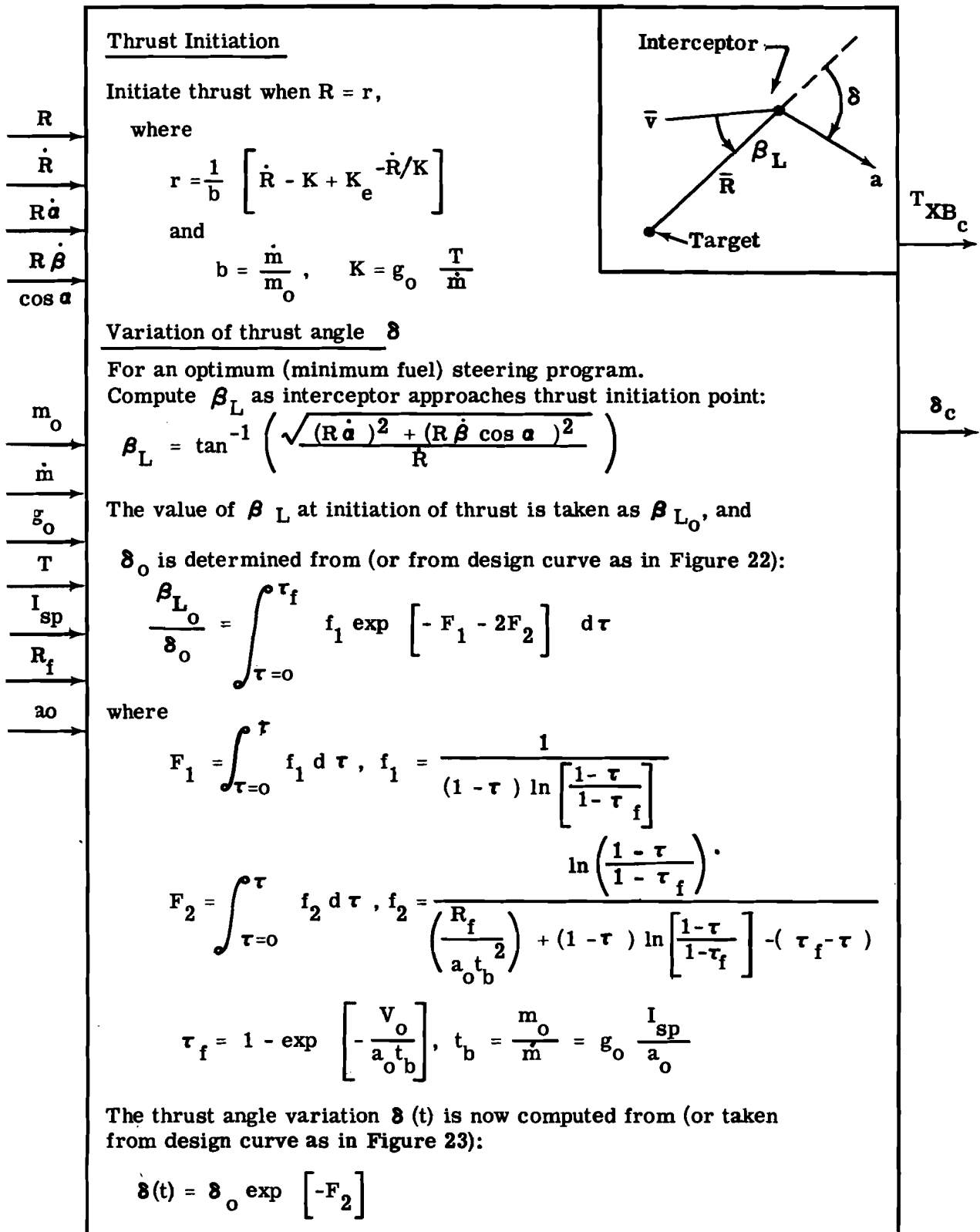


Figure 21. Guidance Command System of Reference 10

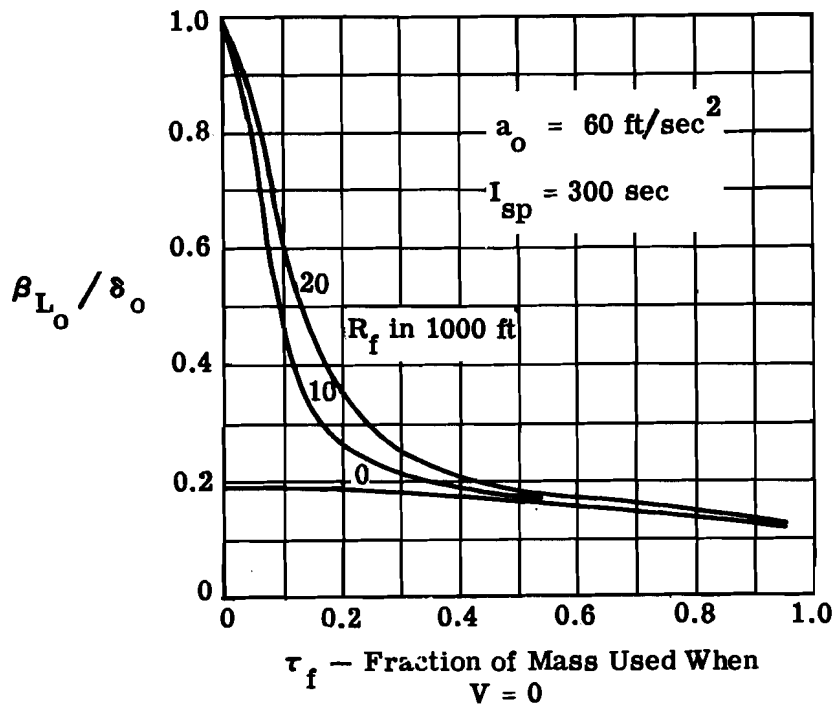


Figure 22. Variation of the Ratio β_{L_0} / δ_0 with τ_f
(Reproduced from Figure 12 of Reference 10)

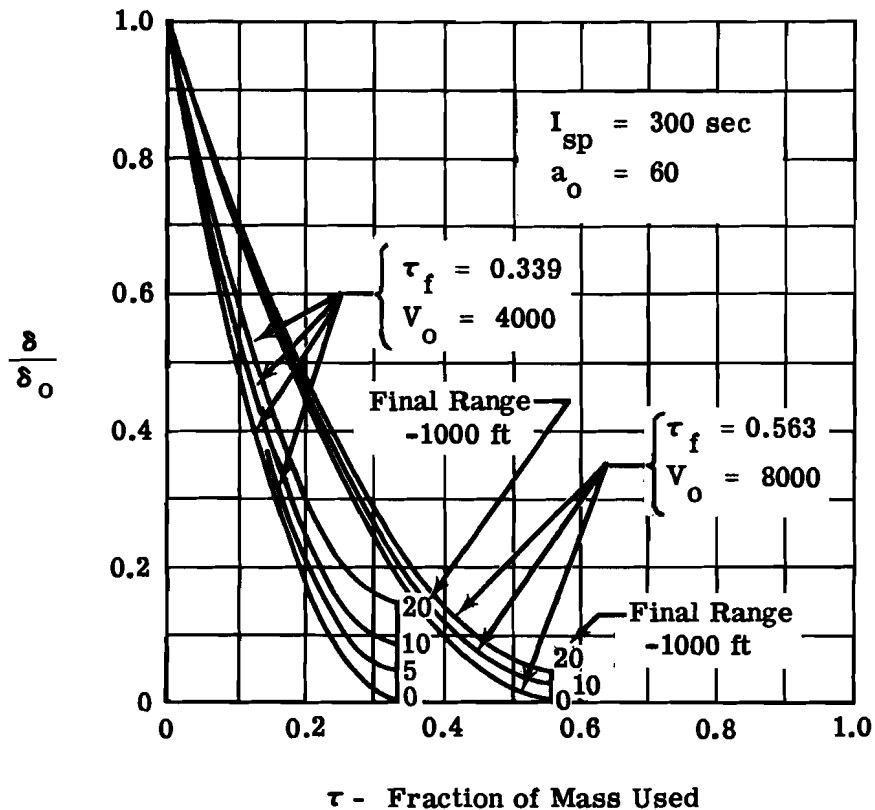


Figure 23. Variation of Thrust Angle with Time
Time for Various Conditions
(Reproduced from Figure 10 of Reference 10)

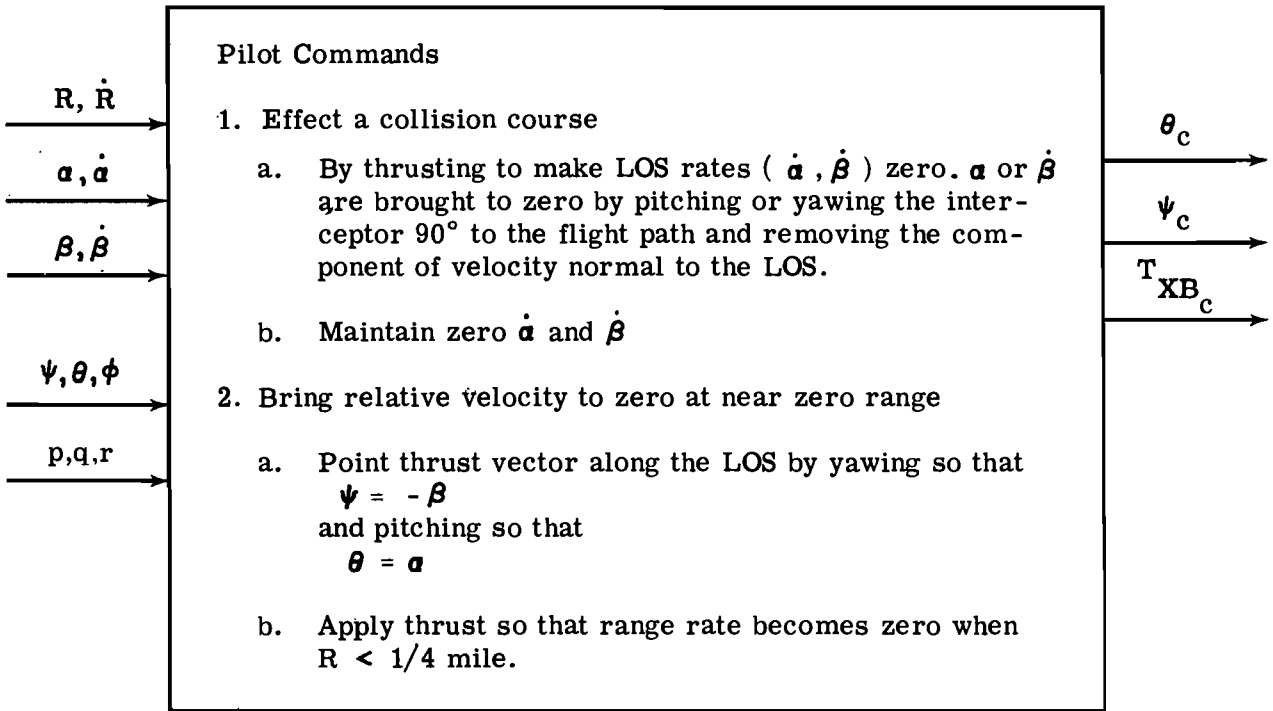


Figure 24. Guidance Command System of Reference 15

For this configuration, the first step of the pilot's task is accomplished by aligning the vehicle normal to the line of sight and thrusting to remove the velocity normal to the line of sight. The second step of the pilot's task is accomplished by aligning the vehicle along the line of sight and thrusting so that the range and range rate are simultaneously driven to zero.

As described in Reference 15, a small analog simulation was set up and the technique evaluated to determine if a pilot could accomplish rendezvous if provided the proper information. The initial conditions assumed for a series of test cases were mild, compared with those of Reference 10:

$$\begin{aligned}
 R_0 &\leq 50 \text{ n. mi.} \\
 \dot{R}_0 &\leq -875 \text{ ft/sec} \\
 R\dot{\beta} &\leq 275 \text{ ft/sec} \\
 R\dot{\alpha} &\leq 250 \text{ ft/sec}
 \end{aligned}$$

The simulation results showed that it was possible to bring about a rendezvous condition adequate to initiate docking.

In order to rendezvous successfully, the following displays were deemed necessary by the pilots:

$$\begin{aligned}
 &R \text{ and } \dot{R} \\
 &\alpha \text{ and } \dot{\beta} \\
 &\theta, \phi, \psi \\
 &p, q, r \\
 &\dot{\alpha} \text{ and } \dot{\beta}
 \end{aligned}$$

The following arrangement of the displayed quantities was found to be best suited to the pilot's needs:

$\psi + \beta$ or β	dial indicator	} the combined displays, $\psi + \beta$ and $\theta - \alpha$ are preferred or $R \dot{\alpha}$ and $R \dot{\beta}$ (oscilloscope)
$\theta - \alpha$ or α	dial indicator	
$\dot{\alpha}$ and $\dot{\beta}$	dial indicator	
ψ	dial indicator	
θ and ϕ	2-axis "8 ball"	
p, q, and r	dial indicator	
\dot{R}	dial indicator	
R	dial indicator	

2. Orbital Mechanics Systems

- a. NASA TN D-883; Eggleston and Dunning, and NASA TN D-1029; Eggleston (References 9 and 11)

The rendezvous system proposed in these two reports utilizes the orbital mechanics technique for rendezvous guidance. Figure 25 presents the equations used to generate guidance commands. These commands are in the form of velocity corrections and are generated by comparing the actual relative velocity vector of the interceptor with the velocity vector which will result in a desired rendezvous trajectory. The required velocity vector is obtained from the solution of a simplified set of equations of motion. The form of equations of motion used (block diagram Figure 25) is the most general set having a known closed form solution. They were first suggested in References 16 and 17 and are generally used in systems of this type (see also Reference 12). Simplifying assumptions include: (1) spherical earth; (2) target in a circular orbit; and (3) a first order gravity field.

Although the type of thrusters and attitude control system are not specified, impulsive thrust has been assumed. Satisfactory operation of this system should also be possible with a continuous, variable thrust at a low level. This system has been demonstrated for initial closing velocities up to 2000 ft/sec, out-of-plane errors of 50 miles, and ranges in excess of 450 miles. The limit of the approximate guidance equations was found to be dependent upon the earth arc angle to rendezvous, $\theta_R = \omega\tau$. For values of $\omega\tau > 90^\circ$, large errors in the computation of velocity corrections result.

Two techniques (options "a" and "b" of Figure 25) for preventing input errors from causing over-corrections in velocity were investigated. The first was a "dead band"; the second consisted of decreasing the ΔV commands by a "factor" before sending them to the rocket systems. Both techniques result in a series of corrective impulses rather than the ideal two firings that would result if the command equations were exact and the data errorless.

- b. ARS Paper 62-155-1849; Shapiro (Reference 12)

Figure 26 shows the equations employed by this system. Like Reference 9, this is a system using the orbital mechanics technique where aiming and thrusting commands are generated from solutions of a simplified set of equations of motion. In this case, however, closed loop operation is obtained by successively increasing the desired time to reach the intercept point. Thus, the second impulse of a two-impulse transfer is changed into continuous or a series of finite thrustings. This system requires the use of a computer to determine the

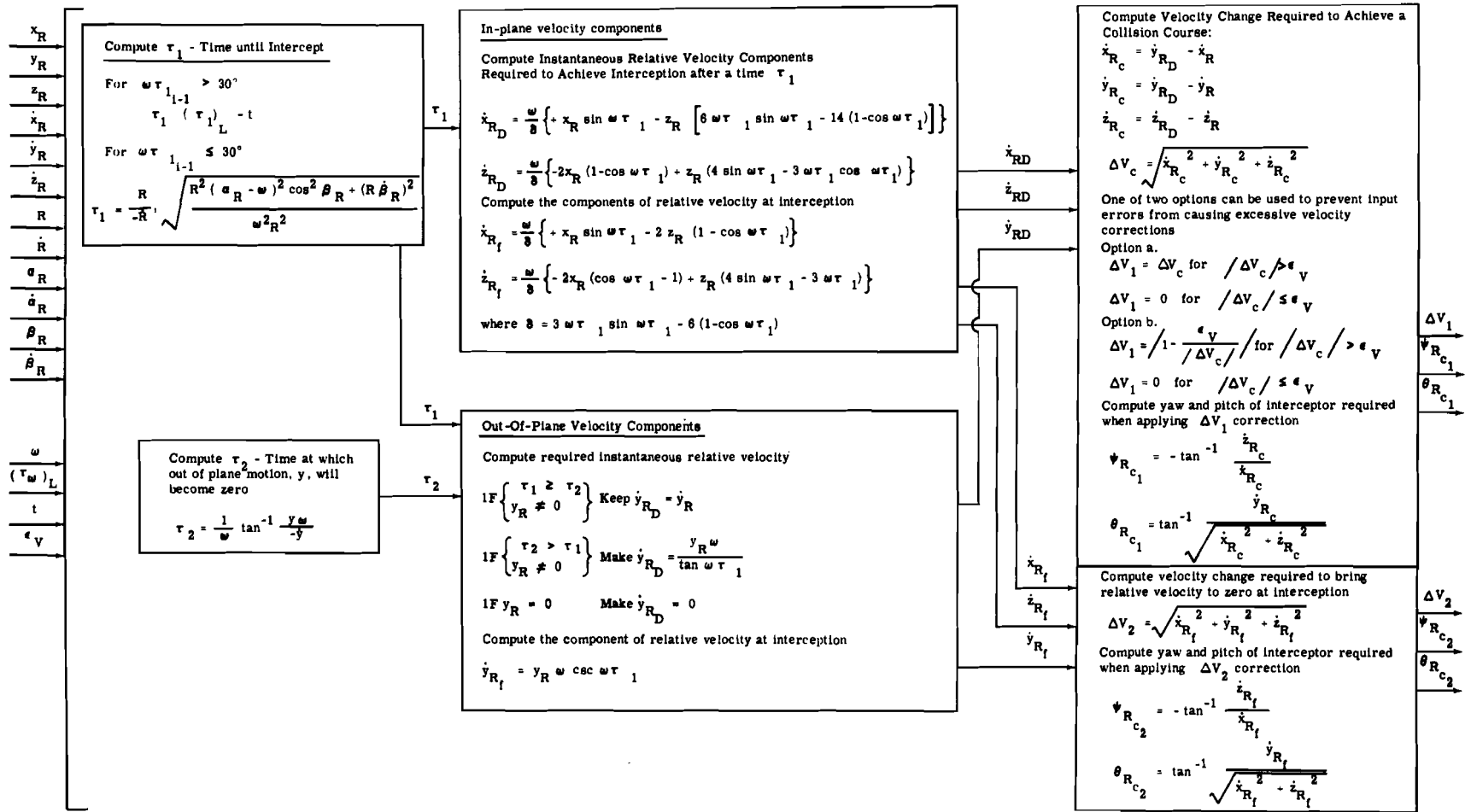


Figure 25. Guidance Command System of References 9 and 11

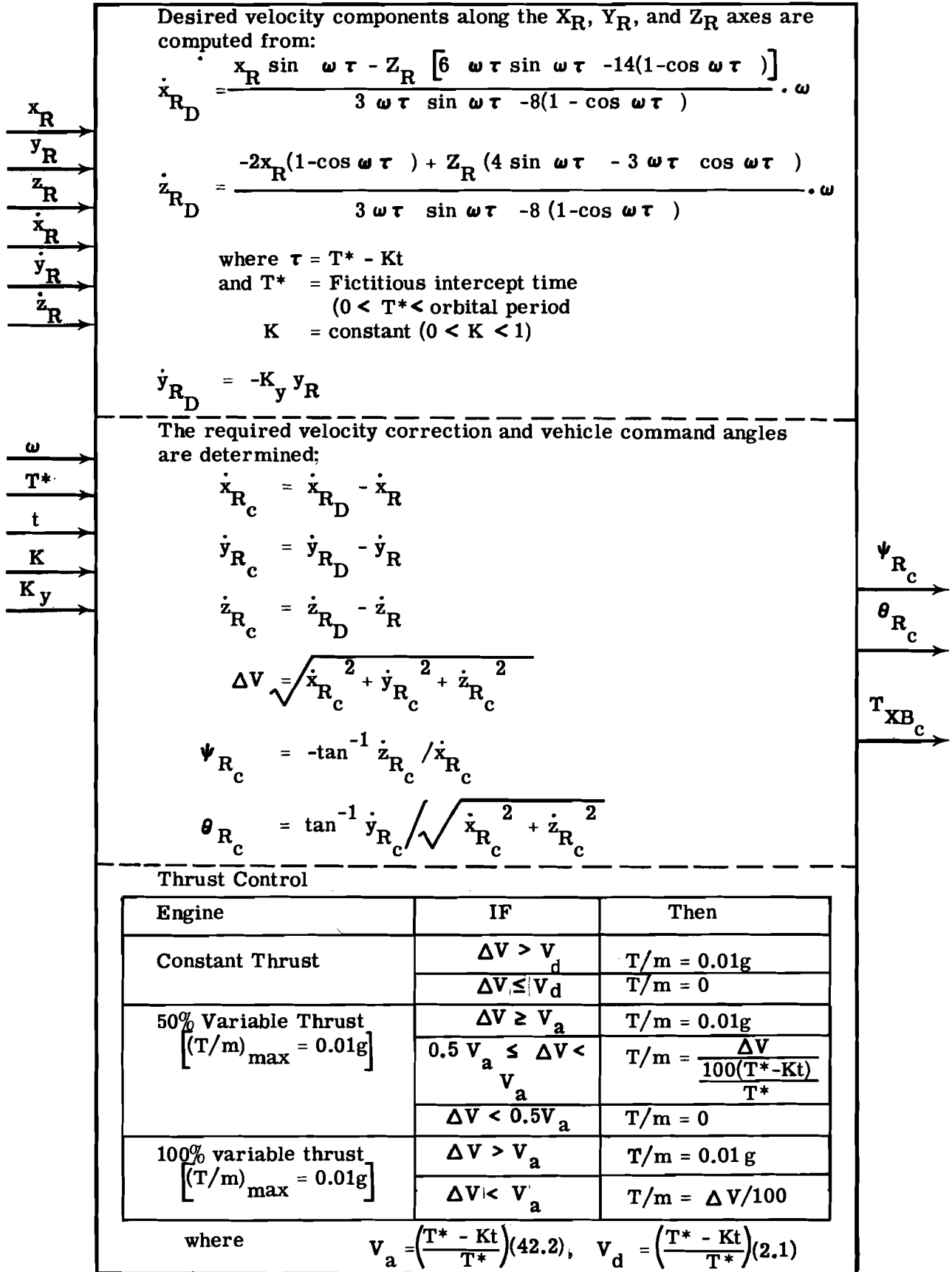


Figure 26. Guidance Command System of Reference 12

desired ΔV 's and direction of thrust application from the relative distances, velocities and target motion inputs.

This system computes the velocity increment, ΔV , that is to be added and the Euler angles, θ_c and ψ_c , at which the vehicle is to be oriented during the firing. A time varying dead band, given by the equations for V_a and V_d , was used to keep engine firings to a reasonable number. The tabulation in Figure 26 indicates how V_a and V_d are used to determine whether or not to fire the engine.

The system can be implemented with multiple start nonthrottleable engines, although the use of variable thrust control was found to give small fuel savings. Attitude rates up to 2 deg/sec were assumed. No limits on the initial conditions were specified. In a test case, initial conditions of range = 50 miles, associated look angle (α) = -30° , and a relative velocity = 217 ft/sec were used. T/W ratios of 0.001 and 0.04 were used. Times required for rendezvous were very long (i.e., of the order of 1 to 2 hours).

3. Docking Phase

The end of the terminal guidance phase and the beginning of the docking phase is difficult to define for many rendezvous systems since there is no sudden change in mode of system operation that marks this transition. With other systems there may be a change from one type of sensor to another or from automatic to visual determination of range, range rate, etc. With still other systems, the docking phase can be defined as starting when attitude alignment of the two vehicles becomes an important consideration. Various authors have considered docking to be initiated at ranges from 100 feet to a mile, with closing velocities of 5 to 100 ft/sec. Thus, if a definition of the start of the docking phase is desired, it will generally be necessary to either make a separate definition for each system or to make an arbitrary definition.

The docking phase ends when the two vehicles become secured to one another so that material or personnel can be transferred or some other mission function can be accomplished. Thus, the final range and relative velocity will be zero. Actually, it may not be necessary to have a simulation which is valid all the way to these zero-zero conditions because the docking mechanisms will be designed to absorb some shock. Closing velocities of the order of 0.1 to 1.0 ft/sec prior to initial contact seems to be typical. Also, for many purposes it may be sufficient to show that relative velocities have been reduced to near zero when the vehicles are as much as 50 to 100 feet from one another.

Literature on control systems for docking is not nearly so extensive as that for the terminal guidance phase. One reason for this is that docking of manned vehicles will probably be done with manual control based on visual observations. The pilot will probably effect docking similar to the system described in Section III-D-1 (Reference 14) which is presented for the terminal guidance operation; i.e., by keeping the vehicle x-axis pointed at the docking mechanism on the target and using body fixed thrusters to brake the vehicle as it approaches its target. Reference 12 is one of the few references in which an automatic docking system is described. This system is summarized at the end of this section.

Many of the docking reports and papers that have been written deal with mechanical details of coupling and latching mechanisms rather than with the vehicle control to be used for docking. Reference 19 is an example of reports of this type. Reference 20 summarizes many docking concepts and coupling devices. It would appear that an accurate simulation of the very last phase of docking, in which physical contact is made, will require physical mockups of these actual docking mechanisms and portions of the vehicles, and either low friction supports for these mockups or a simulated frictionless environment.

Such simulators may employ servo systems to overcome friction, to generate simulated rocket forces and moments, to compensate for the fact that the mockup masses and inertia may not be the same as those of the real vehicles, and to counteract moments which will be produced in the 1g environment if the centers of gravity deviate from pivot points which provide attitude freedom. Although computers could be employed to determine input signals to these servo mechanisms, the determination of computer requirements for such specialized simulators was considered to be beyond the intended scope of the present study. Consequently, details of the docking mechanisms are of immediate concern only because they influence the final ranges, velocities, attitudes, and relative positions for the portion of docking which ends just prior to the establishment of physical contact. From the summary presented in Reference 20, it appears that physical contact may occur with the pilot of the maneuvering vehicle only a few feet from and nearly in a direct line with the axis of a probe type mating mechanism. Such mechanisms will probably require closing velocities of 1 ft/sec or less and angular alignment to within a degree or two. At the other extreme, physical contact can be defined to occur when a harpoon type device finds its mark. This could occur when the vehicles are 50 or more feet from one another. In these cases, relative velocities could be several ft/sec and the only attitude requirement would be that required for a direct view of the target. Thus, attitude tolerances of the order of several degrees are acceptable. Even the latter requirement might be unnecessary if remote sighting devices are provided.

ARS Paper 62-155-1849; Shapiro (Reference 12)

This report presents some modifications to the terminal phase guidance system, described in Section III-D-2, that will permit docking along any predetermined docking axis. Figure 27 presents the equations used by this system. Reference 12 assumed that the target vehicle is oriented to the local vertical and that the two vehicles will initially be within the arbitrarily selected limits. $R < 1/2$ mile and $\dot{R} < 20$ ft/sec.

The energy management system for docking (Figure 27) differs from the energy management system for the terminal phase of rendezvous (Figure 26) in two respects. First, the equations for determining the desired velocity components are simplified to:

$$\begin{aligned}\dot{x}_{R_D} &= -\frac{x_R}{k_x (T' - t)} - z_R \omega \\ \dot{y}_{R_D} &= -\frac{y_R}{k_y (T' - t)} \\ \dot{z}_{R_D} &= -\frac{z_R}{k_z (T' - t)} + x_R \omega\end{aligned}$$

where T' = a predetermined docking time, $\frac{T^*}{k_x} = \frac{T^*}{k_y} = \frac{T^*}{k_z}$

k_x, k_y, k_z = gain constants defining response speed along the X_R, Y_R, Z_R axes, respectively.

Appropriate choice of these gains will drive the interceptor along any desired docking axis.

The second change from the terminal phase energy management is a different thrust on line to comply with docking requirements. Thus,

$$V_a = K_{T'} \left(\frac{T' - t}{T'} \right) + \dot{R}_R$$

where \dot{R}_R = residual velocity (0.1 ft/sec), defined as a servo compensating factor.

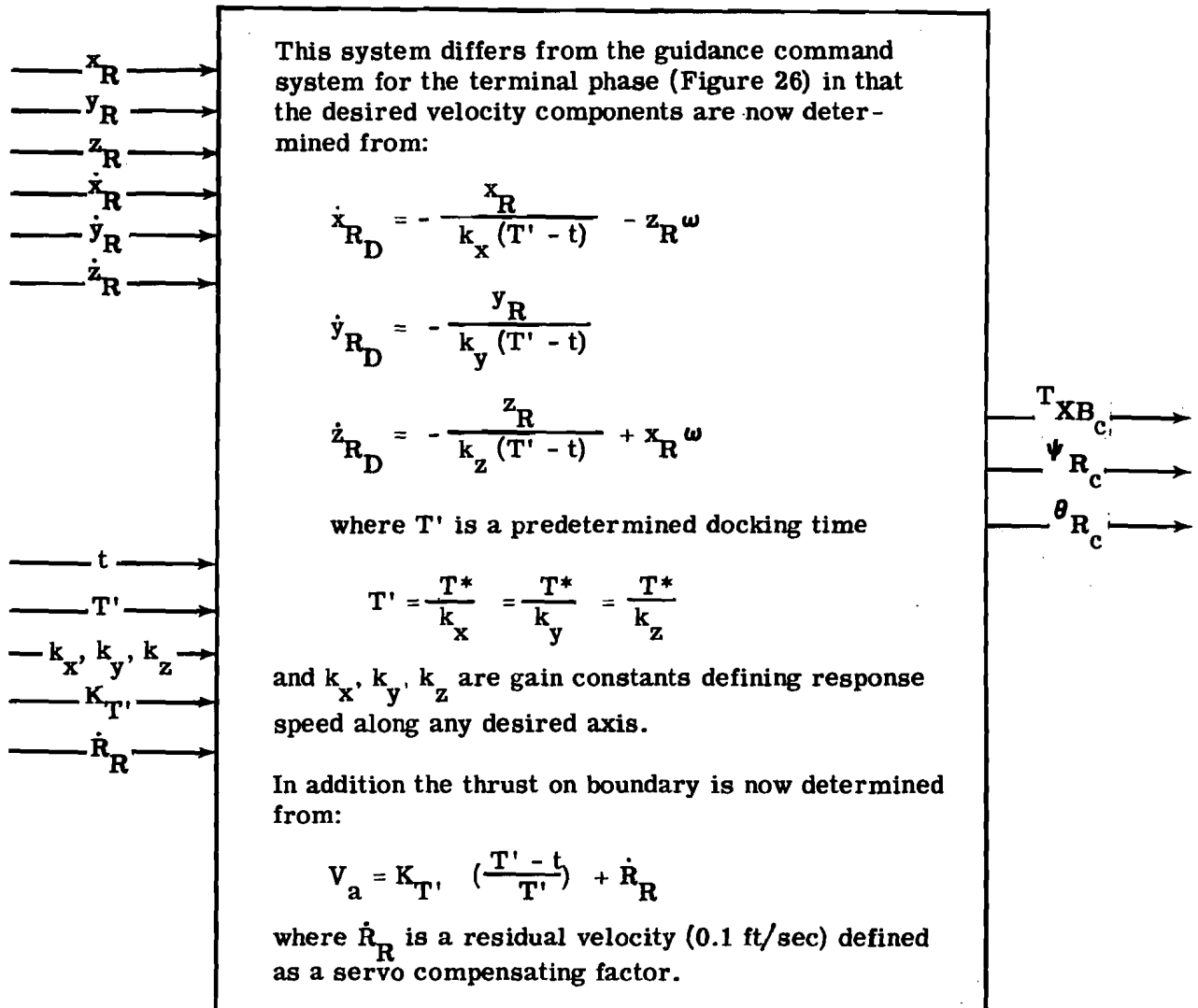


Figure 27. Docking Guidance Command System of Reference 12

IV. SIMULATOR ELEMENTS AND ASSOCIATED EQUATIONS

A. GENERAL

In Section III, rendezvous and docking systems, techniques, and equations that are used to generate ΔV or thrust commands and vehicle attitude commands were described. In a complete rendezvous and docking simulation, illustrated in block diagram form in Figure 28, these rendezvous and docking control equations must be solved and several other major computations must be performed. These include computations to determine the interceptor vehicle's translational and rotational response to commands; its position, attitude, and velocity relative to the target, the earth, and celestial background; and appropriate parameters for recording and actuating displays.

In this section each of the major computations are discussed and a complete representative set of equations are formulated for all elements of the diagram of Figure 28 except the rendezvous and docking system element. Although no particular rendezvous and docking system is specified, transformations are provided for making inputs and outputs available in the desired coordinate system, as required for any of the systems described in Section III. The computations performed within the rendezvous and docking system element will vary with the technique employed and, hence, these computations will be mechanized as a subroutine in a digital simulation. Computations performed in each of the other elements are presented in figures as indicated for each element of Figure 28.

B. DESCRIPTION OF SIMULATOR ELEMENTS

The various elements of the typical system of Figure 28 are described in the following.

1. Vehicle Equations of Motion

Any two of three basic sets of equations can be used to describe the motions of the target and interceptor. These are: "vehicle relative motion equations" describing the motion of the two vehicles with respect to each other; "target vehicle equations" describing the motion of the target vehicle with respect to a reference frame; and "interceptor vehicle equations" describing the motion of the interceptor with respect to the same reference frame. Since there are only two vehicles involved, any two of these sets of differential equations will provide all the needed data. That is, solutions of two of the sets can be used algebraically to obtain the desired quantities of the third set.

Thus, for example, the position of the target vehicle with respect to the earth can be obtained by integrating Keplerian equations which describe a nonmaneuvering vehicle in orbit. Likewise, the position of the interceptor vehicle with respect to the earth can be obtained by integrating interceptor differential equations of motion. (A typical example of these equations is given in Reference 21.) From the solutions of these two sets, all information is available to calculate the position and rates of the interceptor with respect to the target vehicle. In this case, the position of the maneuvering vehicle relative to the target could be determined by performing some relatively simple arithmetic and trigonometric calculations to determine the difference in radii from the center of the earth to the two vehicles, the range angle between them, etc. If the origin were at the earth's center, this would involve subtracting two numbers of the order of magnitude of 24×10^6 feet from each other, to an accuracy of 1 foot, at docking.

$R, \dot{R}, \alpha, \beta, R\dot{\alpha}, R\dot{\beta}, \tau, t$

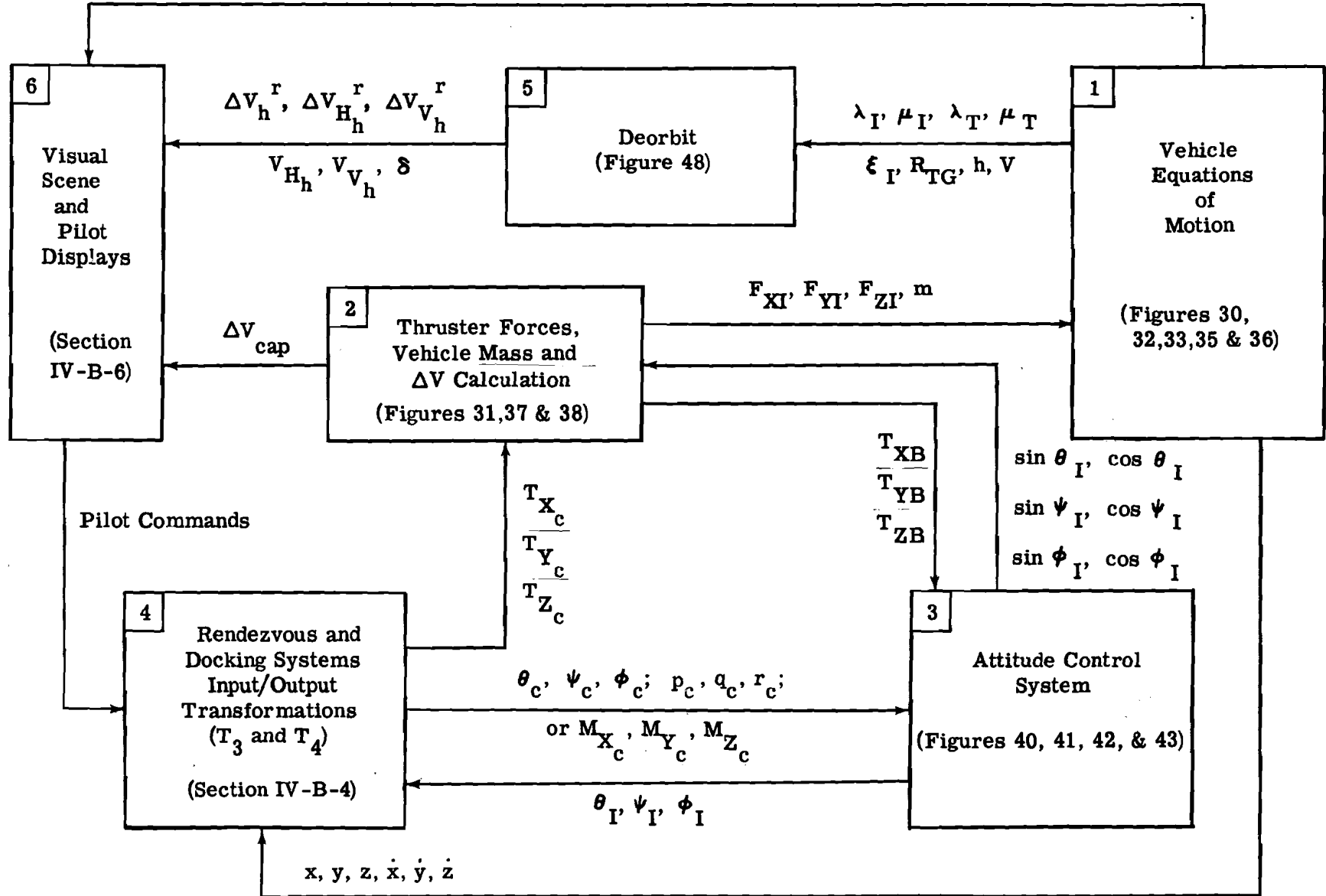


Figure 28. Major Elements of Rendezvous Simulator

To obtain an accuracy of 1 foot would require a computation good to 8 significant figures. This would require a digital computer having a minimum of 25 bits. Although there are computers available that may accomplish the task with this accuracy requirement, a better approach is to use differential equations which determine the relative positions, rates, etc., of the two vehicles. The other required set of equations can then be either the equations of motion of the target vehicle with respect to the earth, or the equations of motion of the interceptor with respect to the earth. Since the target is in a fixed orbit, the equations for target position relative to the earth are simpler.

a. Reference Axis Systems

Two major axis systems are appropriate as references for vehicle attitude angles and position. These are:

- (1) Axes which do not rotate relative to inertial space. For example, a system referenced to the star field defined by using right ascension, elevation, and roll of the body axes as inertial Euler angles.
- (2) Reference axes frames which rotate so that one axis is aligned with the line from either the interceptor or the target to the center of the earth. Although many orientations for the other two reference axes are possible, the most natural system is one which has two of its axes in the orbital plane of the target. With such an axis system, a sequence of rotations ψ_R , θ_R , ϕ_R , from a reference, has the following meaning: ψ_R is the angle in the horizontal plane that the vehicle is yawed out of the orbit plane of the target; θ_R the amount it has pitched from the local horizontal plane; and ϕ_R is the roll angle about vehicle's longitudinal axis.

Some of the rendezvous and docking systems described in Section III use an inertially referenced axis frame, while others use a rotating set. Some use rectangular and others spherical coordinate systems. If the simulation is to be capable of simulating all of these systems it must be able to provide either of the above sets of Euler angles and the rates of change of the angles and to provide displacements and rates in either rectangular or spherical coordinate form.

There are also several possible locations for the origins of the axes systems to be used in the simulator. For example, separate sets of differential equations describing motions of the target and maneuvering vehicle could be referenced to the center of the earth. This choice of an origin has the disadvantage of requiring the differencing of two radii which are very large to obtain the altitude differential between the two vehicles. Although the origin could be placed in the interceptor, this has not been done in any proposed system because the equations describing interceptor motion relative to the target vehicle become much more complicated for out-of-plane interceptor motions. Therefore, the most desirable location of the origin is in the target vehicle.

If the simulator is to be capable of quickly switching from a simulation of one rendezvous and docking system to another, it will be desirable to provide several sets of transformations so this basic simulation (including all elements but the rendezvous and docking equations) can be matched to a number of rendezvous and docking systems that utilize different coordinate systems. It has been assumed that the simulator will be used for simulating many different rendezvous techniques; hence, this flexible approach has been taken in this program.

b. Equations of Interceptor and Target Relative Motion

The desirability of having equations of motion describing the relative position and rate of the interceptor with respect to the target vehicle is described in Section III. Discussions and derivations of relative equations of motion are given extensively in the literature (References 8 through 15). In fact, an extensive table of equations of motion has been set up in Reference 11 and repeated in Reference 15. These tables give a variety of the forms that the equations may have, expressed in inertially fixed axes and rotating axes, in vector form and rectangular coordinates, and in order of simplification: exact, spherical earth, spherical earth with target vehicle in a circular orbit, spherical earth and circular orbit with a first order gravity field, spherical earth with circular orbit, and constant gravity, and finally no gravity. In all cases, the origin of the reference axis system is in the target vehicle.

The equations of motion selected are based on an inertially oriented rectangular system (X_T , Y_T , Z_T) with origin in the target vehicle as shown in Figure 29. These equations (derived in Reference 15) utilize approximations to the relative gravity effects as described in Reference 18. These approximations assume a first order gravity field and neglect small effects such as solar radiation, moon gravity and such. They are summarized in Figure 30.

It is assumed that the thrusters in the interceptor may apply thrust along the \pm directions of each of the vehicle body axes. The vehicle relative motion equations require thrusts along the inertial (X_I , Y_I , Z_I) axes. Thus, since the interceptor is oriented with respect to the inertial axes through the inertial Euler angles ψ_I , θ_I and ϕ_I ,

$$\begin{Bmatrix} F_{XI} \\ F_{YI} \\ F_{ZI} \end{Bmatrix} = \begin{bmatrix} \psi_I' \\ \theta_I' \\ \phi_I' \end{bmatrix} \begin{bmatrix} \theta_I' \\ \phi_I' \end{bmatrix} \begin{Bmatrix} T_{XB} \\ T_{YB} \\ T_{ZB} \end{Bmatrix}$$

where $[\phi_I']$, $[\theta_I']$, $[\psi_I']$ are transposed matrices representing rotations about X_B , Y_B , and Z_B axes, respectively. The equations which result when these matrices are multiplied out are given in Figure 31.

c. Target Equations of Motion

The target is a nonmaneuverable vehicle and may be in either a circular or an elliptical orbit. Kepler equations expressing target position and velocity with respect to the inertial axes centered in the earth are:

$$\ddot{\sigma}_T - \sigma_T \omega^2 + \frac{g_e R_E^2}{\sigma_T^2} = 0$$

and $\omega = C_S / \sigma_T^2$

where σ_T = radius of target from center of the earth

C_S = constant of angular momentum per unit mass of the station

R_E = radius of the earth

g_e = acceleration of gravity at the surface of the earth

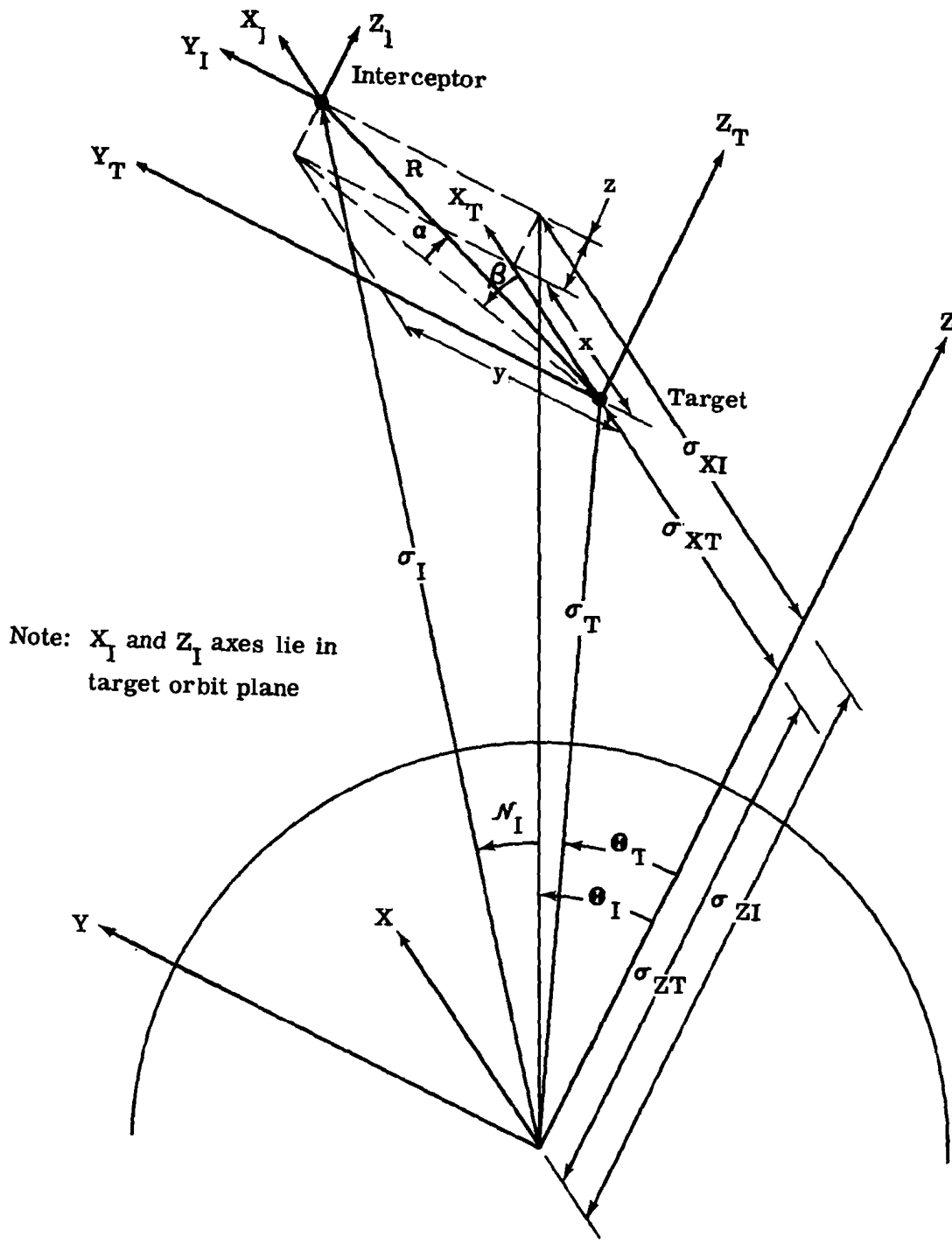


Figure 29. Sketch Illustrating Relative Motion Parameters

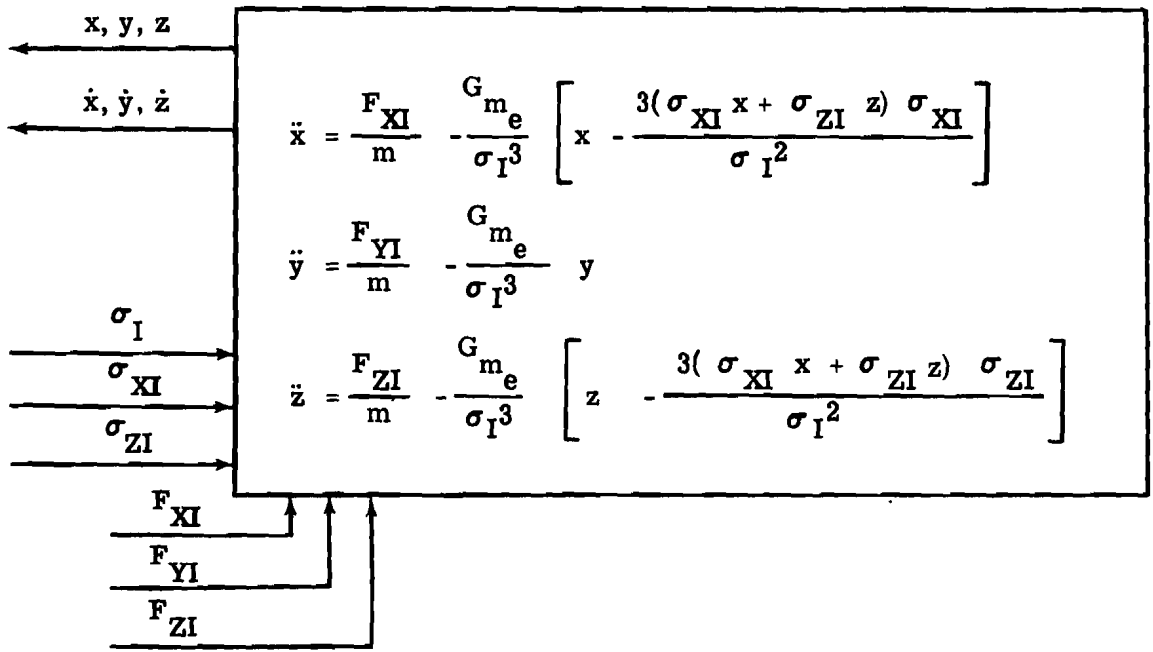


Figure 30. Equations of Interceptor and Target Relative Motion

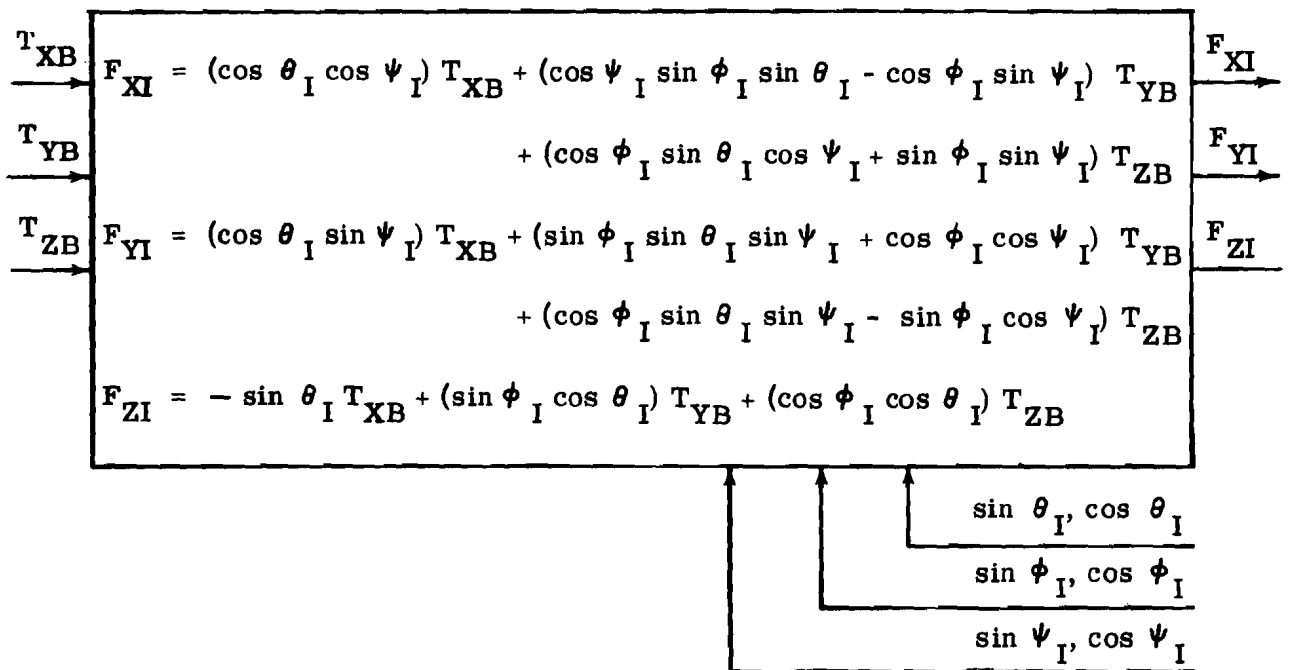


Figure 31. Transformation from Body Axes to Inertial Axes

It is necessary to calculate σ_I , σ_{XI} , and σ_{ZI} for the relative equations of Figure 30. Also, for purposes of locating the interceptor with respect to the latitude and longitude of the earth, it is necessary to calculate Θ_I and \mathcal{N}_I (see Figure 29). Thus, referring to Figure 29, the following calculations are defined:

$$\Theta_T = \int_0^t \omega dt + \Theta_{T_0}$$

where
$$\omega = \dot{\Theta}_T = \frac{C_S}{\sigma_T^2}$$

Θ_{T_0} = the value of Θ_T when $t = 0$.

Also, from Figure 29, the following expressions can be obtained:

$$\sigma_{XT} = \sigma_T \sin \Theta_T$$

$$\sigma_{ZT} = \sigma_T \cos \Theta_T$$

$$\sigma_{XI} = \sigma_{XT} + x$$

$$\sigma_{ZI} = \sigma_{ZT} + z$$

$$\sigma_I = \sqrt{\sigma_{XI}^2 + \sigma_{ZI}^2 + y^2}$$

If a maximum separation of the order of 50 miles between vehicles is allowed, $y \ll \sigma_{XI}$ or σ_{ZI} :

then,
$$\sigma_I \approx \sqrt{\sigma_{XI}^2 + \sigma_{ZI}^2}$$

Even if this maximum separation distance is in the σ_I direction, it is probably valid to set $\sigma_I = \sigma_T$, because 50 miles is small relative to the earth's radius.

From trigonometry:

$$\Theta_I = \sin^{-1} \frac{\sigma_{XI}}{\sqrt{\sigma_{XI}^2 + \sigma_{ZI}^2}}$$

and
$$\mathcal{N}_I = \sin^{-1} \frac{y}{\sigma_I}$$

Figure 32 diagrams the target equations, showing 3 input variables, 6 output variables, and 5 input constants.

d. Interceptor Flight Conditions Relative to the Earth

The position of the interceptor relative to the target and its velocity relative to the target vehicle are obtained from equations in Figure 30. The expressions given in

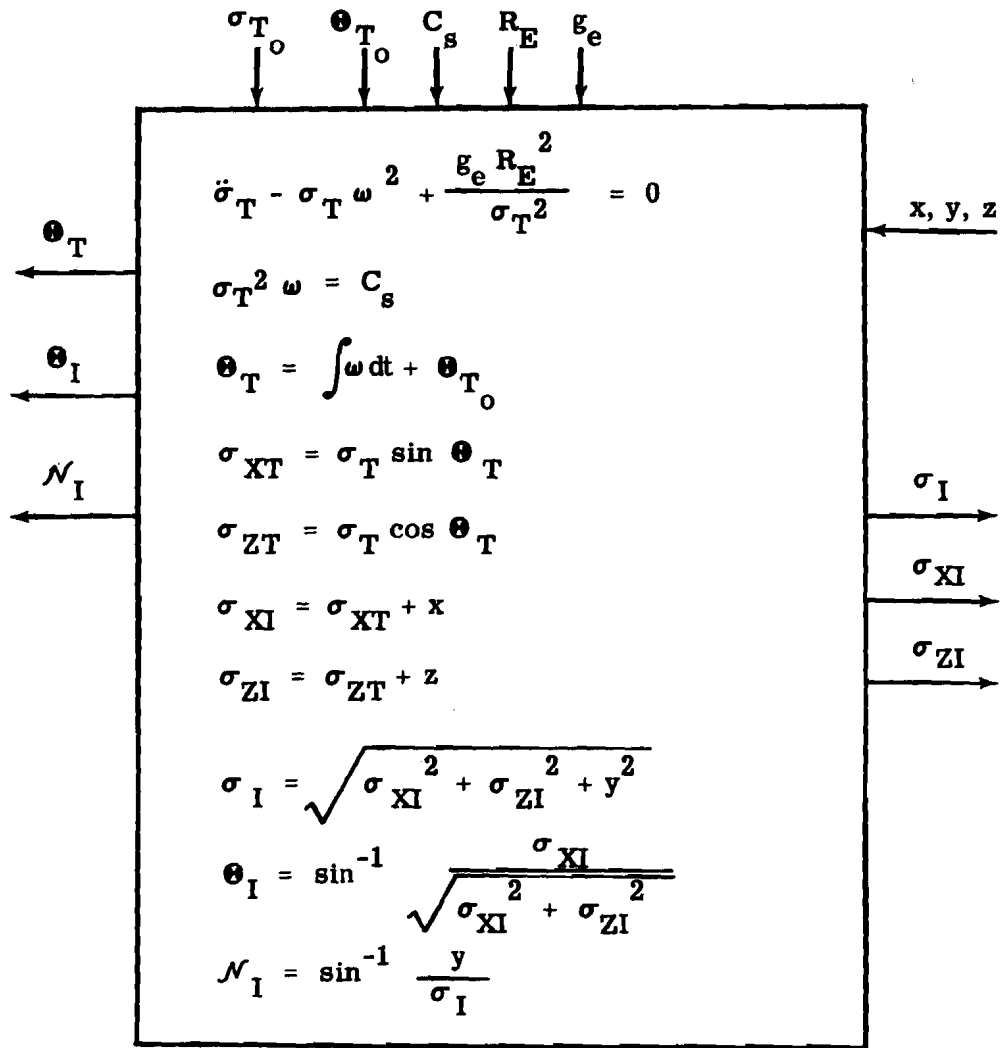


Figure 32. Target Equations of Motion

Figure 33 define the position of the interceptor relative to the earth. These expressions are sufficient to determine the interceptor's colatitude, longitude, flight path angle with respect to local East, and altitude. A diagram of the parameters involved in the calculations is given in Figure 34.

Although these expressions are suitable for use in the simulator, the fact that the interceptor vehicle will be within a few hundred miles, and generally within 50 miles, of the target vehicle indicates that a flat earth assumption in immediate area of the two vehicles may be used to simplify or eliminate some of the expressions used to determine the interceptor's latitude and longitude. When this approximation is worked into the equations, the resulting expressions will appear as those given in Figure 35. As can be seen, these new expressions reduce the required computations by about one-half.

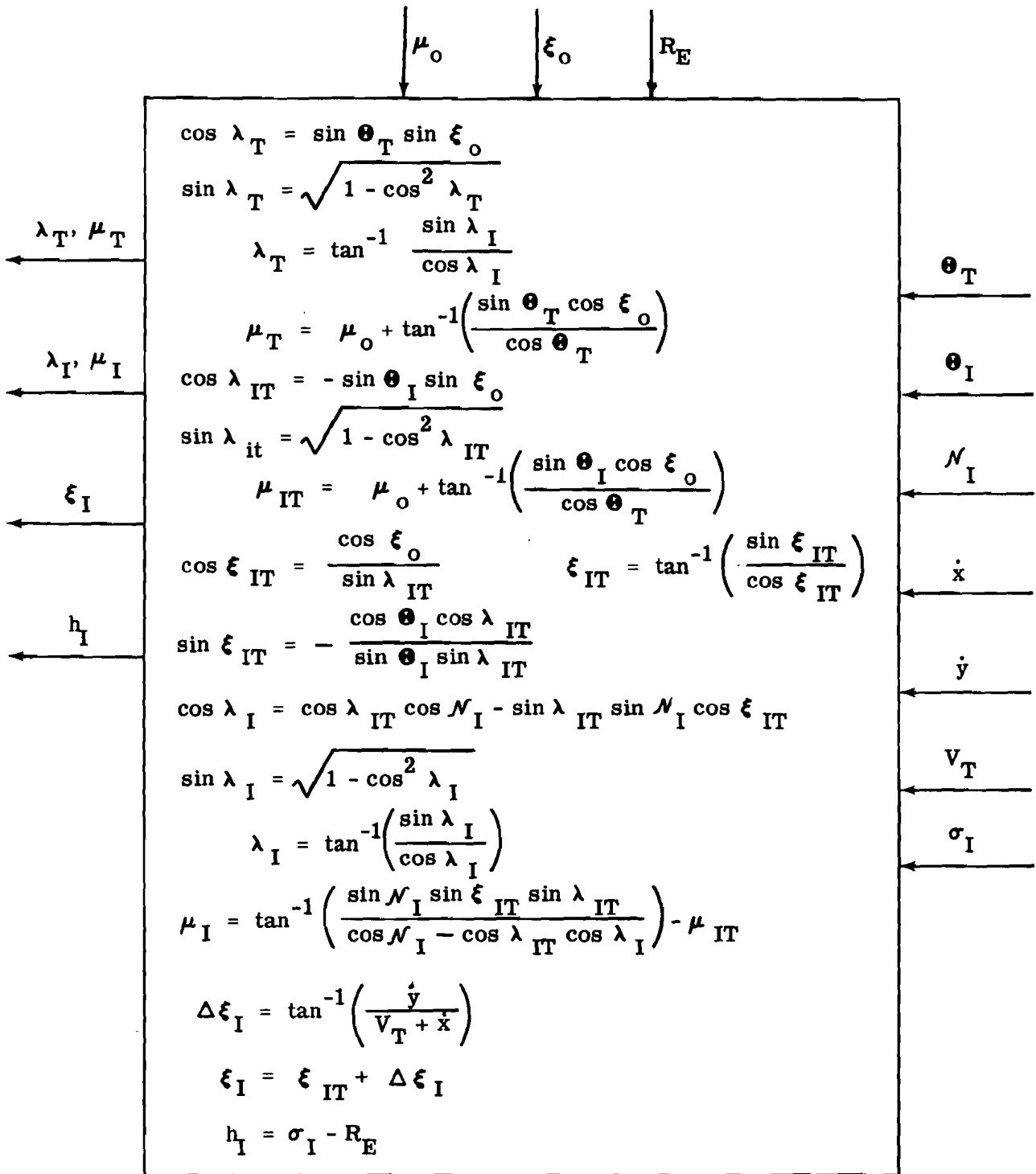


Figure 33. Interceptor Flight Conditions Relative to the Earth

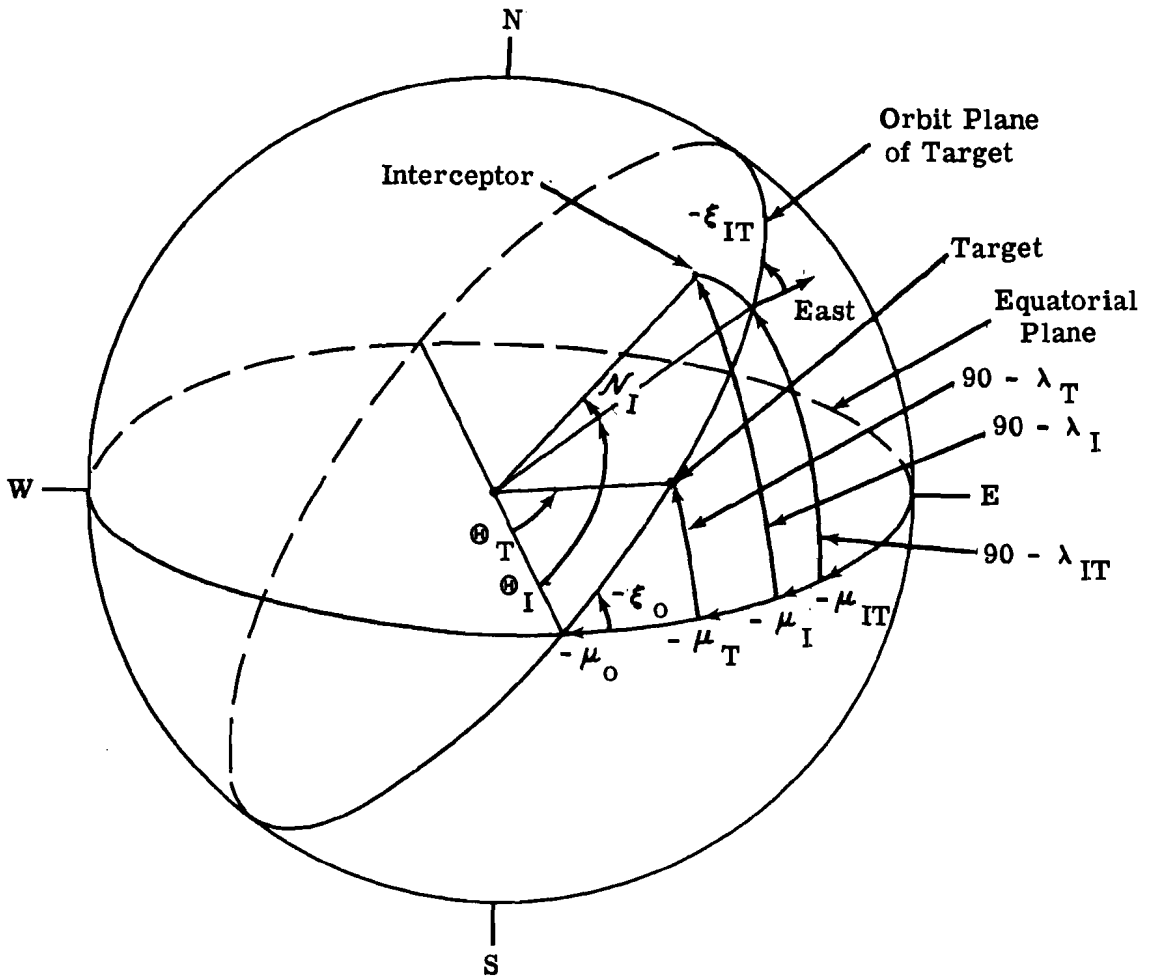


Figure 34. Sketch Illustrating Earth Reference Parameters

The expressions for determining the velocity of the interceptor with respect to a rotating earth are presented in Figure 36. The inertial velocity of the interceptor in the target's local horizontal plane is

$$V_{I_{XY}} = \sqrt{[\dot{x}_R + \sigma_T \omega]^2 + \dot{y}^2}$$

where

\dot{x}_R is the component of the interceptor's velocity relative to the target which lies in the target's orbital plane in the target's local horizontal plane.

$\sigma_T \omega$ is the horizontal component of the target's inertial velocity.

\dot{y}_R is component of the interceptor's velocity relative to the target that is normal to the target's orbital plane in the target's local horizontal plane.

The vertical velocity of the interceptor is

$$\dot{h} = (\dot{z}_R + \dot{\sigma}_T)$$

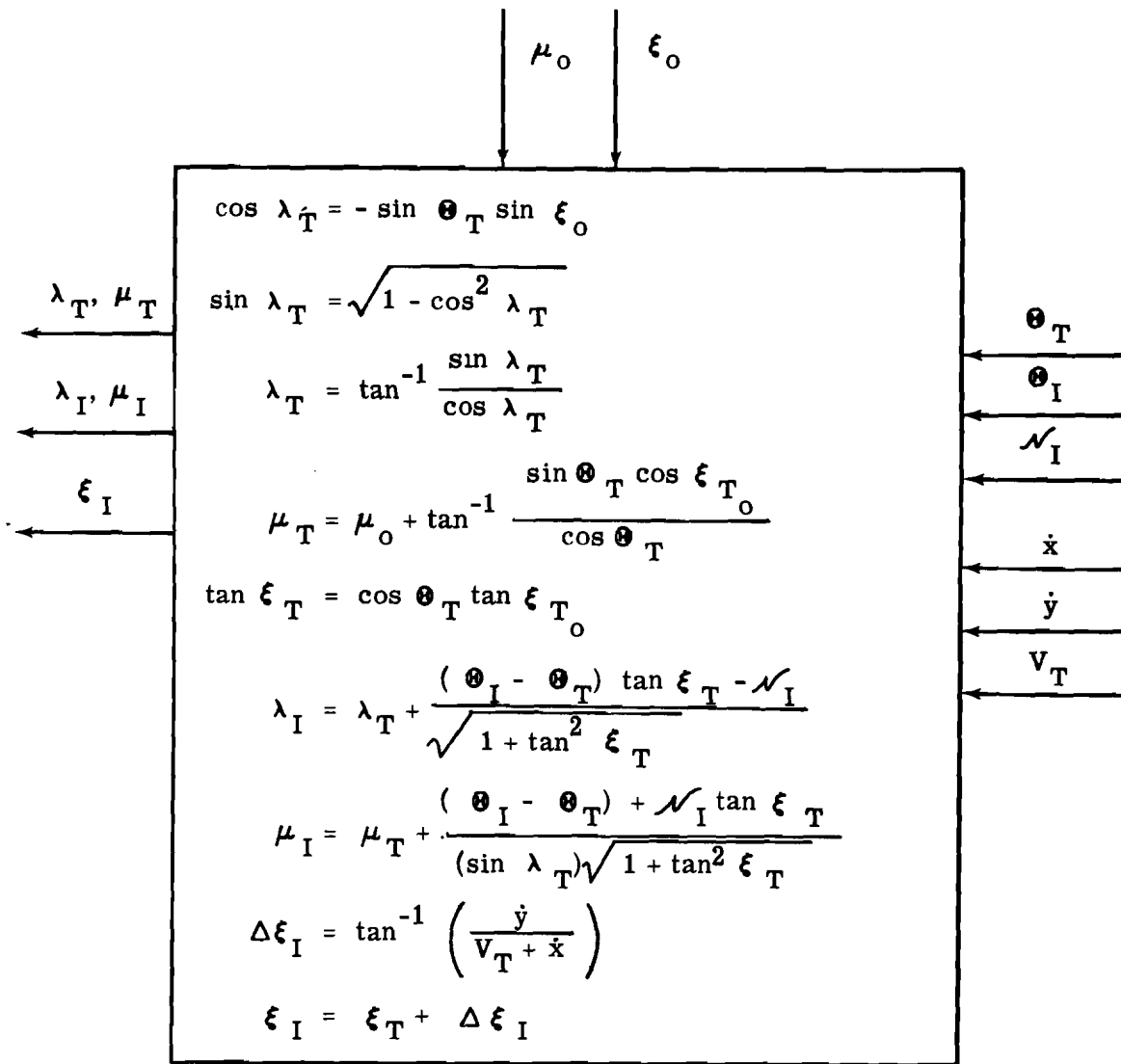


Figure 35. Simplified Interceptor Flight Conditions

where \dot{z}_R is the component of the interceptor's velocity relative to the target along the target's local vertical.

The \dot{x}_R , \dot{y}_R , \dot{z}_R components of velocity can be obtained from inertial \dot{x} , \dot{y} , \dot{z} components of the interceptor's velocity relative to the target by the transformation T_{3B} described in Section IV-B-8.

The component of inertial velocity of the interceptor in the target's local horizontal plane along east is $V_{I_{XY}} \cos \xi_I$, Thus, its easterly velocity relative to the earth is;

$$V_{I_{XY}} \cos \xi_I - \sigma_T \Omega \sin \lambda_I$$

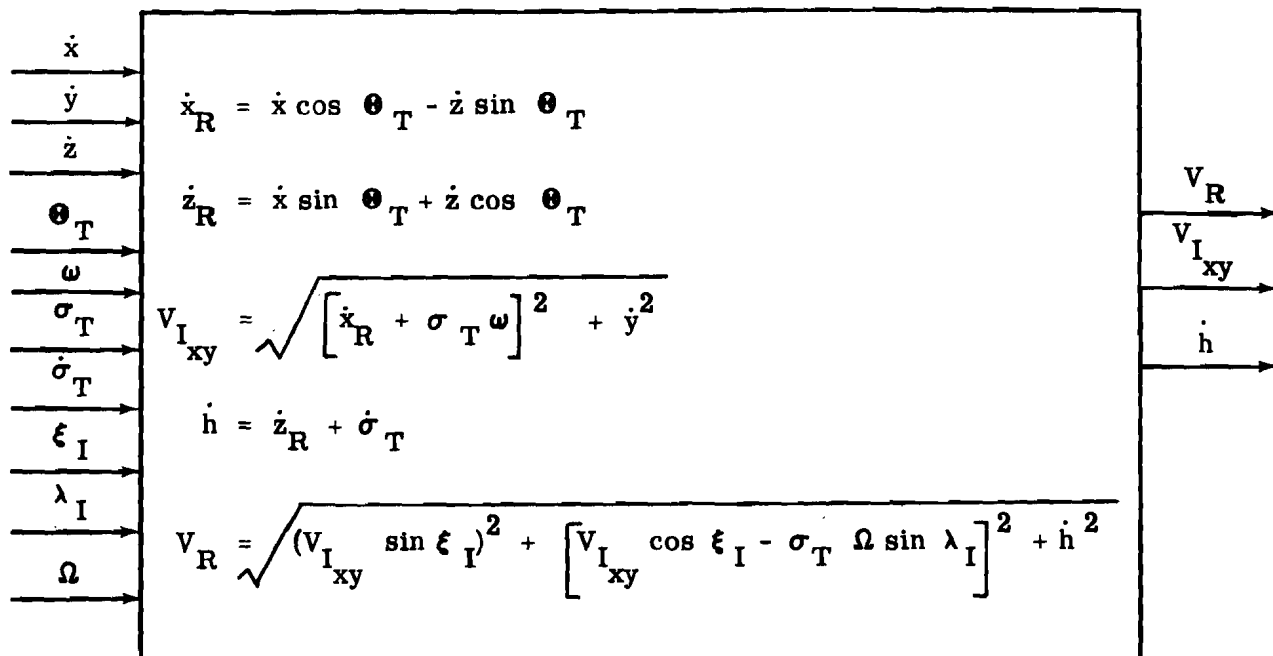


Figure 36. Velocity of the Interceptor Relative to the Earth

Where the latter term is the inertial velocity of a point on the earth under the interceptor due to earth rotation. The component of $V_{I_{XY}}$ to the north is $V_{I_{XY}} \sin \xi_I$, and the interceptor's radial velocity is \dot{h} . Thus, the velocity of the interceptor relative to the rotating earth is

$$V_R = \sqrt{(V_{I_{XY}} \sin \xi_I)^2 + [V_{I_{XY}} \cos \xi_I - \sigma_T \Omega \sin \lambda_I]^2 + \dot{h}^2}$$

2. Thruster Forces, Vehicle Mass and ΔV Calculations

a. Interceptor Rockets for Maneuvering

As discussed in Section II, the interceptor may have one or several rocket engines for maneuvering. These may have one or more fixed thrust levels or they may be throttleable. To cover the more general case, it is assumed for simulation purposes that the interceptor will have rocket thrusters for translational control located in both directions in each body axis. Along the body longitudinal axis there may be two separate thrusters; one of large thrust for braking operations and one of small thrust for docking operations.

In simulations, two engines which produce thrusts in opposite directions can be represented as a single engine with plus and minus thrust capability. Thus, a maximum of three engine firing signals (one for each body axis) will be required.

Usually, in a simulator designed for training purposes, lags (thrust rise and decay times) of the rocket engines can be neglected. However, since these rockets are often operated in automatic control loops during rendezvous and docking, a transfer function

$T = \left(\frac{K}{\tau s + 1} \right) T_c$ has been included. For small docking engines, the time constant τ will be of the order of a few milliseconds; and for very large rendezvous engines probably less than a tenth of a second.

If the engine is a simple on-off type, K in the transfer function for thrust will be the value of the thrust and the thrust command will be a suitable discrete signal. If the engine is throttleable, the upper and lower thrust levels can be provided by inserting a limiting function in series with the above transfer function as shown in the accompanying sketch.

In this case, T_c can be an actual desired thrust and K can be set equal to unity; or K can be maximum thrust as before with T_c scaled accordingly.

Figure 37 shows inputs and outputs required for the simulation of rocket engines for maneuvering. The thrust versus thrust command function shown can be used to represent fixed thrust or variable thrust engines. If more than one engine is provided for maneuvering, it will generally be necessary to provide a separate representation for each engine. However, if each engine has only one fixed thrust level, and if the engine time constants are negligible, the transfer function for engine simulation becomes unity and the actual thrusts can be set equal to the commanded values.

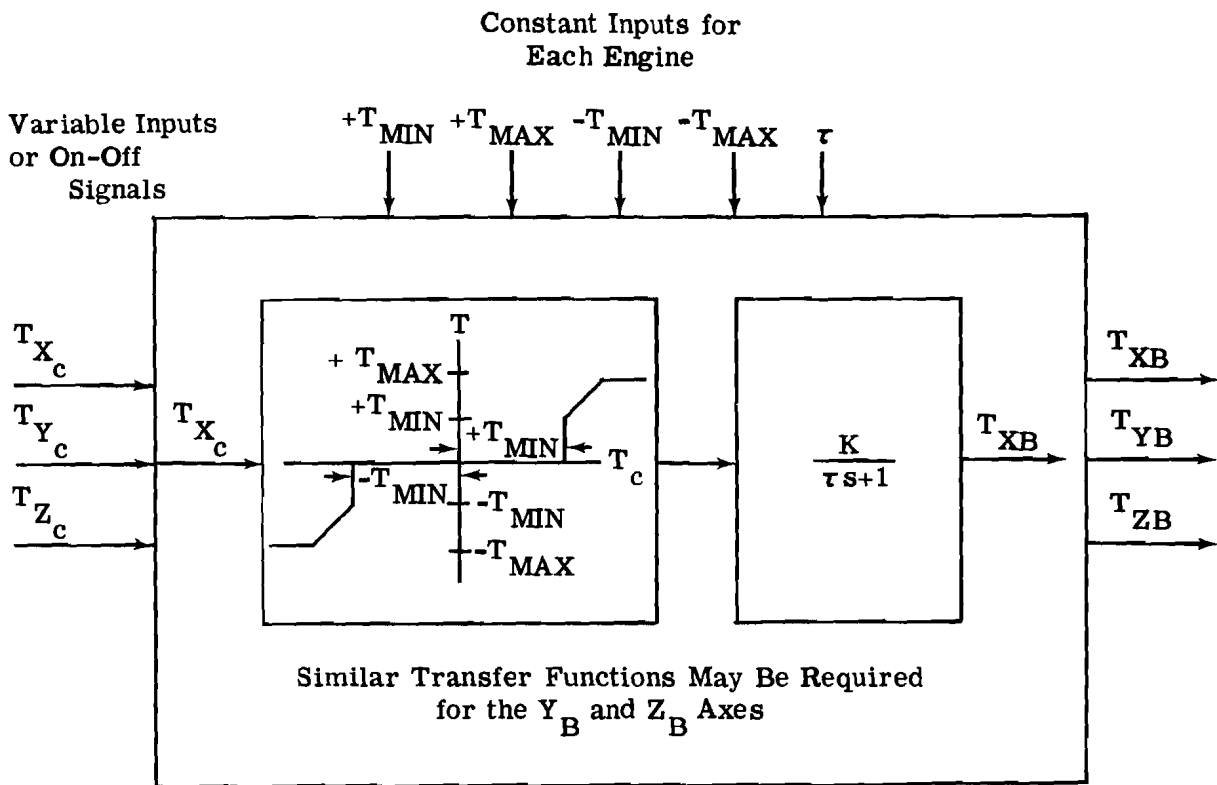
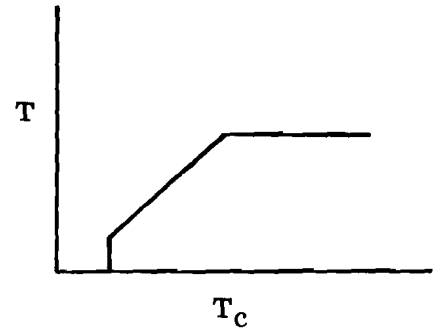


Figure 37. Interceptor Rockets for Maneuvering

b. Computation of the Instantaneous Vehicle Mass and ΔV

As the interceptor applies thrust, propellants are consumed and the total mass of the vehicle is reduced. For a variable thruster, the rate of propellant consumption is very nearly proportional to the thrust generated, thus $\dot{W}_{VX} = \frac{T_{VXB}}{I_{sp}}$. Knowing \dot{W}_{VX} , the amount

of propellant consumed is the integral of \dot{W}_{VX} with respect to the burning time; i.e., mass loss due to t_b seconds burning of the variable thruster is

$$\int_0^{t_b} \frac{\dot{W}_{VX}}{g_0} dt_b$$

For the engines of fixed thrust, the propellant rate, \dot{W}_{F_i} , is constant. Thus, the propellant consumed is \dot{W}_{F_i} times the total time the i thruster has burned. The final expression for total propellant consumed, assuming three fixed \pm thrusters, one aligned along each of the vehicle body axes, X_B , Y_B , and Z_B , and one variable thruster along X_B is:

$$\frac{1}{g_0} \left[\dot{W}_{FXB} t_{b1} + \dot{W}_{FYB} t_{b2} + \dot{W}_{FZB} t_{b3} \right] + \int_0^{t_b} \frac{T_{VXB}}{g_0 I_{sp}} dt_b$$

Firing the reaction control jets creates moments M_{XB} , M_{YB} , and M_{ZB} about the vehicle body axes. The forces in the body axes directions due to these moments can be computed from

$$\begin{aligned} (F_X)_M &= \frac{M_{XB}}{d_x} \\ (F_Y)_M &= \frac{M_{YB}}{d_y} \\ (F_Z)_M &= \frac{M_{ZB}}{d_z} \end{aligned}$$

where d_x , d_y , d_z are moment arms along the X_B , Y_B , Z_B axes, respectively.

The amount of fuel used in attitude control can be expressed as

$$\Delta W_{fuel} = \int_0^t \frac{(F_{total})_M}{I_{sp}} dt$$

where $(F_{total})_M = (F_X)_M + (F_Y)_M + (F_Z)_M$

The amount of fuel consumed by thrusting plus the amount of fuel used in attitude control represents the total amount by which the mass has been diminished. Subtracting this amount from the initial total mass of the vehicle, m_0 , gives m , the instantaneous mass of the vehicle.

The amount of ΔV remaining if the remaining useable propellants were consumed by firing one of the engines (with a specific impulse, I_{sp}) is given as $\Delta V_{cap} = -g_0 I_{sp} \ln \frac{m_{empty}}{m}$

where m_{empty} is the present mass of the vehicle minus the mass of the useable propellants remaining.

It may be desirable to determine the ΔV equivalent of the propellant expended. This can be done by using m in place of m_{empty} and the initial mass, m_0 , in place of m , in this equation.

Figure 38 summarizes the vehicle mass and ΔV equations, with a listing of the constants and variables needed as inputs and the outputs obtained by performing the indicated calculations.

3. Interceptor Attitude Control System

a. Interceptor Attitude Dynamics

The equations of motion for interceptor body axis rates are standard in form and may be found in most dynamics books.

$$\dot{p} = \frac{M_{X_{\text{total}}}}{I_x} - \frac{I_z - I_y}{I_x} qr$$

$$\dot{q} = \frac{M_{Y_{\text{total}}}}{I_y} - \frac{I_x - I_z}{I_y} pr$$

$$\dot{r} = \frac{M_{Z_{\text{total}}}}{I_z} - \frac{I_y - I_x}{I_z} pq$$

where: p, q, r are rates of rotation about the X_B, Y_B, Z_B interceptor body axes (see Figure 39). $M_{X_{\text{total}}}, M_{Y_{\text{total}}},$ and $M_{Z_{\text{total}}}$ are the total moments being applied around these axes and I_x, I_y, I_z are the moments of inertia of the interceptor about these body axes.

From these equations and Euler angles in the sequence ψ, θ, ϕ , the Euler angle rates may be obtained from the equations:

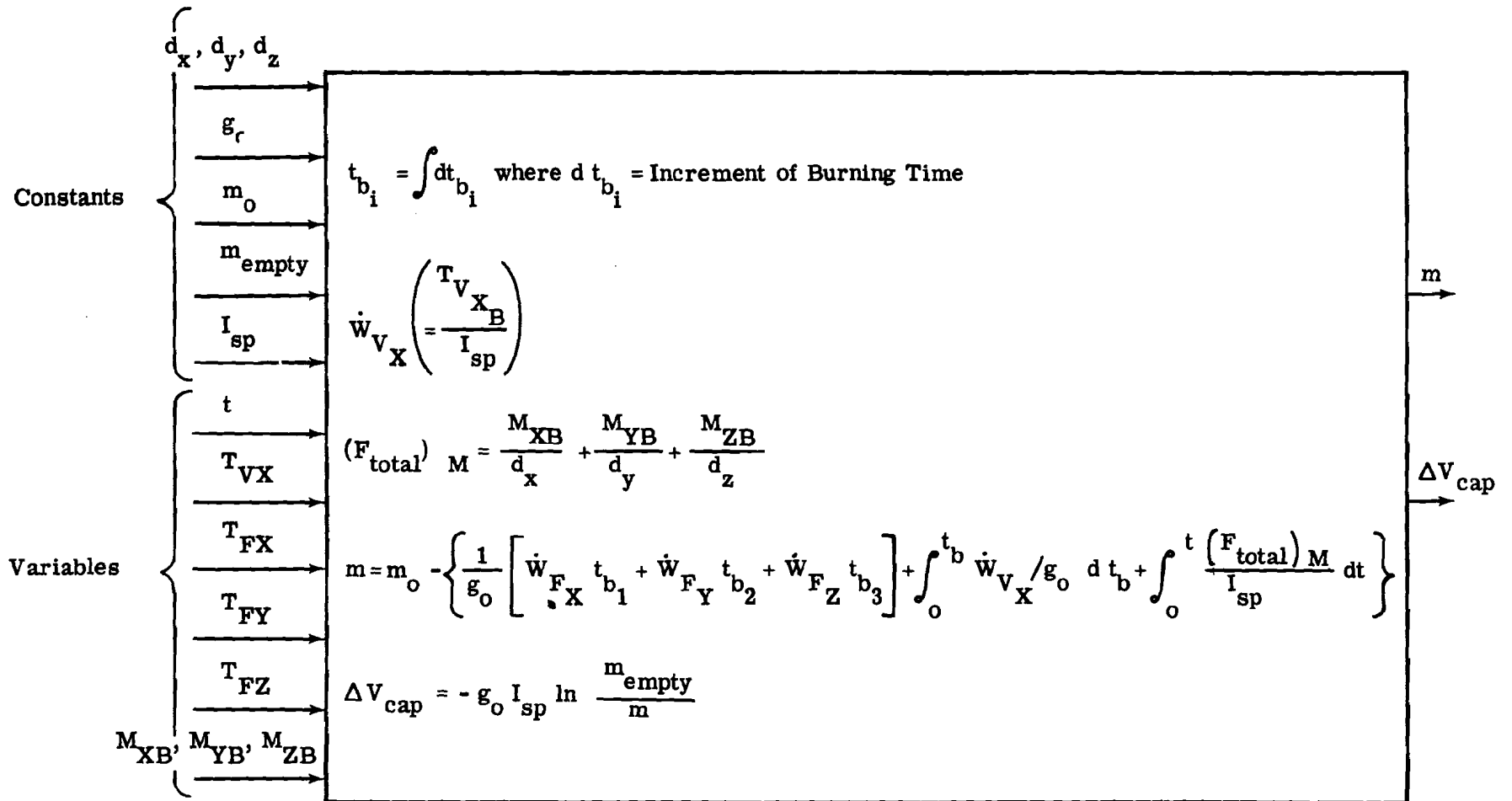
$$\dot{\phi}_I = p + \dot{\psi}_I \sin \theta_I$$

$$\dot{\theta}_I = p \cos \phi_I - r \sin \phi_I$$

$$\dot{\psi}_I = \frac{q \sin \phi_I + r \cos \phi_I}{\cos \theta_I}$$

The equations representing the interceptor attitude dynamics are summarized, together with inputs and outputs, in Figure 40.

For study purposes, the conventional order of rotation $\psi, \theta,$ and ϕ has been selected. However, when it comes to an actual case of applying these equations in a simulation with a visual display of a specific design, the Euler order must be compatible with the hardware items which are to use the Euler angles or rates as inputs. An example of this is given in Reference 23, where a planetarium was designed to produce a view of a star field

Figure 38. Vehicle Mass and ΔV Equations

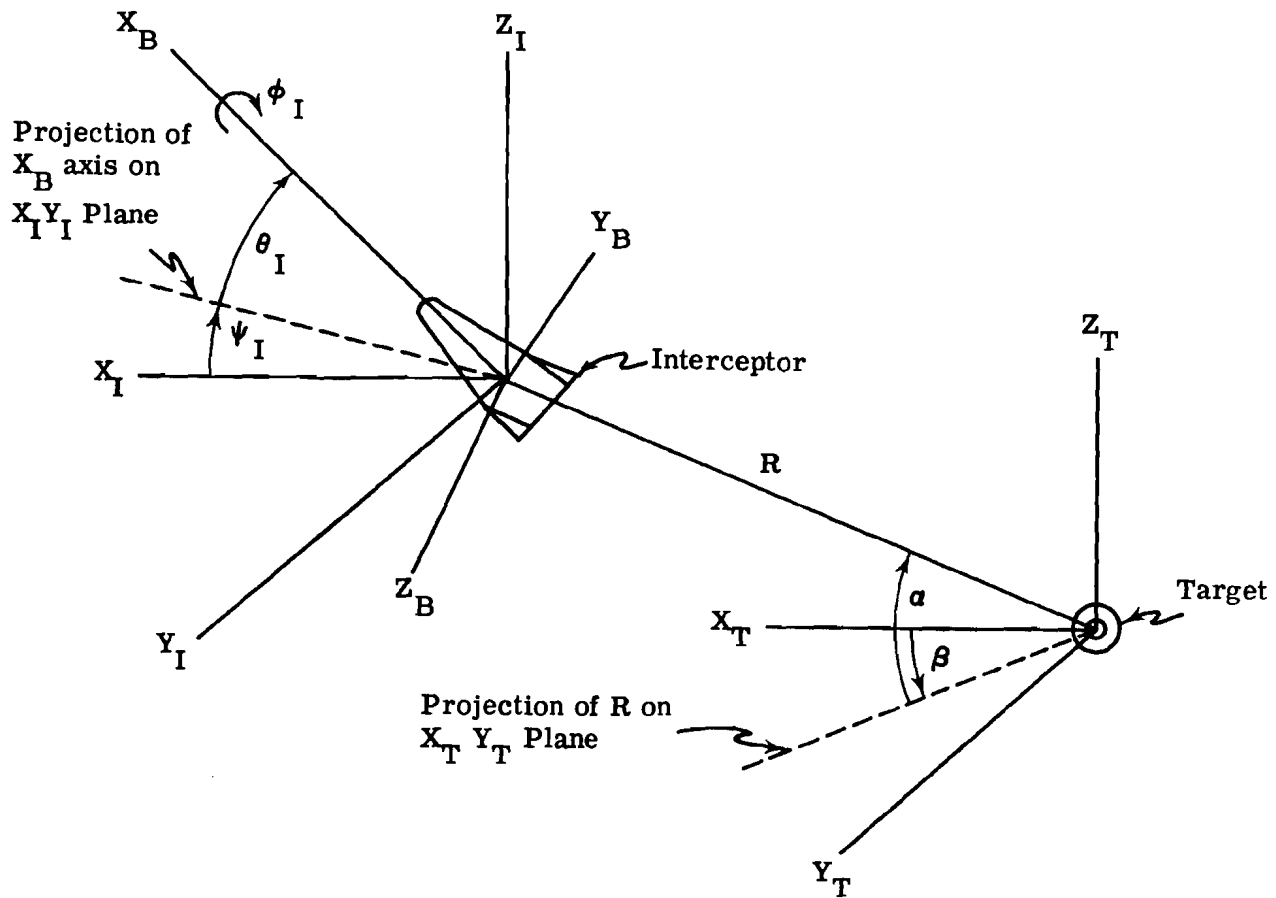


Figure 39. Interceptor Body Axes

and of the earth's horizon as seen through the porthole of an orbiting space vehicle. A TV camera was placed in the center of the planetarium where it picked up the view of the stars and earth and relayed it to a TV monitor screen. In this design, the outer sphere of the planetarium rotated representing pitch of the interceptor. The TV camera inside was allowed to yaw and roll. Thus, the equations had to be written in the Euler angle sequence; pitch θ , yaw ψ and roll ϕ . This form or any other form for the Euler angles has no appreciable influence on computational requirements.

The question of gimbal lock arises for whatever set of Euler transformations are assumed. The conventional set chosen, i.e., the order ψ , θ , and ϕ allows for yaw attitude changes up to 180 degrees, but θ is limited to less than 90 degrees. Other orders have been studied extensively by other authors (viz., References 15 and 24). In particular, Reference 15 includes a concise definition of the problems associated with the orders θ , ψ , ϕ ; θ , ϕ , ψ as well as the conventional set ψ , θ , and ϕ . In order to overcome the 90-degree limit on θ , Reference 15 describes a "gimbal flip" circuit which the authors believe would have worked, had there been time to incorporate it into their studies. Reference 28 also describes techniques for obtaining an all-attitude capability. Although this problem was not pursued further in the present study, it is believed that the additional computing requirements needed to overcome gimbal lock, in those instances where it represents a problem, will not add appreciably to the overall computing load.

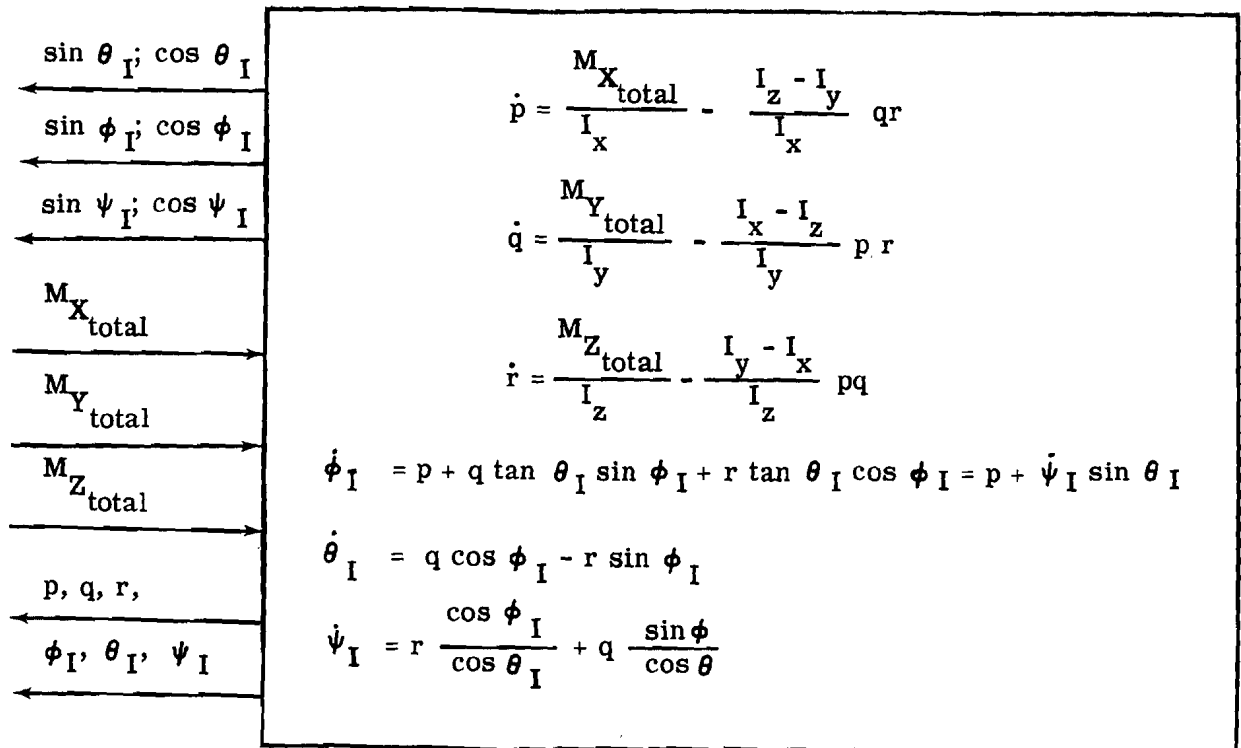


Figure 40. Interceptor Attitude Dynamics

b. Automatic Attitude Control

The attitude commands associated with the rendezvous and docking techniques described in Section III are varied in form. But, regardless of the set considered, the ultimate purpose is to position the interceptor at some desired attitude. This may be accomplished under manual or automatic control, or by a combination of these.

In the simulation of the attitude control system, facility must be provided to satisfy three requirements:

- (1) It must be capable of simulating an automatic, closed loop system controlling the vehicle to a given set of commanded Euler angles ψ_c , θ_c , and ϕ_c .
- (2) It must accept commands given for specified body angular rates p , q , and r and control the attitude control jets to maintain these rates.
- (3) It must accept attitude jet on-off, thrust level, or moment commands so that direct pilot control of the attitude jets can be simulated.

A schematic diagram which incorporates provisions for all three of these modes of operation is presented in Figure 41. This diagram represents the conventional method of mechanization of attitude, rate, and acceleration command systems. It also includes provisions for minimizing couplings between channels when Euler angles are commanded. Note, for example, the term $\psi_c \sin \theta_I$ feeding into the roll rate channel and $\theta_c \sin \phi_I$ feeding into the yaw rate channel.

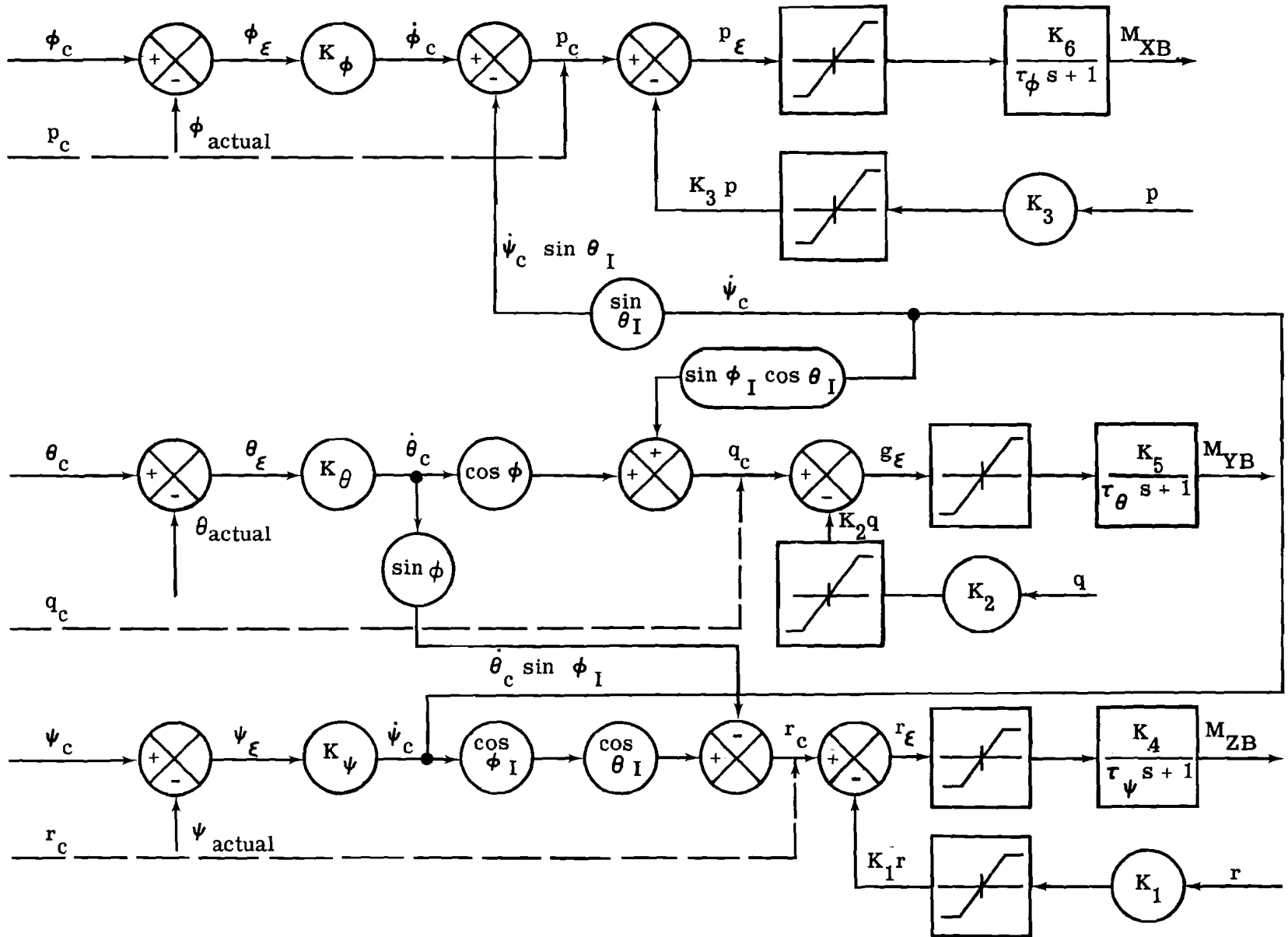
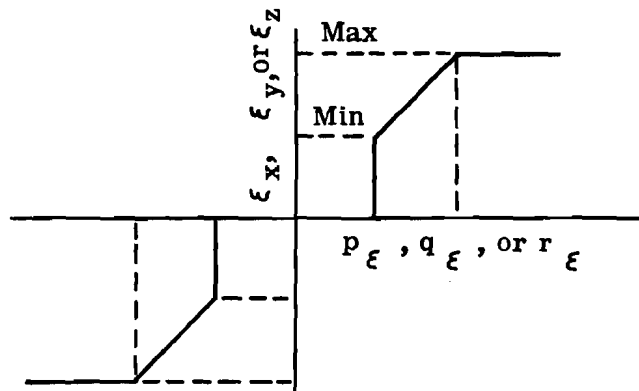


Figure 41. Schematic Diagram of Attitude Control System

Figure 42 expresses this diagram in equation form. The symbols used in these equations are defined as:

- K_ϕ, K_θ, K_ψ = position gains constants in ϕ , θ , and ψ , respectively.
 ϕ_c, θ_c, ψ_c = commanded inertial Euler angles.
 K_3, K_2, K_1 = rate gains constants in p, q, and r channels, respectively.
 $\tau_\phi, \tau_\theta, \tau_\psi$ = lags associated with thrust buildups in the attitude jets.
 K_6, K_5, K_4 = gain constants in p, q, r, respectively, relating $p_\epsilon, q_\epsilon, r_\epsilon$ to M_x, M_y, M_z .
 f_1, f_2, f_3 = attitude rate limiting functions.

Attitude changes are obtained by firing reaction control rocket engines. For the general case, variable thrust attitude rockets in all three axes are assumed. The error signal, ϵ_x, ϵ_y and ϵ_z , used to generate the M_{XB}, M_{YB} , and M_{ZB} moments, respectively, are a function of p_ϵ, q_ϵ , and r_ϵ as shown in the following sketch.



The max and min represent the maximum and minimum thrust limits of the attitude rockets. On-off rockets are simulated by making the minimum error signals equal to the maximum.

c. Thrust Misalignment Moments

Interceptor thrust for translation (T_{XB}, T_{YB}, T_{ZB}) will generate unintentional moments about the interceptor body axes, X_B, Y_B, Z_B , due to misalignments, thrust unbalance and c.g. shifts. The contribution of these unwanted moments to the total moments about each of the interceptor body axes is indicated by the equations of Figure 43.

In this figure, M_{XB}, M_{YB}, M_{ZB} are moments from the attitude jets, and ϵ_{ij} are generalized moment arms of the thrust vectors about the c.g. The ϵ_{ij} can result from linear displacement of the thrust vectors, the c.g. and/or angular misalignment of the thrust vectors.

4. Input/Output Transformations Associated with Rendezvous and Docking Systems

Several rendezvous command generation systems for the terminal phase of rendezvous have been outlined in Section III of this report. Two systems for docking have also been presented. In order to have general application, a complete rendezvous simulation should be

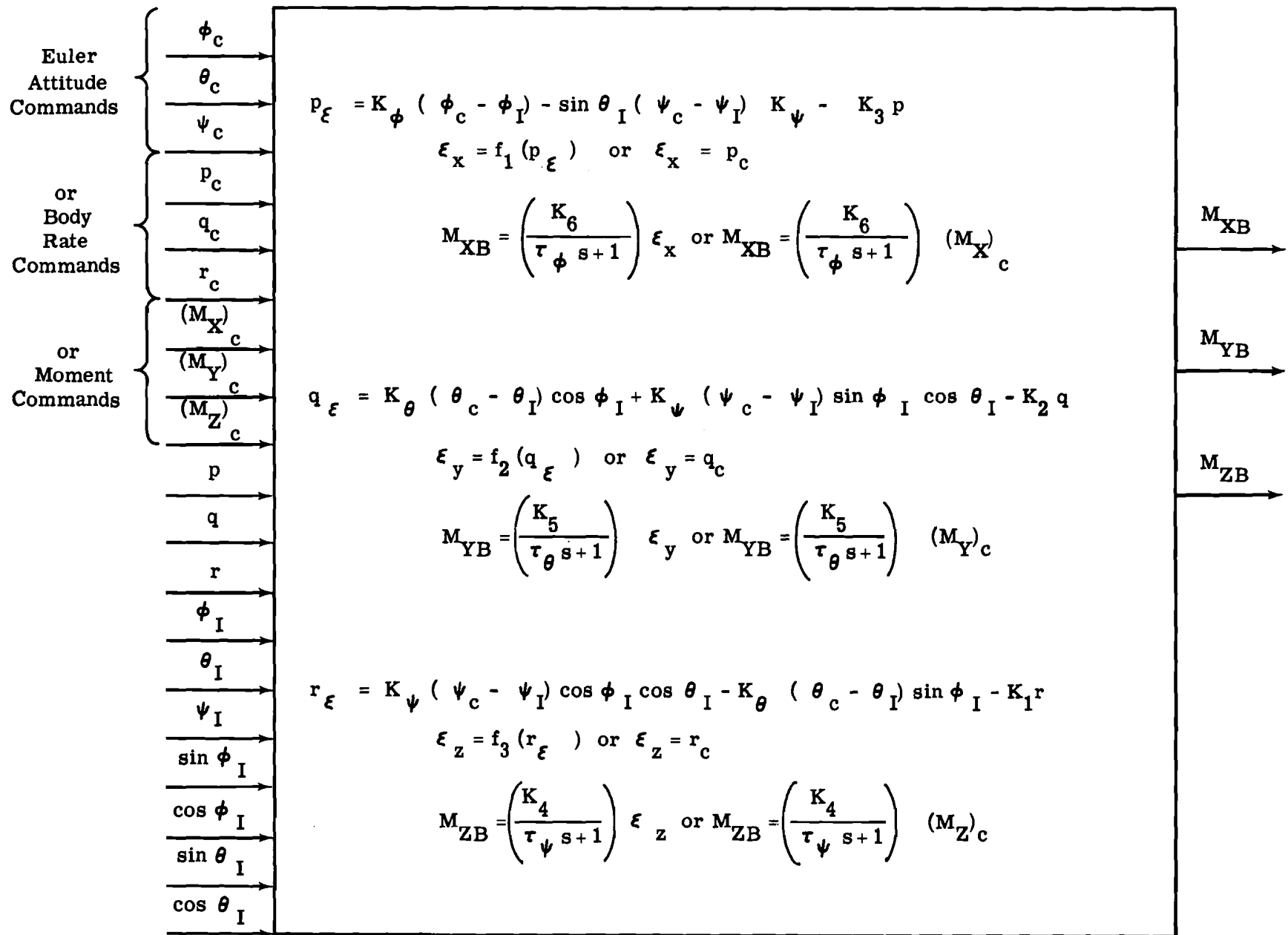


Figure 42. Interceptor Attitude Control System

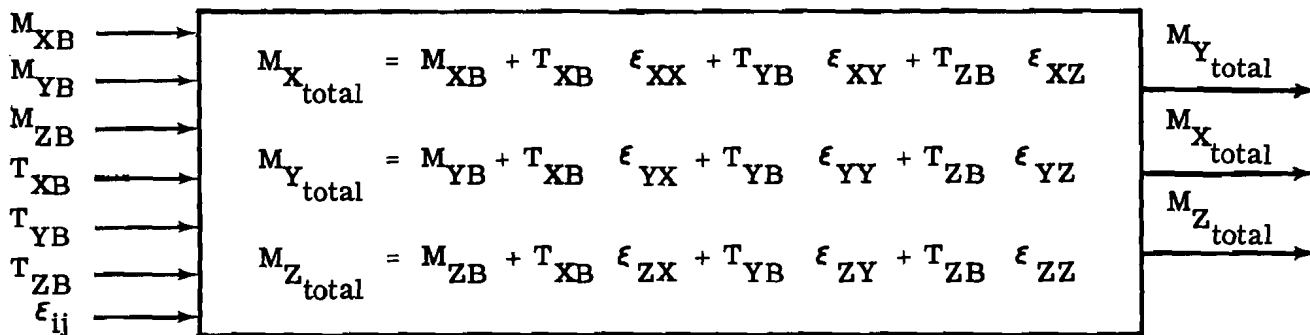


Figure 43. Thrust Misalignment Moments

capable of accommodating each of these as well as other similar systems, one at a time. This means that the simulator computer or computers must have the capability of:

- (1) Supplying each simulated rendezvous system with the required inputs.
- (2) Accepting the outputs of each of the simulated rendezvous systems.
- (3) Supplying sufficient computing speed, accuracy, and capacity either to perform the computations that would be performed in each of the actual rendezvous systems, or in some other manner produce the required outputs.
- (4) Supplying sufficient computational speed, accuracy, and capacity to generate other data required for cockpit displays and a visual display.

In the following paragraphs the input and output requirements of each of the rendezvous systems have been summarized. The input and output transformations required for each system to make it compatible with other elements of the rendezvous simulation (Section IV-B) are also presented.

In Section V, the number of mathematical operations and computational speed requirements for each guidance command system, including the input and output transformations, are determined. The computer equipment requirements for the rendezvous command generation portion of the complete rendezvous simulation are then determined so that the most complex and/or demanding of the known rendezvous systems can be simulated.

a. Summary of Inputs

The inputs required for each of the rendezvous and docking systems which are described in Section III are summarized in Table II.

TABLE II
INPUT AND OUTPUT TRANSFORMATION REQUIREMENTS

	Inputs	Input Transformations Required	Outputs	Output Transformations Required
NASA TN D-747 Brissenden, Burton Foudriat & Whitten (Reference 15)	$R, \dot{R}, \alpha, \dot{\alpha}, \beta, \dot{\beta}$	T_{3A}	$T_{XB_c}, \theta_c, \psi_c$	None Required
NASA D-883, Eggleston & Dunning; NASA TN D-1029, Eggleston (References 9 & 11)	x_R, y_R, z_R $\dot{x}_R, \dot{y}_R, \dot{z}_R$	T_{3B} and T_{3D}	$\Delta V_1, \Delta V_2$ θ_{R_c}, ψ_{R_c}	T_{4B}
IAS-ARS Paper 61-206 Soule & Kidd (Reference 10)	$R, \dot{R}, \alpha, \beta$ $R \dot{\alpha}, R \dot{\beta} \cos \alpha$	T_{3A}	T_{XB_c}, δ_c	T_{4A}
IAS-ARS Paper 61-155 Shapiro (Reference 12)	x_R, y_R, z_R $\dot{x}_R, \dot{y}_R, \dot{z}_R$	T_{3B}	$T_{XB_c}, \theta_{R_c}, \psi_{R_c}$	T_{4B}
NASA TR R-128 Lineberry, Jr. & Foudriat (Reference 13)	Technique 1. (See Figure 17). $R, \dot{R}, \alpha, \dot{\alpha}, \beta, \dot{\beta}$	T_{3A}	$T_{XB_c}, \theta_c, \psi_c$	None Required
	Techniques 1 simplified and 2 (Figure 17) $R, \dot{R}, \alpha', \dot{\alpha}'$	T_{3A} and T_{3C}	$T_{XB_c}, \theta_c', \psi_c'$	T_{4C}
AAS Preprint 62-10 Stapleford (Reference 14)	$R, \dot{R}, \alpha, \beta$ $R \dot{\alpha}, R \dot{\beta} \cos \alpha$	T_{3A}	$T_{XB_c}, T_{YB_c},$ T_{ZB_c}, ψ_c θ_c, ϕ_c	None Required (optional T_{4D})

These various command systems are to be used in the rendezvous simulation shown in Figure 28 and discussed in Section IV-B. It is usually necessary to transform the relative motion parameters into inputs which are acceptable for a specific system. A generalized block diagram of this operation is given as Figure 44. As can be seen from Figure 44, the following inputs are available from the relative motion equations and target equations of motion

$$\left. \begin{array}{l} x, y, z \\ \dot{x}, \dot{y}, \dot{z} \end{array} \right\}$$

The relative position and rates of the interceptor vehicle relative to the target vehicle as measured in an inertially oriented coordinate system with center in the target vehicle. (Figure 29)

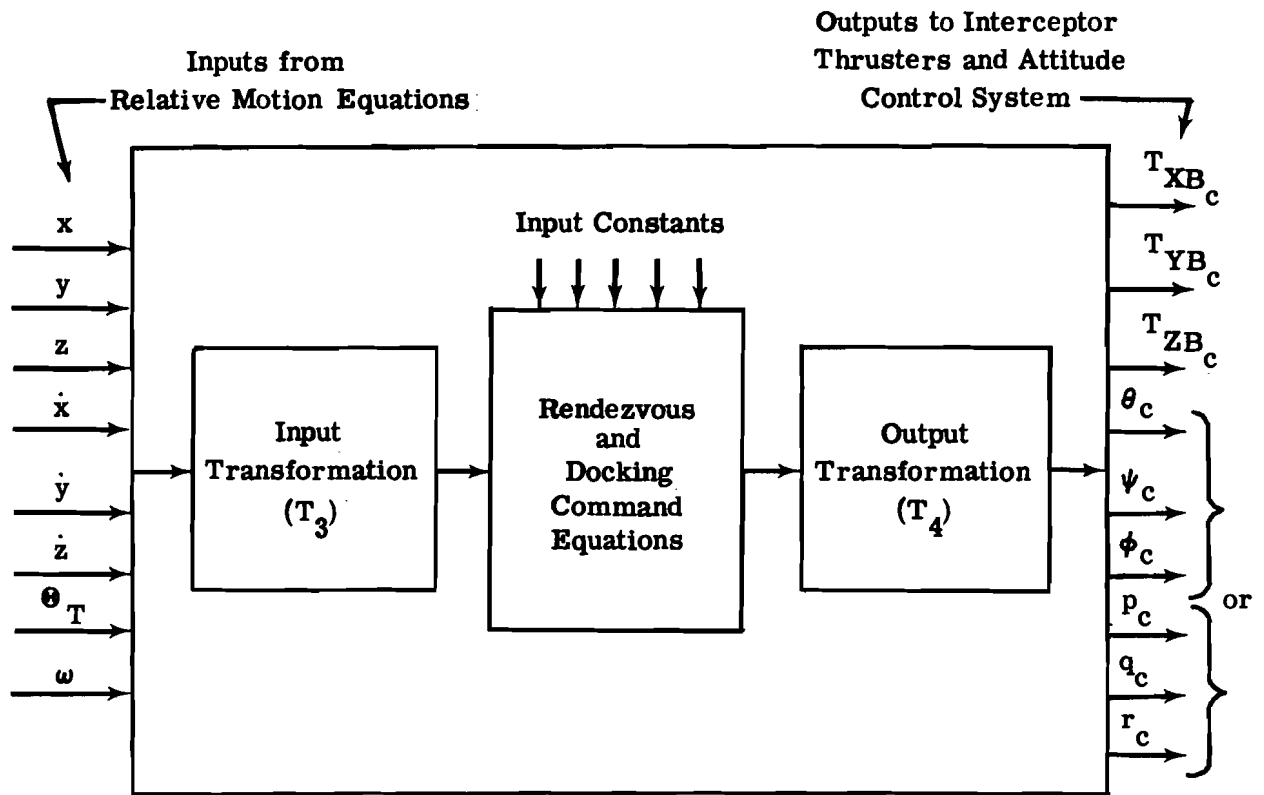


Figure 44. Inputs and Outputs of the Rendezvous and Docking Command Systems

- θ_T Angle of the target vehicle measured in the orbit plane and about the earth from some reference position.
- $\omega \approx \dot{\theta}_T$ Angular velocity of the target vehicle

Using one or more of three basic transformations, it is possible to obtain the required inputs for each of the rendezvous systems from the above terms. These input transformations are:

Transformation T_{3A} - from the rectangular $X_T Y_T Z_T$ coordinate system to a spherical system: (Figure 45a)

$$R = \sqrt{x^2 + y^2 + z^2}$$

$$\alpha = \tan^{-1} \frac{z}{\sqrt{x^2 + y^2}}$$

$$\beta = \tan^{-1} \frac{y}{x}$$

$$\dot{R} = \dot{z} \sin \alpha + \cos \alpha (\dot{x} \cos \beta + \dot{y} \sin \beta)$$

$$R \dot{\alpha} = \dot{z} \cos \alpha - \sin \alpha (\dot{x} \cos \beta + \dot{y} \sin \beta)$$

$$R \dot{\beta} = \frac{\dot{y} \cos \beta - \dot{x} \sin \beta}{\cos \alpha}$$

Transformation T_{3B} - from the rectangular inertial coordinate system (X_T, Y_T, Z_T) to a rectangular rotating coordinate system (X_R, Y_R, Z_R) : (Figure 45b)

$$\begin{aligned}x_R &= x \cos \theta_T - z \sin \theta_T \\y_R &= y \\z_R &= x \sin \theta_T + z \cos \theta_T \\\dot{x}_R &= \dot{x} \cos \theta_T - \dot{z} \sin \theta_T - z_R \dot{\theta}_T \\\dot{y}_R &= \dot{y} \\\dot{z}_R &= \dot{x} \sin \theta_T + \dot{z} \cos \theta_T + x_R \dot{\theta}_T\end{aligned}$$

Transformation T_{3C} - from the spherical coordinate system associated with the X_T, Y_T, Z_T inertial axis system (see Transformation T_{3A}) to the spherical coordinate system associated with an inertial coordinate system centered in the target vehicle where initially the X_T axis passes through the interceptory vehicle: (Figure 45c)

$$\begin{aligned}\dot{\alpha}' &= \dot{\alpha} \cos \phi + \dot{\beta} \cos \alpha \sin \phi' \\\dot{\beta}' &= -\dot{\alpha} \sin \phi' + \dot{\beta} \cos \alpha \sin \phi'\end{aligned}$$

where $\phi' = \tan^{-1} \left\{ \frac{-\sin(\beta - \beta_0) \sin \alpha_0}{\sin \alpha \cos(\beta - \beta_0) \sin \alpha_0 + \cos \alpha \cos \alpha_0} \right\}$

α_0 and β_0 are the initial values of α and β

A fourth transformation, although not necessary, may be beneficial in implementing the rendezvous system of References 9 and 11. This is Transformation T_{3D} :

Transformation T_{3D} - from a rectangular rotating coordinate system (Figure 45b) to a spherical rotating coordinate system (Figure 45d). The rectangular rotating coordinates can be obtained from transformation T_{3B} and then transferred to spherical coordinates in a manner similar to transformation T_{3A} ; that is

$$\begin{aligned}R &= \sqrt{x_R^2 + y_R^2 + z_R^2} \\\alpha_R &= \tan^{-1} \frac{z_R}{\sqrt{x_R^2 + y_R^2}} \\\beta_R &= \tan^{-1} \frac{y_R}{x_R}\end{aligned}$$

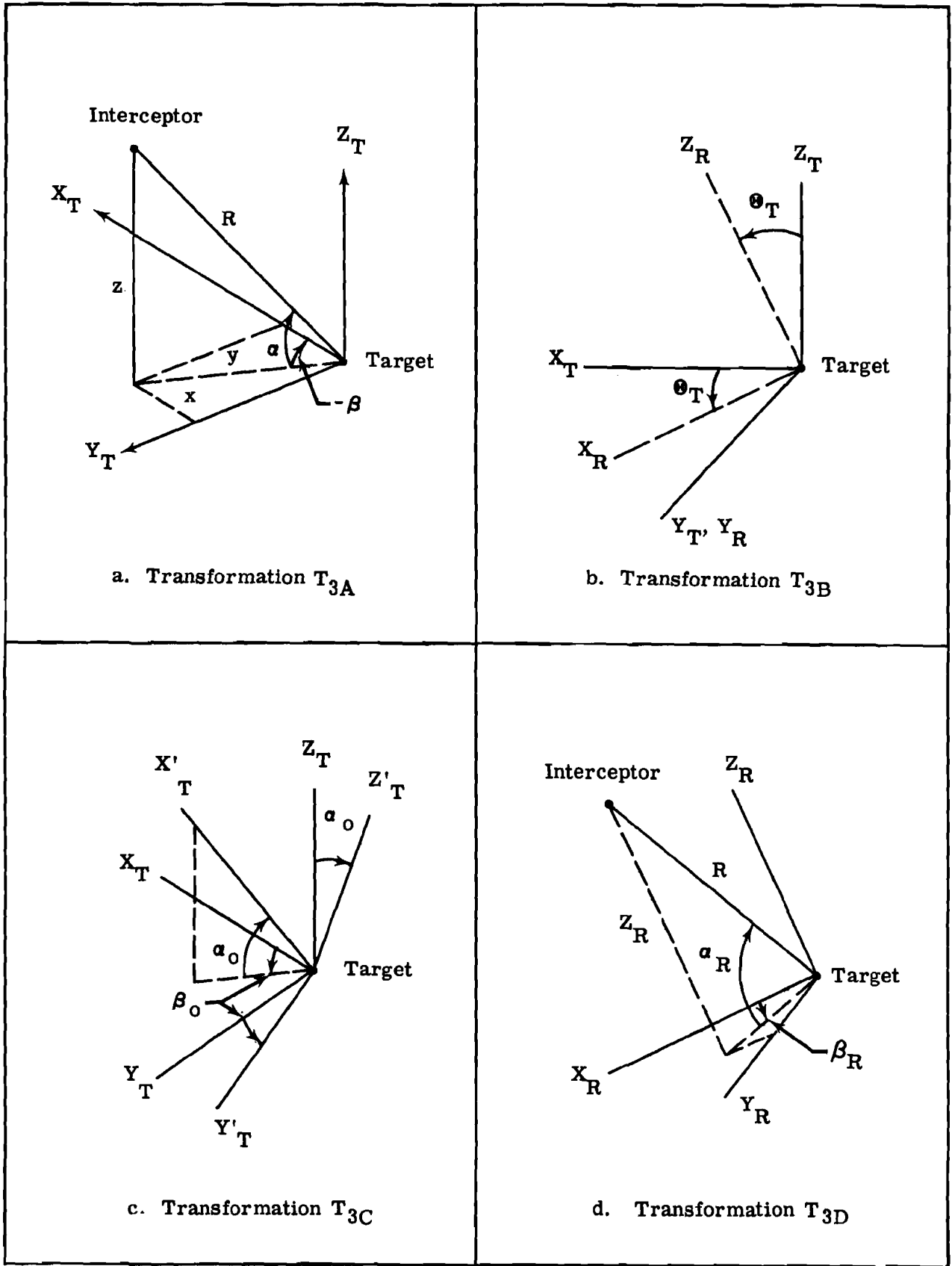


Figure 45. Input Transformation Coordinate Systems

$$\begin{aligned} \dot{R} &= \dot{z}_R \sin \alpha_R + \cos \alpha_R (\dot{x}_R \cos \beta_R + \dot{y}_R \sin \beta_R) \\ R \dot{\alpha}_R &= \dot{z}_R \cos \alpha_R - \sin \alpha_R (\dot{x}_R \cos \beta_R + \dot{y}_R \sin \beta_R) \\ R \dot{\beta}_R &= \frac{\dot{y}_R \cos \beta_R - \dot{x}_R \sin \beta_R}{\cos \alpha_R} \end{aligned}$$

Table II summarizes the input transformations necessary in order to use each of the rendezvous command systems in the rendezvous simulation.

b. Summary of Outputs

The outputs available from each of the energy management systems have been summarized in Table II.

In order to use some of these energy management systems in the complete rendezvous simulation, the outputs must be transformed into a form compatible with other portions of the simulator. As shown in Figure 28, the vehicle body thruster and attitude control system portions of the simulation are capable of implementing the following commands:

T_{XB}, T_{YB}, T_{ZB}	Components of thrust commanded along the interceptor vehicle body axes
ψ_c, θ_c, ϕ_c	yaw, pitch, and roll Euler attitude commands in an inertially oriented reference frame
$\dot{\psi}_c, \dot{\theta}_c, \dot{\phi}_c$	yaw, pitch, and roll Euler angle rate commands
p_c, q_c, r_c	roll, pitch, and yaw rate commands about the interceptor body axes

Using one of three transformations, it is possible to obtain compatible guidance commands from the outputs of each of the energy management systems. These output transformations are:

Transformation T_{4A} - this transforms a command angle, δ , which is angle between the required thrust direction and the LOS in the plane of the LOS and the velocity vector into θ_c and ψ_c command angles. (Figure 46a)

$$\psi_c = \tan^{-1} \left\{ \frac{\cot \delta \cos \alpha - \sin \phi_V \cot \beta + \cos \phi_V \sin \alpha}{\cot \delta \cos \alpha \cot \beta - \sin \phi_V - \cos \phi_V \sin \alpha \cot \beta} \right\}$$

$$\theta_c = \sin^{-1} \left\{ \cos \delta \sin \alpha - \sin \delta \cos \phi_V \cos \alpha \right\}$$

$$\text{where: } \phi_V = \tan^{-1} \left[\frac{R \dot{\beta} \cos \alpha}{R \dot{\alpha}} \right]$$

Transformation T_{4B} - from command angle with respect to a rotating coordinate system (Figure 45b) to command angles with respect to the inertial coordinate system. (Figure 46b)

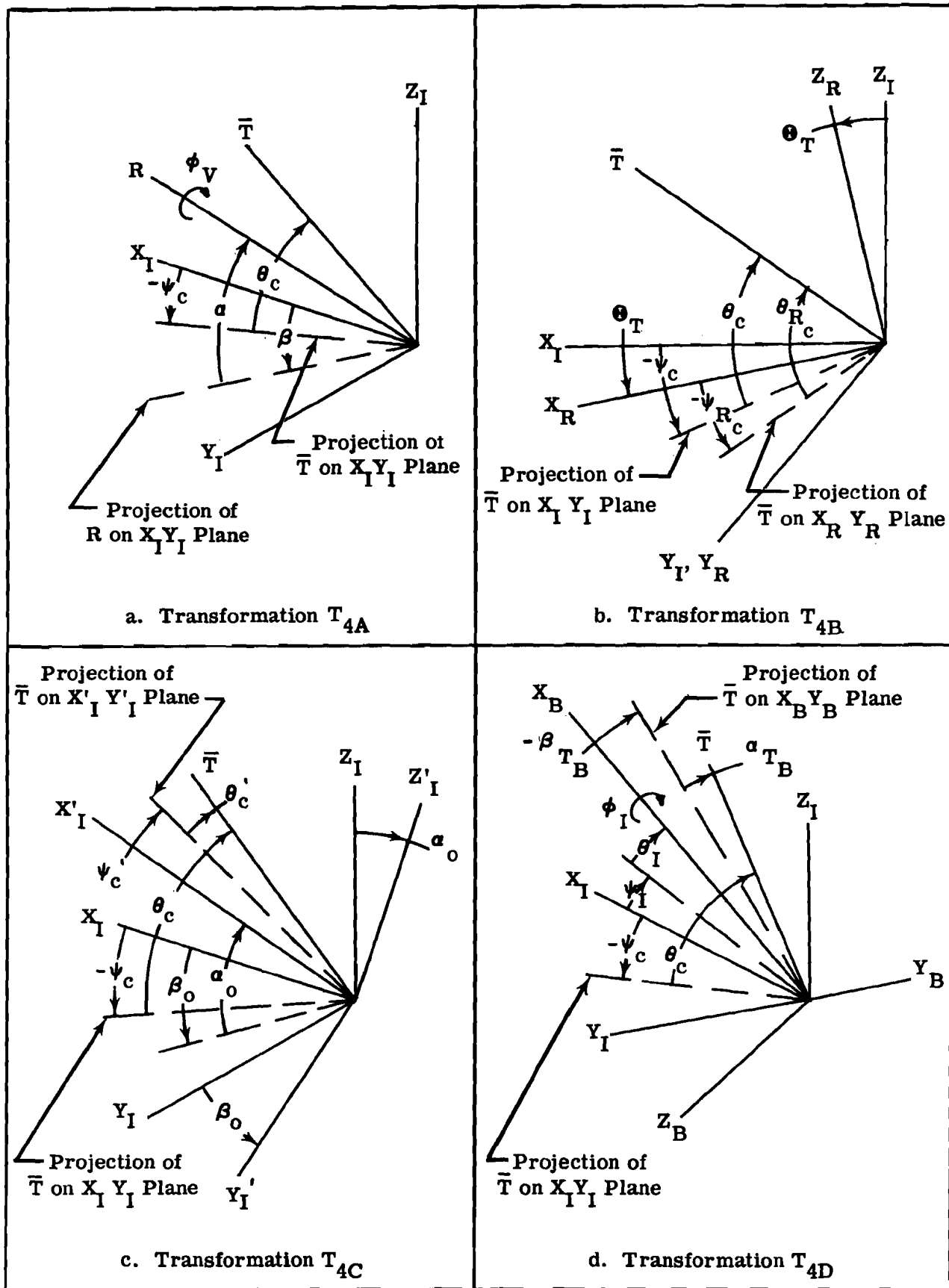


Figure 46. Output Transformation Coordinate Systems

$$\psi_c = \tan^{-1} \left\{ \frac{\sin \psi_{R_c}}{\cos \psi_{R_c} \cos \theta_T + \tan \theta_{R_c} \sin \theta_T} \right\}$$

$$\theta_c = \sin^{-1} \left\{ -\cos \theta_{R_c} \cos \psi_{R_c} \sin \theta_T + \sin \theta_{R_c} \cos \theta_T \right\}$$

Transformation T_{4C} - from command angles in the inertial axis system with center in the target and where initially the X_T' axis passes through the interceptor to command angles with respect to the inertial $X_T Y_T Z_T$ axis system (Figure 46c).

$$\psi_c = -\beta_o + \tan^{-1} \left\{ \frac{-\sin \psi_c' \cos \theta_c'}{\sin \theta_c' \sin \alpha_o - \cos \theta_c' \cos \psi_c' \cos \alpha_o} \right\}$$

$$\theta_c = \sin^{-1} \left\{ \cos \theta_c' \cos \psi_c' \sin \alpha_o + \sin \theta_c' \cos \alpha_o \right\}$$

A fourth transformation which can be used with the rendezvous system of Reference 14 has been developed. This transformation is not required in order to use this system, but merely makes it possible to change a T_{XB_c} , T_{YB_c} , T_{ZB_c} guidance command output such as might be obtained from the system of Reference 14 to a T_{XB_c} , θ_c , ψ_c output which is the form of the guidance commands that are obtained from the other rendezvous command systems. This output transformation is:

Transformation T_{4D} - from thrust commands along the interceptor vehicle body axes to a body longitudinal thrust command and command angles (Figure 46d).

$$T_{XB_c} = \sqrt{T_{XB}^2 + T_{YB}^2 + T_{ZB}^2}$$

$$\psi_c = \psi_I + \tan^{-1} \left\{ \frac{-\cos \alpha_{TB} \sin \beta_{TB} \cos \phi_I + \sin \alpha_{TB} \sin \phi_I}{\cos \alpha_{TB} \cos \beta_{TB} \cos \theta_I - \cos \alpha_{TB} \sin \beta_{TB} \sin \phi_I \sin \theta_I - \sin \alpha_{TB} \cos \phi_I \sin \theta_I} \right\}$$

$$\theta_c = \sin^{-1} \left\{ \cos \alpha_{TB} \cos \beta_{TB} \sin \theta_I + \cos \alpha_{TB} \sin \beta_{TB} \sin \phi_I \cos \theta_I + \sin \alpha_{TB} \cos \phi_I \cos \theta_I \right\}$$

where: $\alpha_{TB} = \tan^{-1} \frac{T_{ZB}}{\sqrt{T_{XB}^2 + T_{YB}^2}}$

$$\beta_{TB} = \tan^{-1} \frac{T_{YB}}{T_{XB}}$$

Table II summarizes the output transformations necessary in order to use each of the energy management systems in the rendezvous simulation of Figure 28.

5. Deorbit System

The energy management system of Reference 1 uses a single "optimum" retro firing to deorbit a vehicle from circular orbits. This procedure is adequate for vehicles of interest and altitudes up to an estimated maximum of 500 miles. However, as altitude increases, the temperature and skip boundaries (as defined in Reference 1) will, for some vehicles, be exceeded for the single retro case. This means that if the reentry is made shallow enough to avoid temperature troubles, the vehicle will skip back out of the atmosphere. In such cases, a two-impulse transfer can be used. With this technique, a descent will be made from a high altitude orbit to a low altitude with the first impulse; then, a second impulse will take the vehicle from the low orbit to reentry.

A brief review of the single-impulse method led to the conclusions that there would be a basic limitation of impracticality for very high altitudes. On the other hand, the two-impulse method will allow deorbit theoretically from any altitude. Therefore, in view of its more universal application, the two-impulse method was chosen for further study.

The steps in this method are indicated in Figure 47 and the equations to be solved are listed in Figure 48. The altitude for the second firing, the range from this point to the destination, and the range from this point to the reentry point are fixed values specified for each vehicle on the basis of preflight studies. They would be selected to give a reentry with adequate margins with respect to temperature limits and skipping. If the initial orbit is circular, the transfer from the initial orbit to the second firing point would be a 180-degree or Hohmann transfer. Thus, the vehicle would arrive at the second firing point with its velocity vector horizontal.

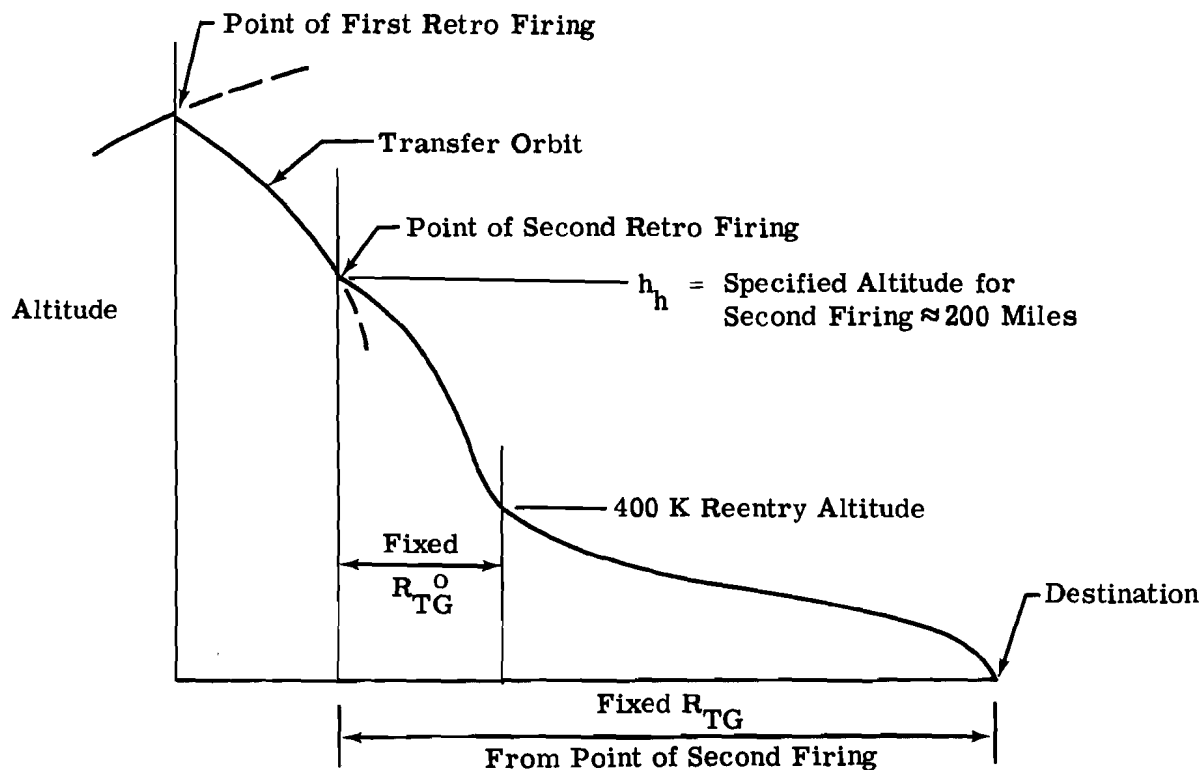


Figure 47. Deorbit Maneuver

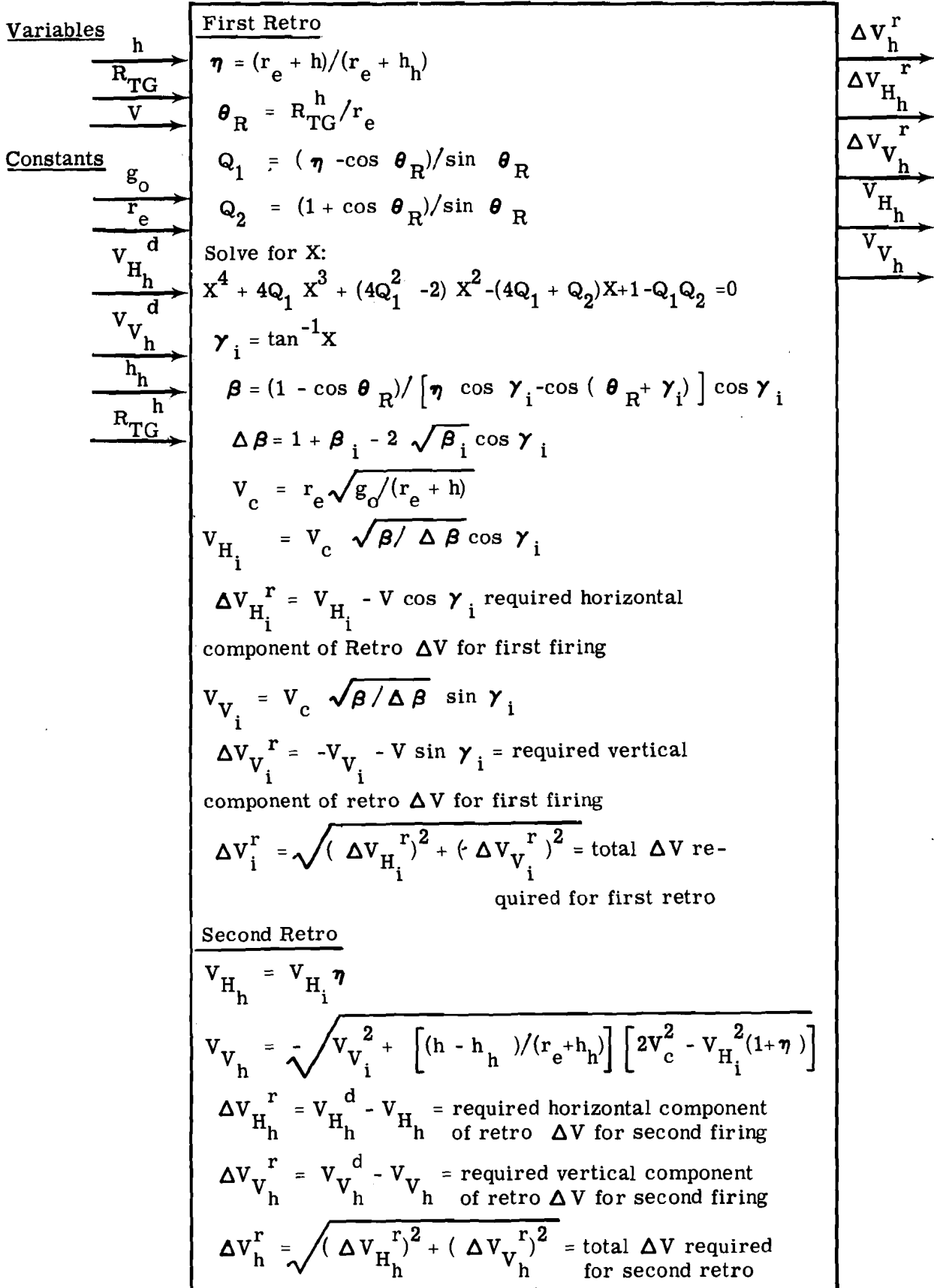


Figure 48. Deorbit Mode Equations

Before initiating the deorbit maneuver, the interceptor must depart a sufficient distance from the target vehicle to avoid collision and to prevent hot gases from impinging on the target during retro firing. For this departure it will be assumed that the interceptor will be released with a small relative velocity. The direction in which the interceptor departs is subject to two considerations.

- (1) If the departure velocity is imparted so as to slow the interceptor down (-x direction) and thus, lower its altitude (-z direction), the amount of fuel required for deorbit retro will be reduced.
- (2) If the departure velocity is imparted in a purely y or z direction, and for some reason the pilot decides not to deorbit, the two vehicles (except for minor disturbing influences) will come back into contact again, in 180 degrees for y direction departure and 360 degrees for z direction departure. Thus, a velocity in either direction simply limits the distance the two vehicles will be separated.

The safety factor makes the second alternative appear more desirable, and a departure in the y direction has been selected for the present study (see Section V).

6. Visual Scene and Pilot Displays

a. Visual Scene

The methods of producing a visual scene in the rendezvous and docking simulator are numerous and the methods selected for a given application will depend to a large extent upon cost factors. If the final steps of docking and latching are to be accurately simulated, it may be important to have a three dimensional hardware mockup, such that the pilot may make full use of his depth perception in estimating distances and rates. In such cases, a large mechanical simulator, such as that discussed in References 25 and 26 may be used. A star background in this case is probably not important.

At the other extreme, when the target vehicle is at a distance great enough to blend it in with the stars, a star background and/or a view of the horizon is usually very important. In such cases it may be necessary to simulate not only the stars and their intensity, but also the rate at which the target vehicle is moving in the celestial sphere and/or relative to the horizon. This case may be simulated a number of ways; electronically, mechanically, or with combinations of physical models and electronic signals. However, regardless of how the simulated visual scene is obtained, the rendezvous simulator must provide inputs to drive the mechanisms or black boxes which create the simulated view.

If the visual scene is complete, it will consist of the following items:

- (1) A view of the target.
- (2) A celestial background, including the sun and moon, as well as stars.
- (3) The horizon, and surface details of the earth or other planet near which the rendezvous is to take place.

The specific variables that will be required to drive a visual display in order to present these three main items will depend on the mechanical and electrical details of the display. For example, in one simulator, a TV camera may be driven to represent all attitude and linear motions of the interceptor. In such a situation, either angular and linear

rates and/or positions relative to inertial space could be supplied to the camera drives. In another simulation, the required inputs might be the bearing angles of the target vehicle relative to the interceptor body axes. This simulator would also require angles describing the attitude of the target relative to the line of sight.

In a general study such as this, it is difficult to anticipate and to provide the equations that may be required for all possible means of implementing the visual scene. However, efforts have been made to provide the visual scene inputs, as described in following paragraphs, which are most likely to be required.

(1) Target Vehicle

Assuming that the target vehicle is not symmetrical, its orientation relative to the line of sight from the interceptor may be required. In order to describe this orientation, the target satellite attitude relative to the inertial coordinate axis has been expressed by the Euler angles ψ_T , θ_T , and ϕ_T shown in Figure 49. The order of these rotations are first, about Z_{TB} giving ψ_T ; second, about Y_{TB} , giving θ_T ; and third, about X_{TB} , giving ϕ_T . Now assume that the interceptor is oriented such that the X_B axis is pointed straight at the target vehicle at zero Euler roll. If the pilot is looking along the interceptor X_B axis which is coincident with the line of sight, the target will appear to him as if the axis of the target vehicle, starting from a position with its body axes parallel to those of his own vehicle, has been rotated consecutively through the angles $-\alpha$, $+\beta$, ψ_T , θ_T , and ϕ_T , where α and β define the orientation of the line of sight as

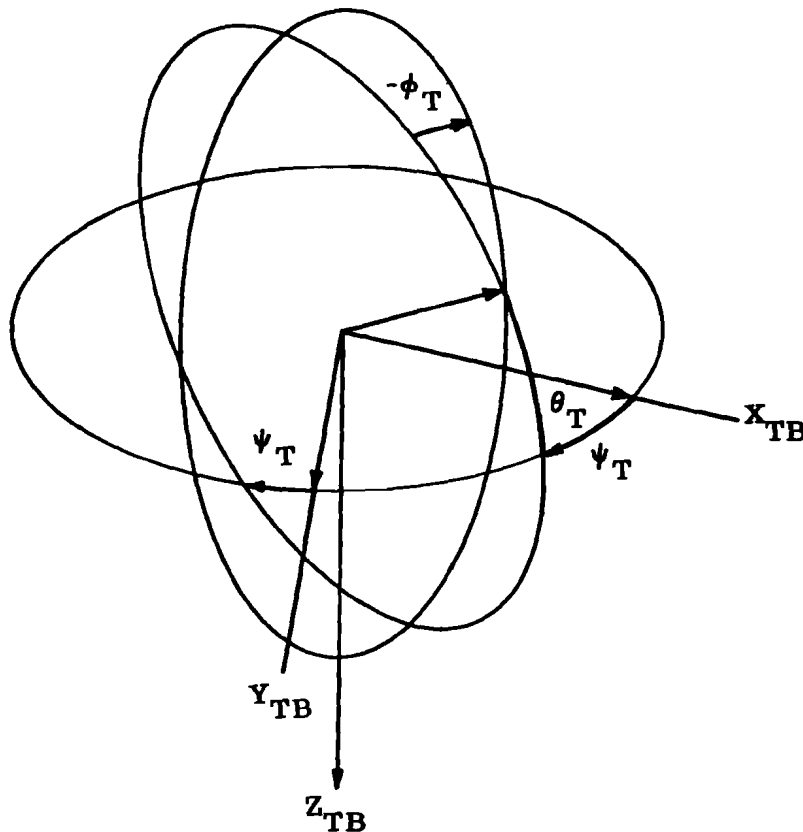


Figure 49. Euler Angles of the Target Vehicle

shown in Figure 16. This position of the target could also be reached by rotating the target vehicle from the same initial position through three angles, ψ_1 , θ_1 , and ϕ_1 . These latter angles can be used in the simulation to describe the target orientation relative to the line of sight.

Thus, the following angular relationships exist:

$$\begin{bmatrix} \phi_1 \\ \theta_1 \\ \psi_1 \end{bmatrix} = \begin{bmatrix} \phi_T \\ \theta_T \\ \psi_T \end{bmatrix} \begin{bmatrix} +\beta \\ -\alpha \end{bmatrix}$$

Multiplying these matrices together and equating like elements results in the following equations from which the simulator computer can obtain the desired angles, ϕ_1 , θ_1 , and ψ_1 .

$$\sin \theta_1 = -\sin \alpha \cos \theta_T \cos(\psi_T + \beta) + \cos \alpha \sin \theta_T$$

$$\cos \phi_1 \cos \theta_1 = \sin \phi_T \sin(\psi_T + \beta) \sin \alpha + \cos \phi_T \sin \theta_T \cos(\psi_T + \beta) \sin \alpha + \cos \phi_T \cos \theta_T \cos \alpha$$

$$\cos \theta_1 \sin \psi_1 = \cos \theta_T \sin(\psi_T + \beta)$$

If the target is stabilized in an arbitrary position with respect to inertial axes, ψ_T , θ_T , and ϕ_T are constant, and the equations reduce to

$$\sin \theta_1 = -C_A \sin \alpha \cos \beta + C_B \sin \alpha \sin \beta + C_C \cos \alpha$$

$$\cos \phi_1 \cos \theta_1 = C_H \cos \beta \sin \alpha + C_J \sin \beta \sin \alpha + C_G \cos \alpha$$

$$\cos \theta_1 \sin \psi_1 = C_B \cos \beta + C_A \sin \beta$$

where the C's are constants involving ψ_T , θ_T , and ϕ_T .

If the target body axes are always aligned with the reference inertial axes, so that $\psi_T = \theta_T = \phi_T = 0$, the equations further reduce to:

$$\sin \theta_1 = -\sin \alpha \cos \beta$$

$$\cos \phi_1 \cos \theta_1 = \cos \alpha$$

$$\cos \theta_1 \sin \psi_1 = +\sin \beta$$

If instead of being inertially stabilized, the target vehicle $X_{TB} Y_{TB}$ plane is always parallel to the earth and the $X_{TB} Z_{TB}$ plane is always in the orbit plane, then $\psi_T = 0$, $\phi_T = 0$, $\theta_T = \Theta_T$, and the equations become:

$$\sin \theta_1 = -\cos \Theta_T \cos \beta \sin \alpha + \sin \Theta_T \cos \alpha$$

$$\cos \phi_1 \cos \theta_1 = \sin \Theta_T \cos \beta \sin \alpha + \cos \Theta_T \cos \alpha$$

$$\cos \theta_1 \sin \psi_1 = +\cos \Theta_T \sin \beta$$

If the target vehicle is toroid shaped, symmetrical about its Z_{TB} axis, and there are no markings to make one side distinguishable from another, we can assume $\psi_T = 0$ and the original equations reduce to

$$\sin \theta_1 = -\sin \alpha \cos \theta_T \cos \beta + \cos \alpha \sin \theta_T$$

$$\cos \phi_1 \cos \theta_1 = +\sin \phi_T \sin \beta \sin \alpha + \cos \phi_T \sin \theta_T \cos \beta \sin \alpha + \cos \phi_T \cos \theta_T \cos \alpha$$

Since yaw of a toroidal shaped vehicle will not change its appearance in the window, it doesn't matter where the X_{TB} axis is pointing. Therefore, assume it to be always coincident with the plane containing the line of sight and its projection on the $X_T Y_T$ plane. Thus, $\psi_T = -\beta$ and the equations reduce to

$$\theta_1 = \theta_T - \alpha$$

$$\phi_1 = \phi_T$$

$$\psi_1 = 0$$

If in addition to the assumption $\psi_T = -\beta$, it is assumed that $\theta_T = \phi_T = 0$, the equations become

$$\theta_1 = -\alpha$$

$$\phi_1 = 0$$

$$\psi_1 = 0$$

These various sets of equations for ψ_1 , θ_1 , and ϕ_1 can be used to describe the target vehicles attitude relative to a window in the interceptor, if α and β are known. α and β will be computed in the "Equations of Relative Motion" portion of the simulator, as described in Section IV-B-1.

In order to determine the apparent size of the target, it will also be necessary to know the range, R , between the two vehicles. This will be obtained by transforming outputs of the relative motion equations to polar form (Section IV-B-4).

If the interceptor body axes are not coincident with the line of sight, the interceptors Euler angles ψ_I , θ_I , and ϕ_I must be combined with α and β in order to locate the target with respect to the interceptor window. If the center of the window is defined to be coincident with the interceptor X_B axis, and the roll of the interceptor is zero, the y_w and z_w coordinates of the target image projection on the interceptor window will be

$$y_w = -\left(\frac{d}{R}\right) R \sin(\psi_I + \beta) \cos \alpha$$

$$z_w = \left(\frac{d}{R}\right) R \left[\sin \theta_I \cos \alpha \cos(\psi_I + \beta) - \cos \theta_I \sin \alpha \right]$$

where d = distance from pilot's eye to the window

R = distance from pilot's eye to target

y_w , z_w are coordinates of the center of the target image relative to the center of the window.

y_w , and z_w are calculated assuming that the pilot is turned around in his vehicle sighting along the $-X_B$ axis.

In this position:

- (1) if the interceptor yaws to the right (+) the image will move to the left (-) y_w

- (2) if the target is in $+\beta$, the image will be left, or $(-)$ y_w
- (3) if the interceptor pitches up $(+)$ (i.e., nose up), the pilot, who is facing rearward in the vehicle, sees the image move up $(+)$ z_w
- (4) if the target is in $+\alpha$, the image will be down, or $(-)$ z_w

If the interceptor rolls about its X_B axis, these coordinates of the target become:

$$y_w = d \left\{ -\sin(\beta + \psi_I) \cos \phi_I \cos \alpha + \left[\sin \theta_I \cos \alpha \cos(\psi_I + \beta) - \cos \theta_I \sin \alpha \right] \sin \phi_I \right\}$$

$$z_w = d \left\{ \left[\sin \theta_I \cos \alpha \cos(\psi_I + \beta) - \cos \theta_I \sin \alpha \right] \cos \phi_I + \sin(\beta + \psi_I) \cos \alpha \sin \phi_I \right\}$$

(2) Celestial Background

The Euler angles ψ_I , θ_I , and ϕ_I define the position of the interceptor body axes with respect to a set of axes that do not rotate with respect to space. Hence, these angles, together with three constant angles which orient the reference axes with respect to a celestial coordinate system, are sufficient to determine which celestial bodies will be in view through an interceptor window and the orientation (roll) of this star pattern about the vehicle X_B axis. The interceptor Euler angles will be obtained from the interceptor attitude dynamics element of the simulator (Section IV-B-3).

A transformation from the ψ_I , θ_I , ϕ_I to a corresponding set of coordinates measured relative to a standard celestial sphere (right ascension, declination, and roll) may be required in some simulators. This will be a standard two-angle transformation involving the inclination of the target orbit to the celestial equator, and the angle that the zero range angle line ($\theta_T = 0$) makes with the line defined by the intersection of the orbit plane and the equatorial plane of the celestial sphere.

(3) The Earth

If a view of the earth is to be included in the visual scene, it will be necessary to know the position of the earth with respect to a convenient reference. It appears that one of the most convenient ways to describe the position of the earth is with the angles θ_I and \mathcal{N}_I (see Figure 29). These angles describe the orientation of the radius vector from the center of the earth to the interceptor, with respect to an inertially fixed set of axes with its origin at the center of the earth. If these axes at the earth's center are selected so they are parallel to the X_I , Y_I , and Z_I set in the interceptor, the angles θ_I and \mathcal{N}_I can be used to position the center of a model or other representation of the earth, relative to these reference axes in the interceptor. Thus, the center of the earth can be thought of much as if it were just another star in the celestial sphere. Equations for the determination of θ_I and \mathcal{N}_I are presented in Section IV-B-1.

If surface details of the earth are to be shown, or if a deorbit to a prescribed destination is to be made, it will also be necessary to compute the latitude, longitude, and heading of the interceptor with respect to the earth. Equations for determining these variables are also given in Section IV-B-1. In some simulators the earth scene may be obtained by scanning a model of the earth with a camera which is translated in response to signals representing interceptor angular rates with respect to inertial space. With this technique, the camera drive motors do the required integration of the equations and result in the camera seeing the desired portion of the earth. The latitude, longitude, and heading information could then be obtained either from pickoffs on the camera carriage or by solving the previously mentioned equations.

The altitude or distance of the interceptor from the center of the earth determines the curvature of the horizon and the size of features on the earth as seen by the pilot. Because altitude will usually change by only a small percentage of the earth's radius during the terminal guidance and docking phases of rendezvous, it will usually not be necessary to provide curvature and size changes in the presentation of the earth. If it is desired to include such refinements, the required altitude or radius information can be obtained from the interceptor flight conditions described in Section IV-B-1.

b. Cockpit Displays

Table III lists displays which are believed to be necessary and/or desirable if a pilot is to play a significant role with the rendezvous and docking systems of Section III. These displays may be used by the pilot in generating guidance commands, in monitoring automatic system operation, or in acting in an override or backup mode with a completely automated system. In systems such as that of Reference 15, the guidance commands are determined by the pilot from displays of basic flight data. In other systems, which require the use of computing equipment to determine the guidance commands, the normal pilot participation may be limited to supplying inputs to the computer and executing the attitude and thrust commands determined by the computer.

The display requirements of each of the rendezvous and docking systems of Section III and Table III are briefly discussed in the following paragraphs. It will be noted that the displays which the authors of Reference 15 determined to be necessary for pilot control during rendezvous form a basic set of displays which could be used (with minor changes in some cases) for all the rendezvous systems regardless of whether the pilot actively participates in or merely observes the rendezvous maneuver. In addition to these basic displays certain other displays appear to be desirable for each of the systems.

In addition to the instrument displays described in this section, a view of the target as seen from windows or periscopes in the interceptor will be desirable with all systems. This is particularly true for the docking phase where the maneuver will probably be controlled primarily from visual cues.

NASA TN D-747; Brissenden, Burton, Foudriat, and Whitten (Reference 15)

As shown in Table III, the following quantities were found from this investigation to be necessary for proper control during the rendezvous maneuver:

Range and range rate (R, \dot{R})

Elevation and azimuth of the line-of-sight (α, β)

Rates of change of the line-of-sight elevation and azimuth ($\dot{\alpha}, \dot{\beta}$)

Interceptor attitude angles (ψ, θ, ϕ)

Interceptor attitude angle rates ($\dot{\psi}, \dot{\theta}, \dot{\phi}$)

Displays of the above quantities on dial instruments proved to be most satisfactory. Display of R versus \dot{R} was found to be unsatisfactory and a display of $R \dot{\alpha}$ versus $R \dot{\beta}$ could not be read with the necessary accuracy. Display of $\theta - \alpha$ and $\psi + \beta$ was found to be helpful. These angular differences indicate how far the interceptor X_B axis is removed from the line of sight.

TABLE III
SUMMARY OF DISPLAY REQUIREMENTS

Parameter	Rendezvous System					
	Ref 15 NASA TN D-747	Ref 9 NASA TN D-883	Ref 10 IAS-ARS 61-206	Ref 12 IAS-ARS 61-155	Ref 13 NASA TR R-128	Ref 14 AAS 62-10
R	x	\dot{x}_R x	x	\dot{x}_R x	x	x
\dot{R}	x	\ddot{x}_R x	x	\ddot{x}_R x	x	x
α	*x	y_R x	x	y_R x	x	x
$\dot{\alpha}$ or $R\dot{\alpha}$	x	\dot{y}_R x	x	\dot{y}_R x	x	x
β	*x	z_R x	x	z_R x	x	x
$\dot{\beta}$ or $R\dot{\beta}$	x	\dot{z}_R x	x	\dot{z}_R x	x	x
θ_c and θ_I	*x	x	x	x	x	x
ψ_c and ψ_I	*x	x	x	x	x	x
ϕ_c and ϕ_I	x	x	x	x	x	x
ϕ_I	x	x	x	x	x	x
θ_I	x	x	x	x	x	x
ψ_I	x	x	x	x	x	x
t		x		x		
τ_1		x		T^*-kt x		
ΔV_{avail}		x		x		
ΔV_1		x		x		
ΔV_2		x				
Thrust On-Off Switching Criterion			x(Range)	x $\begin{cases} \dot{R}_{MAX} \\ \dot{R}_{MIN} \end{cases}$	x $\begin{cases} \frac{\dot{R}^2}{2R} \text{ rela-} \\ \text{tive} \\ \text{to} \\ T_{MAX}/m \\ \text{or} \\ A_1 T/m \\ \text{and} \\ A_2 T/m \end{cases}$	x $\begin{cases} \dot{R} \text{ relative} \\ \text{to} \\ R_{MAX} \\ \text{and} \\ R_{MIN} \end{cases}$
Operating Mode		x				

* Presentation of $\theta_I - \alpha$ and $\psi_I + \beta$ was found to be helpful

With this system it seems logical to display:

- (1) Displacements and velocities along the three axes of the rotating coordinate system $(x_R, \dot{x}_R, y_R, \dot{y}_R, z_R, \dot{z}_R)$ instead of the $R, \dot{R}, \alpha, \dot{\alpha}, \beta, \dot{\beta}$ information of Reference 15. These quantities provide the relative position and rate information for the guidance computer.
- (2) The ΔV_1 and ΔV_2 velocity corrections necessary to establish an intercept course and to bring about a soft rendezvous. Also, the ΔV available.
- (3) The pilot selected or computer determined time for the rendezvous maneuver (τ) and, t , actual time since the start of the maneuver.
- (4) The command angles θ_c and ψ_c at which thrust should be applied in order to bring about the velocity corrections or display of $\theta_c - \theta$ and $\psi_c - \psi$.
- (5) An indication of whether the pilot has requested the computer to give him an intercept in a specified time, a rendezvous in a specified time, or a rendezvous with a specified ΔV .

IAS-ARS Paper 61-206; Soule and Kidd (Reference 10)

Other than basic attitude and attitude rate displays, it is believed that displays for this command system should include:

- (1) A display of the range at which thrust should be initiated if rendezvous is to be accomplished with a fixed thrust engine, and a display of the actual range.
- (2) Attitude commands ψ_c, θ_c, ϕ_c or $\psi_c - \psi, \theta_c - \theta, \phi_c - \phi$ that will orient the thrust vector so as to give the desired angle δ between the thrust and the line of sight.

IAS-ARS Paper 61-155, Shapiro (Reference 12)

Display requirements for this command system are similar to those of

Reference 9:

- (1) Basic displays of attitude and attitude rate as described for Reference 15.
- (2) The components of displacement and velocity of the interceptor relative to the target, along the three axes of the rotating rectangular coordinate system. These displacements are the relative position inputs required by the computer.
- (3) Time since start of the maneuver (t), the time dilation term ($T^* - kt$) and the required velocity correction (ΔV). Unless optimum $T^* - kt$ has been computed and used, a display of ΔV for several values of $T^* - kt$ may be presented to enable the pilot to select an improved course.

- (4) Thrust on-off switching criteria, V_a and V_d , for pilot activation of thrust commands.
- (5) The command angles θ_c and ψ_c , needed for proper thrust application. Again, a display of $\theta_c - \theta$ and $\psi_c - \psi$ may be helpful.

NASA TR R-128 Lineberry, Jr., and Foudriat (Reference 13)

Basic display requirements for this command system are essentially the same as those of Reference 15. Other displays which may be useful are:

- (1) (a) For a modulated thrust system

$$\frac{\dot{R}^2}{2R} \text{ versus } \frac{T_{MAX}}{m}$$

where $\frac{T_{MAX}}{m}$ is the acceleration available

- (b) For an on-off thrust system

$$\frac{\dot{R}^2}{2R} \text{ relative to the switching criteria}$$

$A_1 \frac{T}{m_0}$ and $A_2 \frac{T}{m_0}$, where A_1 and A_2 are constant with values

less than one. These displays would permit pilot control of the thrusters.

- (2) Displays of the command angles θ_c , and ψ_c , would be desirable for pilot attitude control. Displays of $\theta_c - \theta$ and $\psi_c - \psi$ should be helpful.

AAS Preprint 62-10, Stapleford (Reference 14)

In addition to the basic displays as evolved in Reference 15, a presentation of \dot{R} relative to the \dot{R}_{MAX} and \dot{R}_{MIN} on-off switching criteria for the longitudinal rocket engine appears desirable.

Display Requirements - Docking

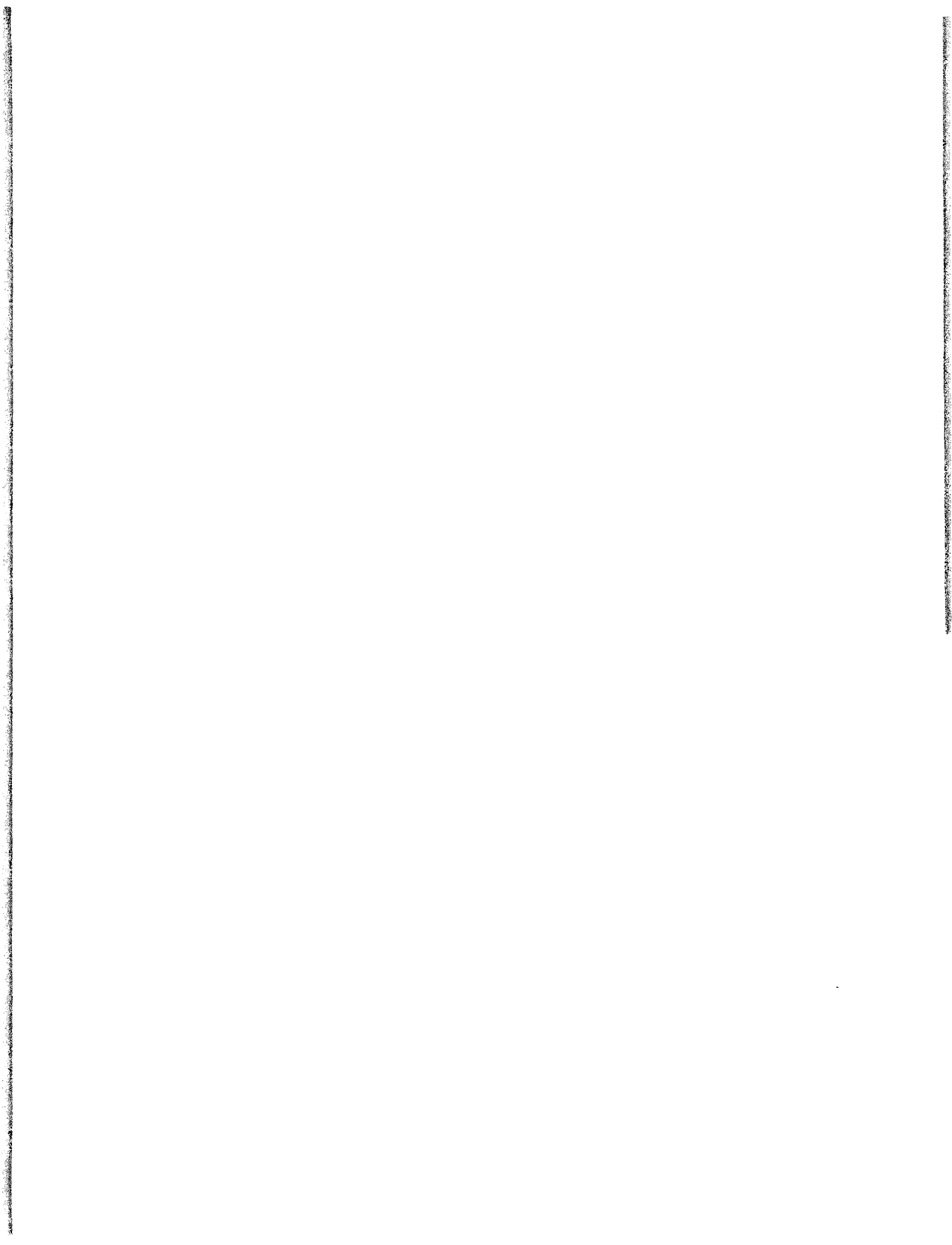
During docking, the interceptor's attitude angles will generally be restricted. Hence, if any displays are used in this phase, they will probably be similar to those listed for the system of Reference 14. It is quite likely, however, that the pilot will rely almost entirely on the view seen through windows and/or periscopes.

Display Requirements - Deorbit and Reentry

The information the pilot needs for deorbit and reentry has been discussed in References 1 and 29. However, the deorbit system described in Section IV-B-5 may utilize two retro firings instead of one. Thus, for deorbit, the pilot should be aware of:

$$R_{TG} = \text{range to go to his destination}$$

- R_c = cross range to his destination
 R_{TG}^h = range (or time) to go to his deorbit point
 ΔV_i^r = Impulse that will be required during the first firing of his rockets
 ΔV_{avail} = available ΔV
 θ_{c1} and θ_{c2} (one at a time) = the desired vehicle pitch attitude during the retro firings
 ΔV_h^r = impulse that will be required during the second firing of his rockets



V. DIGITAL SIMULATION

A. GENERAL

This section presents a description of a digital simulation made to determine the important computing requirements of the system illustrated by the diagram of Figure 28 and described in the preceding section. Important computer requirements include the computer inputs and outputs, accuracies, resolutions and ranges, the nature and amount of data which must be stored, the type of mathematical operations involved, computation cycle time, and flow chart functional diagrams. With this simulation, various mission runs have been made and are reported here. These runs confirm the adequacy and capabilities of the simulation and control techniques programmed. Detailed studies of the computing requirements based on this simulation are presented in this section also. Results obtained from an analog simulation are reported in Section VI.

This simulation, programmed on the IBM 7090 digital computer, incorporates a completely automatic system for both the aiming and thrusting commands. Because of the many possible configurations, operating modes and types of control, the digital program was made flexible so that a change of inputs or minor reprogramming in some of the subroutines is all that would be required for changing configurations or modes of operation.

Section B presents a description and general flow chart of the digital program. Section C presents a discussion and selection of data and gains used in the program, together with illustrative mission runs. Requirements for a digital computer are presented in Section D.

B. EQUATIONS AND FLOW DIAGRAMS

The general flow diagram of the simulation covering all phases of the rendezvous mission from radar acquisition through departure from docking is presented as Figure 50. The general format of the program follows the pattern of the 5 major blocks of Figure 28, each block being a separate subroutine in the program.

Features of the digital program are as follows:

- (1) ΔT was defined as the integration interval and unless specified otherwise, was used for all integrations in the program with two exceptions: First an integration interval, t_1 , was defined for use in the attitude loop. The value t_1 was made a factor N_3 of ΔT . By doing this, the integration interval of the attitude equations could be controlled separately from the rest of the program. Second, an integration interval t_2 was defined for the equations of motion involving the target and the interceptor (element No. 1 of Figure 28). Therefore, these equations too, could be integrated at time intervals smaller than the total loop interval, ΔT .
- (2) With regard to the attitude loop equations, ϵ_x , ϵ_y , and ϵ_z as described in Section IV-B-4, are used to generate M_{XB} , M_{YB} , and M_{ZB} moments, respectively. The expressions on Figure 41 for these moments were programmed as follows:

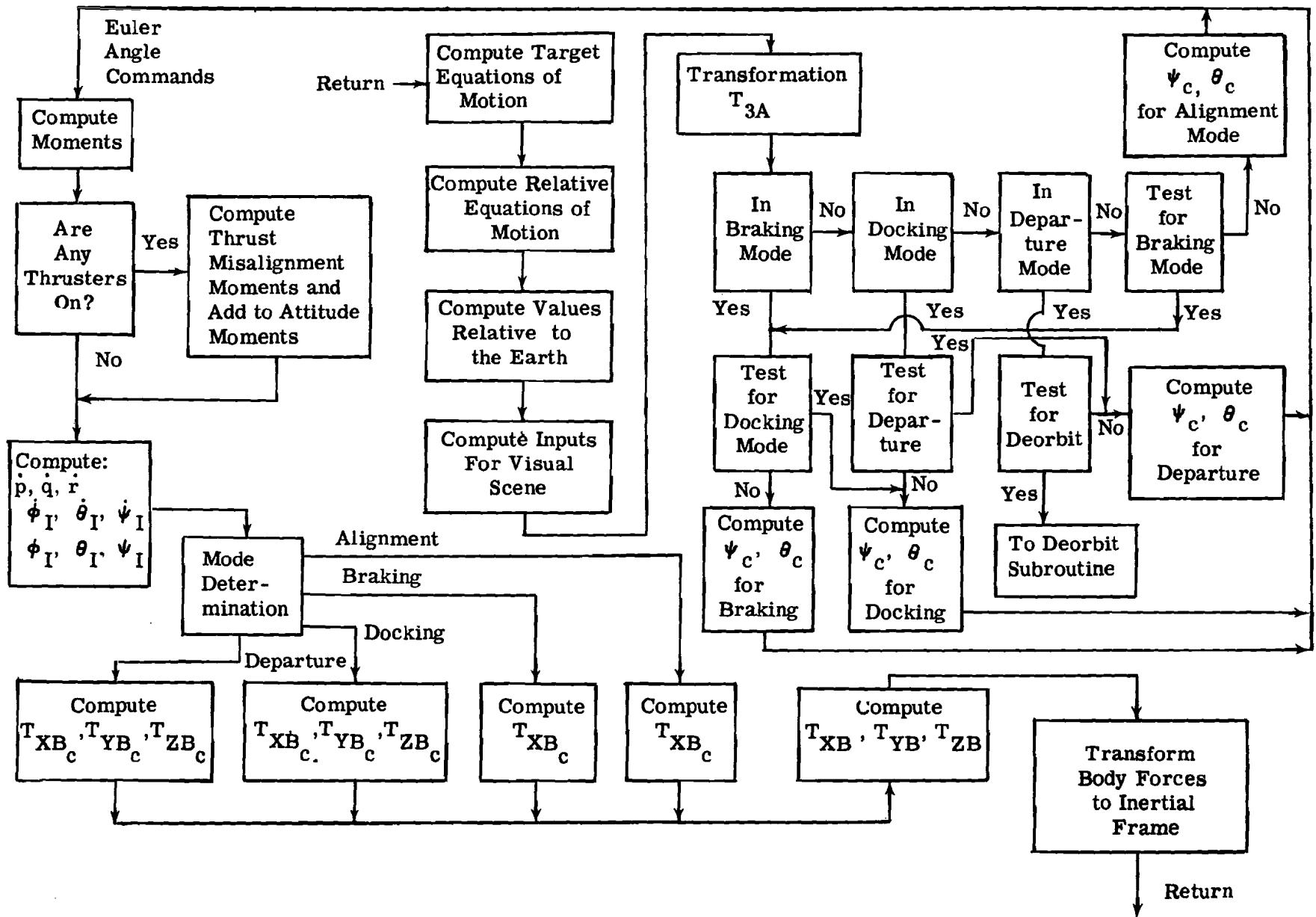


Figure 50. Digital Flow Chart

In roll,

$M_{XB_i} = \frac{K_6}{(\tau_\phi s + 1)} \xi_x$. To make this expression usable in digital format, the denominator was first multiplied through, giving

$$M_{XB} + \tau_\phi \dot{M}_{XB} = K_6 \xi_x$$

Then,

$$\dot{M}_{XB} \text{ was expressed as: } \frac{M_{XB_i} - M_{XB_{i-1}}}{t_1}$$

where t_1 = digital cycling time.

Replacing \dot{M}_{XB_i} in the equation above:

$$M_{XB_i} = \frac{K_6 \xi_x + M_{XB_{i-1}} - 1 \left(\frac{\tau_\phi}{t_1} \right)}{1 + \frac{\tau_\phi}{t_1}}$$

Likewise, similar expressions for $M_{Y_{Bi}}$ and $M_{Z_{Bi}}$ were formulated.

- (3) For purposes of the digital simulation, the system of Reference 13, as described in Section III, was chosen for the rendezvous phase (from acquisition to docking). This system is essentially an automated version of Reference 15. As described in Section III, this system is a proportional type, with three alternate techniques for accomplishing rendezvous: (1) A basic method (Technique 1) where the velocity normal to the line of sight is removed first, the closing speed is controlled afterward as a function of range. (2) A method for allowing a minimum time rendezvous within the fuel limits available for such a maneuver (Technique 2a). (3) A minimum energy method (Technique 2b). Two transformations are needed to supply the required inputs to the command equations; T_{3A} and T_{3C} , as given on page 70. An output transformation, T_{4C} , as given on page 71 will also be required, if technique 2a or 2b is used. The rendezvous phase was terminated when the range R was less than a specified value R_S , and, the relative velocity $\sqrt{\dot{x}^2 + \dot{y}^2 + \dot{z}^2}$ was less than R_S . When these tests are both satisfied, the docking mode is employed.
- (4) In docking, it is important that the interceptor maintain specified attitudes for visual control and latching purposes. The docking technique used in this program is the terminal rendezvous system proposed and studied by R. L. Stapleford in Reference 14 (Figure 19, Section III) scaled to the docking situation. In essence, expressions of \dot{R} , $R \dot{\alpha}$ and $R \dot{\beta} \cos \alpha$ versus R are used to command thrusts in the X_B , Y_B and Z_B directions, respectively, while the interceptor's X_B axis is aligned with the line of sight, and the interceptor's roll angle, ϕ_I , is maintained at zero. A selection of the gains and thrust command lines is given in the next section.
- (5) In element No. 4 of Figure 28, thrusts are commanded according to various expressions and control lines (discussed in Section V-C). The object of element No. 4 is to determine what forces can actually be employed, consistent with the thrusters which are available on the interceptor. To do this, logic has been included in the

program to supply the nearest thrust level to that commanded. The digital program also includes the calculation of the interceptor's mass as fuel is consumed for translational and attitude maneuvering, the ΔV potential of the remaining fuel, and the transformation of the forces applied along the interceptor's body axes to the inertially oriented coordinate system chosen for the relative equations of motion.

- (6) The method used for the departure was not changed from that presented in Section IV-B-9. The system for deorbit which was used is that of Reference 1, using a single retro. It is described in detail there and again in Section IV. In cases where deorbit was studied, the terminal conditions of the departure mode were used to update the deorbit subroutine, and the problem proceeded according to the flow chart of page 7 of Reference 1.

C. SIMULATED INTERCEPTOR

The vehicle configuration which has been selected is typical of interceptors in the current planning stage. In order to stay within the published capabilities of current boosters, a gross weight of 300 slugs was selected. Because vehicles of the Mercury and Gemini class are short, a length of 20 feet was also selected, with a radius of gyration in the Y_B and Z_B directions of 5 feet.

The interceptor employs 6 fixed thrusters for docking; 2 mounted in opposite directions in each of the three vehicle body axes. The X_B thruster magnitude is 200 pounds and the Y_B and Z_B thrusters are each 100 pounds.

For the terminal guidance phase, one thruster, fixed along the interceptor longitudinal axis ($-X_B$ direction as defined in Figure 38) was assumed. For most of the studies, this engine was provided with a variable thrust level, from 1000 pounds minimum to 10,000 pounds maximum.

Discussion as to why many of the above were chosen is presented in subsequent portions of this section. The various configuration parameters of the simulated vehicle are summarized in Table IV.

TABLE IV
SIMULATED VEHICLE PARAMETERS

A. PHYSICAL CHARACTERISTICS	
Mass	full = 300 slugs empty = 100 slugs
Length	= 20 feet
Radius of Gyration	X_B direction = 2 feet Y_B direction = 5 feet Z_B direction = 5 feet
Moments of Inertia	$I_x = 1800 \text{ slug feet}^2$ $I_y = 7500 \text{ slug feet}^2$ $I_z = 7500 \text{ slug feet}^2$

TABLE IV (CONT)

B. REACTION CONTROL ROCKETS FOR ATTITUDE CONTROL	
Maximum Control Moments (Minimum values are 10% of the maximum)	$M_{XB} = 150 \text{ ft lb}$ $M_{YB} = 800 \text{ ft lb}$ $M_{ZB} = 800 \text{ ft lb}$
C. TRANSLATIONAL THRUSTERS	
<u>1. Terminal Rendezvous Phase</u>	
X_B direction	$T_{V_{XB}} = 1000 \text{ to } 10,000 \text{ lb}$
<u>2. Docking Phase</u>	
X_B direction	$T_{XB} = 200 \text{ lb}$
Y_B direction	$T_{YB} = 100 \text{ lb}$
Z_B direction	$T_{ZB} = 100 \text{ lb}$

D. DATA INPUTS, GAIN SELECTIONS, AND MISSION RUNS

1. Attitude Control System

The proportional thrust attitude control system as illustrated in Figure 41 has been employed in this digital simulation. A number of separate attitude control system test runs were made to determine satisfactory values for the gains and constants required for this system. In these test runs, a very short cycling time (0.010 second) was used to insure that computer cycling time did not interfere with the operation of the attitude control loop while gains and constants were being selected. The following values were found to provide a reasonably well damped performance and, therefore, have been selected as typical:

<u>Parameter</u>	<u>Description</u>	<u>Value</u>
K_{ψ}	Yaw Attitude Gain	1.1
K_{θ}	Pitch Attitude Gain	1.1
K_{ϕ}	Roll Attitude Gain	4.0
K_1	Yaw Rate Gain	1.0
K_2	Pitch Rate Gain	1.0
K_3	Roll Rate Gain	4.0
K_4	Yaw Max. Moment/Inertia	25,300
K_5	Pitch Max. Moment/Inertia	25,300
K_6	Roll Max. Moment/Inertia	1800

To limit overshoots resulting from large angular commands, p_{ξ} , q_{ξ} , and r_{ξ} values (see Figure 42) were limited to 14 deg/sec.

In order to determine what computer cycling time, t_1 , would be reasonable in the attitude control loop, a series of runs were made with step command inputs and with computer cycling time varying from 0.025 to 0.25 second. The results of some of these runs are presented in Figure 51 where it is seen that for the long cycling time ($t_1 = 0.25$ second), a transient appears in the ψ_I trace which, if allowed further running time, would continue to oscillate (periodically). For cycling times of 0.025 and 0.050 second, the time histories are smooth and faithfully computed.

Since an attitude control system based on fixed on-off jets is a real possibility, the effects of various cycling times on such a system were also studied. For this system, only the maximum values of reaction control thrust as used in the previous case with variable jets were retained. Thrusts were turned on when corresponding error signals called for

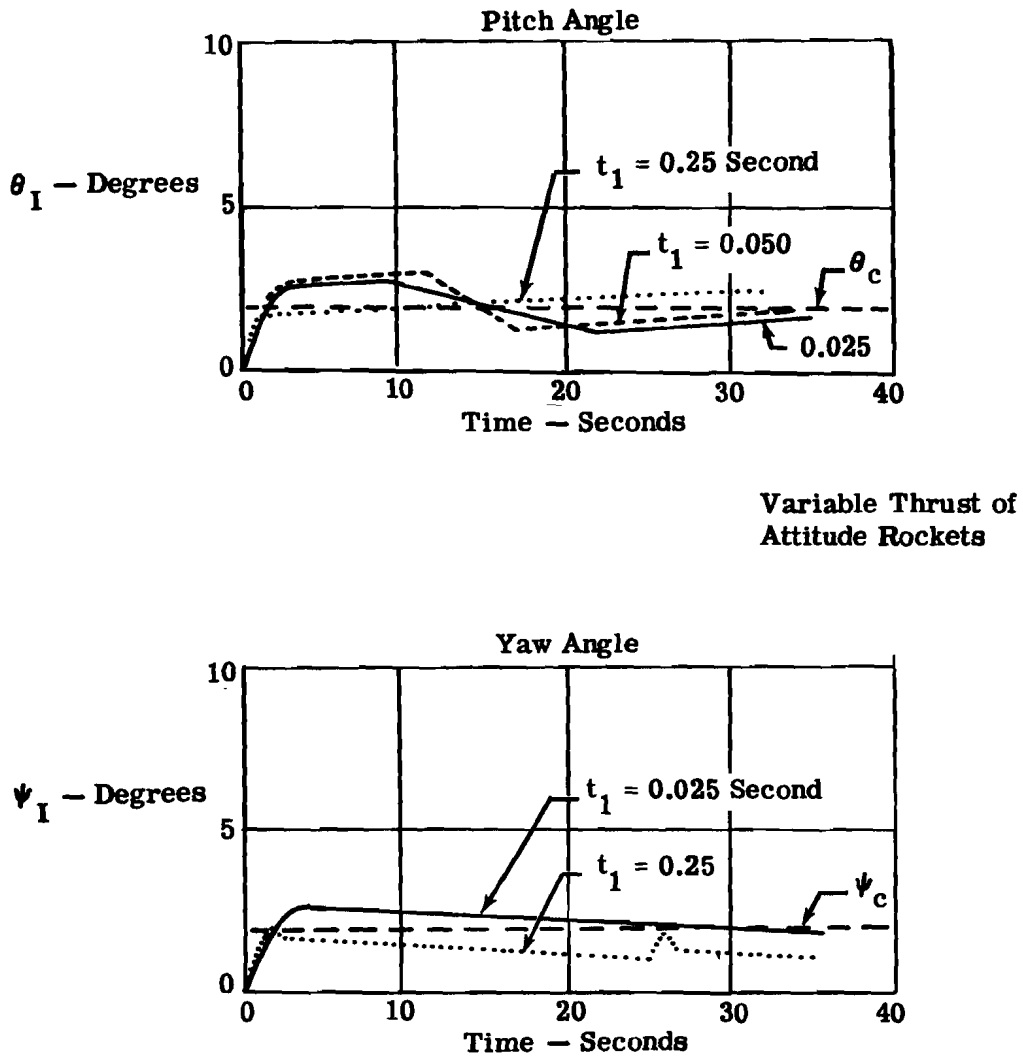


Figure 51. Attitude Loop Cycle Time Studies - Case 1

thrust over one-half the values supplied by the jets. For a series of test runs, the interceptor was oriented such that $\psi_I = 0$ and $\theta_I = 0$. A command of 20 degrees was put in for ψ_C and 10 degrees for θ_C . In successive runs of this series, t_1 was varied from 0.025 to 0.250 second. Results for this system show that computer cycling times of 0.025 and 0.050 produce long limit cycle times which should not interfere with the operation of the attitude loop. As the computer cycling times were increased to 0.125 and 0.250 second, a somewhat higher frequency limit cycle resulted (Figure 52).

From these studies, involving both variable and fixed thrust levels, it was concluded that a cycling time, t_1 , of 0.050 second for the attitude loop should suffice in most, if not all, cases. Except where noted, this integration interval has been used for the attitude loop during the mission runs reported later in this section.

2. Docking Translational System

As an aid to the selection of gains and command lines for automatically controlled docking, terminal conditions of range = 80 ± 20 feet and range rate = 1 ± 0.4 ft/sec have been selected.

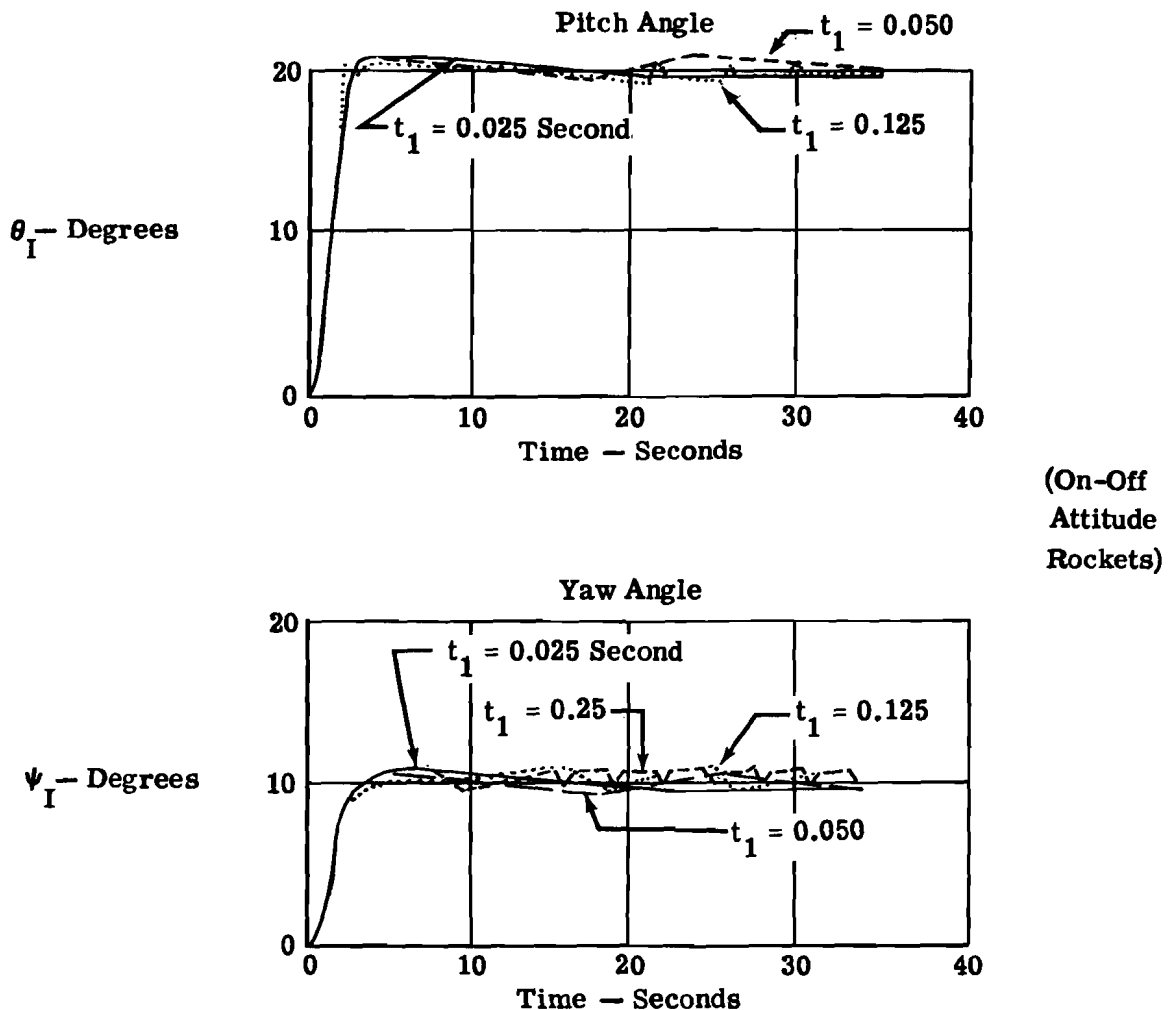


Figure 52. Attitude Loop Cycle Time Studies - Case 2

a. Command Gains for Range and Range Rate Control

The final range and range rate conditions for the terminal guidance phase correspond to the initial conditions for docking. Although the dividing line between the terminal guidance phase and docking is somewhat arbitrary, for purposes of this study, a closing speed of 50 ft/sec ($-\dot{R}$) at a separation distance of 3000 ft (R) have been selected as typical "start of docking" conditions. Since the main thruster will be turned off when the docking phase is entered, it is necessary to supply sufficient thrust to the docking thruster to easily handle this remaining velocity. The minimum acceleration needed for these conditions (50 ft/sec at 3000 ft) is given by

$$a_T = \frac{\dot{R}^2}{2R} = 0.013 \text{ g}$$

In the digital simulation, 0.02 g was selected as the minimum longitudinal thrust for docking. This thruster has the capability of controlling over 60 ft/sec at 3000 feet, or of eliminating 50 ft/sec within 2000 feet. This gives a margin of 10 ft/sec or 1000 feet, both of which appear adequate. To establish the thruster "on" boundary, a plot of \dot{R} versus R was made and a line was drawn from the origin to 50 ft/sec at $R = 2300$ feet (Figure 53). A separation distance of 80 feet was taken between the "off" and "on" command lines, and the "off" line was drawn parallel to the "on" line. The "on" command line passes through 60 feet at 1.4 ft/sec and the "off" command line through 0.6 ft/sec at 100 feet. Thus, the limits for end of "automatic docking" discussed above are respected.

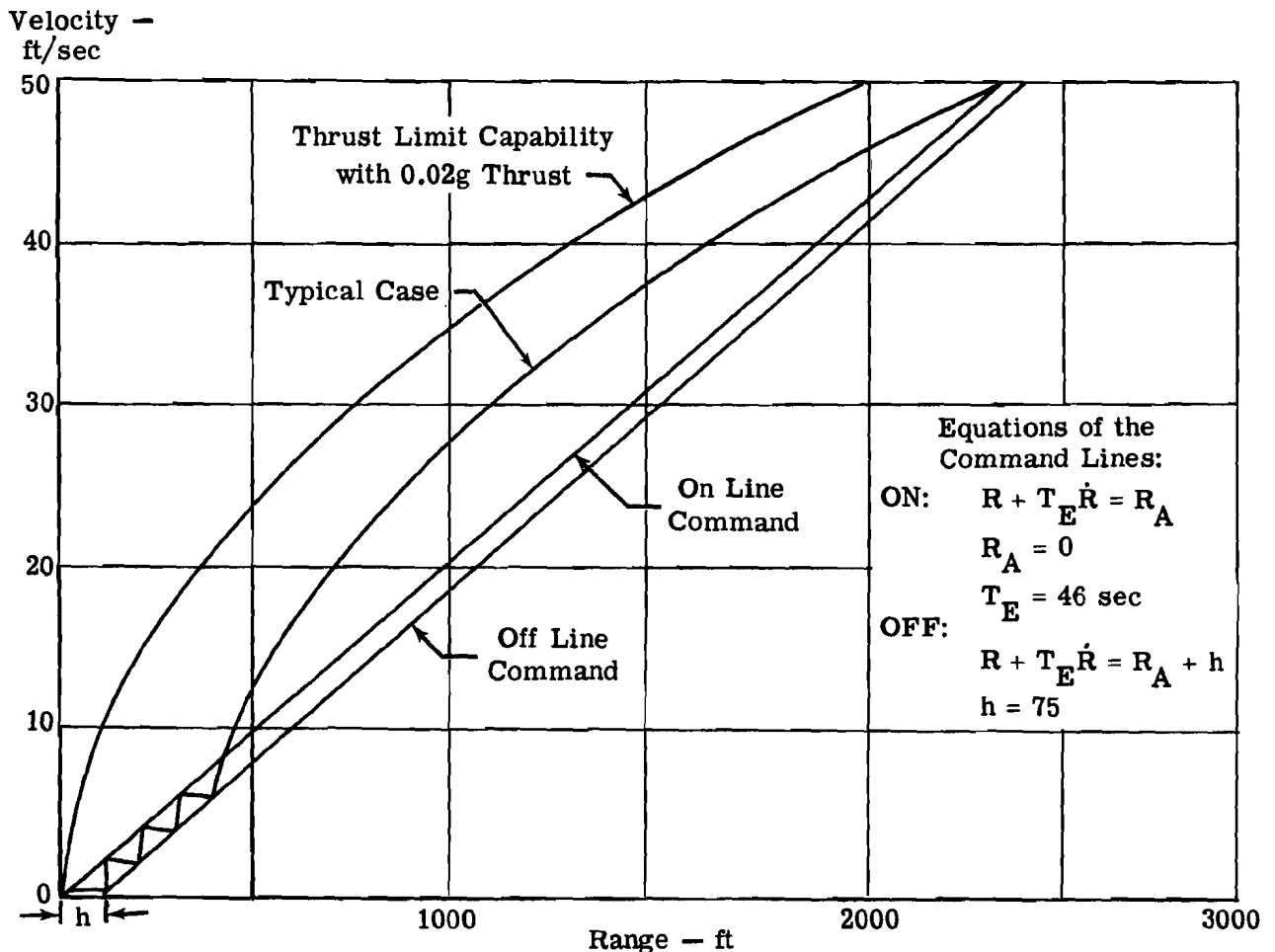


Figure 53. Command Lines for Range and Range Rate Control

With the command lines shown on Figure 53, the interceptor, after the end of a typical braking mission, will continue to close without thrust until the "on" command line is crossed. At this point thrust is actuated in the X_B axis, which is aligned with the line of sight. Thrust will remain "on" until \dot{R} and R are reduced to the point where the "off" command line is crossed. From this point to the end of docking, the thrust will be turned "on" and "off", as is appropriate to keep \dot{R} between the command lines until the terminal docking conditions are met.

b. Command Gains for $R\dot{\alpha}$ and $R\dot{\beta} \cos \alpha$

If braking has been properly executed, $R\dot{\alpha}$ and $R\dot{\beta} \cos \alpha$ values will be reduced to a few ft/sec when docking is initiated. For thruster sizing, however, a maximum of 14 ft/sec has been assumed. Therefore, the interceptor should have thrust great enough to keep both $R\dot{\alpha}$ or $R\dot{\beta} \cos \alpha$ below a linear command line, passing through 14 ft/sec and 3000 feet as shown in Figure 54.

Using the "on" command line of this figure, the minimum acceleration needed in the $R\dot{\alpha}$ and $R\dot{\beta} \cos \alpha$ directions was calculated as 0.00675 g. To be conservative, 0.01 g was selected. The "on" command line for control along the Y_B axis, as discussed above, can be expressed as:

$$R\dot{\beta} \cos \alpha > a + bR$$

where $a = 0$; $b = 0.00435$

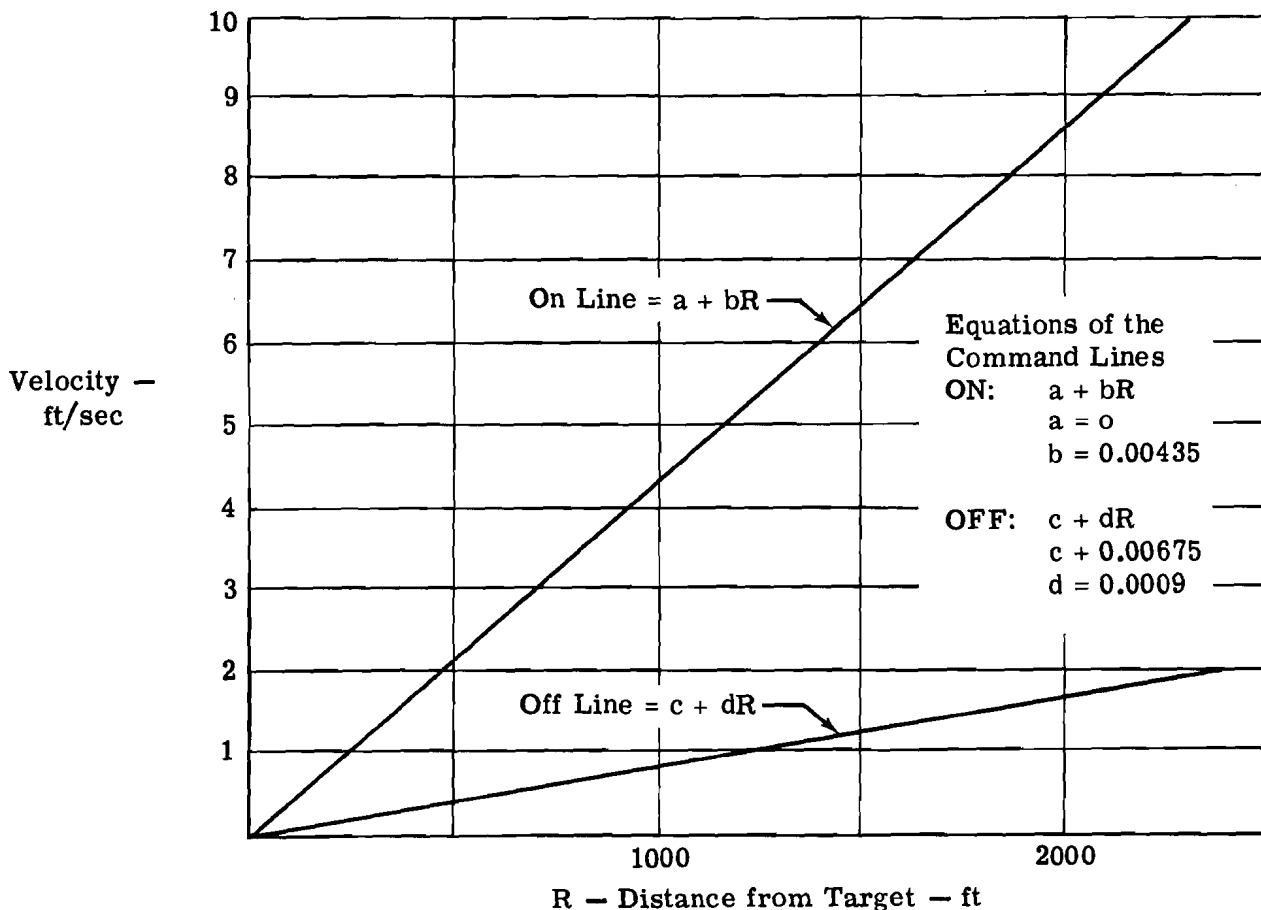


Figure 54. Command Lines for $R\dot{\alpha}$ and $R\dot{\beta} \cos \alpha$

The "off" equation is less restrictive. It should be such that $R \dot{\beta} \cos \alpha$ are small values. Thus, the "off" line has been drawn through $R = 80$ feet to 2 ft/sec at 2300 feet. This results in the expression:

$$R \dot{\beta} \cos \alpha < c + dR$$

where $d = 0.00090$

and $c = -0.00675$

The above constants also apply to $R \dot{\alpha}$ control, hence,

$$e + fR: e = 0; f = 0.00435$$

$$g + hR: g = -0.00675; h = 0.0009$$

A summary of these results is shown in Figure 54.

Mission Run No. 1 - Docking

In order to demonstrate the program, the input gains and constants, and the capabilities of the docking mode, a typical run (Mission Run No. 1) was made. The following constants and initial starting values were used.

Altitude, h , = 1,824,000 ft

$$\theta_o = -30^\circ$$

$$\dot{\theta}_o = 0$$

$$\psi_o = 0$$

$$\dot{\psi}_o = 0$$

$$\phi_o = 0$$

$$\dot{\phi}_o = 0$$

$$\alpha_o = -30^\circ$$

$$\beta_o = 0$$

$$R = 3000 \text{ ft}$$

t_1 = the integration interval for the attitude loop = 0.125 second

$$\dot{R} = -50 \text{ ft/sec}$$

$$R \dot{\alpha} = 10 \text{ ft/sec}$$

$$R \dot{\beta} \cos \alpha = 9.6 \text{ ft/sec}$$

$$t_2 = \text{the integration interval for the relative equations of motion} = 0.25 \text{ second}$$

$$\Delta T = \text{the loop integration interval} = 0.25 \text{ second}$$

Results of this run are given in Figures 55 through 57, which illustrate satisfactory operation of the simulation. Docking end conditions were satisfied at 181 seconds, with the interceptor 100 feet away, closing directly at the target at 0.77 ft/sec.

3. Rendezvous - Selection of Gains and Constants

a. Braking Mode

A configuration has been selected (Table IV) which has a 1 g thrust capability at gross weight. The command equation for braking thrust, T_{X_c} , as obtained from the system of Reference 13, is:

$$T_{X_c} = m \left\{ a_{LOS} - K_a \left[a_{LOS} - \frac{\dot{R}^2}{2(R - R_a)} \right] \right\}$$

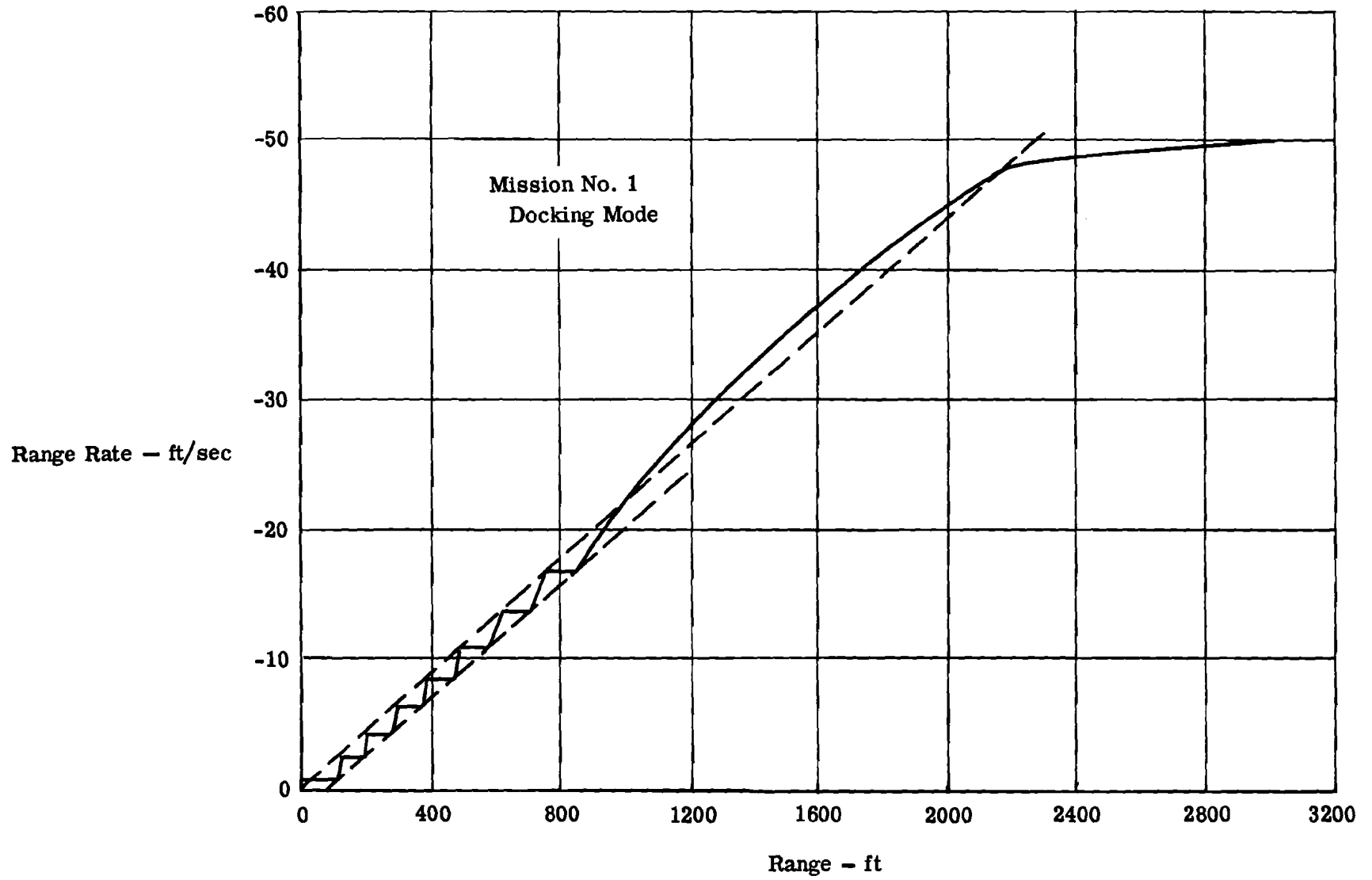


Figure 55. Mission Run No. 1 -- Range Rate versus Range

$R\dot{\beta} \cos \alpha$ and $R\dot{\alpha}$
(ft/sec)

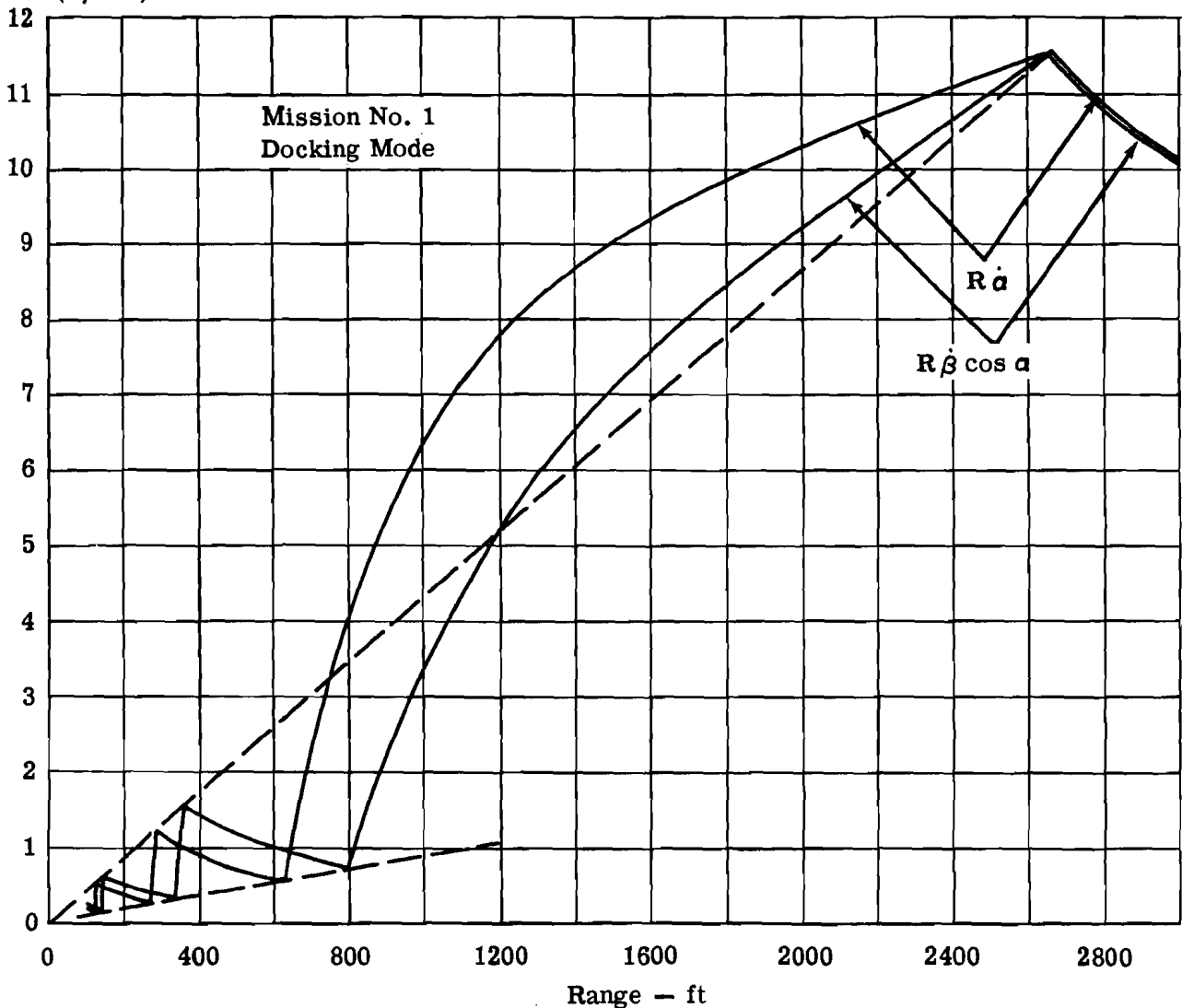


Figure 56. Mission Run No. 1 - $R\dot{\alpha}$ and $R\dot{\beta} \cos \alpha$ versus Range

In this expression, a_{LOS} represents a "nominal" type of acceleration; the term $\left(\frac{\dot{R}^2}{2(R-R_a)}\right)$ by itself represents an acceleration required of the interceptor to reduce \dot{R} to zero at a range $R = R_a$, and K_a represents a gain constant. In this expression, if \dot{R} versus R is such that the term $\frac{\dot{R}^2}{2(R-R_a)}$ is greater than a_{LOS} (point 1 of Figure 58), T_{X_c} will be increased in a manner such that the interceptor will accelerate greater than a_{LOS} . If $\frac{\dot{R}^2}{2(R-R_a)}$ is less than a_{LOS} (point 2), T_{X_c} will be commanded at a value proportionally less than needed for a_{LOS} , and point 2 will proceed toward the "nominal" a_{LOS} line. a_{LOS} was selected at 0.5 g; thus, at a maximum distance of 300,000 feet (50 n. mi.), the time to rendezvous, if flying nominally, is 140 seconds.

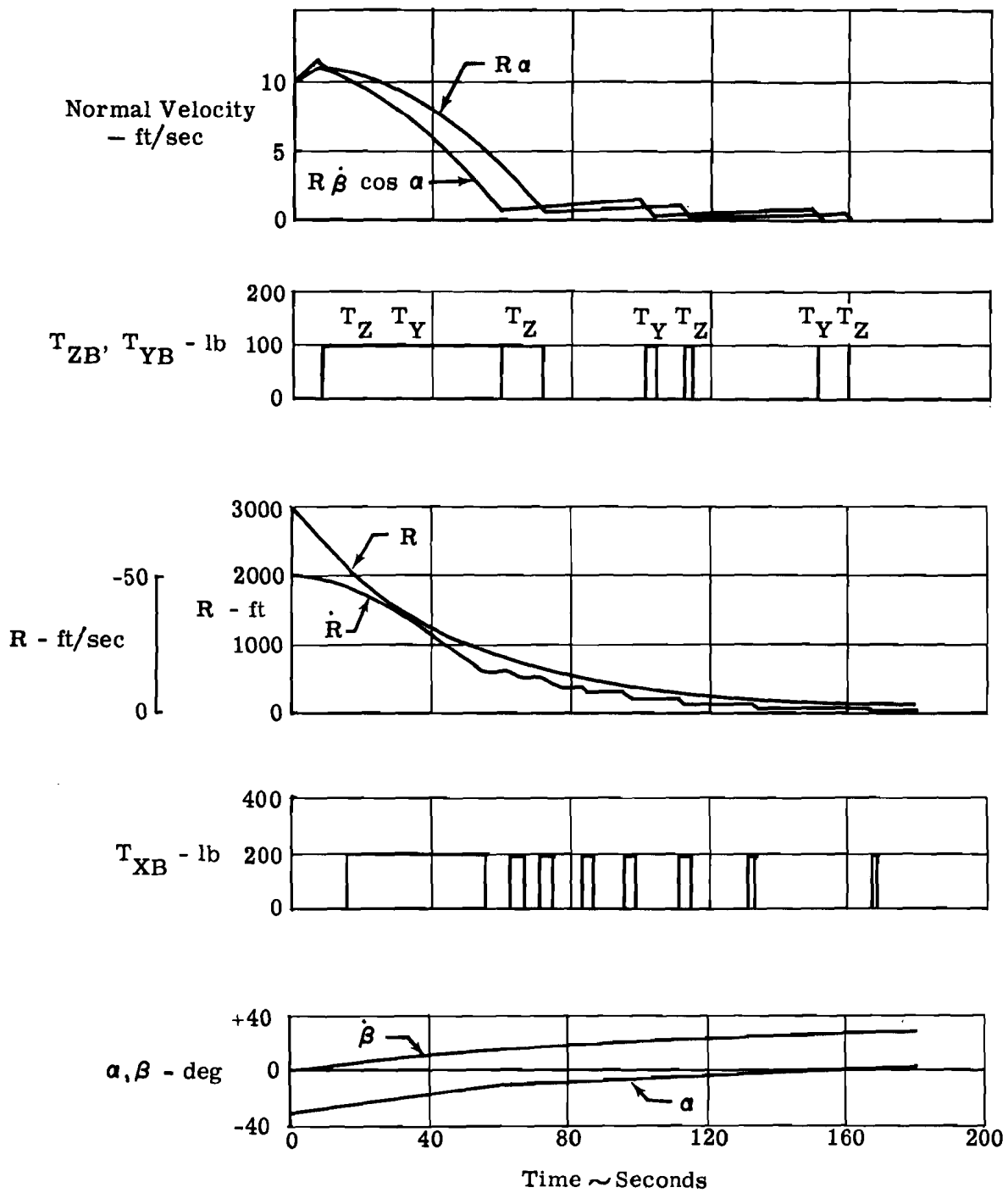


Figure 57. Mission Run No. 1 - Time History

In setting up the expressions for docking, it was assumed that the braking mode reduces the velocity of the interceptor to 50 ft/sec by the time $R = 3000$ feet. This requires an offset distance, R_a , of 2922 feet.

The minimum value for K_a is 1.0; otherwise $(T_{X_c})_{\max}$ will not be commanded when \dot{R} versus R is at the maximum capability line (Figure 58). However, if this minimum value were used, the command equation would degenerate to $T_{X_c} = m_1 \left(\frac{\dot{R}^2}{2(R-R_a)} \right)$. In other

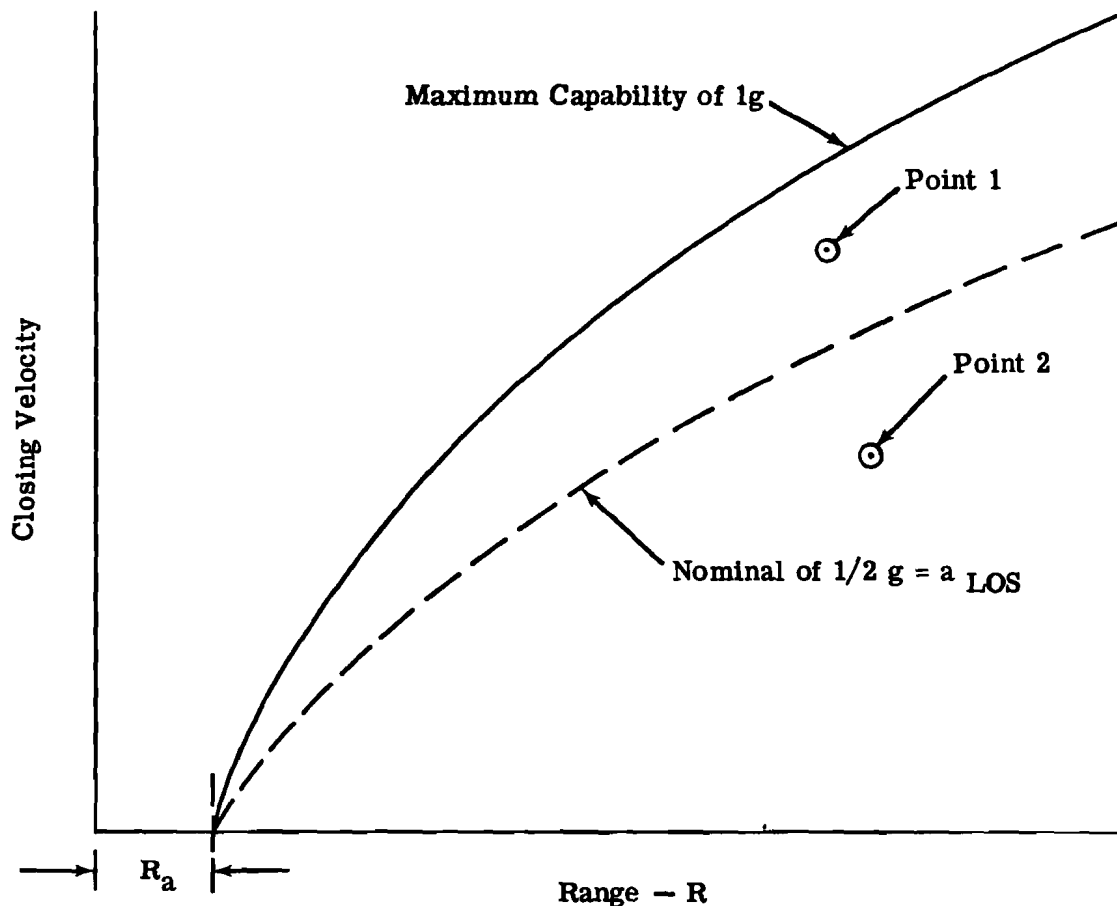


Figure 58. Acceleration Capabilities

words, the nominal 0.5 g line would not be reached until the end of flight. In order to return the vehicle to "nominal" in a reasonable time, $K_a = 3$ was selected.

During braking, $R\dot{\alpha}$ and $R\dot{\beta} \cos \alpha$ are controlled by vectoring the thrust off the line of sight by commanding:

$$\psi_c = -\beta + C_1 R \dot{\beta}$$

$$\theta_c = \alpha - C_1 R \dot{\alpha}$$

where C_1 is the gain, determining the angle the thruster makes with the LOS. C_1 should be small enough that $C_1 R \dot{\beta}$ and $C_1 R \dot{\alpha}$ increments remain within reason ($< 40^\circ$). By the same token, C_1 should be large enough to remove $R\dot{\alpha}$ and $R\dot{\beta} \cos \alpha$ promptly.

A series of test runs were made trying various values of C_1 . From these runs, 0.004 rad/ft/sec was found to be a satisfactory value for most cases. Unless otherwise specified, subsequent mission runs presented in this report used this value.

Several runs with varying initial conditions were made to demonstrate operation in the braking mode, the transition to this mode, and continued operation in the docking mode. The first case presented is Mission Run No. 2. Initial conditions for this run are as follows:

Mission Run No. 2 - Braking and Docking

$$\begin{aligned} \alpha_o &= -26.5^\circ \\ \beta_o &= 0^\circ \\ R &= 112,000 \text{ ft} \\ R\dot{\alpha} &= 62 \text{ ft/sec} \\ R\dot{\beta} \cos \alpha &= 50 \text{ ft/sec} \\ \dot{R} &= -1863 \text{ ft/sec} \\ \theta_o &= -26^\circ \\ \psi_o &= 0 \end{aligned}$$

The integration interval used for the attitude loop was 0.050 second.

Under the above starting conditions, the initial Euler angle commands were:

$$\begin{aligned} \psi_c &= 12.8^\circ \\ \theta_c &= -40.8^\circ \end{aligned}$$

Therefore, using the automatic attitude command system described in Section V-D-1, it took 10 seconds to achieve the commanded angles, whereupon thrusting in the X_B direction was initiated. $R\dot{\alpha}$ and $R\dot{\beta} \cos \alpha$ velocities were effectively eliminated during braking and the interceptor entered docking with the conditions: (Figure 59)

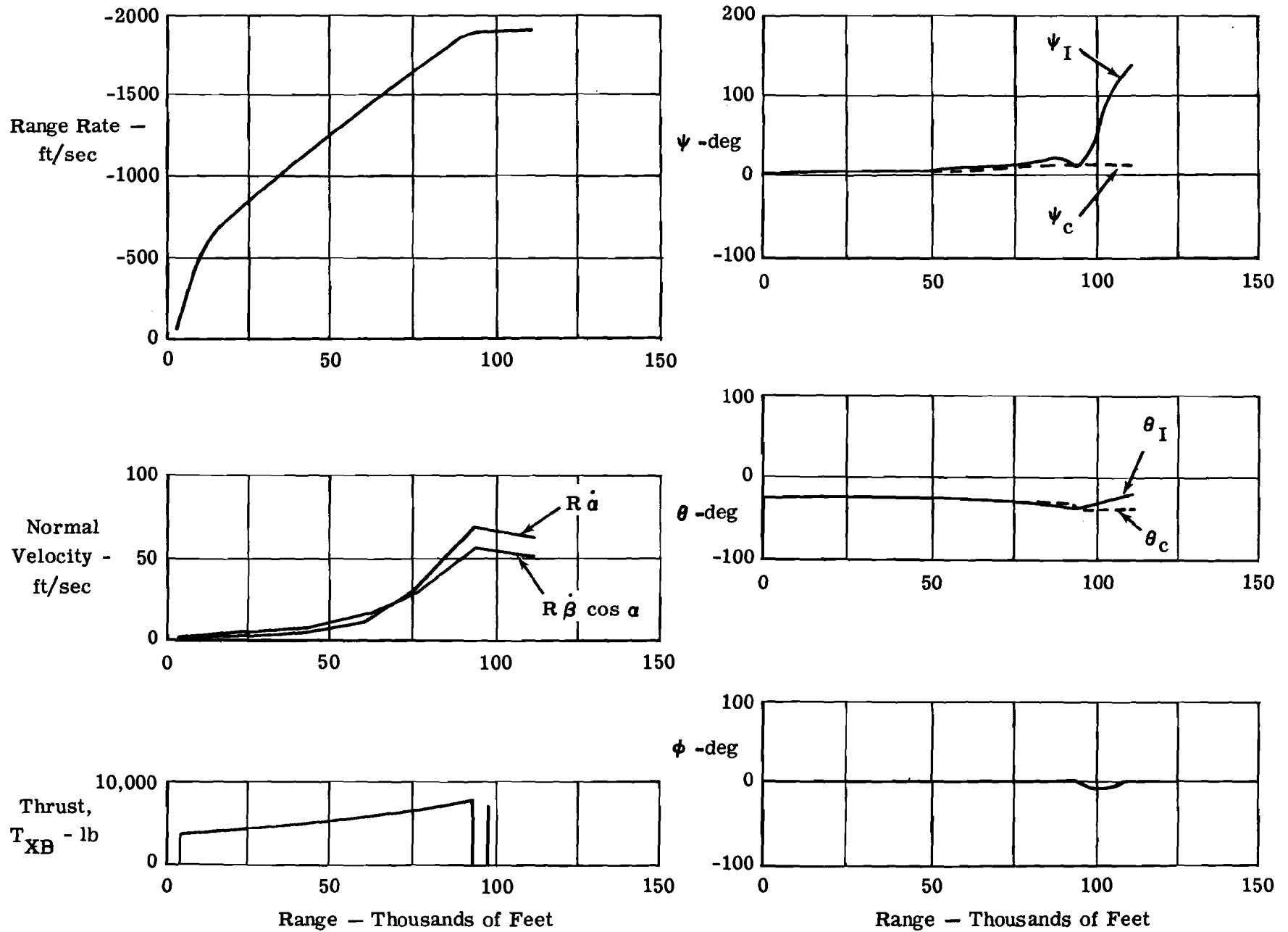


Figure 59. Mission Run No. 2 - Time History of Braking Phase

$$\begin{aligned}
R &= 3000 \text{ ft} \\
\dot{R} &= -47 \text{ ft/sec} \\
R\dot{\alpha} &= 0.28 \text{ ft/sec} \\
R\dot{\beta} \cos \alpha &= 0.90 \text{ ft/sec}
\end{aligned}$$

The conditions at end of the docking phase were:

$$\begin{aligned}
R &= 100 \text{ ft/sec} \\
\dot{R} &= -0.95 \text{ ft/sec}
\end{aligned}$$

with the interceptor proceeding directly toward the target vehicle.

Mission Run No. 3 - Braking and Docking

Mission Run No. 3 was conducted to demonstrate braking and docking with an initial out-of-plane position defined by $\beta = 14$ degrees. Initial conditions were as follows:

$$\begin{aligned}
\alpha_0 &= -25.5^\circ \\
\beta_0 &= -13.6^\circ \\
R &= 113,575 \text{ ft} \\
\dot{R} &= -1760 \text{ ft/sec} \\
R\dot{\alpha} &= 34 \text{ ft/sec} \\
R\dot{\beta} \cos \alpha &= 37 \text{ ft/sec} \\
\theta_0 &= -33.5^\circ \\
\psi_0 &= 23^\circ
\end{aligned}$$

In this case, it was assumed that the interceptor's X_B axis was initially pointed at the target vehicle so that the pilot could view the target. This case is typical of the initial conditions that might exist if the interceptor were boosted from the ground (in a launch trajectory as described in Figure 1 of Section II) where he approaches from a position ahead of and below the target vehicle. Hypothetical errors during boost have also put the interceptor to the target's right. At the start of rendezvous, the interceptor is travelling in a plane which is approximately 1 degree inclined with the orbital plane of the target vehicle.

At the start of this run, the variable X_B thruster was turned on. From this point, the interceptor continued braking, reducing $-\dot{R}$ and $R\dot{\alpha}$ and $R\dot{\beta} \cos \alpha$ as expected. At $t = 336$ seconds, the docking mode was automatically employed.

The interceptor successfully completed this phase. The final conditions were:

$$\begin{aligned}
R &= 73 \text{ ft} \\
\dot{R} &= -1.6 \text{ ft/sec} \\
R\dot{\alpha} \text{ and } R\dot{\beta} \cos \alpha &\text{ virtually negligible}
\end{aligned}$$

Mission Run No. 4. - Braking and Docking

In this run, a complete braking and docking mission starting at 40 n. mi. separation is simulated. The initial conditions listed in the following are typical of those

expected when the interceptor transfers to get into terminal guidance position from a higher orbit, with a slight orbital inclination.

$$\begin{aligned} \alpha_0 &= 2^\circ \\ \beta_0 &= -151^\circ \\ R &= 287,000 \text{ ft} \\ \dot{R} &= -2311 \text{ ft/sec} \\ R \dot{\alpha} &= -19 \text{ ft/sec} \\ R \beta \cos \alpha &= -31 \text{ ft/sec} \end{aligned}$$

The initial attitude was chosen so that the vehicle was aimed straight at the target vehicle; i.e.,

$$\begin{aligned} \psi_0 &= 151^\circ \\ \theta_0 &= 2^\circ \end{aligned}$$

These conditions give an orbital inclination of 2.8 degrees of the interceptor with respect to the target's orbital plane. The braking mode was entered directly, since $R \dot{\alpha}$ and $R \beta \cos \alpha$ normal velocities were low and the interceptor was on a reasonable collision course. Because of the large range relative to the closing velocity, the control system did not command a braking thrust for 15 seconds, until the range had reduced to 250,000 feet.

The braking phase proceeded smoothly and, at 200 seconds, conditions were satisfied for entering the docking phase. At 380 seconds, terminal conditions on docking were satisfied.

b. Alignment Mode

Figures 55 through 64 present three mission runs demonstrating the braking and docking modes as programmed on the IBM-7090. Figures 65 through 68 present three additional runs, including braking and docking, but also employing varieties of Techniques 1 and 2 of the alignment mode. Each case is explained as the mission run is presented.

For the alignment mode, the interceptor vehicle was provided with an on-off fixed thruster aligned along the X_B axis. For Mission Runs No. 5 and 6, a 3000-pound capability was provided. For Mission Run No. 7, a 7500-pound capability was provided.

Mission Run No. 5 - Alignment, Braking, and Docking

The initial conditions for this mission are listed on Figure 65. Here an alignment maneuver using Technique 1 was employed to eliminate the initial $R \dot{\alpha}$ and $R \beta \cos \alpha$ velocities. As discussed in Section III, Technique 1 commands the interceptor into an attitude position such that thrusting along the X_B axis directly eliminates the component of velocity normal to the line of sight; hence, $R \dot{\alpha}$ and $R \beta \cos \alpha$ components of velocity are effectively eliminated.

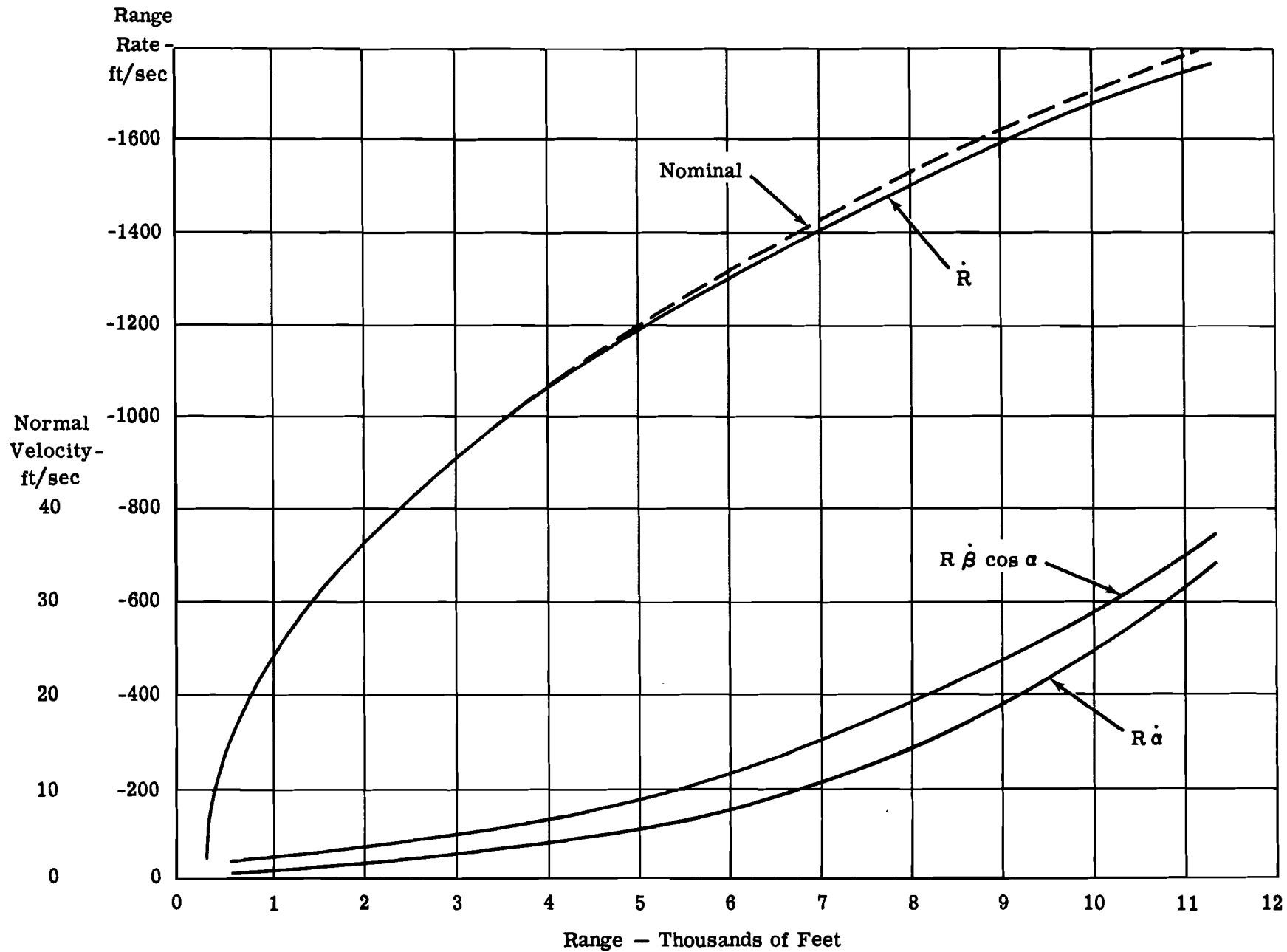


Figure 60. Mission Run No. 3-Range Rate, $R \dot{\alpha}$ and $R \dot{\beta} \cos \alpha$ versus Range for Braking Phase

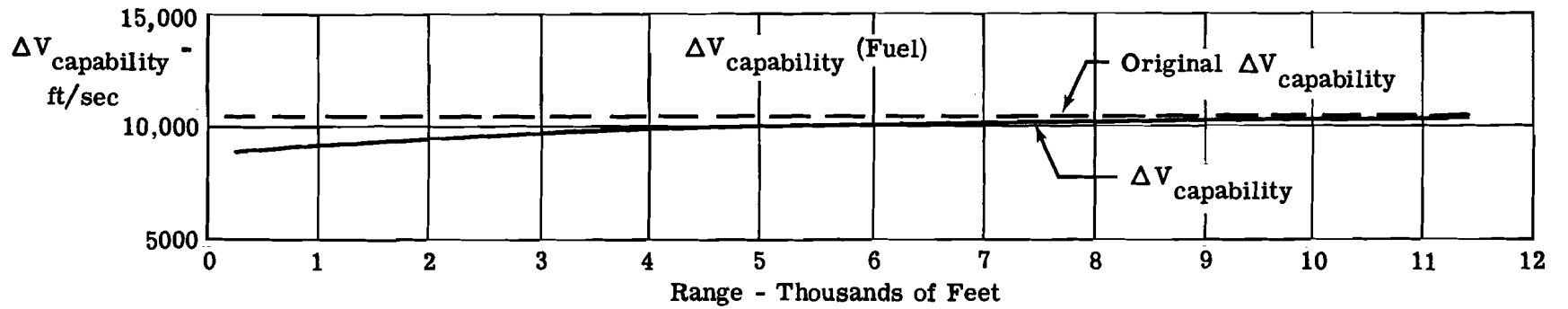
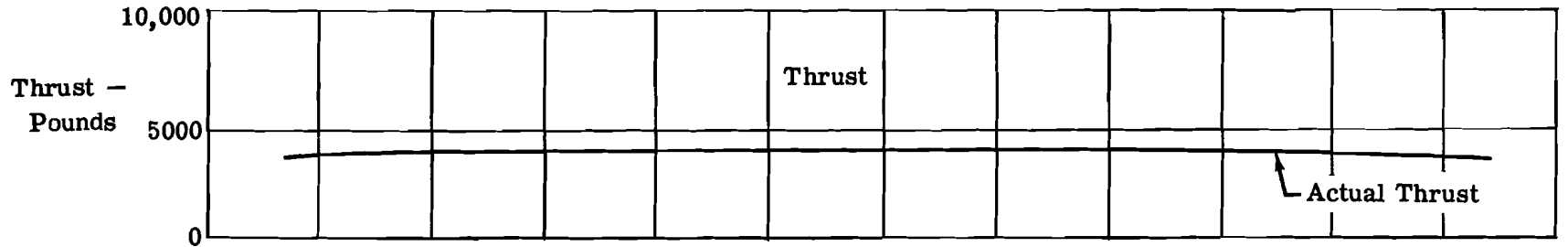
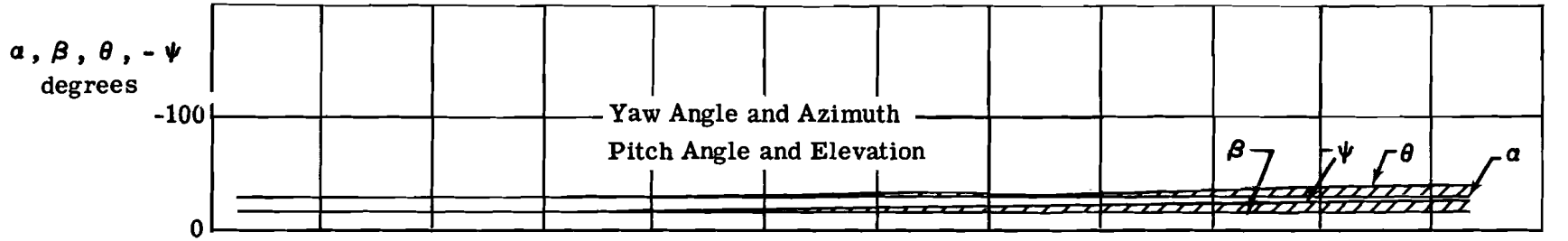


Figure 61. Mission Run No. 3 - Angles, Thrust and ΔV_{cap} versus Range (Braking Phase)

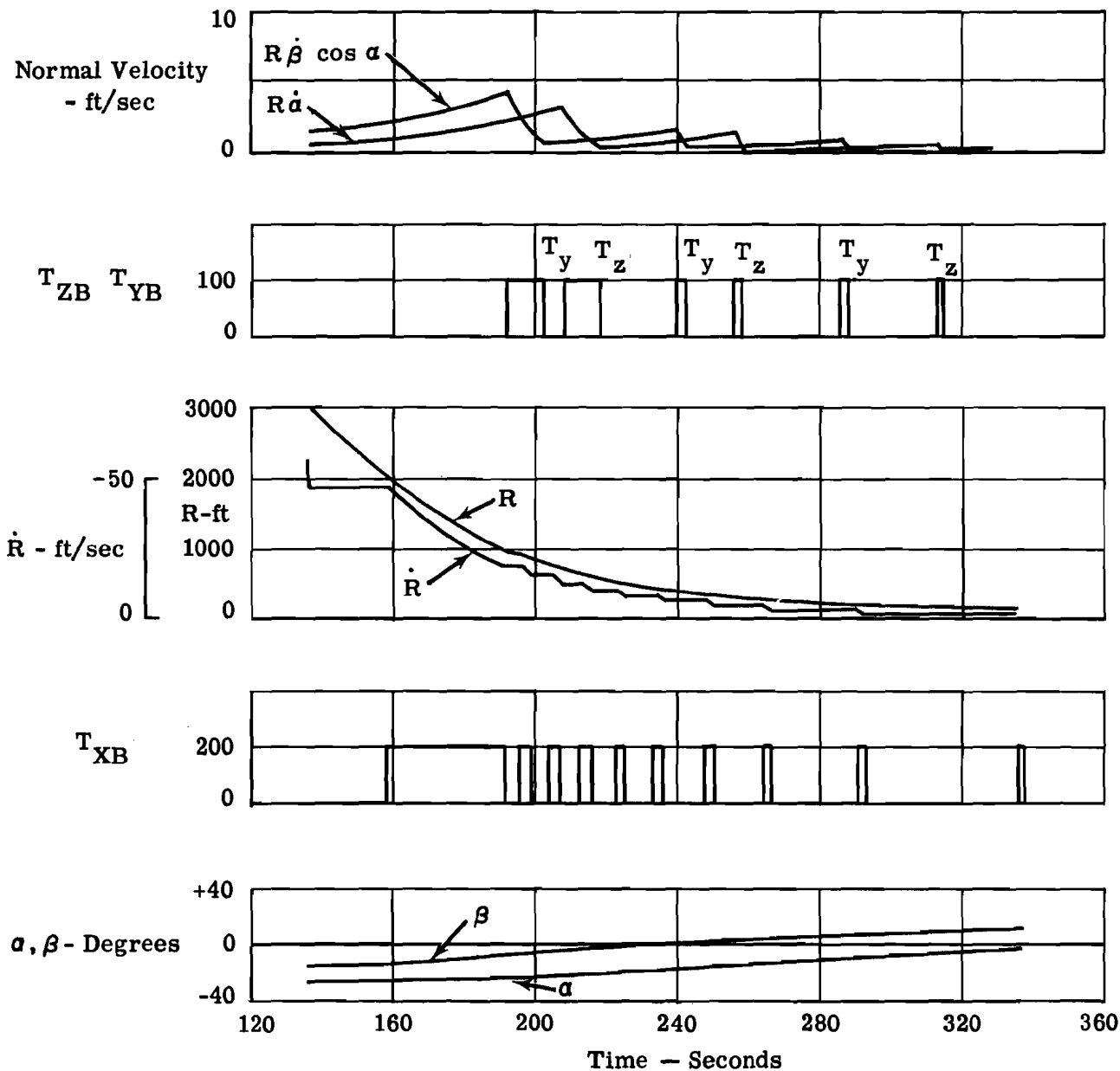


Figure 62. Docking Phase, Mission Run No. 3

At the start of the run, $\psi_c = 129^\circ$ and $\theta_c = -41.2^\circ$. Therefore, from $\psi_I = 13.0^\circ$ and $\theta_I = -26^\circ$, the interceptor pitched and yawed, until the commanded values were obtained. This took approximately 11 seconds, following which 3000 pounds of thrust was applied, reducing the total V_N to 1.86 ft/sec in 9 seconds. At this point, the braking mode was initiated, and ψ_c changed from 126 to 142° and θ_c from -38 to -26°. After another 9 seconds, the interceptor had pitched and yawed to its newly commanded values, and the variable thruster turned on with a near maximum value of 9014 pounds. At 127 seconds, docking mode conditions were satisfied. At $t = 312$ seconds, terminal conditions for docking were satisfied. The interceptor was allowed to approach the target vehicle from this point, without further thrust. It passed within 24 feet of the center of the target vehicle.

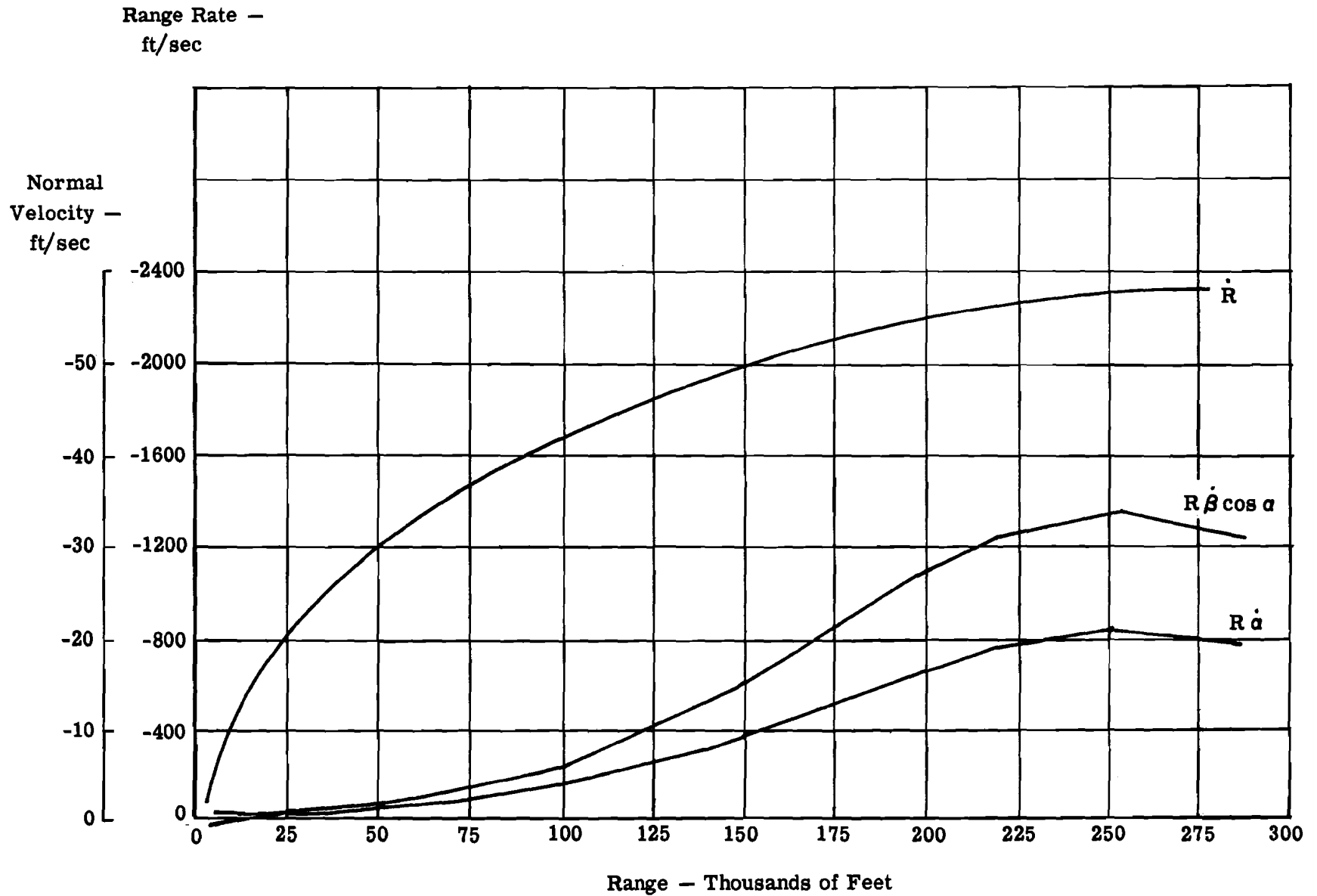


Figure 63. Mission Run No. 4 — Range Rate, $R\dot{\alpha}$ and $R\dot{\beta} \cos \alpha$ versus Range for Braking Phase

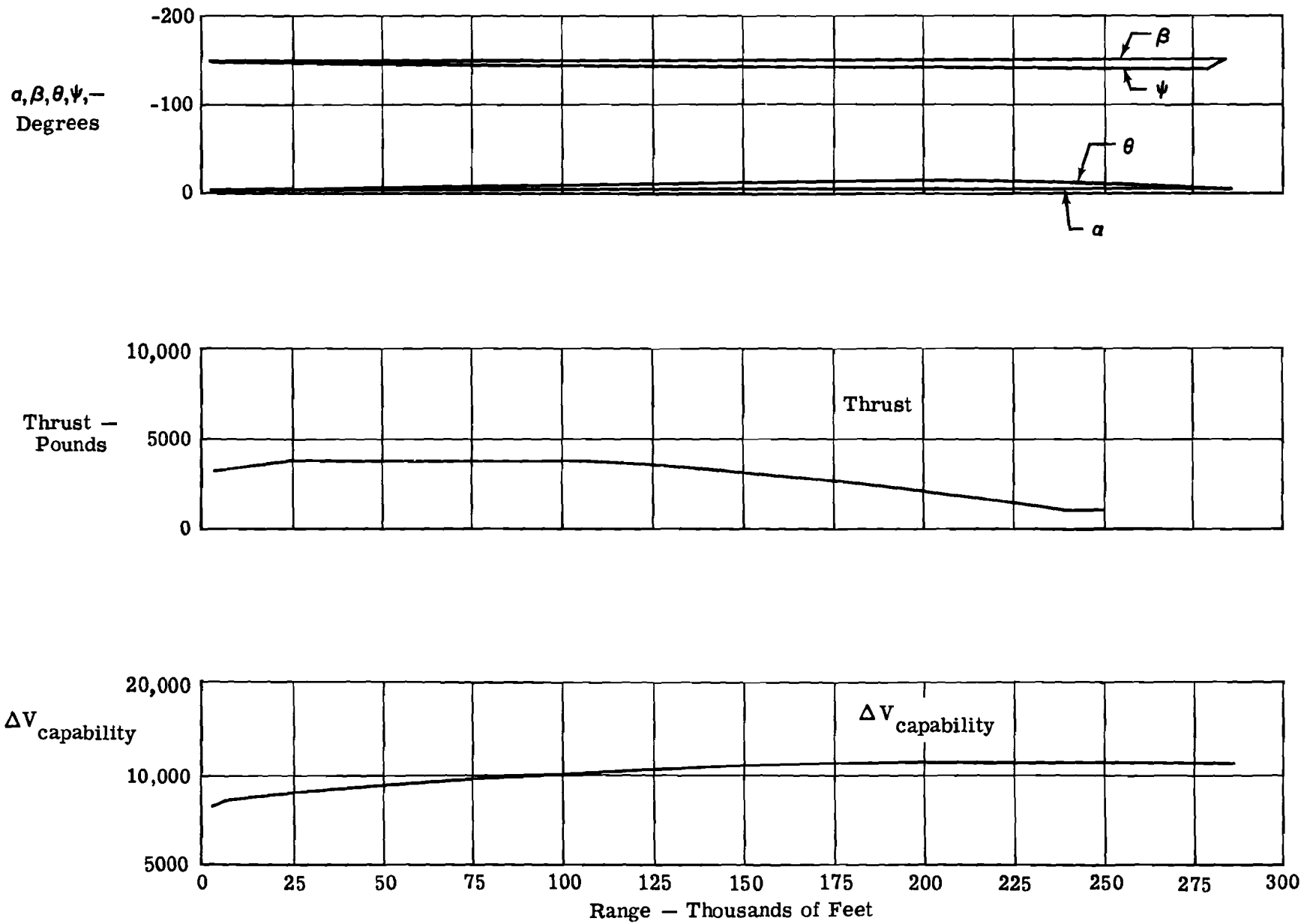


Figure 64. Mission Run No. 4 Angles, Thrust and ΔV_{cap} versus Range for Braking Phase

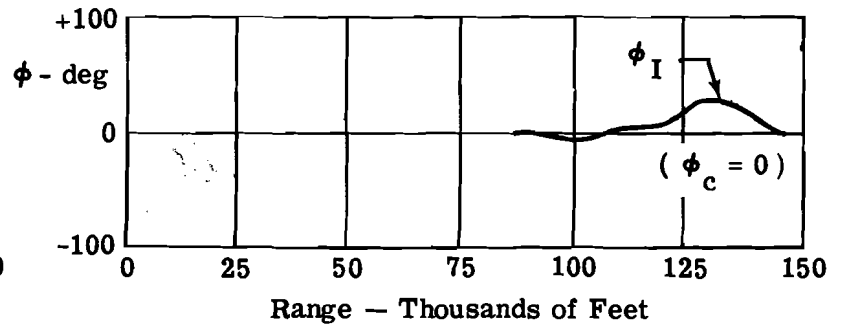
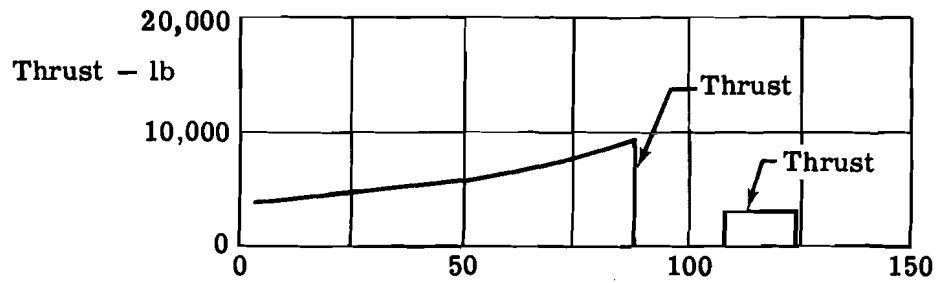
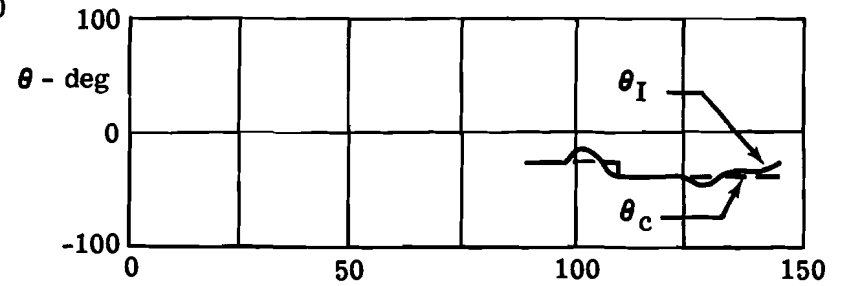
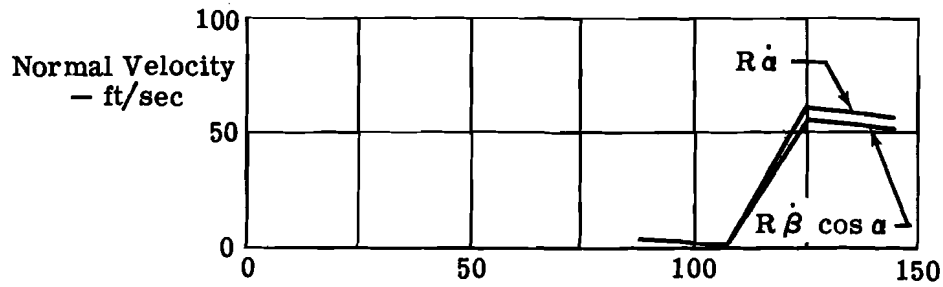
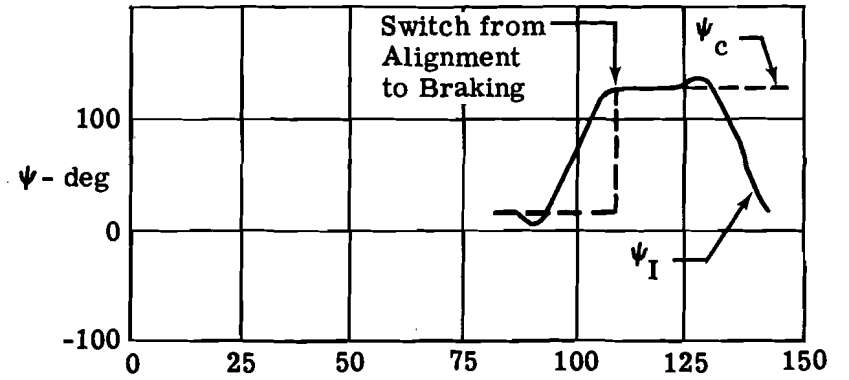
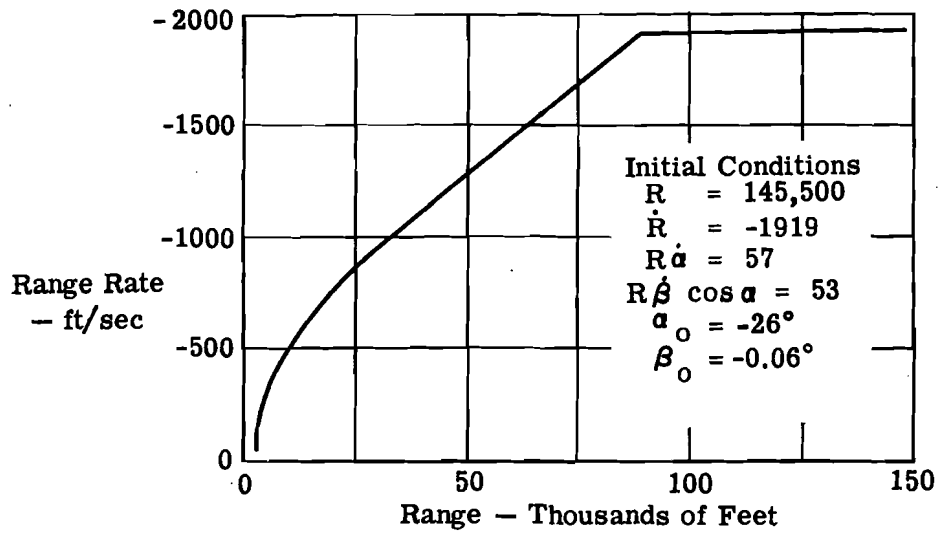


Figure 65. Mission Run No. 5 — Alignment and Braking Phase

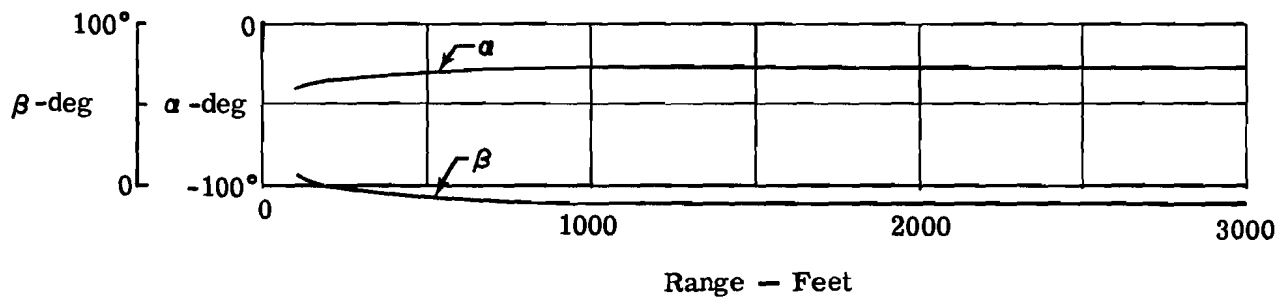
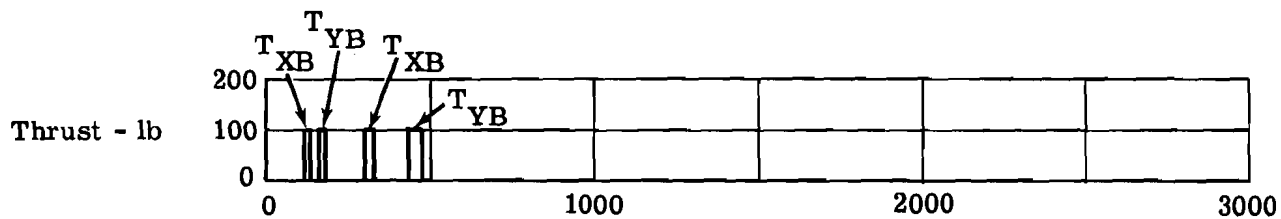
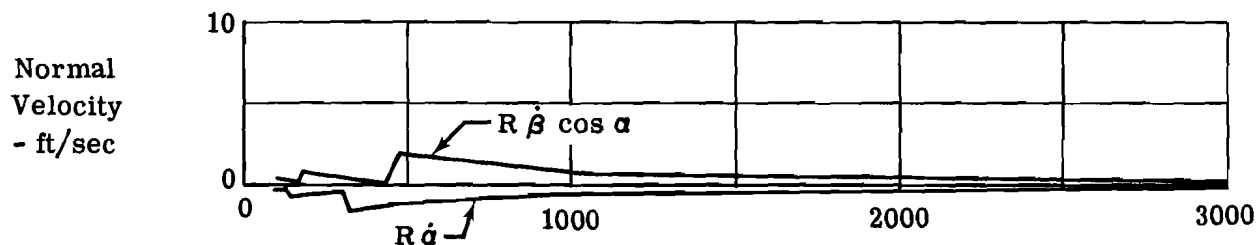
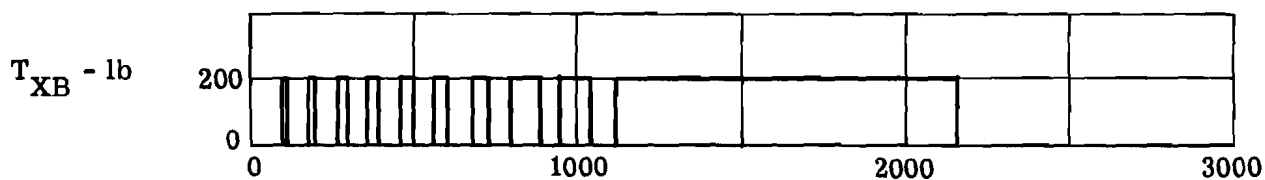
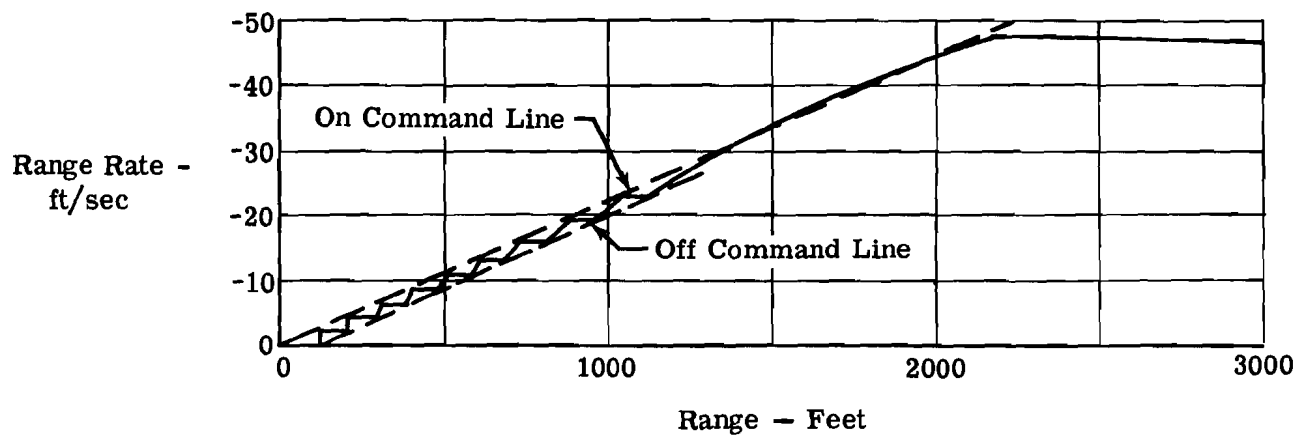


Figure 66. Mission Run No. 5 - Docking Phase

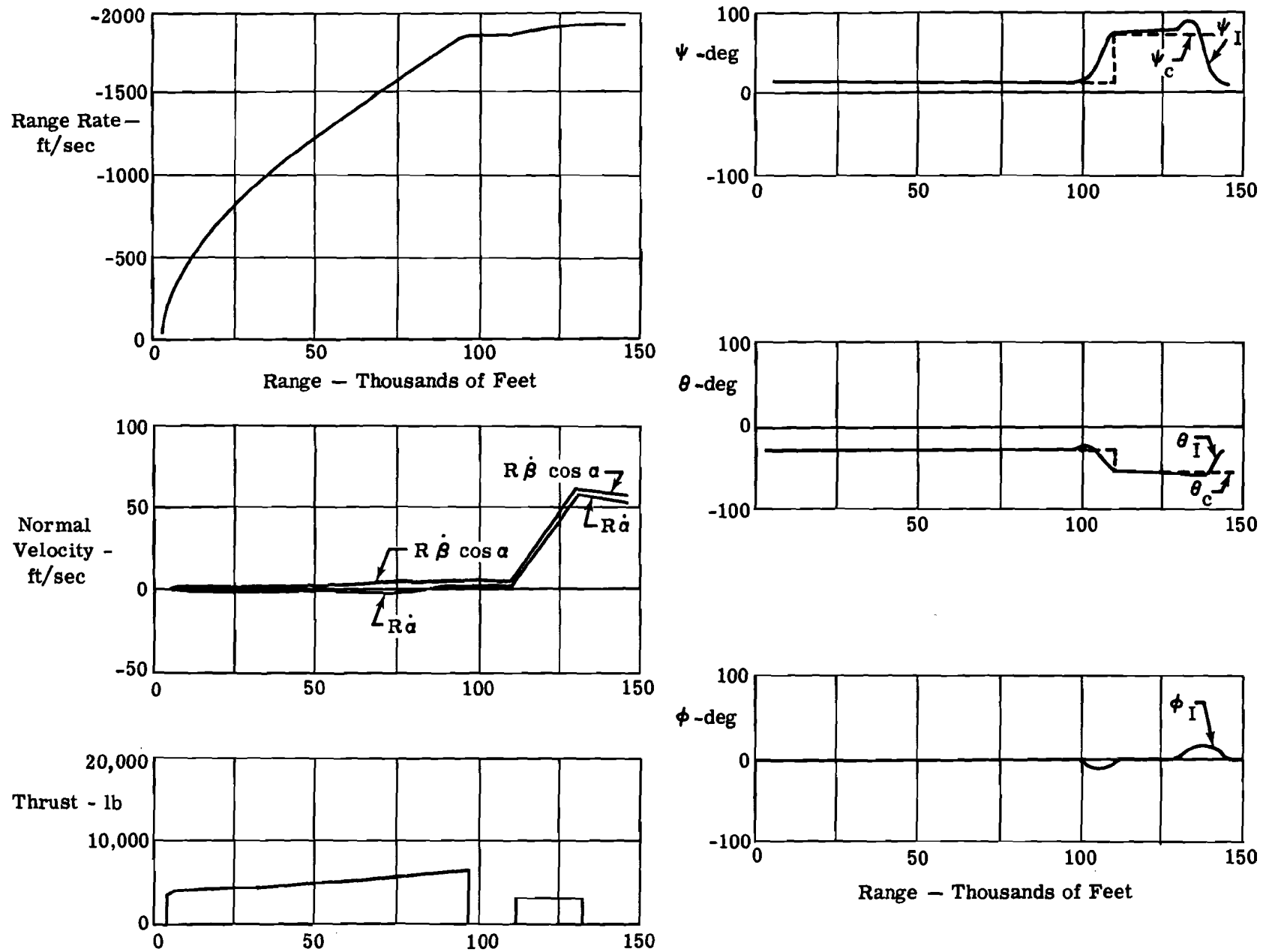


Figure 67. Mission Run No. 6 - Alignment and Braking Phases

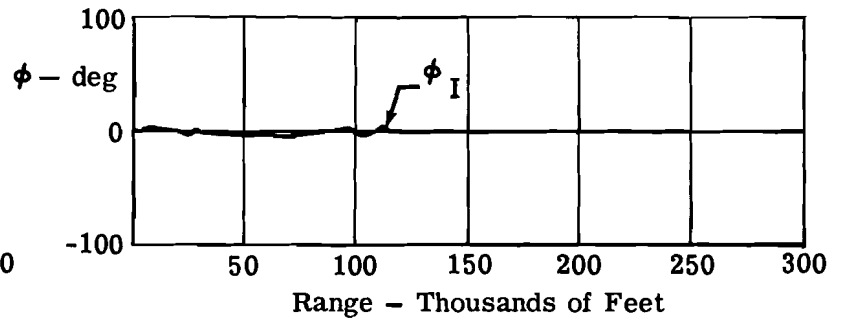
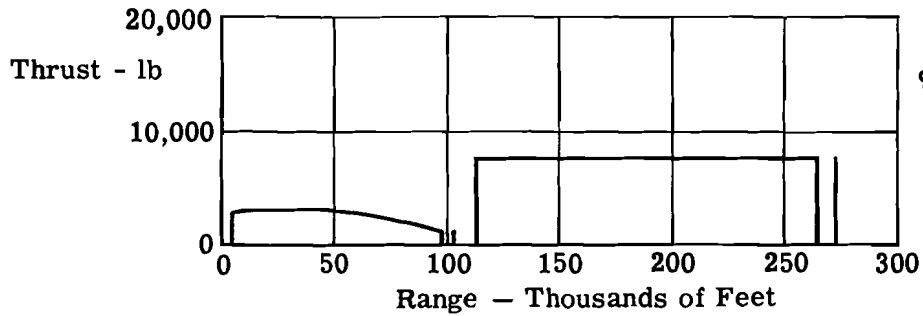
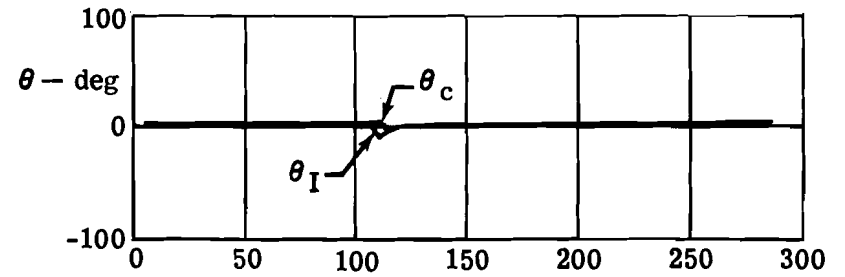
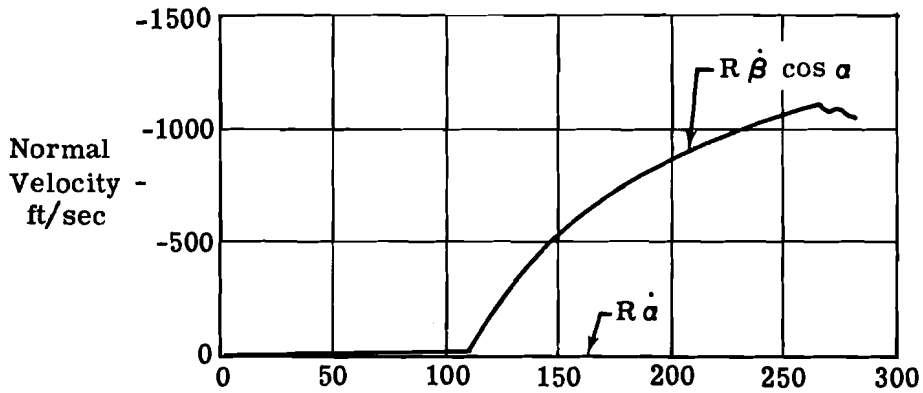
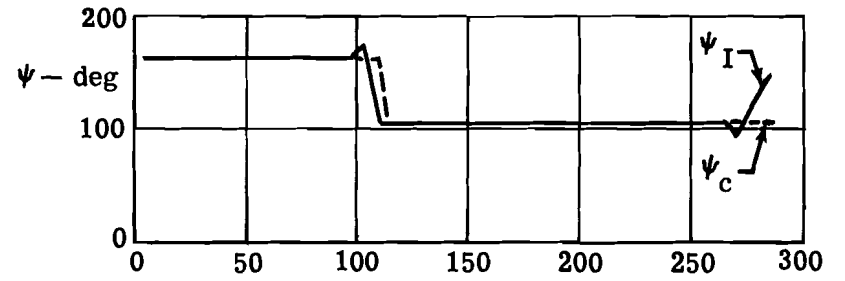
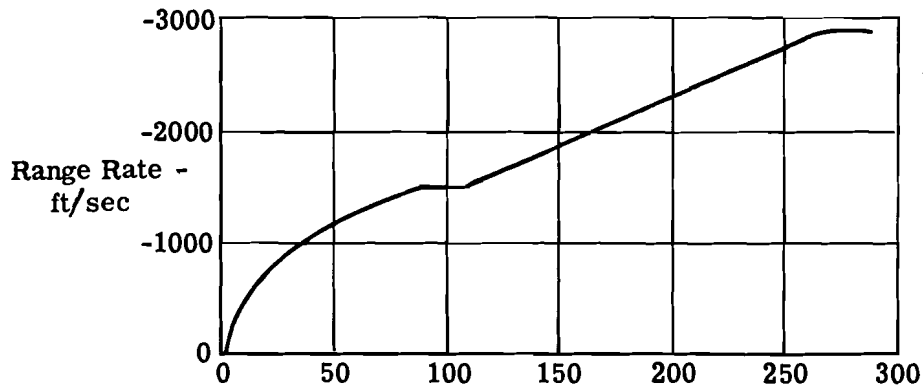


Figure 68. Mission Run No. 7 - Alignment and Braking Phases

Mission Run No. 6 - Alignment, Braking, and Docking

The initial conditions of Mission Run No. 5 were also used for this run. In this case, however, Technique 2 was used to eliminate the normal velocity components, $R\dot{\alpha}$ and $R\dot{\beta} \cos \alpha$ during an initial alignment maneuver.

The process of eliminating $R\dot{\alpha}$ and $R\dot{\beta} \cos \alpha$ by thrusting perpendicular to the line of sight (Technique 1), will use a total velocity increment of 1987 ft/sec, if done perfectly. The absolute minimum value of ΔV needed for rendezvous and docking, on the other hand, is 1920 ft/sec. In Mission Run No. 6, using Technique 2, a ΔV available, V_a , was specified as 1958 ft/sec.

The initial attitude of the interceptor was:

$$\begin{aligned}\psi_o &= 13^\circ \\ \theta_o &= -26^\circ\end{aligned}$$

The initial commanded angles were

$$\begin{aligned}\psi_c &= 77.5^\circ \\ \theta_c &= -52^\circ\end{aligned}$$

It took 7 seconds for the interceptor to achieve this attitude, and to start firing its thruster. By the end of the alignment phase, R had been reduced from -1919 ft/sec to -1855 ft/sec, and $R\dot{\alpha}$, $R\dot{\beta} \cos \alpha$ eliminated. The interceptor continued in the braking phase until the docking conditions were satisfied at 130 seconds. Terminal conditions on docking were satisfied at 331 seconds with a closing rate, $\dot{R} = 1.5$ ft/sec. At this time, a ΔV of 1960 ft/sec had been consumed, which is very close to the predicted 1958 ft/sec.

Mission Run No. 7 - Alignment, Braking, and Docking

Mission Run No. 7 is a long range mission and at acquisition, a large normal velocity, $R\dot{\beta} \cos \alpha$, exists. The initial conditions were:

$$\begin{aligned}\alpha_o &= 2^\circ \\ \beta_o &= -151^\circ \\ R &= 287,000 \text{ ft} \\ \dot{R} &= -2875 \text{ ft/sec} \\ R\alpha &= 100 \text{ ft/sec} \\ R\dot{\beta} \cos \alpha &= -1049 \text{ ft/sec}\end{aligned}$$

Technique 2 was again used for alignment and the total available velocity increment was $V_a = 3305$ ft/sec. A corresponding velocity increment of 3820 ft/sec would be required using Technique 1.

In order to complete the alignment maneuver in time to remain within the thrusting capabilities of the interceptor in the braking mode, the fixed thruster used during alignment was increased to 7500 pounds. The interceptor was assumed aligned with the LOS at the start of the run. A switch to the braking mode was commanded when the velocity normal to the line of sight was reduced to 6 ft/sec.

Results of this run are given in Figure 68. It took 6 seconds for the interceptor to align itself into the command direction. Thrust was applied continuously for 73 seconds, after which time, the velocity normal to the line of sight was approximately 1 ft/sec. At this point, a ΔV of 1877 ft/sec had been used. With $\dot{R} = -1582$ ft/sec an ideal ΔV at this point was 3459 ft/sec. The program switched to the braking mode, making a satisfactory rendezvous and docking with the target vehicle. Total ΔV used for this mission run was 3547 ft/sec.

Mission Run No. 8 - Alignment and Braking

The eighth mission run was at the long ranges, using Technique 1, with a large velocity normal to the line of sight, and a relatively low closing velocity.

Initial conditions for this case are:

$$\begin{aligned} R &= 195,400 \text{ ft} \\ \dot{R} &= -1060 \text{ ft/sec} \\ R \dot{\alpha} &= 500 \text{ ft/sec} \\ R \dot{\beta} \cos \alpha &= 61 \text{ ft/sec} \\ \alpha_0 &= 0 \\ \beta_0 &= 22.9^\circ \end{aligned}$$

In this case, Technique 1 was employed, with a fixed thrust of 7500 pounds being applied during alignment, and the variable thruster (1000 to 10,000 pounds) for braking. The attitude loop had on-off type attitude control rockets, with the system described in Section V-D-1.

Results of this run are given in Figure 69. It took 16 seconds for the interceptor to align itself into the commanded direction. The alignment mode was completed at 37 seconds, after which time, the interceptor entered the braking mode. At a range of 54,000 feet, the thrust command had built up sufficiently to turn on the thruster, at its minimum value of 1000 pounds. The braking operation proceeded routinely until the initial conditions for docking were achieved. The docking mode for this mission run was not attempted.

c. Terminal Guidance Phase Using an On-Off Thruster

In simulation tests of the rendezvous operation with an on-off main thruster, a thrust level of 7500 pounds was selected.

From Reference 13, the "on" command line, $A_1 (T/m_0)$ should correspond to approximately $1/2$ the acceleration capability of the interceptor. Therefore, $A_1 (T/m_0)$ was taken as 12 ft/sec^2 . The "off" command line: $A_2 (T/m_0)$ was taken as $1/4$ the capability, therefore, 6 ft/sec^2 .

The "on" and "off" command equations were then expressed as:

$$\begin{aligned} \frac{R^2}{2(R-R_a)} &= 12 \text{ ft/sec}^2 \\ \frac{\dot{R}^2}{2(R-R_a)} &= 6 \text{ ft/sec}^2 \end{aligned}$$

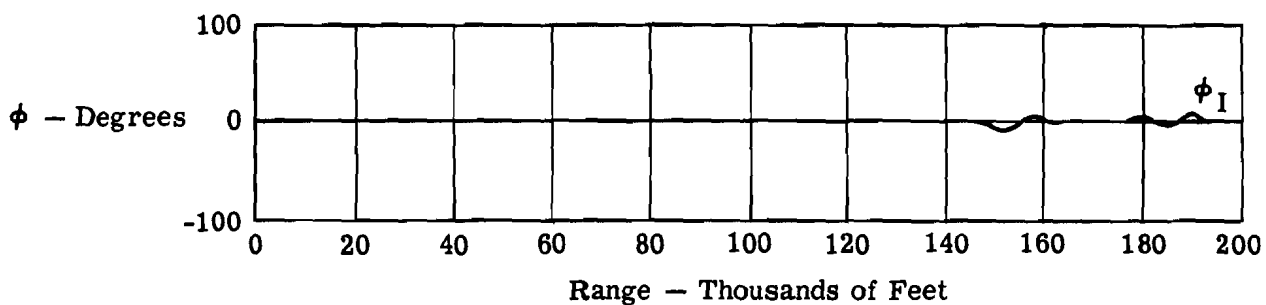
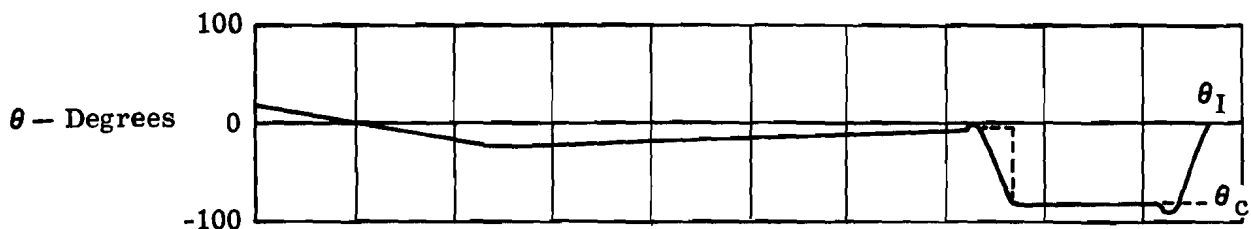
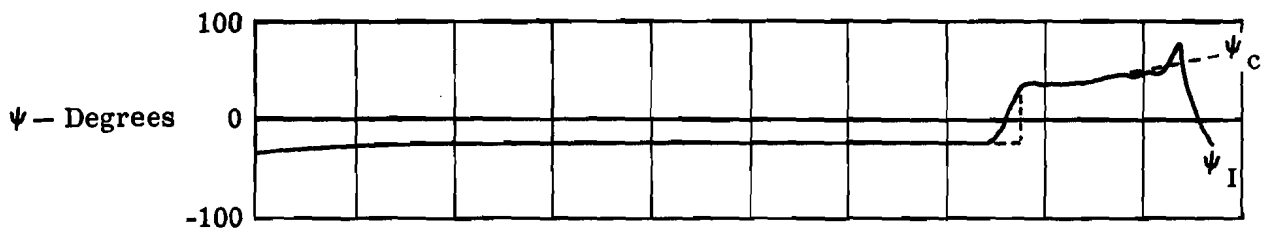
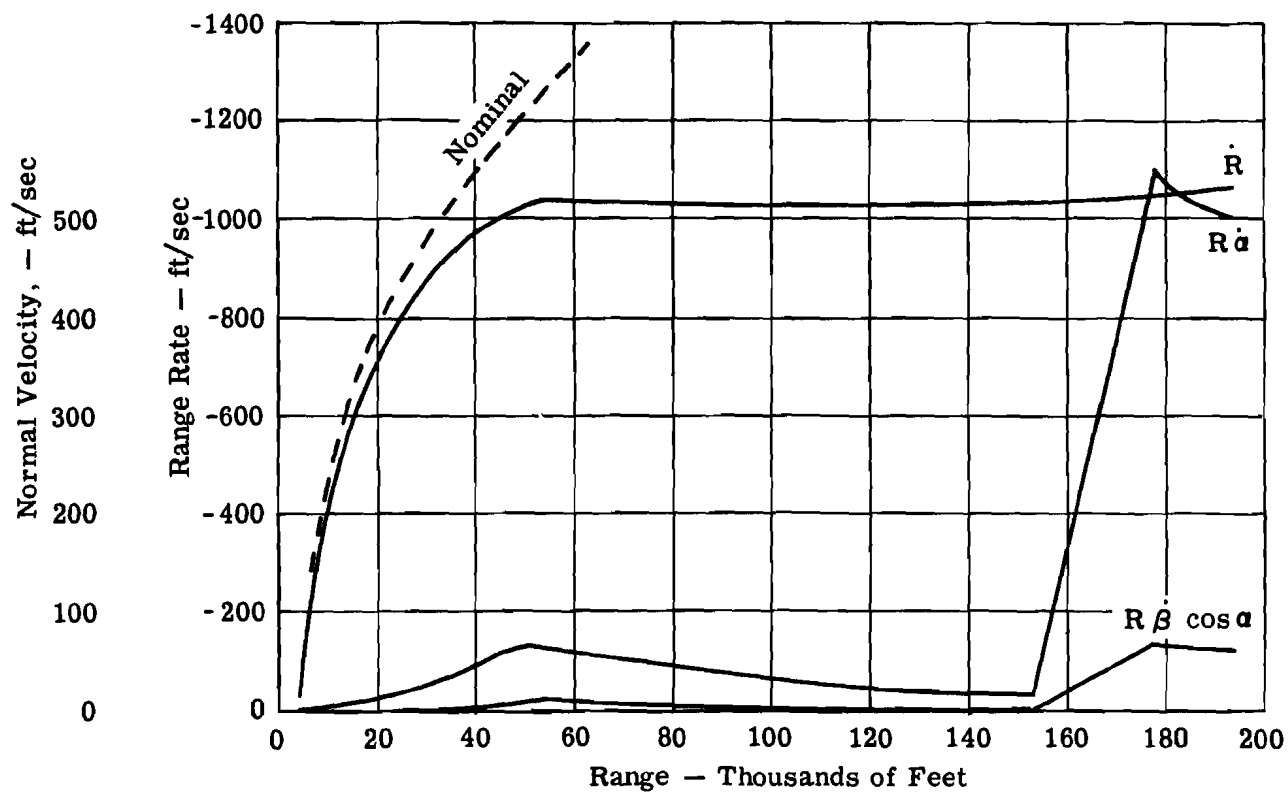


Figure 69. Mission Run No. 8 - Alignment and Braking Phases

To achieve desirable terminal conditions for the end of braking (which are the initial conditions for docking), the R_a offset distance was taken as 2792 feet.

The command lines are shown in Figure 70.

Mission Run No. 9

In this run, the on-off thruster capability described above was employed.

The command constants are:

$$A_1 = 0.48$$

$$A_2 = 0.24$$

$$T/m_0 = 25$$

$$R_a = 2792$$

Other constants in the system are

$$T_1 = 200 \text{ lb}$$

$$T_2 = 7400 \text{ lb (dummy value - for command purposes)}$$

$$T_{\text{fixed}} = 7500 \text{ lb}$$

No. 2. The initial conditions used for this run were similar to those of Mission Run

$$\alpha_0 = 26.6^\circ$$

$$\beta_0 = 0$$

$$R = 112,000 \text{ ft}$$

$$\dot{R} = -1850 \text{ ft/sec}$$

$$R \dot{\alpha} = 0$$

$$R \dot{\beta} = 0$$

$$\theta_0 = -26^\circ$$

$$\psi_0 = 0$$

d. Complete Mission Runs Involving Departure and Deorbit

For departure, the vehicle was assumed in a starting position of

$$x = 0$$

$$y = 20 \text{ ft}$$

$$z = 0$$

$$\dot{x} = 0$$

$$\dot{y} = 1 \text{ ft/sec}$$

$$\dot{z} = 0$$

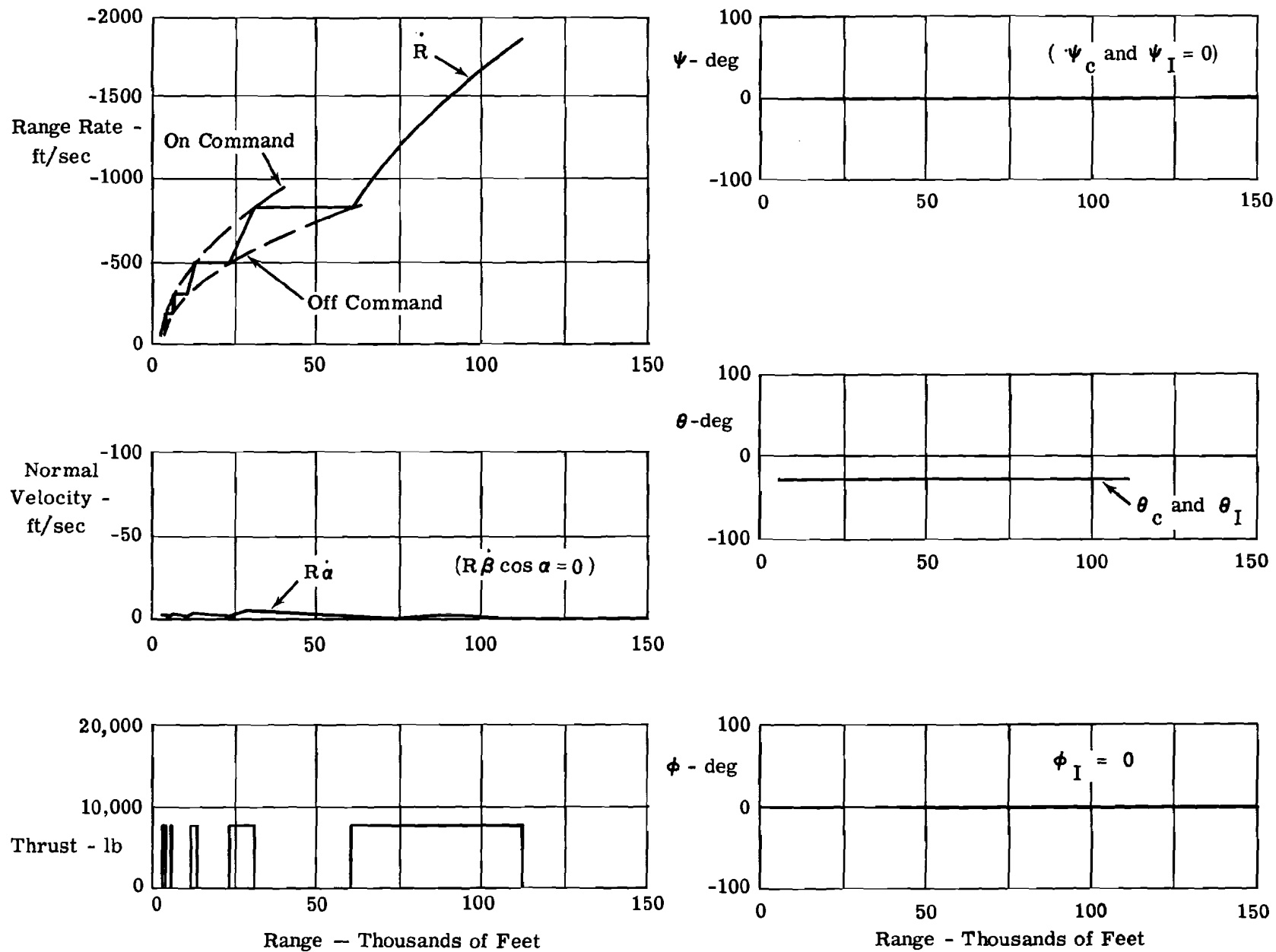


Figure 70. Mission Run No. 9-Braking Phase

It was decided that the interceptor would depart from docking with the target by applying a small thrust in the y direction; thus serving only to incline the orbit slightly. The velocity imparted was such that the greatest separation distance between vehicles would be 1000 yards. This was calculated to be 4.5 ft/sec. Thus, with a $T_{YB} = 100$ pounds, and a vehicle mass of approximately 250 slugs, a firing time of 8.75 seconds was selected.

The deorbit phase of the program was essentially the program developed in Reference 1. Data tables and other stored information used in the program are given in that report. For convenience, the following reference is made to information in that report which was used to deorbit:

<u>Symbol</u>	<u>Definition</u>	<u>Figure of Report No. MRL-TDR-62-6</u>
S'	Reentry Criticality Factor	Figure 4, page 9
ΔV_H^*	Desired Horizontal Velocity Increment Between Vehicle Velocity for Reentry and Circular Speed	Figure 5, page 11
ΔV_V^*	Desired Vertical Velocity of Vehicle Required for Reentry	Figure 6, page 12

The satisfactory operation of the automatic rendezvous and docking modes have been demonstrated by mission runs 1-9. In the following, complete mission runs are described starting at acquisition and continuing through terminal guidance, docking, departure and deorbit to the earth's atmosphere. For this series, the initial conditions at acquisition are:

$$\begin{aligned} (R\dot{\alpha})_0 &= 300 \text{ ft/sec} \\ (R\dot{\beta})_0 &= 300 \text{ ft/sec} \\ \dot{R}_0 &= -1105 \text{ ft/sec} \\ R_0 &= 206,155 \text{ ft} \\ \alpha_0 &= -45^\circ \\ \beta_0 &= 14^\circ \end{aligned}$$

The vehicle configuration had an on-off X_B thruster of 7500 pounds. The size of the docking thrusters were the same as before.

Input constants for the thrust control loop were the same as for Mission Run 9; that is,

$$\begin{aligned} A_1 &= 0.48 \\ A_2 &= 0.24 \\ T/m_0 &= 25 \\ R_a &= 2792 \text{ ft} \\ T_1 &= 200 \text{ pounds} \end{aligned}$$

$$T_2 = 7400 \text{ lb (dummy value for command purposes)}$$

$$T_{\min} = 7500 \text{ lb}$$

$$T_{\max} = 10,000 \text{ lb (dummy value for command purposes)}$$

Table V presents a summary of the conditions chosen for the series of four mission runs. A typical set of plots from these mission runs is given in Figures 71 through 74. The rendezvous and docking portions of the missions proceeded routinely. As expected, altitude had little effect on the rendezvous and docking phases. The departure and deorbit modes operated satisfactorily.

TABLE V
ORBITAL CONDITIONS

Start of Rendezvous	Orbital Conditions	Mission Objectives
1. $\lambda_T = 0$ $\mu_T = 136^\circ$ $\xi_o = -36.39^\circ$	$\ddot{\sigma}_{T_o} = 0$ $h = 300 \text{ n. mi.}$ $\omega_o = 0.00111 \text{ rad/sec}$ $C_S = 572 \times 10^9 \text{ ft}^2/\text{sec}$ $\ominus_{T_o} = 0$	Rendezvous and dock Wait for 10 minutes Depart and continue orbiting earth At the proper time - retro and deorbit to the earth's atmosphere under conditions which will permit glide and landing at Edwards AFB.
2. $\lambda_T = 0$ $\mu_T = 159.1^\circ$ $\xi_o = -36.39^\circ$	$\ddot{\sigma}_{T_o} = 0$ $h = 220 \text{ n. mi.}$ $\omega_o = 0.001159 \text{ rad/sec}$ $C_S = 560 \times 10^9 \text{ ft}^2/\text{sec}$ $\ominus_{T_o} = 0$	Rendezvous and dock Wait for one complete orbit Depart and continue orbiting earth. At the proper times - retro and deorbit to the earth's atmosphere under conditions which will permit glide and landing at Edwards AFB.
3. $\lambda_T = 0$ $\mu_T = 136^\circ$ $\xi_o = -36.39$	$\ddot{\sigma}_{T_o} = 0$ $h = 160 \text{ n. mi.}$ $\omega_o = 0.001159 \text{ rad/sec}$ $C_S = 557 \times 10^9 \text{ ft}^2/\text{sec}$ $\ominus_{T_o} = 0$	Same as (1) but this case involves deorbiting at a much lower altitude $\sim 160 \text{ n. mi.}$
4. $\lambda_T = 0$ $\mu_T = 159.1^\circ$ $\xi_o = -36.39^\circ$	$\ddot{\sigma}_{T_o} = 0$ $h = 100 \text{ n. mi.}$ $\omega_o = 0.001188 \text{ rad/sec}$ $C_S = 550 \times 10^9 \text{ ft}^2/\text{sec}$ $\ominus_{T_o} = 0$	Same as (2) but this case involves deorbiting from only a 100 n. mi. altitude.

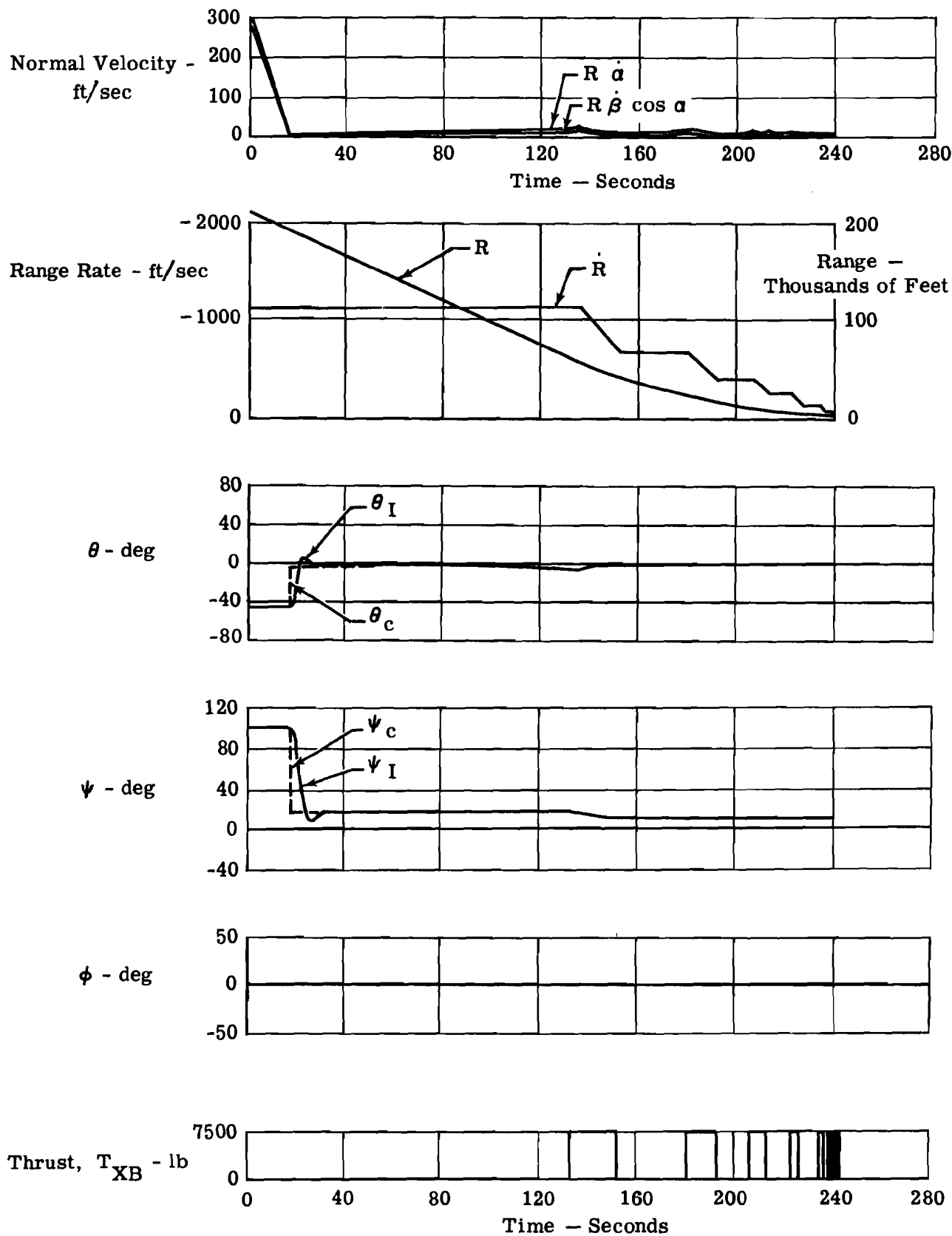


Figure 71. Complete Mission Phase Involving Departure and Deorbit - Alignment and Braking

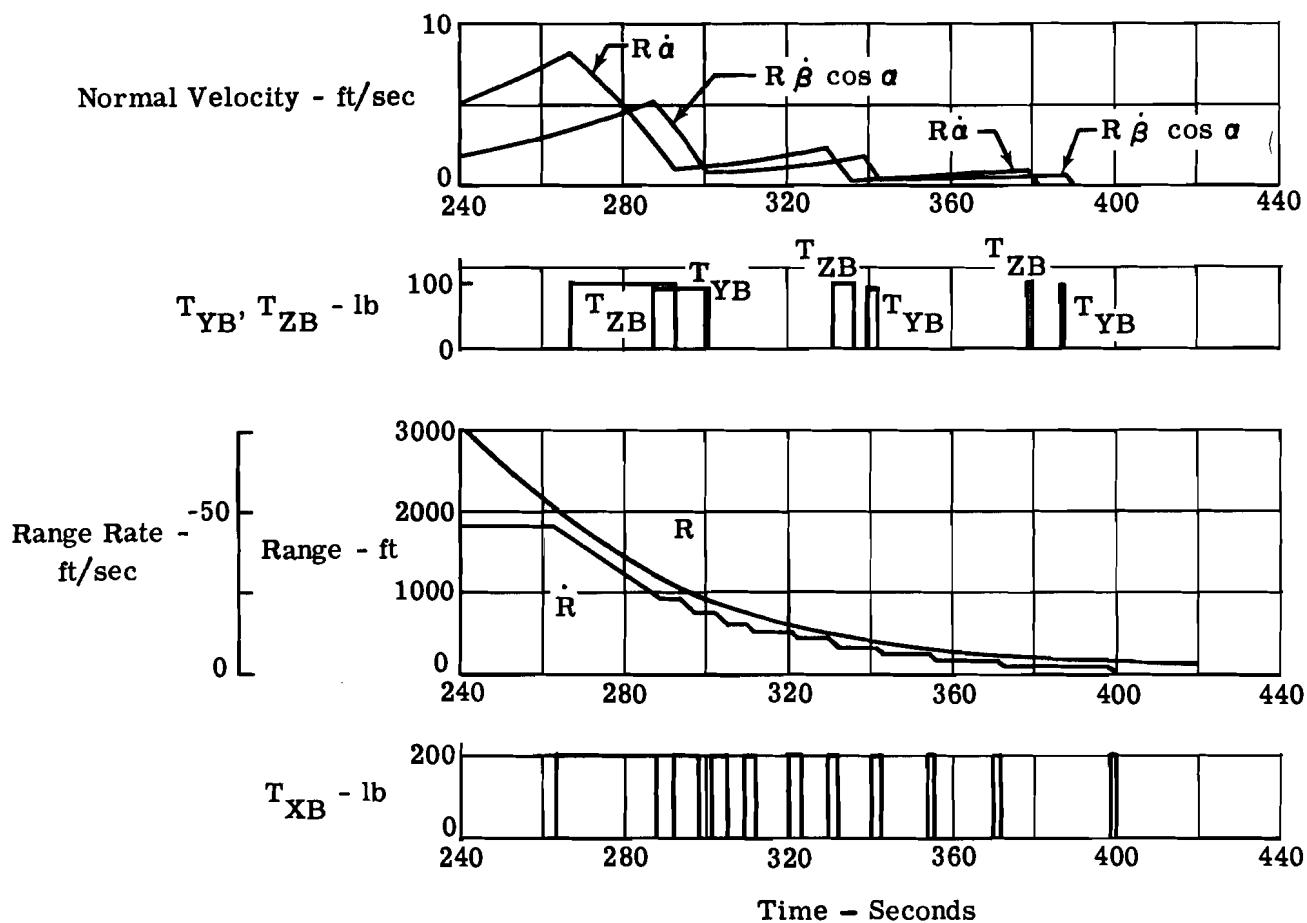


Figure 72. Complete Mission Phase Involving Departure and Deorbit - Docking Phase

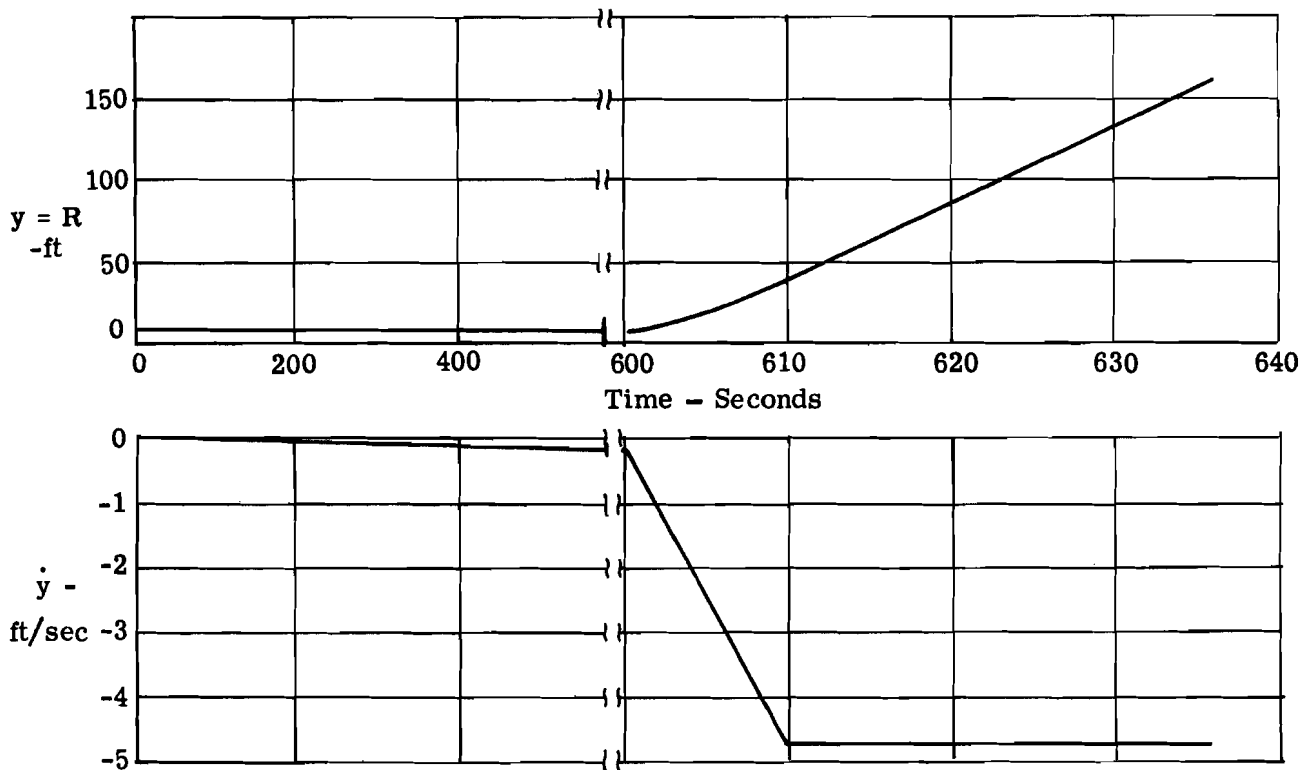


Figure 73. Complete Mission Phase Involving Departure and Deorbit - Departure Phase

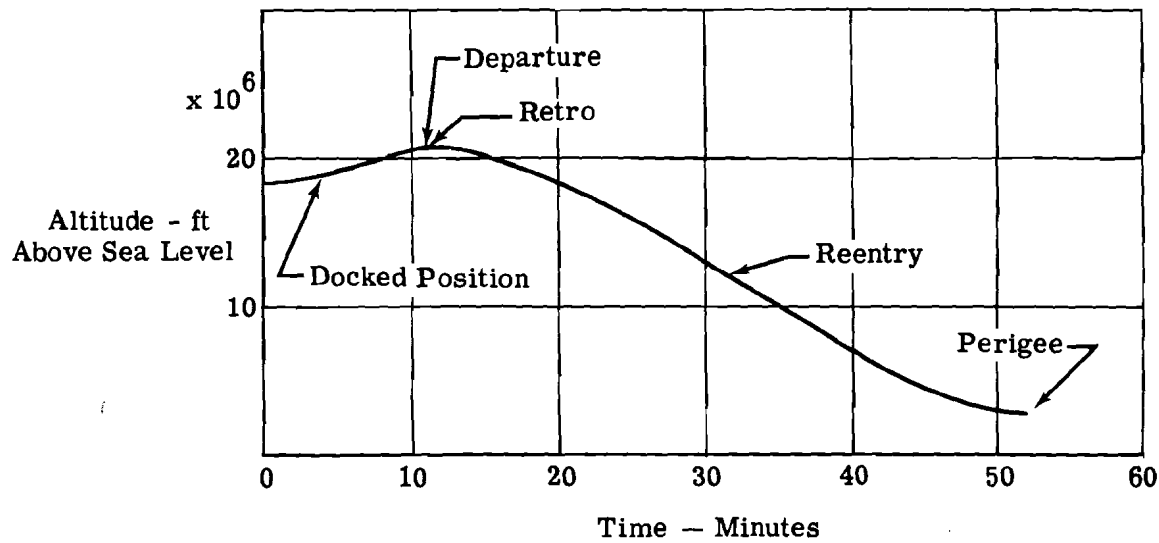
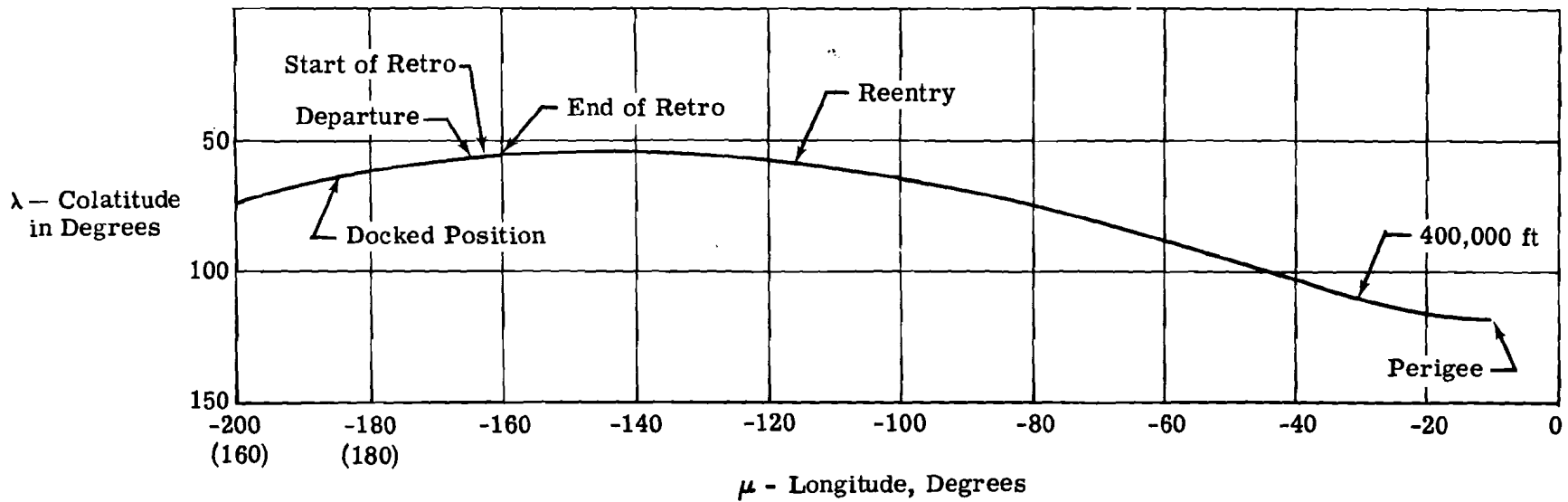


Figure 74. Complete Mission Phase Involving Departure and Deorbit - Deorbit

E. REQUIREMENTS FOR A DIGITAL COMPUTER SIMULATION

1. Accuracy Requirements

The determination of accuracy requirements for the computations which must be made in the simulation of rendezvous and docking systems is a somewhat intangible problem since the performance and accuracies of the airborne sensors, computers, and other hardware can vary considerably. Generally, however, it may be said that the computational errors should not be sufficiently large that they: (1) produce influences on the rendezvous and docking operation which are noticeable to the pilot; (2) significantly influence the ability of the systems and/or the pilot to accomplish the mission; and (3) significantly influence the figure of merits of a system such as the amount of propellant required to accomplish a given mission.

The principle function of all of the rendezvous and docking systems, whether automatic or manual, is to generate and execute two commands; the angle (δ) at which the thrust is applied, and the thrust magnitude and duration.

In most rendezvous and docking systems which have been proposed, these commands are computed and executed on essentially a continuous basis throughout the mission. Thus, control errors which are incurred early in a mission will tend to be "washed out" as the mission progresses. However, noncontinuous control systems such as those based upon the two impulse transfer technique, do not realize the benefit of this "wash out" and, hence, errors in the computation of the δ and ΔV have a more adverse influence on the mission. The allowable errors in δ and ΔV for this most adverse case (two-impulse transfer) have been used in establishing the computational accuracy requirements for the rendezvous and docking computations.

It is important that these errors in δ and ΔV not influence the second firing to the degree where considerable increase in fuel is required, or where repeatability of the simulation is lost. As a criterion, a maximum value of 3 percent for range error at second impulse/initial range $\pm \frac{R_{\epsilon}}{R_0}$ due to errors in ΔV and δ , has been selected. With this criterion as a guide, a series of runs were performed on the digital program described in Section V-D to determine allowable ΔV and δ errors.

Figure 75 presents values of the maximum miss distance per degree error in the angle δ at which the thrust is applied. Results are shown for various initial conditions which are considered typical and for two rendezvous times, 200 seconds and 300 seconds. The inputs to these curves were calculated from simplified formulae and then confirmed by running selected cases on the digital simulation. From these graphs, it is seen that the region below the $\frac{R_{\epsilon}}{R_0} = 3$ percent line encompasses most of the range of practical initial

conditions. A one-degree error in thrust direction results in a miss distance of less than one nautical mile for all cases except the extreme range condition, $R_0 = 300,000$ feet.

Figure 76 gives the total allowable velocity error normal to the line of sight as a function of separation distance, and the time to rendezvous for a total miss distance ratio, $\frac{R_{\epsilon}}{R_0} = 0.03$. In this figure, it can be seen that at the longer ranges (30 to 50 n. mi.) and at the shorter times (100 to 200 seconds or less) the allowable $V_{N_{\epsilon}}$ is relatively large. However, at the shorter ranges and longer times, the $V_{N_{\epsilon}}$ allowable becomes small. As a result, the rocket shutdown time or minimum impulse the pilot may impart to the interceptor may become critical. In reviewing the range of initial conditions concerned

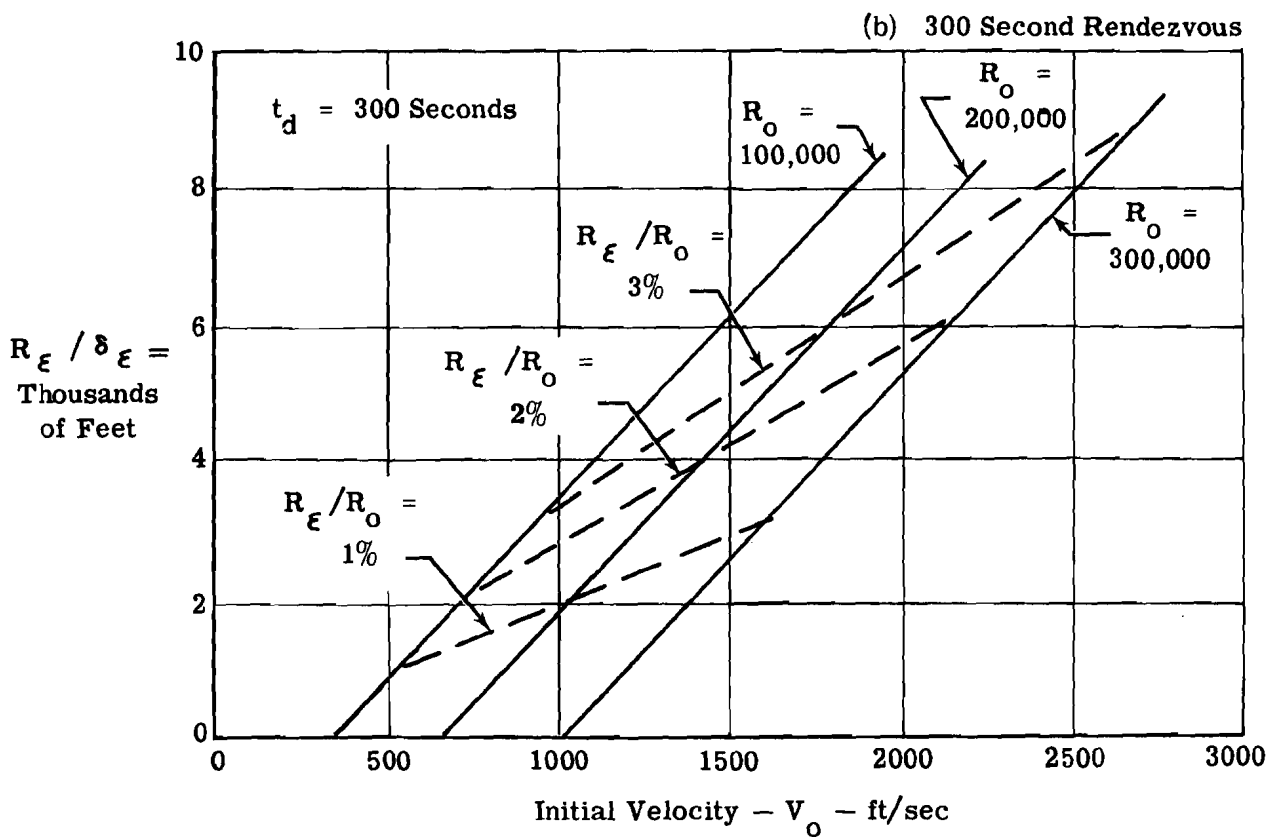
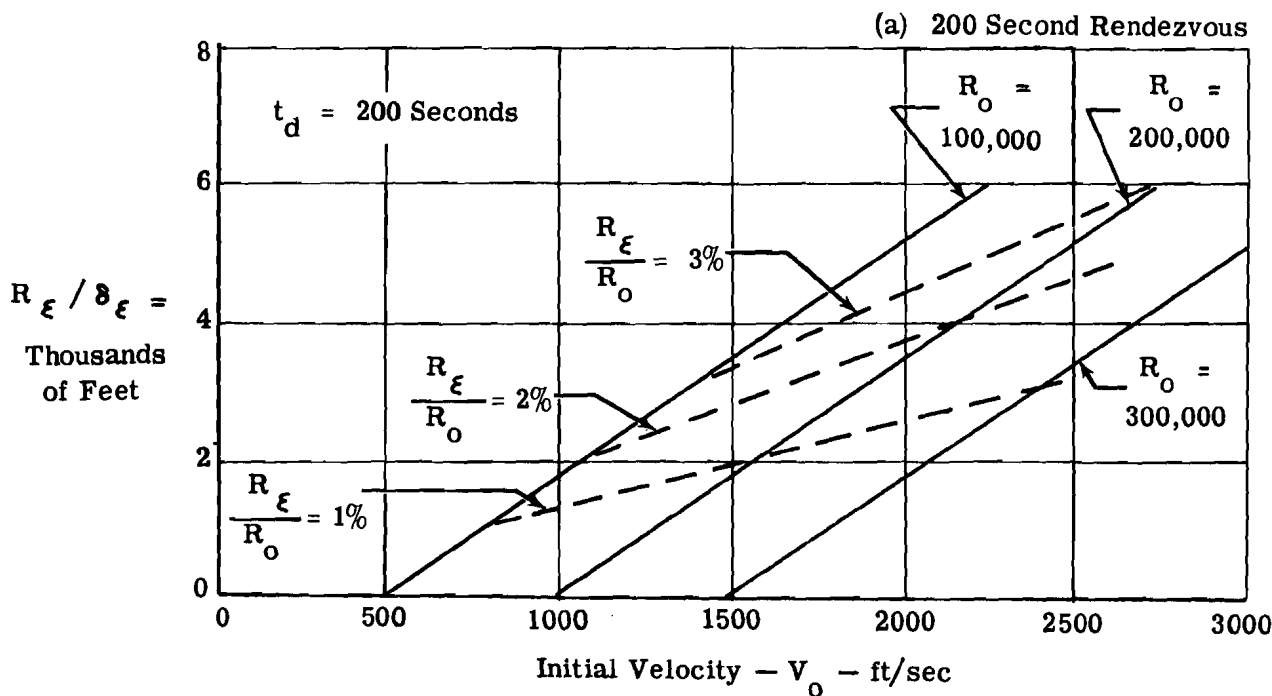


Figure 75. Miss Distance Per Degree Aiming Error

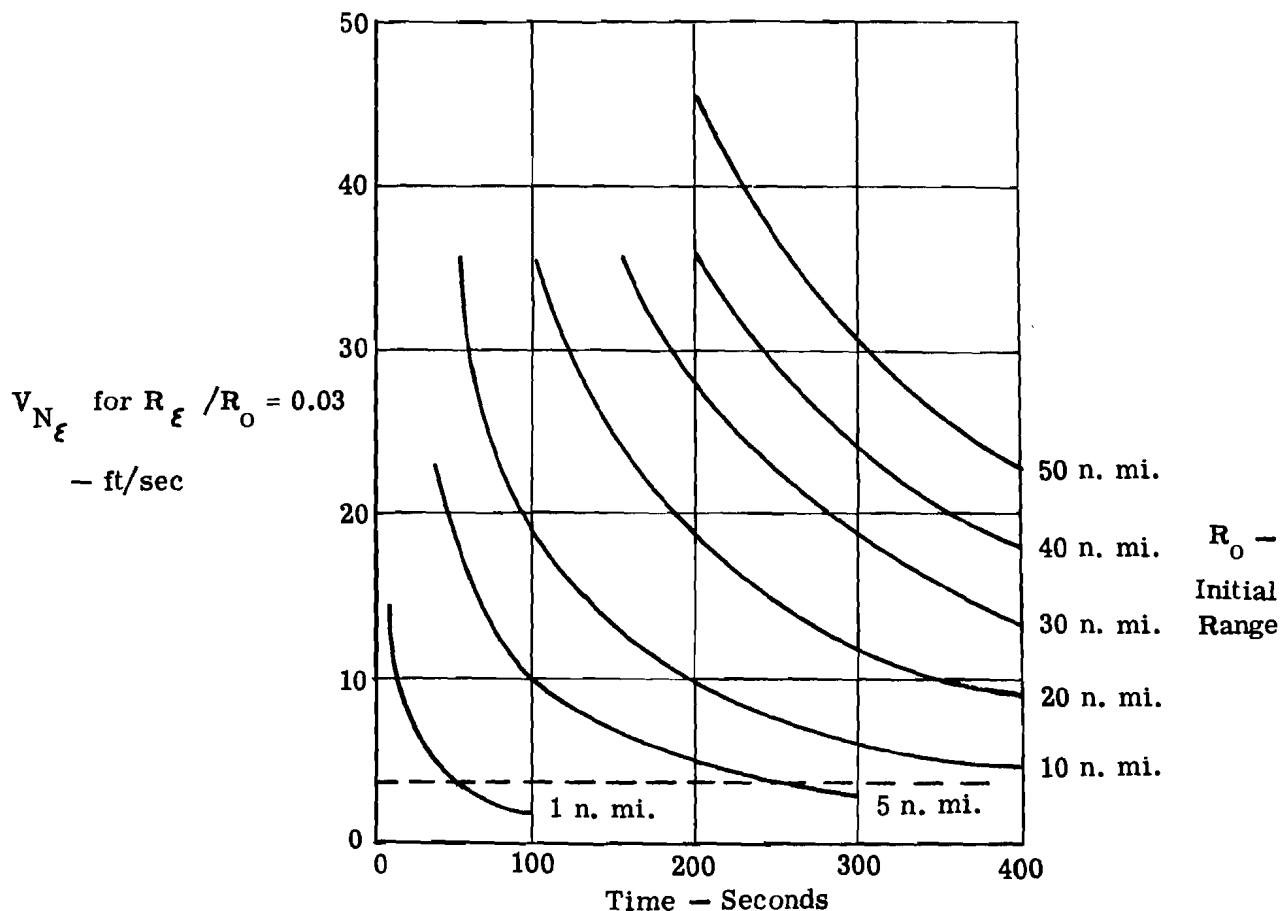


Figure 76. Allowable Velocity Error Normal to the Line of Sight

in this study, all reasonable conditions are satisfied with a $V_{N_{\epsilon}}$ value of 3 ft/sec. Therefore, this value was selected as an accuracy requirement for the normal velocity component and command values.

Based upon the allowable errors in δ and ΔV obtainable from Figures 75 and 76, and the equations and logic upon which they are based, the corresponding errors allowable in the various terms in the equations and logic can be determined. This has been done, and from supporting information obtained from mission runs, other accuracy studies, and from literature in general, a set of accuracy and resolution requirements has been formulated and presented in Table VI. This table also includes estimates of the maximum range for each of the variables together with maximum rate of the variable and estimated requirement on resolution.

2. Cycling Time

In the process of rendezvous and docking, the cycle time requirements are highly dependent on how rapidly problem position variables are accelerating. When forces are not being applied to the interceptor, a cycle time as high as 0.5 second may be perfectly adequate. When large thrust forces are applied, or when it is applied and should be removed, computational time delays will generally be important. In the total maneuver, from the beginning of the terminal guidance phase to docking, three areas are critical: first is the

TABLE VI
COMPUTER VARIABLES, RANGES, ACCURACIES AND RESOLUTIONS

	Max. Range Of The Variable	Max. Rate Of The Variable	Accuracy	Resolution
R	0 to 50 n. mi.	0 to 6000 ft/sec	1% of R + 2 ft	0.1% of \dot{R} + 0.5 ft
\dot{R}	0 to 6000 ft/sec	0.03 to 60 ft/sec ²	1% of R + 0.5 ft/sec	0.1% of \dot{R} + 0.2 ft/sec
α (1)	$\pm 180^\circ$	0 to 10 deg/sec	0.25° + 10% of $\dot{\alpha}$ in deg	0.1° + 5% of $\dot{\alpha}$ in deg
$\dot{\alpha}$	0 to 10 deg/sec	0 to 2 deg/sec ²	0.02 deg/sec + 10% of $\ddot{\alpha}$ in deg/sec	0.005 deg/sec + 5% of $\ddot{\alpha}$ in deg/sec
R $\dot{\alpha}$	0 to 500 ft/sec	0 to 60 ft/sec ²	1% of R $\dot{\alpha}$ + 0.5 ft/sec	0.1% of R $\dot{\alpha}$ + 0.2 ft/sec
β (1)	$\pm 180^\circ$	0.25° + 10 deg/sec	0.25° + 10% of $\dot{\beta}$ in deg	0.1° + 5% of $\dot{\beta}$ in deg
$\dot{\beta}$	0 to 10 deg/sec	0 to 2 deg/sec ²	0.02°/sec + 10% of $\ddot{\beta}$ in deg/sec	0.005 deg/sec + 5% of $\ddot{\beta}$ in deg/sec
R $\dot{\beta}$	0 to 500 ft/sec	0 to 60 ft/sec ²	1% of R $\dot{\beta}$ + 0.5 ft/sec	0.1% of R $\dot{\beta}$ + 0.2 ft/sec
θ_c and $\dot{\theta}$	360°	30 deg/sec	$\pm 0.25^\circ$ + 10% of $\dot{\theta}_c$ in deg	5% of $\dot{\theta}_c$ in deg + 0.1°
ψ_c and $\dot{\psi}$	360°	30 deg/sec	$\pm 0.25^\circ$ + 10% of $\dot{\psi}_c$ in deg	5% of $\dot{\psi}_c$ in deg + 0.1°
ϕ_c and $\dot{\phi}$	360°	30 deg/sec	$\pm 0.25^\circ$ + 10% of $\dot{\phi}_c$ in deg	5% of $\dot{\phi}_c$ in deg + 0.1°
$\ddot{\phi}$	30 deg/sec	30 deg/sec ²	10% of $\ddot{\phi}$ in deg/sec + 0.01 deg/sec	5% of $\ddot{\phi}$ in deg/sec + 0.005 deg/sec
$\ddot{\theta}$	30 deg/sec	30 deg/sec ²	10% of $\ddot{\theta}$ in deg/sec + 0.01 deg/sec	5% of $\ddot{\theta}$ in deg/sec + 0.005 deg/sec
$\ddot{\psi}$	30 deg/sec	30 deg/sec ²	10% of $\ddot{\psi}$ in deg/sec + 0.01 deg/sec	5% of $\ddot{\psi}$ in deg/sec + 0.005 deg/sec
t	0 to 20 min		± 0.5 sec	
τ_1	0 to 10 min		$\pm 1\%$	
ΔV_{avail}	0 to 10,000 ft/sec		± 20 ft/sec	
ΔV_1	0 to 5000 ft/sec	60 ft/sec ²	± 3 ft/sec	
ΔV_2	0 to 5000 ft/sec	60 ft/sec ²	± 0.5 ft/sec	

Note (1) - Although α and β may vary 360°, unless the interceptor flies past the target, α and β will be limited to 0 to +90° or 0 to -90°.

alignment mode using Technique 1 or 2, where high thrust is used, and must be terminated quickly; second is the end of the terminal guidance phase when the main thrust is terminated and the docking mode is entered; and third, at the end of docking, when the interceptor is only a few feet away from the target vehicle and short bursts of the thrusters are needed for maneuvering. The first two cases were studied analytically, the third case was investigated using the rendezvous and docking simulation described in Section VI. Case 3 involves the analog simulation. However, these results bear on digital requirements and are presented in this section.

Cycle time requirements for the attitude control loops were discussed in Section V-D where it was shown that a 50 ms interval was acceptable. In the following, the cycle time demands by these other critical operations on the system are described.

Alignment Mode - Cycle Time Requirements

When the interceptor is at a large distance from the target vehicle, the rendezvous system, if automatic, may call for turning the interceptor 90 degrees to the line of sight and thrusting to eliminate the velocity normal to the line of sight (see Reference 13.) If the pilot is in control, it is assumed that he may wish to perform a similar maneuver manually. In this maneuver, if thrust is being applied to the interceptor the velocity error that may result due to computational lags is given by the expression

$$\dot{R}_\xi = \frac{32.2 (t_c) (T/W)}{1000}$$

where t_c = cycle time, or elapsed time between solutions in the computer in milliseconds

T/W = thrust to weight ratio

If a thrust equivalent to $T/W = 2.0$ is applied, the minimum cycling time, t_c , is given in Figure 77 for values corresponding to V_{N_ξ} of Figure 76. From the conditions involved in rendezvous, it is likely that the pilot (for the command system) will not attempt to turn the vehicle a full 90 degrees to eliminate the normal velocity when the interceptor is

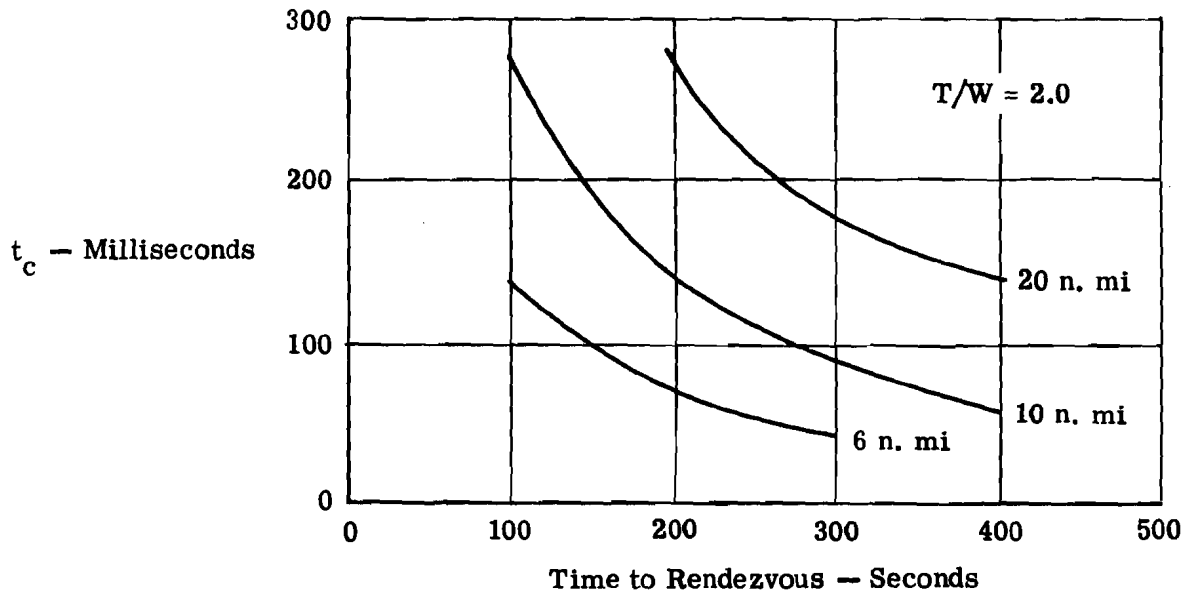


Figure 77. Allowable Cycling Time

less than 5 n. mi. from the target. At this distance, and at shorter distances, acceleration along the line of sight will invariably be required. Therefore, an intermediate value of δ to obtain thrust, both normal and along the line of sight, will probably be commanded, thus reducing the effective T/W normal to the line of sight. Using T/W = 2.0 and an \dot{R}_ϵ value of 3 ft/sec as described previously, t_c is 50 milliseconds. This appears to be a reasonable value for the minimum cycling time.

Terminal Braking Phase - Cycle Time Requirements

Another of the critical items affecting the cycling time of the simulation is how fast a thruster must be shut down once the simulated rendezvous command system equations (or the pilot) signal for zero thrust. In other words, how much error is introduced into the system by not shutting down a thruster immediately when the desired velocities are obtained. A shutdown delay of Δt seconds could result while the computer is performing computations required by other elements of the simulator.

In estimating this value, an extreme vehicle thruster configuration was chosen. This configuration included a single, on-off thruster with a thrust to weight ratio of 2, together with a small thruster, to take care of docking and close-in maneuvering, with a T/W = 0.001. For a 10,000-pound vehicle, this represents rocket engines of 20,000 pounds (T/W = 2) and 10 pounds (T/W = 0.001). It has further been assumed that the docking maneuver is to be done in a matter of minutes. Curve A of Figure 78 gives the maximum velocity \dot{R} versus distance, R, that the interceptor can have, and still dock without overshooting its mark, or restarting the big engine. The time it takes to perform this docking maneuver with T/W = 0.001 from various initial conditions on this curve are marked off along the curve. As a matter of comparison, Curves B, C, and D of the figure indicate the R versus R values it takes for a constant time without thrust to intercept the target vehicle. From the figure, the large thruster must be able to be turned off when R falls below the capability limit of the small thruster, but not so far below that the velocity is driven to zero, or to a value that would result in the interceptor taking an unreasonably long time to rendezvous. For instance, if the large thruster is on, with R = 1 n. mi., it must be turned off when \dot{R} has been reduced to 19.2 ft/sec if the interceptor is to rendezvous in 5 minutes. It should not be turned off before 19.2 ft/sec; otherwise, the interceptor will overshoot the target. Nor should it be allowed to remain on much below 19.2 ft/sec; otherwise, the 5-minute line will be bypassed and a long rendezvous time will result. For this case, a maximum velocity error, \dot{R}_ϵ , of 3 ft/sec has been selected. Thus,

$$\dot{R} = (T/W) g t_c \text{ and } t_c = 50 \text{ milliseconds.}$$

Since this example is an extreme case, the cycling time of 50 milliseconds should be adequate for any reasonable engine combination. If extreme cases are to be studied, 50 milliseconds should be adhered to. If lower T/W's are used, this requirement can probably be relaxed.

Terminal Docking Phase - Cycle Time Requirements

As mentioned earlier, the third case important in establishing digital cycling times, was examined by means of the analog simulation of rendezvous and docking described in Section VI. A series of runs was made to determine what size impulse could be applied to the interceptor vehicle at extremely close ranges (25 feet or less) without producing a change in position or rate noticeable to the pilot. For example, if the interceptor were beside the target vehicle at a distance of 25 feet, what departing velocity could be imparted to the interceptor without the pilot over a short period (one or two minutes) realizing he is travelling away. From simulator tests, this velocity proved to be 0.12 ft/sec. From previous

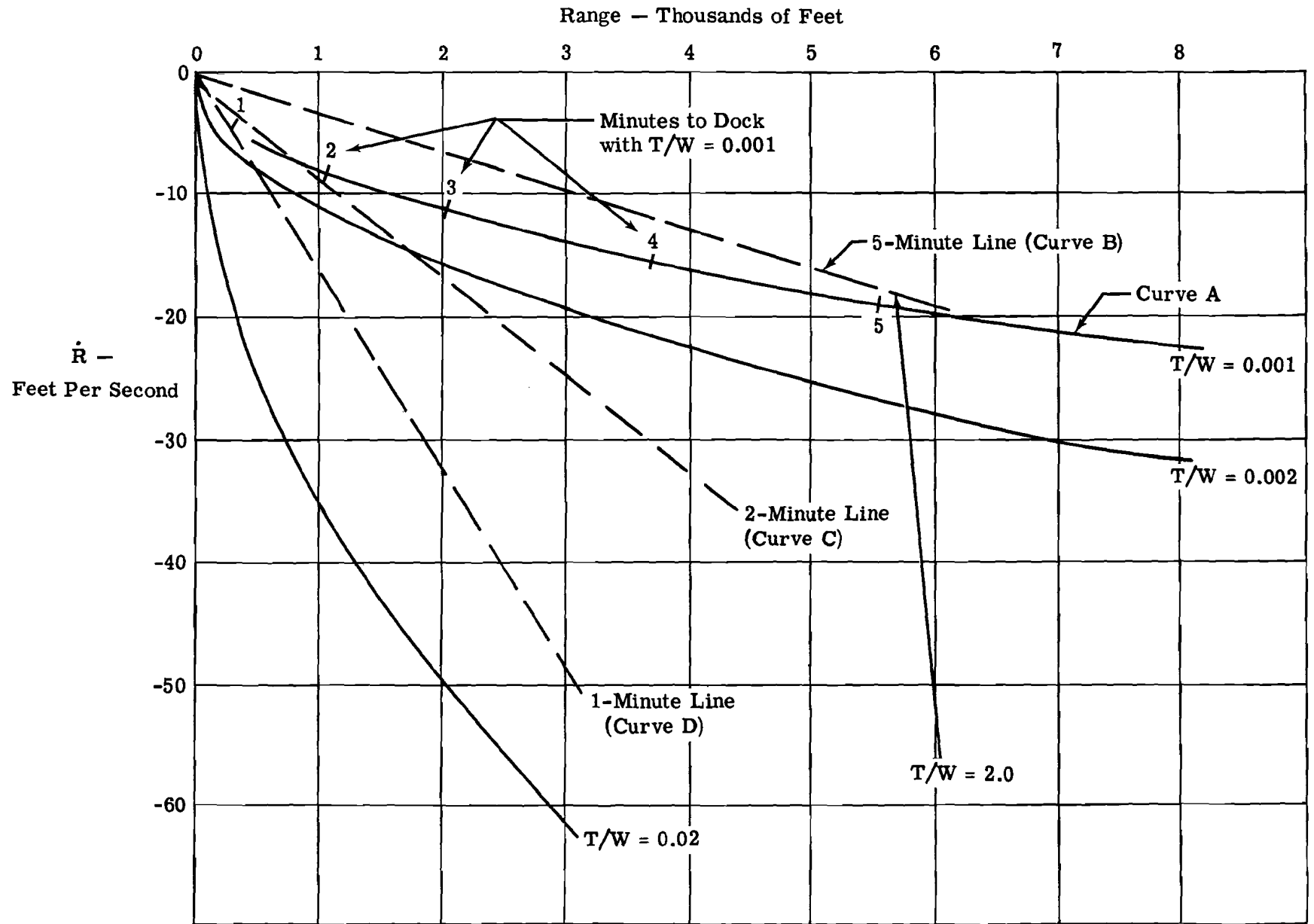


Figure 78. Range Rate versus Range for Several (T/W) Values

testing and design work, it has been fairly well established that the practical limit in acceleration that can be supplied the pilot and still have him maintain acceptable control of the interceptor is 0.08 g. Therefore, the minimum cycling time required of the digital computer at these close ranges can be calculated as

$$t_1 = \frac{\Delta V}{a} = \frac{0.12 \text{ ft/sec}}{32 \times 0.08} = 0.05 \text{ second.}$$

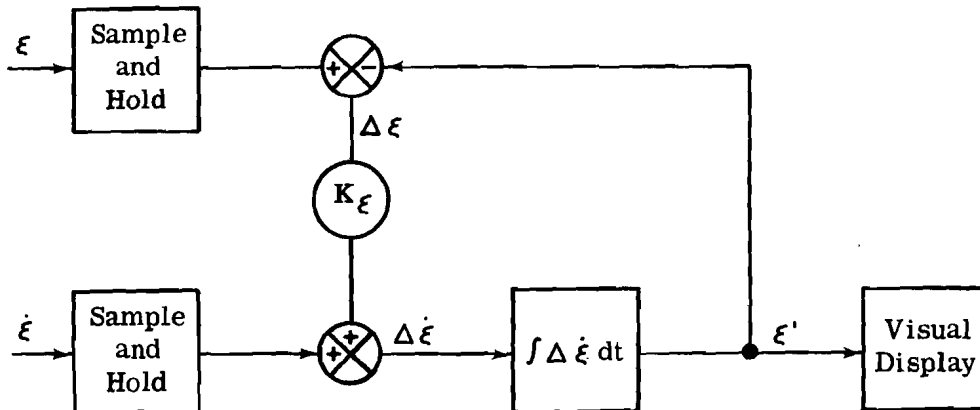
In the mission runs performed on the digital simulation, a longitudinal acceleration of 0.02 g was used. t_1 then, from the standpoint of close-in maneuvering, should be 0.20 second or less. In these runs, however, close-in maneuvering was not attempted; therefore, the 0.25-second cycling time used appears justifiable.

Deorbit Phase - Cycle Time Requirements

A reasonable approximation to the required cycling time for the deorbit mode can be made by referring to the overall range accuracy requirements in Reference 1. Since the total process of deorbit (using the technique in Section IV-B-9) and flight within the atmosphere will usually consume over half an orbit, the minimum range to the destination at the time of the first retro firing can be taken as 10,000 n. mi. With this technique, the position of the interceptor and deorbit conditions need to be calculated only once every few seconds.

Visual Display Cycle Time Requirements

The visual display, if it is to present a smooth coherent picture, must have the picture updated at least 20 times per second, with even a faster rate desirable. Up to this point, it has been argued that an updating of equations once every 50 milliseconds is all that is needed. 50 milliseconds is equivalent to 20 frames per second. However, this frequency can be increased substantially by driving the visual display with rate commands, rather than displacement commands. If the visual display is designed only to accept displacements, an integration loop may be accomplished with auxiliary computing hardware in the computer itself. For example, if ξ is an input signal to be used by the visual display, such an integration loop would take the form shown in the accompanying sketch.



3. Digital Requirements

The digital simulation of rendezvous and docking, used 7219 words of storage, of which 437 were for data, and 6782 for instructions and executions. The average speed of computation on the IBM-7090 computer was 2.7 times real time when the rendezvous and docking modes were employed (without computations relating the interceptor to the earth), and 2.2 times real time when all loops were used. These times were based on a computer cycling time of 0.050 second for the attitude control loop and 0.25 second for the remaining portions of the simulation. Except for standard subroutines, such as square route, trigonometric functions, etc., all programming was accomplished in Fortran machine language. This program was reviewed briefly to determine whether sizable savings in computational time could be picked up by recoding in FAP (an intermediate machine program language). It was concluded that in general, some small savings could be effected, but total benefits would be less than 5 percent. Therefore, no further action along this line was taken.

The IBM-7090 program was modified, however, so that test runs could be made to determine how many computational bits are needed to produce acceptable results. Since the IBM-7090 is designed to use 27-bit word lengths, single precision, a mask was constructed in the program so that wherever an important computation was made, the resulting number was reduced to a specified number (n) of bits. n was controllable from the input sheets, so that for any given run, it could be specified as any number from 1 to 27. Selected portions of the missions were then simulated for various values of n ranging from 10 to 27. From the results of these runs, n could be determined as the minimum number of computational bits required for a digital simulation of rendezvous and docking.

The first series of runs started from the initial conditions of Mission Run No. 3. Three runs were made for the first 10 seconds of flight with 27, 14, and 10 computational bits assumed. Results are shown in Figure 79. As can be seen, the 14-bit computation followed the 27-bit solution reasonably close, while the 10-bit computation was virtually worthless.

A second series of runs with 13, 14, 16, and 27 bits was made using the initial conditions of Mission Run No. 9. In this case (Figure 80), trouble was experienced in the attitude control system where the interceptor failed to stay within the prescribed attitude limits of ± 2 degrees from the commanded values. As can be seen in Figure 80, the 13 and 14-bit cases appear unacceptable, causing the thrust command to oscillate on and off. The 16-bit case is better, but still is marginal. From these results, it was concluded that a digital computer of at least 18 bits will be needed if reliable results are to be obtained in the attitude control system. In examining other parts of the loops, 13 and 14 bits appeared to give sufficient accuracy. Once the braking mode was entered, suitable control in all loops was obtained, even for the 13-bit case.

In performance of the contract, not only was it necessary to consider simulation requirements for the many rendezvous and docking systems and guidance techniques but also to consider all the equations and expressions representing the dynamics elements involved in the rendezvous mission. The amount of computation required to solve the command equations turned out to be a small portion of the computations needed for the entire loop. For example, Table VII presents a summary of the mathematical operations needed for a digital solution of the entire rendezvous simulation. Here, it can be seen that the rendezvous and docking command equations represent from 10 to 25 percent of the total computing operations required. In actually implementing a digital program, however, it became apparent that if a general simulator is to be designed with the capability of using any one of several guidance techniques, each technique will require its own set of inputs. The logical method of accomplishing this is to use one basic set of equations and expressions for simulating the dynamics of the two vehicles, and then use the proper transformation expressions to obtain the inputs needed for the control equations. Outputs from the control equations would then

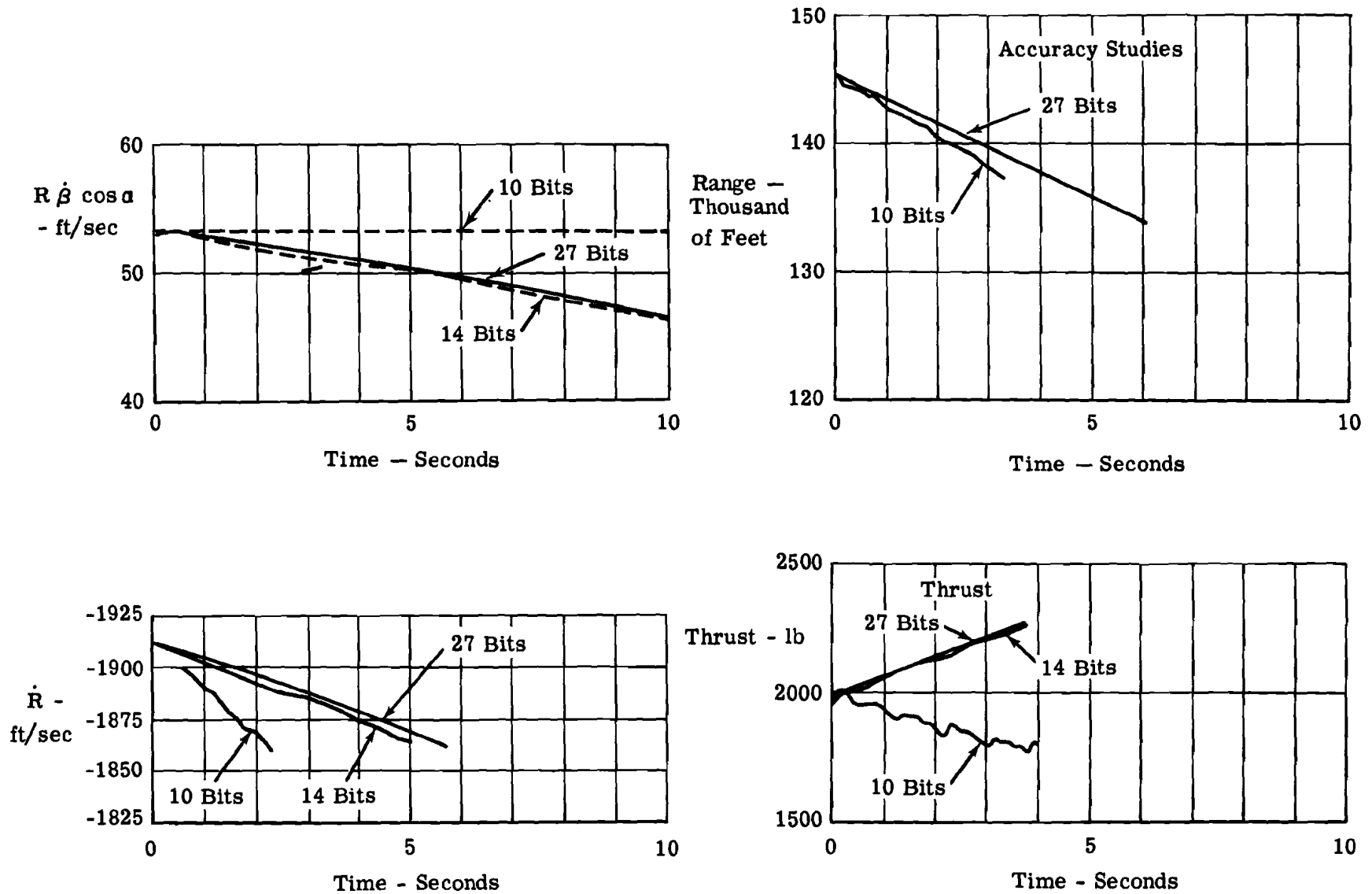


Figure 79. Accuracy Studies, Case 1

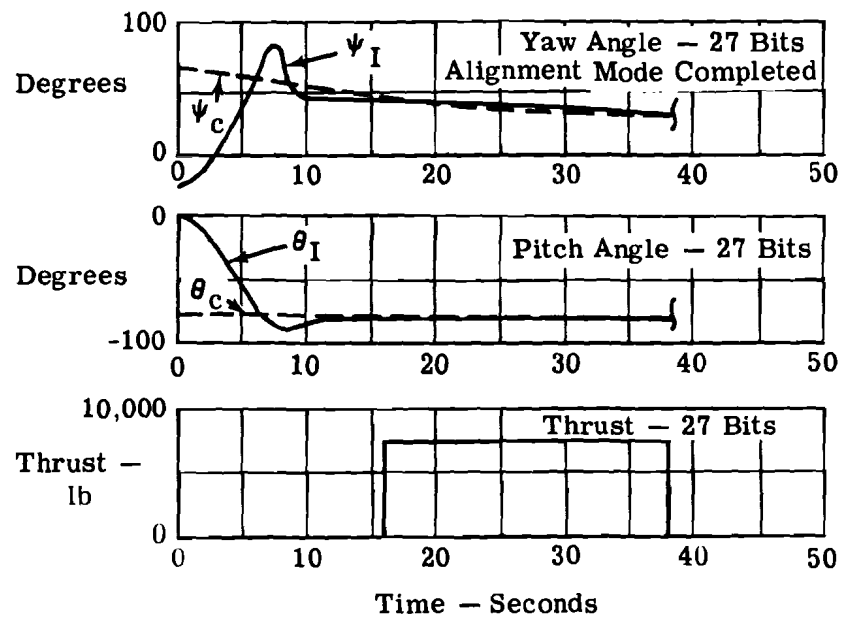
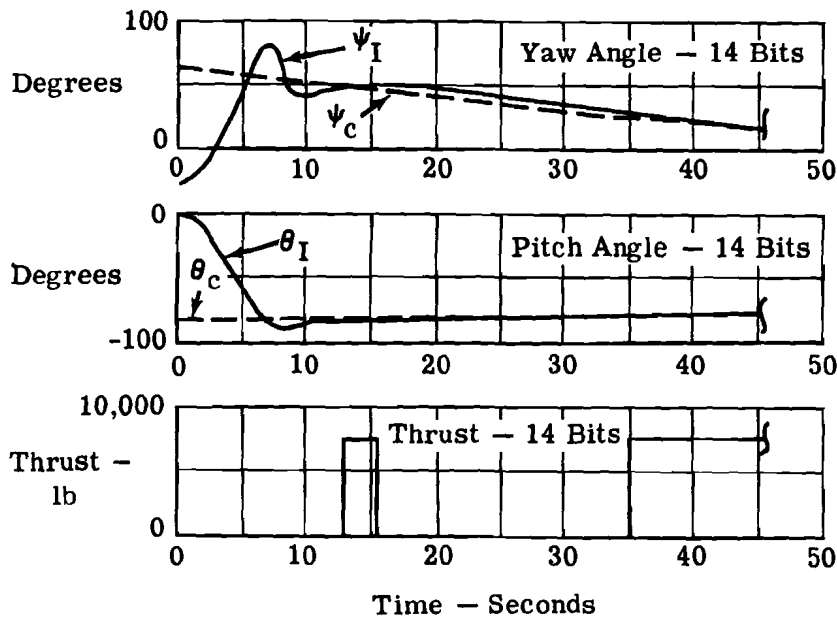
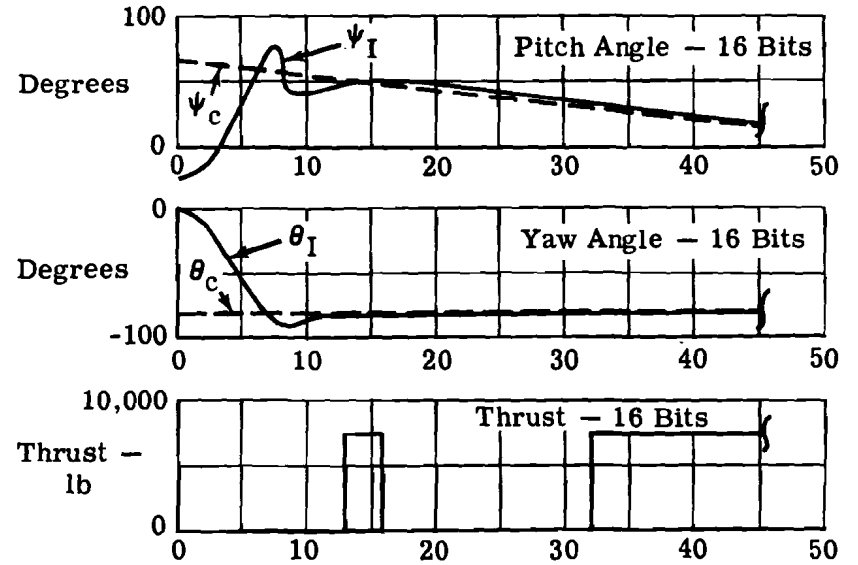
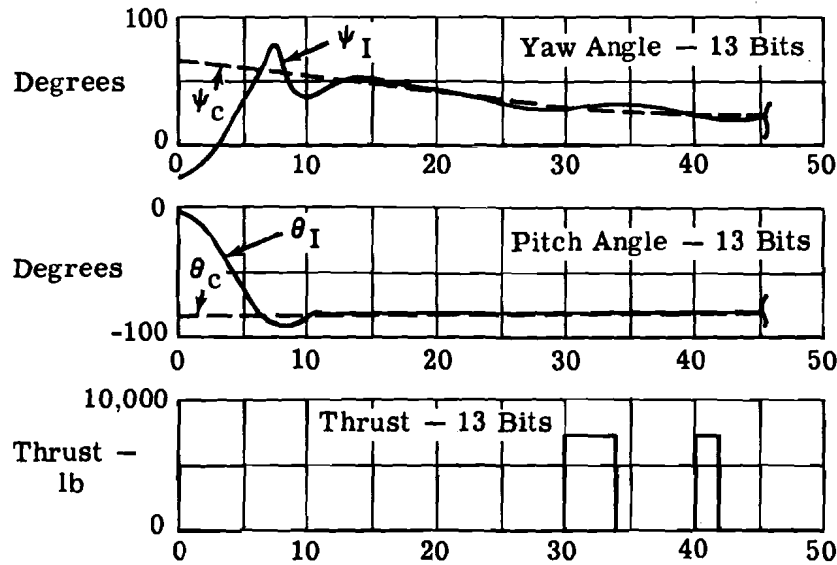


Figure 80. Accuracy Studies, Case 2

TABLE VII
SUMMARY OF MATHEMATICAL OPERATIONS

	Add	Multiply	Divide	Square Root	Trigonometric Functions
Dynamic Simulation of the two vehicles	83	128	19	4	21
Interceptor Flight Conditions Relative to Earth and Deorbit Control	33	40	14	9	20
Input Transformations to the Rendezvous and Docking Command Equations					
T3A	6	12	5	2	6
T3B	6	10	0	0	2
T3C	4	9	1	1	5
T3D	6	12	5	2	6
Rendezvous and Docking Command Equations					
References 9 and 11	20	43	12	5	8
10	11	11	10	0	0
12	16	24	5	3	4
13	6	8	6	1	5
14	14	1	0	0	0
Output Transformations from the Rendezvous and Docking Command Equations					
T4A	4	4	6	0	10
T4B	2	3	0	0	3
T4C	2	3	0	0	3
T4D	10	17	8	2	15

be converted back into the proper form for use in the dynamic equations. It is recommended, then, that the rendezvous and docking command equations be kept separate from the rest of the system by the use of subroutines. Table VIII presents the estimated computing time for the IBM-7090 for various guidance techniques given in Section III. Using these values, together with results of timing studies made of the mission runs, the IBM-7090 is able to solve the most demanding case as approximately twice real time. Therefore, for real time operation, a computer with add times of 60 microseconds and multiplication times of 70 microseconds should be sufficient.

TABLE VIII
ESTIMATED COMPUTING TIME FOR THE IBM-7090

	Milliseconds
Dynamic Simulation of the two vehicles	16.5
Interceptor Flight Conditions relative to Earth and Deorbit Control	14.9
Input Transformations to the Rendezvous and Docking Command Equations	
T3A	14.3
T3B	1.3
T3C	3.2
T3D	14.3
Rendezvous and Docking Command Functions	
References 9 and 11	7.7
10	3.2
12	4.1
13	3.3
14	0.2
Output Transformations from the Rendezvous and Docking Command Equations	
T4A	5.3
T4B	6.0
T4C	6.0
T4D	9.1

VI. ANALOG SIMULATION

A. GENERAL

The primary purpose of the analog simulation program was to permit studies to be made of rendezvous and docking under various degrees of pilot participation, ranging from automatic to fully manual control. This simulation was used in studies to investigate interceptor to target closure rates which are within the pilot's capabilities, the nature and number of displays and controls which are required, and the desirable control techniques for pilot controlled rendezvous and docking.

In addition to these studies relating directly to the rendezvous problem, the analog simulation was also used to study requirements for the analog simulation of rendezvous and docking so that a comparison could be made between analog and digital equipment for this simulation.

The analog simulation consists of three major elements:

- (1) An analog computer program of the equations of motion defining the relative motion between a target in a fixed orbit and a maneuvering interceptor vehicle. Also programmed are equations of automatic control for rendezvous, covering separation distances to 40 nautical miles.
- (2) An interceptor vehicle simulated cockpit permitting manual control in six degrees of freedom. A photograph of the interior of the cockpit is shown in Figure 81.
- (3) An electronic target image generation device capable of generating a toroidal shaped space station as it would be viewed from a window in the interceptor vehicle. This simulated target is presented on a 21-inch cathode ray tube (CRT) which is located behind the viewing port in the simulator. The toroidal target can be seen in the upper center of the photograph in Figure 81.

A detailed description of each of these items, together with the equations used to implement the simulation, is given in the following paragraphs. A block diagram of the simulation is shown in Figure 82.

B. SIMULATION DESCRIPTION

1. Analog Computer Program

a. Equations of Relative Motion

The equations and expressions given in Section IV were used as a basis for programming the rendezvous and docking modes on the analog computer. During the course of implementing the analog simulation, it was necessary to make simplifications to these equations to keep the amount of analog equipment required within reasonable limits. Other modifications were also made to the form of the equations to circumvent the accuracy limitations of the analog computing equipment. A description of what was done and the resulting program follows.

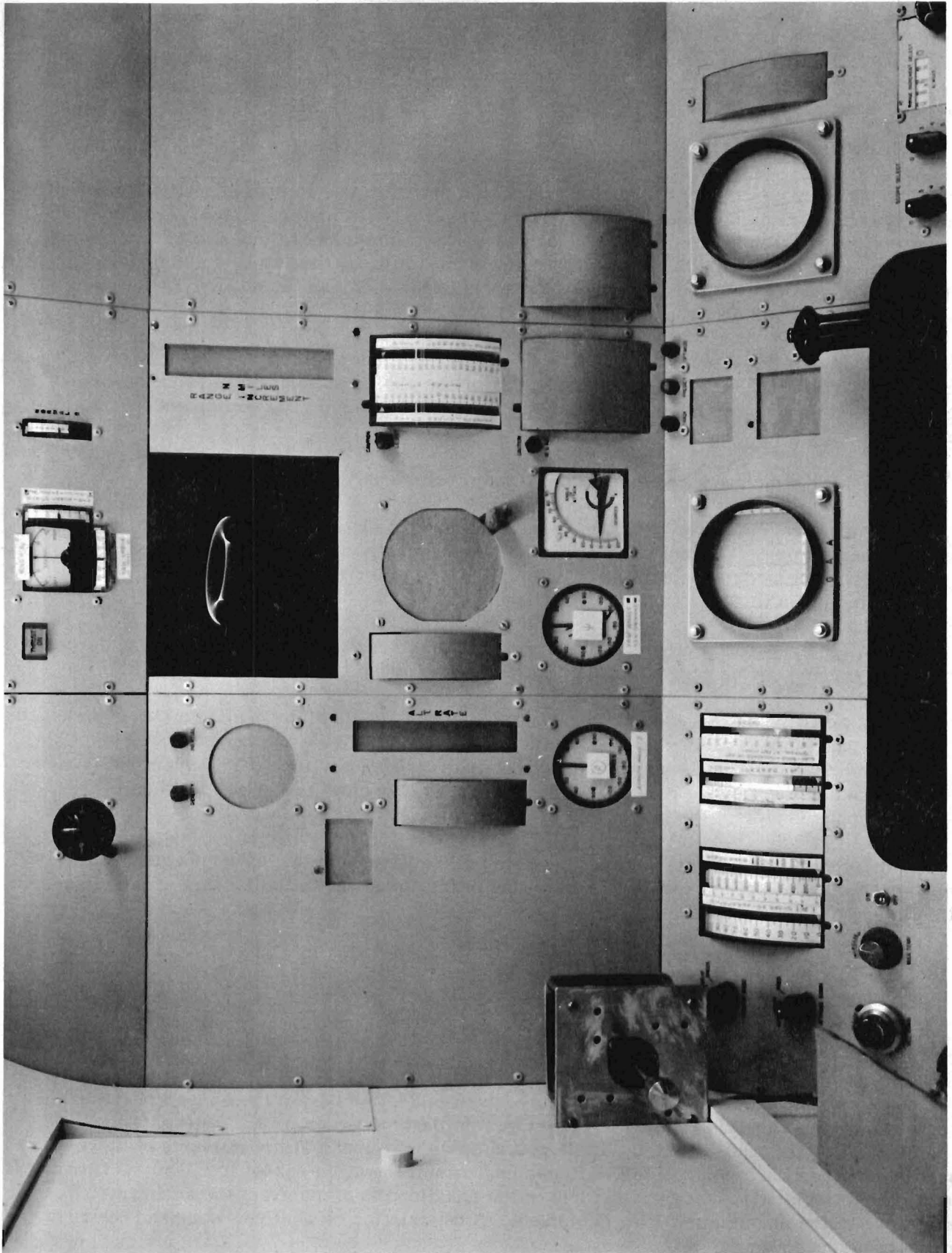


Figure 81. Interior of the Rendezvous and Docking Simulator Cockpit

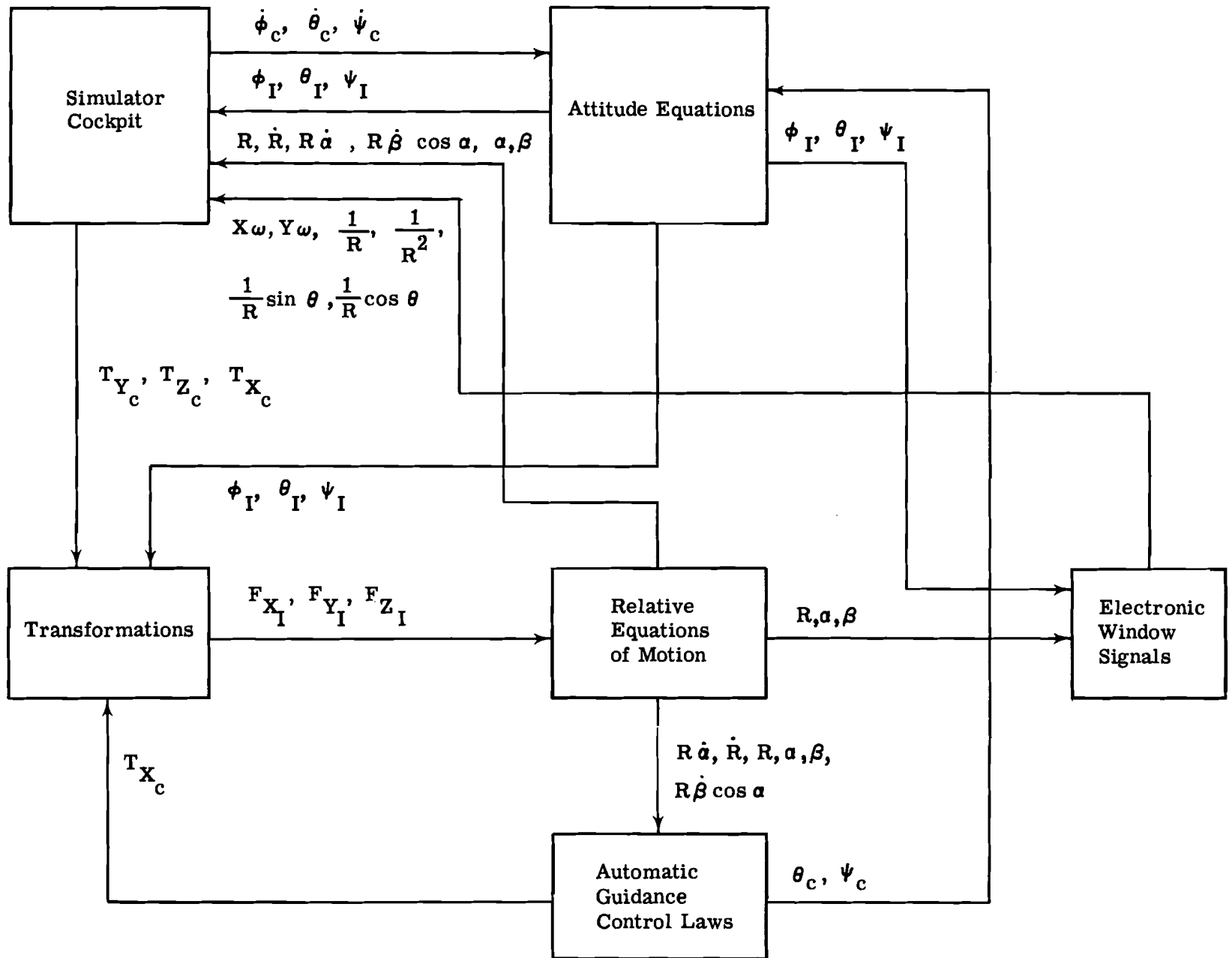


Figure 82. Block Diagram of the Simulation

The relative equations of motion given in Figure 30 of Section IV, which were programmed for the digital simulation, were based on an X_T, Y_T, Z_T , rectangular reference system, whose origin moves with the target, but the direction of the X_T, Y_T, Z_T axes remain inertially fixed. As such, the equations take the general vector form of

$$\frac{d^2 \bar{R}}{dt^2} + \frac{Gm_e}{\sigma_T^3} \left(\bar{R} - 3 \frac{\bar{\sigma}_T}{\sigma_T^2} R \bar{\sigma}_T \right) = \frac{\bar{T}}{m}$$

where \bar{R} is the relative displacement vector between target and interceptor.

$\bar{\sigma}_T$ is the displacement vector of the target from the center of the earth.

\bar{T} is the thrust vector applied to the interceptor.

In a close examination of this equation, it can be seen that the gravity expression which represents the differential acceleration between the two vehicles is small. For example, in digital simulation studies it was noted that accelerations due to these gravity effects typically reached a maximum of about 0.0075 g at 50 n.mi. Since the magnitude of this acceleration is proportional to R , this acceleration approaches zero as the two vehicles approach each other. For example, when 1000 feet apart, the acceleration due to the differential gravity is reduced to a maximum value of 0.0006 g.

This effect was further investigated by plotting the resulting relative displacements of the two vehicles when they are approaching each other. A sample of these trajectories is given in Figure 83. Here it can be seen that in the terminal rendezvous phase, the interceptor travels virtually a straight line with respect to the target vehicle. Since the scope of the present study involves only the terminal phase of rendezvous, the differential gravity terms were neglected. This assumption is also supported in References 13, 15, and 18 where it is shown that in the terminal phase of rendezvous, where closing speeds are sufficient to effect rendezvous within times which are short compared to the orbital period, the differential gravity terms may be neglected. Results obtained from runs made by the analog simulation, when compared with corresponding digital solutions, also bore out the validity of this conclusion.

For accuracy reasons, the standard method as used in the digital simulation for solving the relative equations of motion was modified for the analog program. In the digital simulation, the $\ddot{x}, \ddot{y}, \ddot{z}$ relative accelerations were calculated, then integrated to give the rates $\dot{x}, \dot{y}, \dot{z}$. These rates were in turn integrated to give relative displacements x_R, y_R, z_R . Transformation T_{3A} was then used to convert to spherical coordinates R, α and β

$$\begin{aligned} \text{where } R &= \sqrt{x^2 + y^2 + z^2} \\ \alpha &= \arctan \frac{z}{\sqrt{x^2 + y^2}} \\ \beta &= \arctan \frac{y}{x} \end{aligned}$$

Because of the large range of variables involved (see Table IX), poor accuracy resulted from the nonlinear operations which were required on the analog. To circumvent this problem, a modification to the method of integrating the relative equations of motion was made. First, $\ddot{x}, \ddot{y},$ and \ddot{z} were integrated, giving \dot{x}, \dot{y} and \dot{z} . Then, assuming α and β angles are available, $\dot{R}, R \dot{\alpha}$ and $R \dot{\beta} \cos \alpha$ were obtained from the expressions:

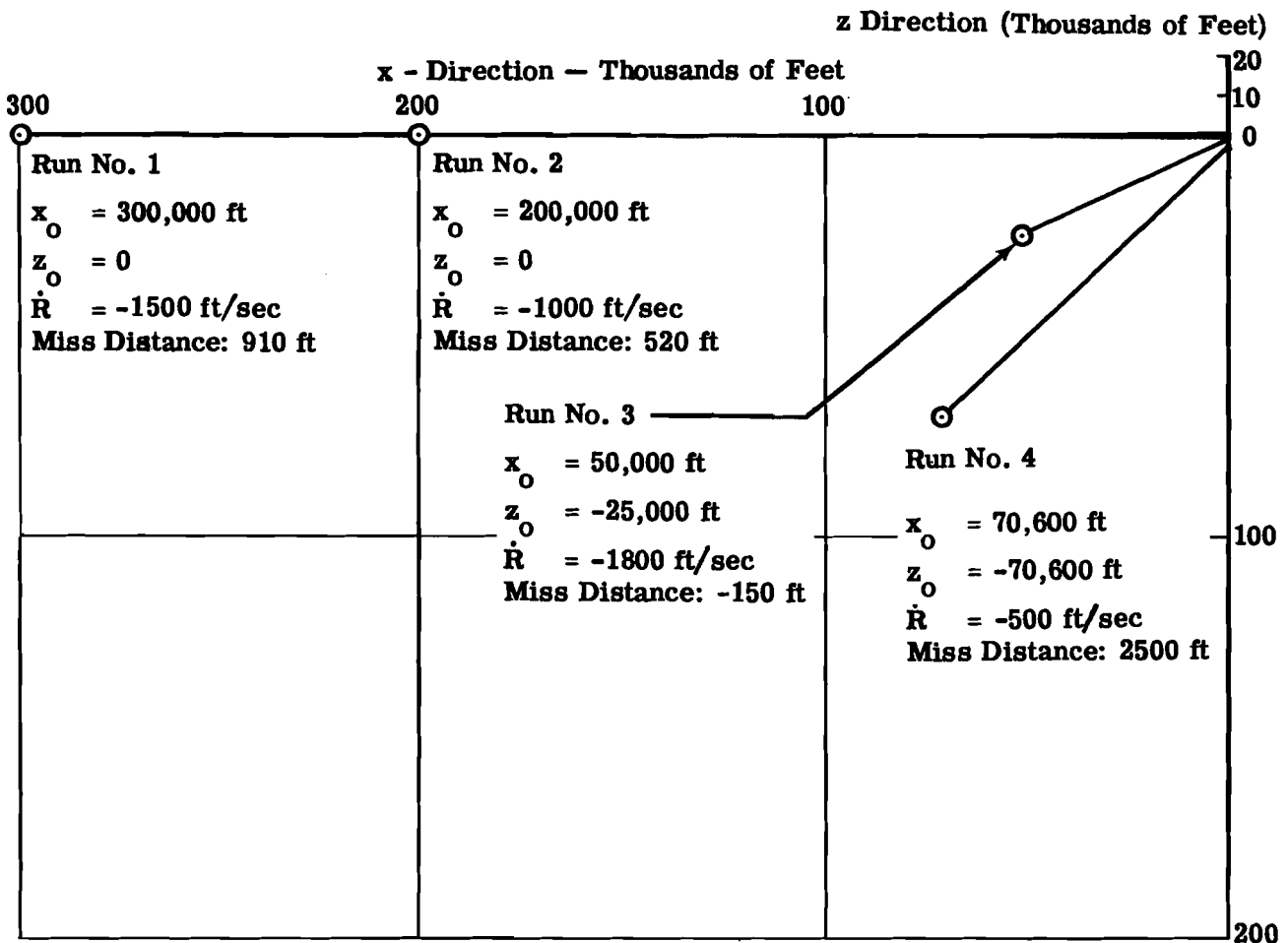


Figure 83. Miss Distances Due to the Effects of Differential Gravity (Inertially Fixed Axes with x Horizontal at the start of each Run)

$$\begin{aligned} \dot{R} &= \dot{z} \sin \alpha + \cos \alpha (\dot{x} \cos \beta + \dot{y} \sin \beta) \\ R \dot{\alpha} &= \dot{z} \cos \alpha - \sin \alpha (\dot{x} \cos \beta + \dot{y} \sin \beta) \\ R \dot{\beta} \cos \alpha &= \dot{y} \cos \beta - \dot{x} \sin \beta \end{aligned}$$

These rates were then integrated, giving R , α , and β , and fed back in the analog circuit, into the expressions requiring them. As a result of this sequence of programming, the requirements on the analog equipment were greatly relieved.

b. Transformation of Forces

To obtain F_{XI} , F_{YI} , and F_{ZI} from the thrust forces applied along the body axes, the transformation through the inertial Euler angles, ψ_I , θ_I and ϕ_I as given on page 48, were made.

$$\begin{bmatrix} F_{XI} \\ F_{YI} \\ F_{ZI} \end{bmatrix} = \begin{bmatrix} \psi'_I \\ \theta'_I \\ \phi'_I \end{bmatrix} \begin{bmatrix} T_{XB} \\ T_{YB} \\ T_{ZB} \end{bmatrix}$$

TABLE IX
DISPLAY QUANTITIES
ALIGNMENT AND BRAKING

Display	Range of Operation	Accuracy of Display
R Range	200,000 to 2000 ft	±50
\dot{R} Range Rate	2,000 to 50 ft/sec	± 3
A_{req} Req'd Accel. (or)	1.0 to 0 g	±0.01 g
$A^* a_{req}/a_{avail}$	1.0 to 0	±0.01
$R \dot{\alpha}$	500 to 0 ft/sec	1% ± 0.5 ft/sec
$R \dot{\beta} \cos \alpha$	500 to 0 ft/sec	1% ± 0.5 ft/sec
α Elevation	±90°	±0.5°
β Azimuth	±180°	±0.5°
θ_I Euler Pitch	±90°	± 0.5°
θ_c Command Pitch	±90°	±0.5°
ψ_I Euler Yaw	±180°	± 0.5°
ψ_c Command Yaw	± 180°	± 0.5°
ϕ_I Euler Roll	± 180°	± 0.5°
T_{X_c} Thrust Command	0-10,000 lb	± 1%
Also desirable		
$(\psi_I - \psi_c)$ Yaw Command Error	± 20°	± 0.5°
$(\theta_I - \theta_c)$ Pitch Command Error	± 20°	± 0.5°

c. Rendezvous and Docking Command Equations

For automatic aiming and thrusting in the terminal guidance phase, Technique 1 (page 27 of Section III) from the system of Reference 13 was programmed for the alignment mode together with the control equations from the same report for the braking mode. (These equations were also used in the digital simulation as described in Section V.)

For technique 1, however, the simplification indicated on page 4 of Reference 13 was used to simplify the command angles and reduce the computational requirements. As pointed out in that report, if the X axis of the reference axes is made coincident with the initial range vector, the initial α is zero. With proper thrust control, the maximum value of α will remain small. Consequently, the command expressions as given in Figure 17 reduce to

$$\psi_c = -\beta + \frac{R\dot{\beta}}{R\dot{\beta}} 90^\circ$$

$$\theta_c = -\arctan \frac{R\dot{\alpha}}{R\dot{\beta}}$$

A fully automatic docking system was not included as part of the control equations. It was judged that control during the docking phase could be handled by the pilot, through the use of the proper displays and visual scene. Both manual and automatic attitude control were provided.

The rendezvous and docking control arrangement programmed on the analog simulator allows for a wide variety of automatic and semi-automatic combinations of interceptor translation and attitude control. These are:

- (1) Alignment and Braking Phases – Automatic or manual translational thrusting with automatic or manual Euler angle commands, Euler angle rate commands, or body angular rate commands.
- (2) Docking Phase – Manual translational thrusting with automatic or manual Euler angle commands, Euler angle rate commands, or body angular rate commands.

d. Attitude System

In the analog simulation, the conventional automatic attitude control loop has been simplified. Whenever Euler angle commands are supplied by the guidance equations, the actual Euler angles are computed by passing these commands through a simple time lag. This provides a reasonably acceptable simulation of the actual attitude response under automatic attitude control operation.

The analog simulation also included a rate command mode wherein the pilot may command Euler rates $\dot{\psi}_c$, $\dot{\theta}_c$, and $\dot{\phi}_c$. From these commands,

$$\psi_I = \frac{\dot{\psi}_c}{s(\tau_\psi s + 1)}; \quad \theta_I = \frac{\dot{\theta}_c}{s(\tau_\theta s + 1)}; \quad \phi_I = \frac{\dot{\phi}_c}{s(\tau_\phi s + 1)}$$

Through this simplification, not only can the attitude control loop as programmed in the digital simulation be eliminated, but also the attitude equations:

$$\dot{p} = \frac{(M_{XB})_c}{I_x} - \frac{I_z - I_y}{I_x} qr$$

$$\dot{q} = \frac{(M_{YB})_c}{I_y} - \frac{I_x - I_z}{I_y} pr$$

$$\dot{r} = \frac{(M_{ZB})_c}{I_z} - \frac{I_y - I_x}{I_z} qp$$

$$\dot{\phi}_I = p + \psi_I \sin \theta_I$$

$$\dot{\theta}_I = q \cos \phi_I - r \sin \phi_I$$

$$\dot{\psi}_I = \frac{q \sin \phi_I + r \cos \phi_I}{\cos \theta_I}$$

can be eliminated.

However, since Euler rate commands $\dot{\psi}_c, \dot{\theta}_c, \dot{\phi}_c$, may be somewhat removed from the values the pilot may wish to command (i.e., r_c, q_c, p_c), the last three equations were added to the simulation.

2. Cockpit Simulator Description

The Bell Spaceflight Cockpit Simulator (see Figure 81) has been used in the rendezvous and docking studies performed under the subject program. A list of the displays which were used for these studies is shown in Tables IX and X. Figure 84 shows miniature illustrations of the key displays with titles and scalings. Cockpit controls for rendezvous and docking are listed in Table XI.

TABLE X
DISPLAY QUANTITIES
DOCKING

Display	Range of Operation	Accuracy
R Range	2000 to 20 ft	$\pm 1\% \pm 1$ ft
\dot{R} Range Rate	100 to 0 ft/sec	$\pm 1\% \pm 0.1$ ft/sec
a_{req} - Req'd Accel or A* Req'd Accel (Nondimensional)	0.03 to 0 g	$\pm 1\% \pm 0.0003$ g
R $\dot{\alpha}$ Normal Vel (In Elevation)	1.0 to 0	± 0.01
R $\dot{\beta} \cos \alpha$ Normal Vel (In Azimuth)	20 to 0 ft/sec	± 0.1 ft/sec
α Elevation	20 to 0 ft/sec	± 0.1 ft/sec
β Azimuth	$\pm 90^\circ$	$\pm 0.5^\circ$
θ_I Euler Pitch	$\pm 180^\circ$	$\pm 0.5^\circ$
θ_c Command Pitch	$\pm 90^\circ$	$\pm 0.5^\circ$
Y_I Euler Yaw	$\pm 90^\circ$	$\pm 0.5^\circ$
Y_c Command Yaw	$\pm 180^\circ$	$\pm 0.5^\circ$
ϕ_I Euler Roll	$\pm 180^\circ$	$\pm 0.5^\circ$
Also desirable: ($\psi_c - \psi_I$) Yaw Command Error	$\pm 20^\circ$	$\pm 0.5^\circ$
($\theta_c - \theta_I$) Pitch Command Error	$\pm 20^\circ$	$\pm 0.5^\circ$

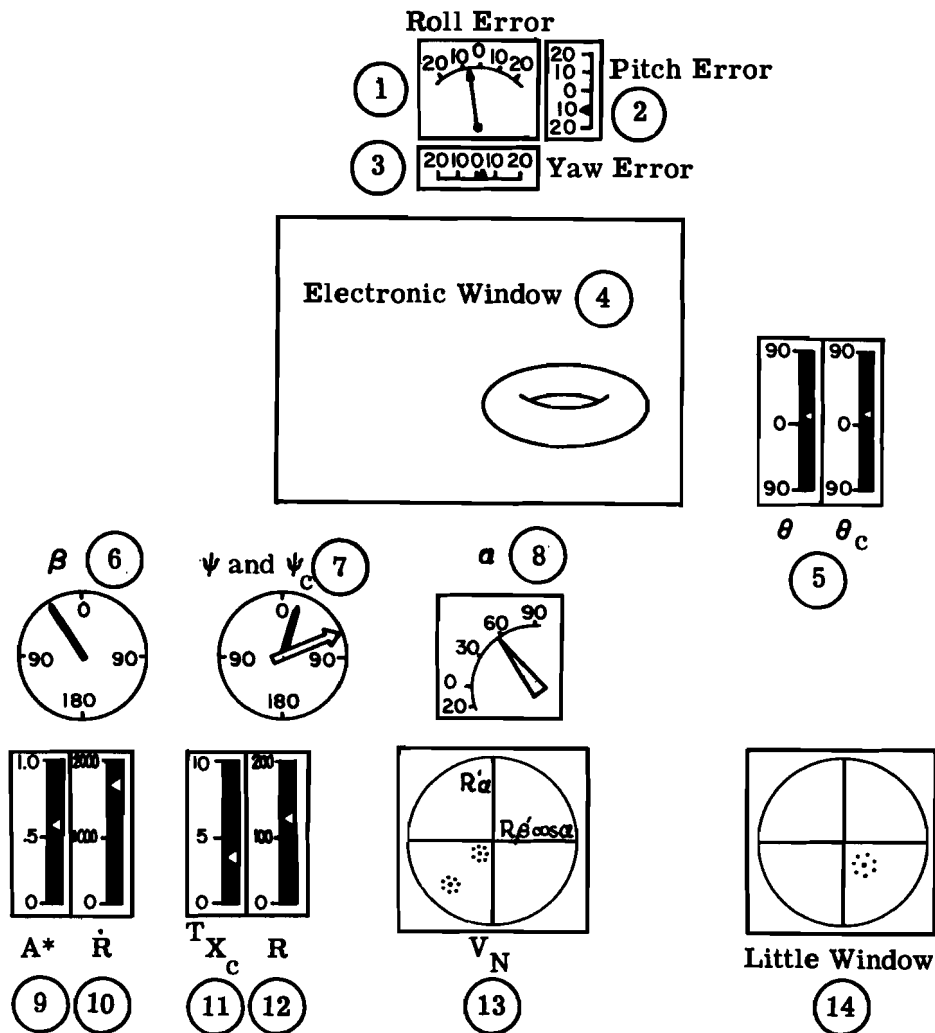


Figure 84. Simulator Cockpit Displays

A brief description of each of the displays and controls is given in the following.

a. Displays

Displays 1, 2 and 3 (Attitude Error Signals)

These instruments present the command error signals $(\phi_c - \phi_I)$, $(\theta_c - \theta_I)$, and $(\psi_c - \psi_I)$, respectively. Since roll command is zero at all times, the error signal represents the actual roll attitude. Pitch and yaw command angles are obtained from command equations of element 4, Figure 28.

Display 4 (Electronic Window)

The electronic window provides a visual representation of a toroidal shaped space station as viewed by the pilot through a forward window in the interceptor. The scene is displayed on a 21-inch CRT which is located 35 inches (17 inches behind panel, 18 inches in front of panel) away from the pilot's eye. With a maximum diagonal of 18 inches avail-

TABLE XI
COCKPIT CONTROLS

Control	Output	Description
Two-axis sidearm controller	Pitch and roll Attitude	Output proportional to deflection
Rudder pedals	Yaw Attitude	Output proportional to deflection
Two-axis sidearm controller	Docking thrust in Y_B and Z_B directions	On-off
Trigger-button on attitude controller	Docking thrust in X_B direction	On-off
Throttle lever	Alignment and/or braking thrust in X_B direction	Output proportional to deflection
Thrust switch	Alignment and/or braking thrust in X_B direction	On-off
Selector Switches: (1)	Signals for either automatic or manual thrust control	
(2)	Signals for either automatic or manual attitude control	
(3)	Signals for alignment braking or docking mode	

able on the CRT, the maximum view angle, θ , is ± 14.42 degrees. A target vehicle of 24 feet in outside diameter has been assumed. Therefore:

- (1) At 3000 feet, the target will subtend an angle of 0.46° , corresponding to a major axis diameter of 0.286 inch.
- (2) At 47 feet, the target will fill the screen.

Display 5 (Pitch Attitude and Pitch Command Indicators)

These are edge reading instruments giving the pilot pitch information within a range of ± 90 degrees.

Display 6 (Azimuth Angle)

This is a servo driven instrument with scaling 0 to ± 180 degrees.

Display 7 (Yaw Angle and Yaw Command Angle)

A dual-channel, servo type instrument with a scaling of 0 to ± 180 degrees. One indicator is being used for yaw angle, the other, yaw command angle.

Display 8 (Elevation Angle)

This is a galvanometer type instrument, with scaling -20 to +90 degrees.

Display 9 (A* - Nondimensional Required Acceleration)

A galvanometer type, edge reading display, scaled from 0 to 1.0.

Display 10 (Range Rate)

Range rate is scaled from 0 to 2000 ft/sec during the alignment and braking modes, and 0 to 100 ft/sec during docking.

Display 11 (Thrust Command)

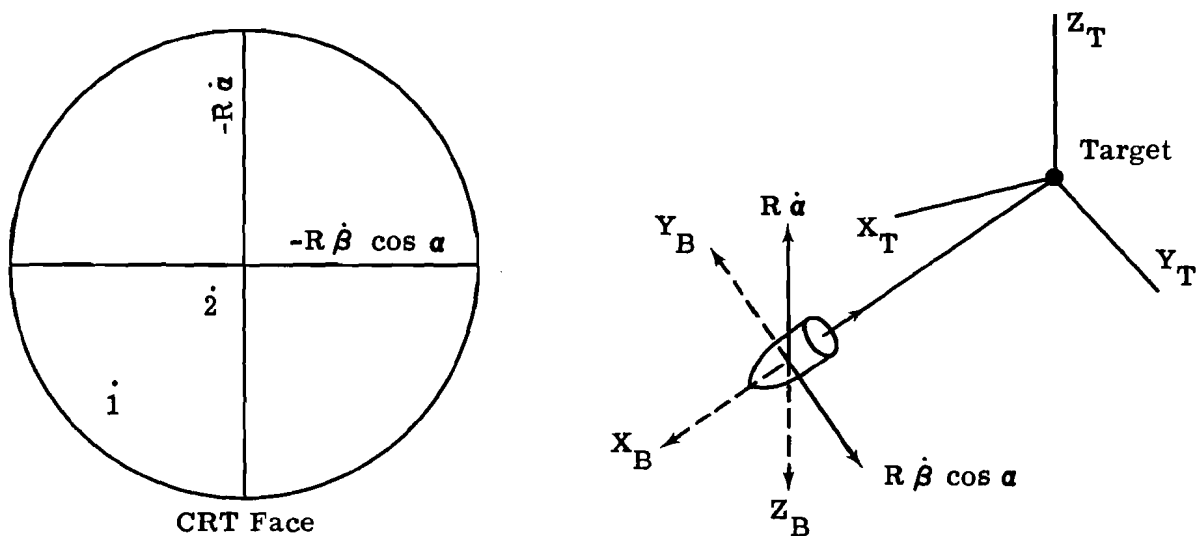
The thrust command is calculated according to the equation in element 4 of Figure 28. This applies only to the braking mode.

Display 12 (Range)

The line-of-sight range is presented on this edge reading display. During alignment and braking, it reads between 0 and 200,000 feet. During docking it is re-scaled to read between 0 and 2000 feet.

Display 13 (Velocities Normal to the Line of Sight)

This is a 5-inch dual-beam CRT which displays $R \dot{\alpha}$ (z input to the CRT), and $R \dot{\beta} \cos \alpha$ (y input to the CRT), the two components of velocity normal to the line of sight. Given any combination of $R \dot{\alpha}$ and $R \dot{\beta} \cos \alpha$, the CRT will display two points, 1 and 2, as illustrated in the accompanying sketch. Point 1 and point 2 represent the same coordinates ($R \dot{\alpha}$, $R \dot{\beta} \cos \alpha$) but with a scaling factor of ten in their display. Thus, if $R \dot{\alpha}$ and/or $R \dot{\beta} \cos \alpha$ are large, information will be derived from point 2; if they are small, point 1 will be utilized.



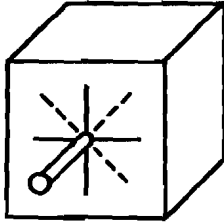
Display 14 (Target Location - Little Window)

Because the electronic window is limited in viewing range to δ less than ± 15 degrees, display 15 has been provided to indicate where the target is with respect to the body axes of the interceptor vehicle when δ is outside the ± 15 -degree range. Because of the small angle assumption made that $(\psi_I + \beta)$ represents the azimuth angle of the target in the window, the position of the target at large angles of $(\psi_I + \beta)$ will be only approximate. However, this display is meant for qualitative information, indicating to the

pilot which way he should pitch and yaw to bring the target image back into the visual range of the electronic window.

b. Pilot Controls

Thrust Controls



In order to control thrusting along the Y_B and Z_B axes during docking, a two-axis side arm controller is provided. It is mounted at the pilot's left and consists of a stick, as shown in the sketch, which operates four microswitches. Pushing up or down operates one pair of switches, corresponding to \pm thrust in the Z_B direction; pushing right or left operates the other pair, corresponding to \pm thrust in the Y_B direction. Diagonal displacement will operate two switches simultaneously, thus commanding thrust in both the Y_B and Z_B directions.

Although thrust values, T_{YB} and T_{ZB} may be assigned in any of several directions, they have been defined as:

- (1) Up fires rockets below, giving a force upward.
- (2) To the right fires rockets at left, giving a force to the right.
- (3) Diagonal fires both T_{ZB} and $T_{YB} \pm$ according to quadrant.

Thus, in conjunction with display 14, the pilot may follow the general rule of moving the sidearm controller to the same quadrant (or direction) in which the point on the CRT appears.

During the docking mode, longitudinal thrust, T_{XB} , is provided by a button and a trigger, on the model T-1, sidearm attitude controller, at the pilot's right. Thus, if the interceptor is aimed at the target, the button will apply thrust to accelerate toward the target; the trigger, away from the target.

Thrust will be available only in the longitudinal direction during braking, and on manual, variable thrust will be controllable by a lever to the pilot's left. Fixed thrust may be applied manually by controlling an on-off switch located on the pilot's left hand console.

In addition to the thrust controls, the pilot will have the following switches:

- (1) Automatic versus manual attitude control
- (2) Automatic versus manual thrust control
- (3) Mode control:
 - (a) Alignment
 - (b) Braking
 - (c) Docking

Automatic attitude control may be dialed in and out at any time in any mode. In addition, any mode may be selected by the pilot at any time. For instance, if the pilot wishes to dial the docking mode while in the braking mode range, he may do so, and use his docking thrusters, if that is his desire.

The pilot will also have the capability to stop his run at any time, then continue or reset to his original initial conditions. However, when he has finished his braking phase and is ready for rescaling for docking, he must go to hold until external switching at the computer console is accomplished. This takes approximately 5 seconds after which time he may continue by pressing the operate button. If he fails to stop for rescaling, the run will be stopped automatically at 2000 feet, at which time rescaling can still be made if desired.

Attitude Control

The pilot was provided with rate command attitude controls. This circumvented the problem of providing trimming switches or controls to maintain a biased attitude. Attitude and roll commands are introduced by a two-axis sidearm controller (Model T-1) to the pilot's right. Rudder pedals provide yaw rate command inputs to the computer. The operating rate command levels were fixed at 20 deg/sec about all three axes.

C. PILOT CONTROL TECHNIQUES FOR RENDEZVOUS

The technique the pilot should use in bringing about rendezvous and docking should be patterned after the control provided by automatic systems for proportional guidance control. To perform in a manner similar to the automatic system, the pilot must be aware of his line-of-sight range, range rate, and the two components of velocity normal to the line of sight, $R\dot{\alpha}$ and $R\dot{\beta}\cos\alpha$. In relation to an inertial reference system, he should be aware of the elevation angle, α , and azimuth angle, β , of the target. With this information, he will be able to locate the target vehicle with respect to his own vehicle's axes and position himself in the correct attitude for thrusting. The following two sections describe the procedure the pilot should use and the displays and controls to be employed for the rendezvous and docking phases of the mission.

1. Rendezvous

a. Braking

If the interceptor is approaching the target with components of velocity normal to the line of sight which are negligible compared to the range rate, R , then the pilot should apply thrust directly along the line of sight as required to control R . If the line-of-sight rotation rate becomes noticeable, then the pilot should thrust at some small angle away from the line of sight so as to drive this unwanted velocity to zero. If available, the automatic systems attitude commands ψ_c and θ_c , are useful to the pilot during braking. More relevant however, are the errors ($\psi_I - \psi_c$) and ($\theta_I - \theta_c$) which have been found to be very helpful on display during manual control.

How and when the pilot applies thrust to control \dot{R} can be determined from a measure of his available acceleration, compared with the acceleration required to just reduce \dot{R} to zero at a desired range to go, R . A good approximation of this required acceleration is given by the expression $a_{req} = \frac{R^2}{2R}$. (This expression is the basis of the thrust command expressions for the braking mode used in the digital simulation studies).

For display purposes, it is convenient to have a_{req} information on display at all times. Rather than a_{req} as such, it is somewhat more meaningful to present the

information in the nondimensional form, $A^* = \frac{a_{req}}{a_{avail}}$, with the general ground rule that

when A^* increases above 0.75, thrust should be applied and when it decreases below 0.25, thrust should be terminated. If a variable thruster is available, the pilot will be able to adjust his thrust until A^* becomes constant at a desired value such as 0.50.

b. Alignment

At acquisition, the interceptor will not generally be directly approaching the target; hence, there will be a rate of rotation of the line of sight. If this rate is sizable, it will be recognizable in a sizable $R \dot{\alpha}$ and/or $R \dot{\beta} \cos \alpha$. In this case, the pilot should pitch and/or yaw his vehicle well away from the line of sight (to a normal direction to the line of sight if the rates are very large) and perform an alignment maneuver wherein thrusting is maintained until both $R \dot{\alpha}$ and $R \dot{\beta} \cos \alpha$ are effectively eliminated. After this is accomplished, he may then follow braking phase maneuvers as described in the preceding paragraph.

When the pilot makes a large angular maneuver away from the line of sight, he will not be able to see the target image in his electronic window. In this case, all that he will have for reference are his displays. In order to position himself correctly, it is anticipated that he will need ψ_C and θ_C , along with the vehicle Euler angles and normal velocities $R \dot{\alpha}$ and $R \dot{\beta} \cos \alpha$.

In review, Table IX lists the displays that are deemed necessary for the pilot for control of alignment and braking. The estimated ranges of operation and accuracies of these displays are also listed.

2. Docking

Typically, docking will be initiated within a range of about 3000 feet or less and a closing speed of 50 ft/sec. Velocities up to 14 ft/sec normal to the line of sight can be handled by the typical thrusters. If V_N exceeds this value, the pilot will not be able to fully correct with his docking jets. In this case, his only alternative will be to fly around the target, where he can approach from the other side.

In the analog simulation, there is no automatic thrust mode during docking. Instead the pilot is responsible for thrusting in the X_B , Y_B , and Z_B directions to modulate R and eliminate $R \dot{\beta} \cos \alpha$ and $R \dot{\alpha}$. This can be done directly if the attitude of the interceptor is such that $\psi_I = -\beta$, $\theta_I = \alpha$ and $\phi_I = 0$. At this attitude, T_{ZB} will act to remove $R \dot{\alpha}$ directly, and T_{YB} will act to remove $R \dot{\beta} \cos \alpha$ directly. Thrusting in the X_B direction can be determined from the A^* display discussed previously, or from cues obtained from the visual scene. The recommended procedure for the pilot to follow upon entering the docking phase is as follows:

- (1) Point the interceptor directly at the target vehicle and maintain this attitude with roll equal to zero. Thus,

$$\psi_I = -\beta; \theta_I = \alpha \text{ and } \phi_I = 0$$

- (2) If $R \dot{\alpha}$ is positive, T_{ZB} should be applied downward until $R \dot{\alpha}$ is effectively eliminated.
- (3) If $R \dot{\beta} \cos \alpha$ is positive, T_{YB} should be applied toward the pilot's right until it also is effectively eliminated.
- (4) T_{XB} should not be applied until A^* builds up to some prescribed value, approximately 0.75. It should then be applied continuously until A^* becomes less than 0.25.
- (5) As closing proceeds, $R \dot{\alpha}$ and $R \dot{\beta} \cos \alpha$ components of velocity should be removed by thrusting with T_{ZB} and T_{YB} , respectively. As A^* builds up, T_{XB} should be applied.

By following these rules, an approximate collision course will be maintained. As the line-of-sight range reduces to values less than about 700 feet, the pilot is able to obtain information from visual cues from the electronic window.

The simulator instrumentation available to the pilot during the docking maneuver is the same as in the case of alignment and braking, although not all displays are required throughout the docking maneuver. However, because of his closer proximity to the target satellite, the ranges and associated accuracies of the displayed parameters will be different. Table X summarizes these displays, with estimates of the associated accuracy and resolution requirements.

D. COMPUTER MECHANIZATION

A schematic of the analog mechanization of the rendezvous and docking simulation is shown in Figure 85. In order to ease the programming problem, several simplifications have been made. Several of these, in connection with the equations of relative motion and the equations for positioning the target image in the window have been described in earlier parts of this section. It should be noted that the "exact" equations were not beyond the capability of analog computers, but rather that the simplifications made were deemed to be fully justified from mathematical as well as operational considerations.

In the following, some additional simplifications that have been made in the computer mechanization are first described. This is followed by a discussion of accuracy considerations inherent in analog computer programming.

1. Simplifications

- (a) No provision was made in the simulation to account for the reduction in the mass of the interceptor resulting from fuel expended during corrective maneuvers. This assumption of a constant mass considerably eased the computing task but did not appreciably compromise simulation results.
- (b) The rotational order of β followed by α produces a "gimbal lock" in β when α is 90° . This phenomenon is reflected in the simulation where $\cos \alpha$ appears in the denominator (Section IV). This situation does not limit the simulation except for the case where the interceptor "flies" directly over (or under) the target as the result of an unsuccessful rendezvous maneuver. It is to be noted that an order of rotation α followed by β would result in a similar "gimbal lock" in α .
- (c) A deficiency in the target image generation produced a false shading effect when the toroid was viewed at negative α (from below). After a few practice runs, the pilots quickly adapted to the situation and were not hindered by this limitation. A technique for correcting this limitation has been devised, but the added cost was not warranted for the present application.

2. Accuracy

In general, the accuracy that can be realized on an analog computer in terms of problem quantities is highly dependent on the range of problem variables that must be covered.

Because the analog computer has a useful signal range of 0 to + 100 volts, all of the problem variables must be scaled such that their operating range does not extend beyond this voltage range. An example illustrating this follows.

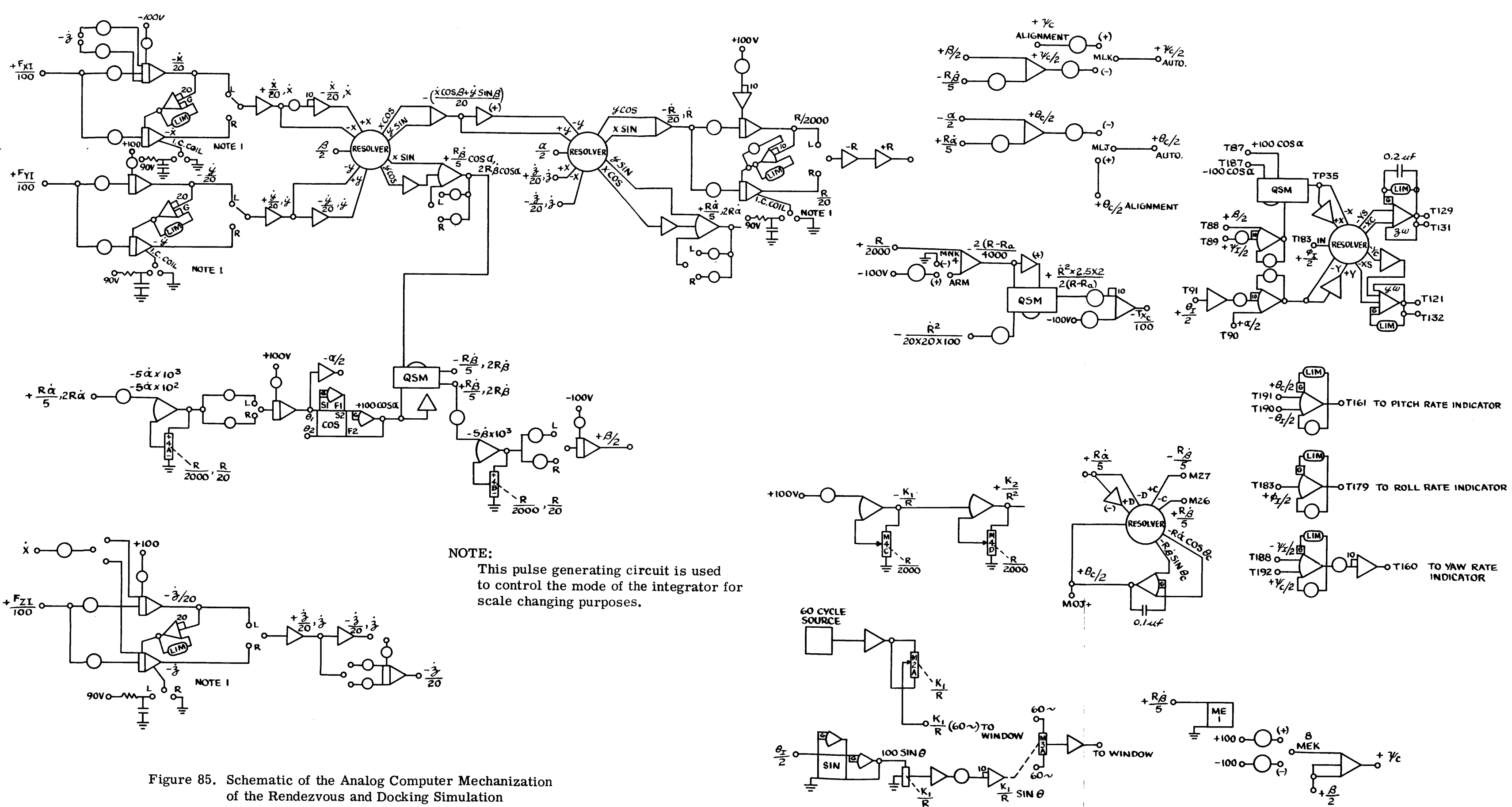


Figure 85. Schematic of the Analog Computer Mechanization of the Rendezvous and Docking Simulation

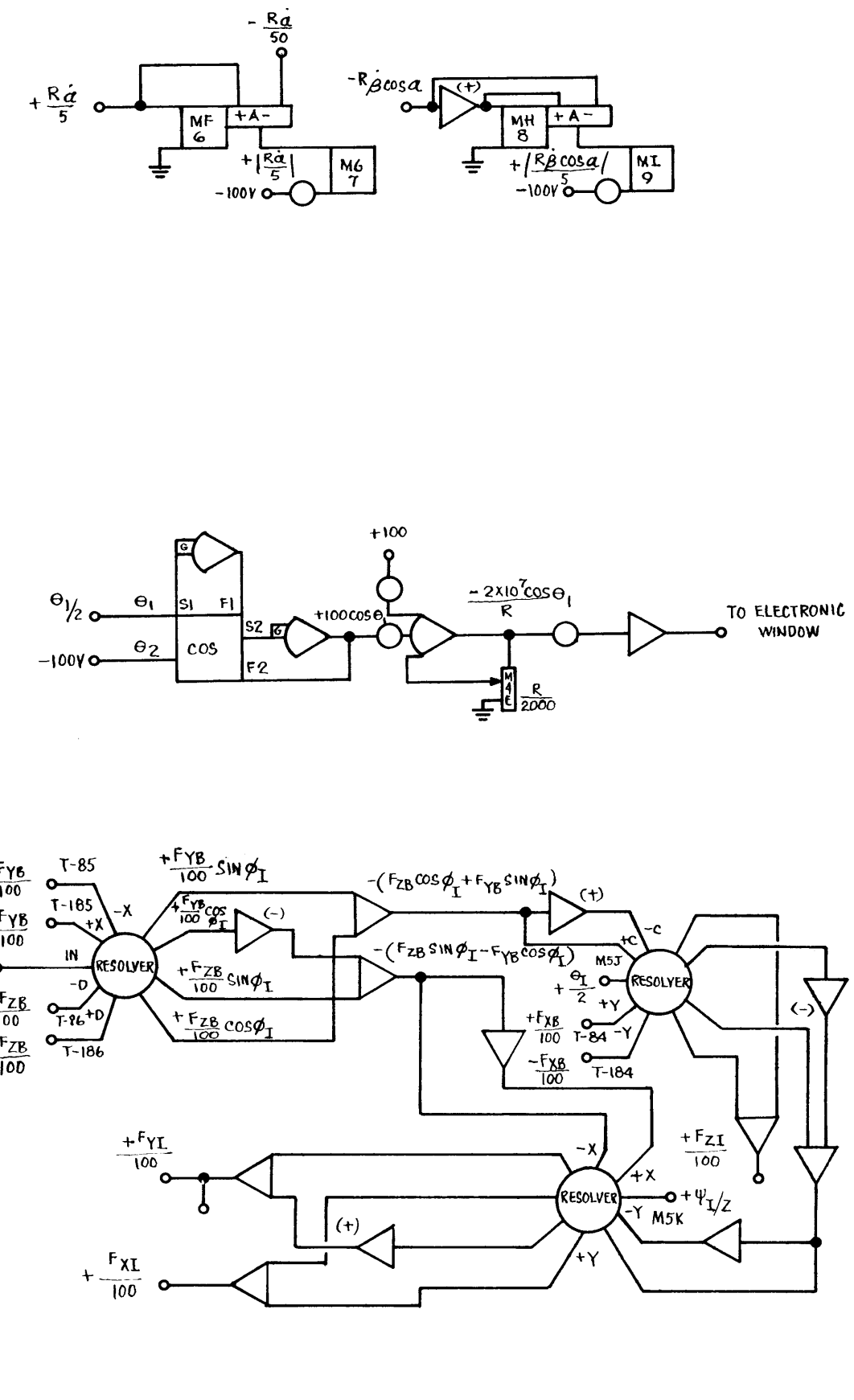
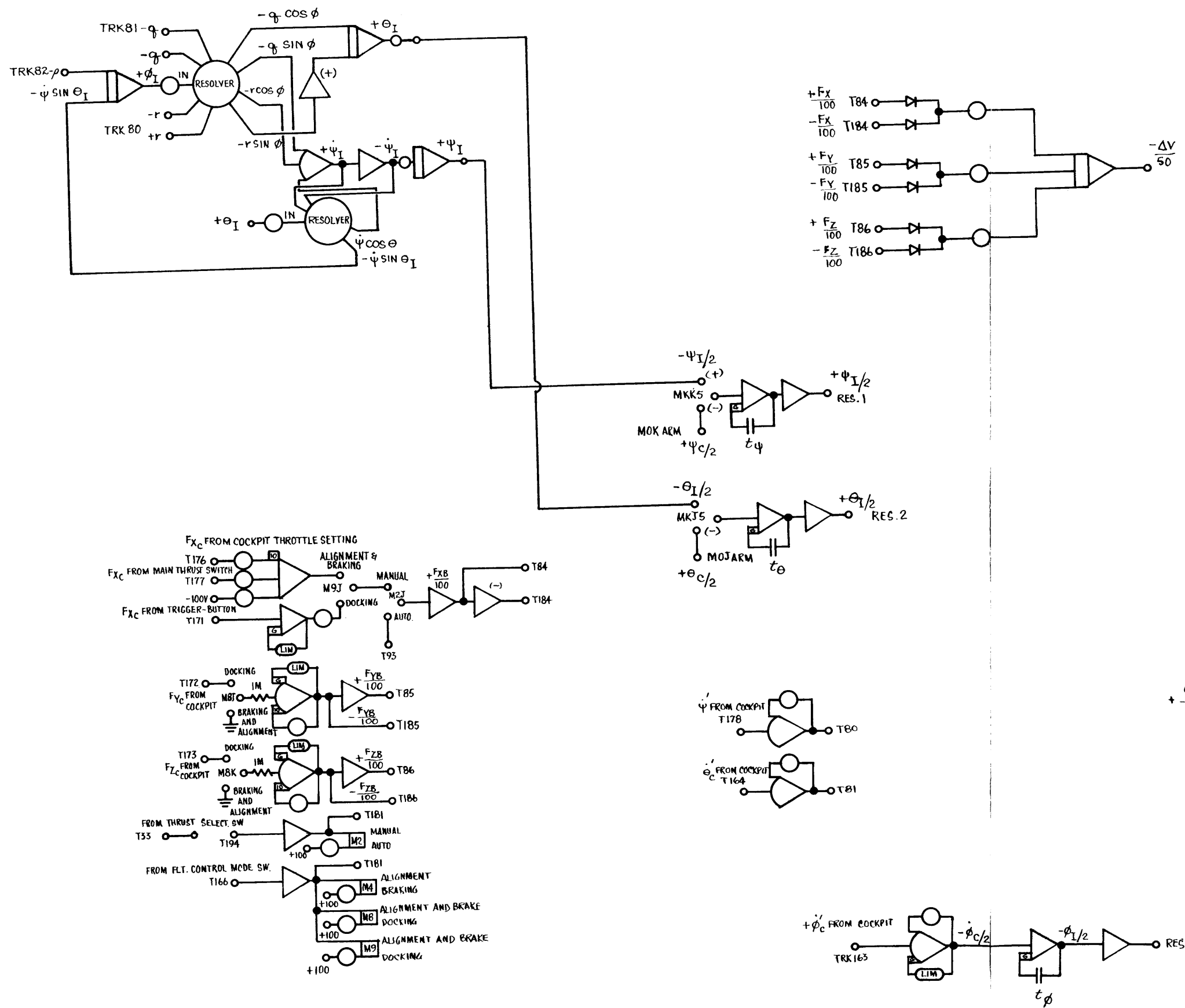


Figure 85. Schematic of the Analog Computer Mechanization of the Rendezvous and Docking Simulation

If the LOS range takes on values from zero to 200,000 feet, a volt in the computer represents 2000 feet. It is possible, of course, to make each volt equal 5000 feet, thus extending the maximum operating range to 500,000 feet. However, since the accuracy of a signal is good to within ± 0.1 volt, the first scaling ($R/2000$) produces a signal good to within ± 200 feet, while the second scaling ($R/5000$) produces a signal good to within ± 500 feet. Therefore, a tradeoff exists between operating range and accuracy.

An overall computer accuracy of 0.4v was used to determine the problem signal accuracies and these are tabulated in Table XII together with the maximum value the parameter may take on.

E. MISSION RUNS AND RESULTS

1. General

In order to check the validity of the analog simulation and to justify the simplifying assumptions used in programming the equations of motion, a series of analog runs was made using automatic and semi-automatic guidance and control loops, and fully manual where the pilot controlled the vehicle at his own discretion. Results were cross-checked with each other and with the corresponding solutions as obtained on the digital simulation.

Further testing was done to determine initial conditions which are within the pilot's capabilities to control and to obtain information as to what roles a pilot may play in the overall rendezvous and docking mission, and to what extent pilot displays will be needed.

TABLE XII
PARAMETER ACCURACY AND RANGE

Parameter		RANGE		ACCURACY	
		Alignment-Braking	Docking	Alignment-Braking	Docking
R	ft	2000 to 200,000	0 to 2000	± 800	± 8
\dot{R}	fps	0 to 2000	0 to 100	± 8	± 0.4
$R \dot{\alpha}$	fps	0 to 500	0 to 50	± 2	± 0.2
$R \dot{\beta} \cos \alpha$	fps	0 to 500	0 to 50	± 2	± 0.2
α	deg	0 to 180	0 to 180	± 0.8	± 0.8
β	deg	0 to 180	0 to 180	± 0.8	± 0.8
ϕ_I	deg	0 to 180	0 to 180	± 0.8	± 0.8
θ_I	deg	0 to 180	0 to 180	± 0.8	± 0.8
ψ_I	deg	0 to 180	0 to 180	± 0.8	± 0.8
$F_{XI} F_{YI} F_{ZI}$	lb	0 to 10,000	0 to 10,000	± 40	± 40
$\dot{x}, \dot{y}, \dot{z}$	fps	0 to 2000	0 to 100	± 8	± 0.4

2. Mission Runs

The first series of analog simulation runs are presented in Figures 86 and 87. In these runs the initial conditions were the same as those of Mission Run No. 3, which involved only the braking mode of the Reference 13 technique described in Section III-D-1 and again in Section V-D-3. Curves (b) of these figures are for the case in which complete automatic aiming and thrusting commands were used. Curves (c) correspond to manual control of the interceptor vehicle from displayed information and visual cues as supplied from the electronic window. Curves (a) correspond to curves (b), except that the solutions were obtained from the digital simulation of Section V.

In examining the results of curves (a) and (b), it can be seen that the analog simulation using automatic control closely matches the solutions obtained from the digital simulation. When the pilot took over the controls, (curves (c) of Figures 86 and 87), he had little difficulty in performing a satisfactory rendezvous. However, his performance did not follow very closely that of the "automatic" runs, in that, he modulated thrust in large steps occasionally turning his thruster off completely, with the result that the time history of \dot{R} versus R (Figure 86), was quite irregular. In addition, the pilot initially thrust to reduce his range rate to a smaller value than that produced by the "automatic" system. This resulted in a somewhat longer rendezvous time. The amount of ΔV used was 1800 ft/sec - virtually the same amount that was used by the "automatic" run. Actually, several manual runs were made of which curves (c) are typical.

Figures 88 and 89 present results similar to Figures 86 and 87 except in this case, the initial conditions of Mission Run No. 8 were used. Because of the large velocities normal to the line of sight ($R \dot{\alpha} = 500$ ft/sec, $R \dot{\beta} \cos \alpha = 50$), Technique 1 was employed to eliminate $R \dot{\alpha}$ and $R \dot{\beta} \cos \alpha$. This operation was then followed by the braking mode. Again, three curves are presented; curves (b) of Figures 88 and 89, respectively, give the results in which complete automatic aiming and thrusting commands were used to control the interceptor; curves marked (c) present the case in which the pilot was controlling the interceptor. Curves (a) present the digital solution using closed loop automatic control. It can be seen in this case that the analog simulation, using automatic control (curves (b)) also correspond closely to the digital results (curves (a)). During the alignment mode, the pilot followed the "automatic" commands displayed to him closely, producing results very similar to those obtained by "automatic" control. During braking, however, he disregarded many of the "automatic" commands, aiming and thrusting as he felt the situation warranted. As shown, he brought the interceptor into conditions suitable for docking without difficulty. Again, the ΔV he used was approximately the same as that used by the "automatic" control loop.

Additional runs were made with the pilot in the loop with displays of command information covered up, but all other displays (presenting \dot{R} , $R \dot{\alpha}$, $R \dot{\beta} \cos \alpha$; i.e., his situation displays) available for use. It was found from these runs that some difficulty was experienced in the alignment portion of flight, where the large velocities normal to the line of sight must be removed. With practice, however, the pilot was able to occasionally conduct a successful rendezvous. Limits of his ability are discussed in the following.

Results presented thus far have dealt with the terminal guidance phase of rendezvous. For docking, another set of runs was made. In this case, the pilot had to monitor his displays and command thrust by means of his sidarm controllers. The technique the pilot should follow is described in detail in Section III. Many runs were made with varying initial conditions, of which Figure 90a presents results of a typical flight. As in the case of the rendezvous phase, it can be seen that the pilot had no difficulty in bringing the interceptor into close proximity to the target vehicle. In the typical run shown in Figure 90a, the pilot had full use of his displays and automatic attitude positioning.

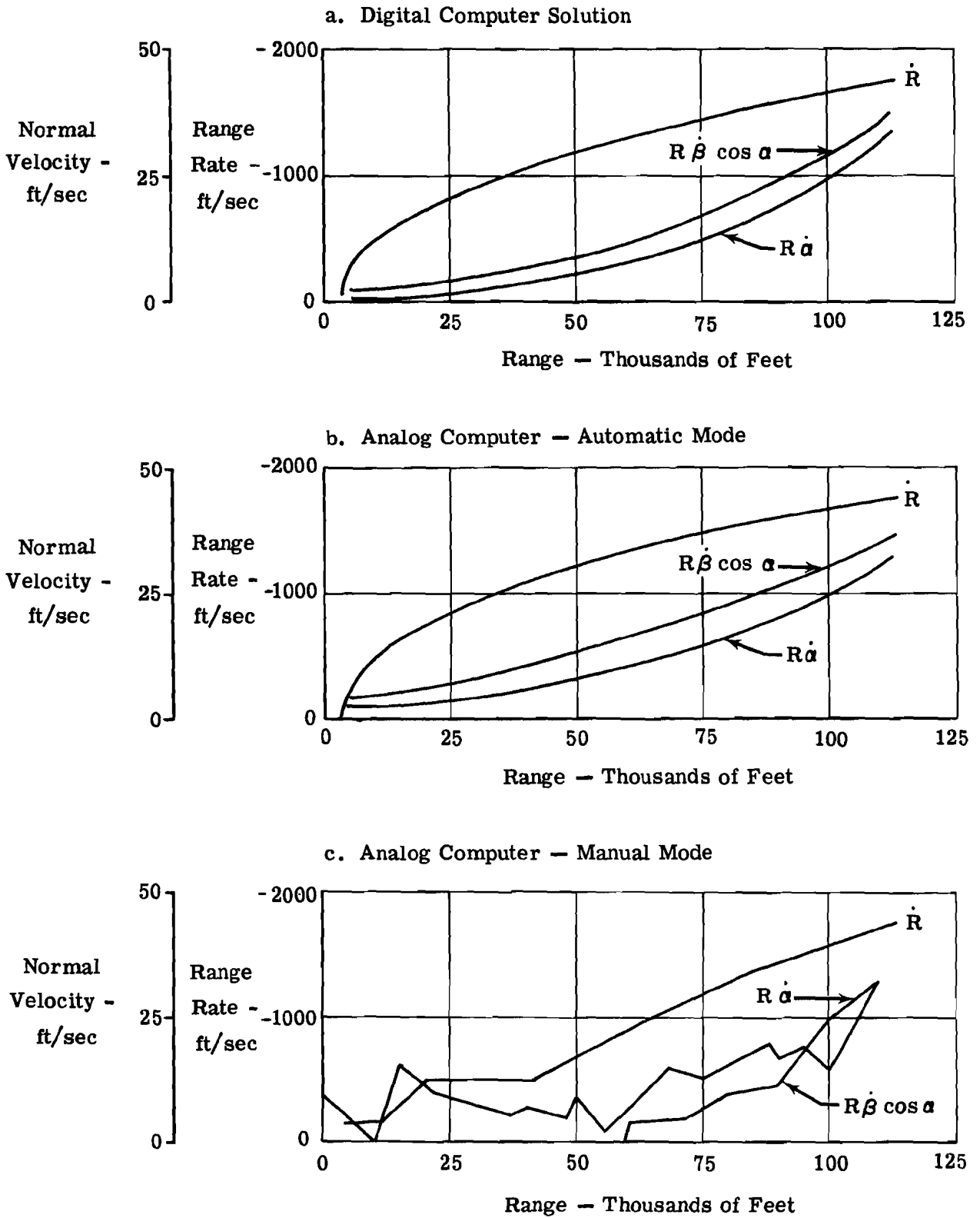
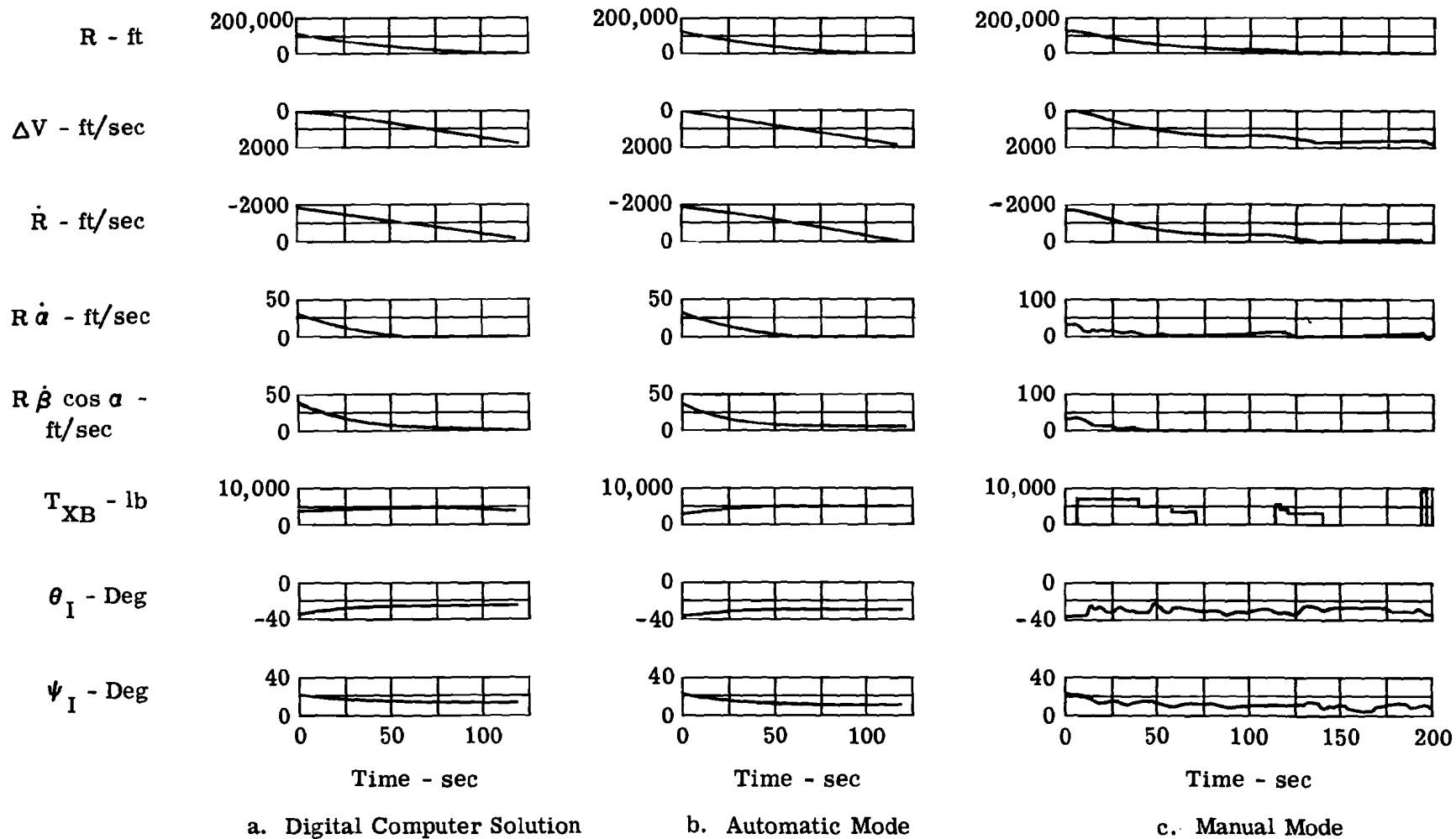


Figure 86. Velocity Trajectories of Mission Run No. 3



Initial Conditions:

$$\begin{aligned}
 R_0 &= 113,575 \text{ ft} & (R \dot{\beta} \cos \alpha)_0 &= 37 \text{ ft/sec} \\
 \dot{R}_0 &= -1760 \text{ ft/sec} & \alpha_0 &= -25.5^\circ \\
 (R \dot{\alpha})_0 &= 34 \text{ ft/sec} & \beta &= -13.6^\circ
 \end{aligned}$$

Figure 87. Time Histories of Mission Run No. 3

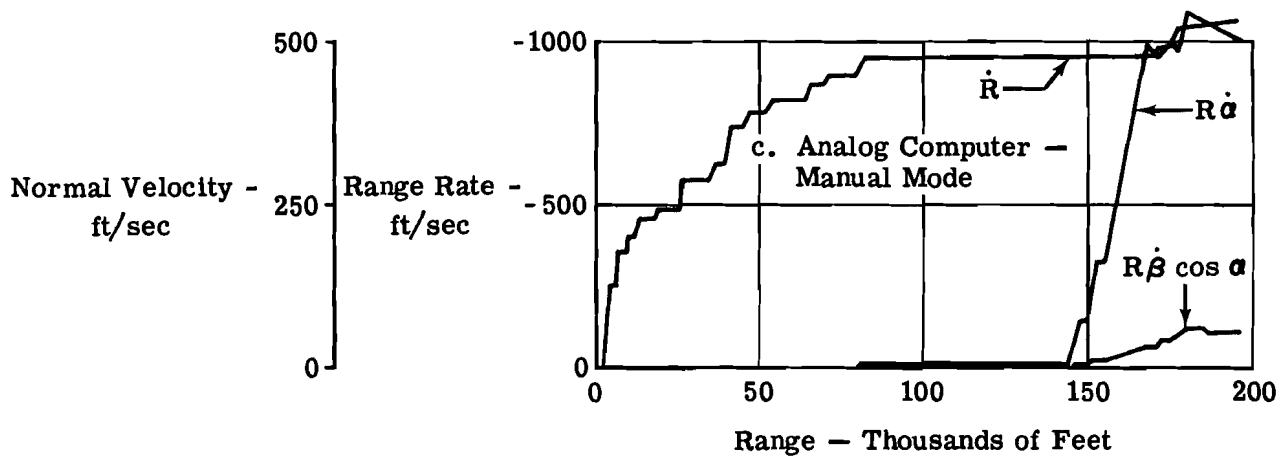
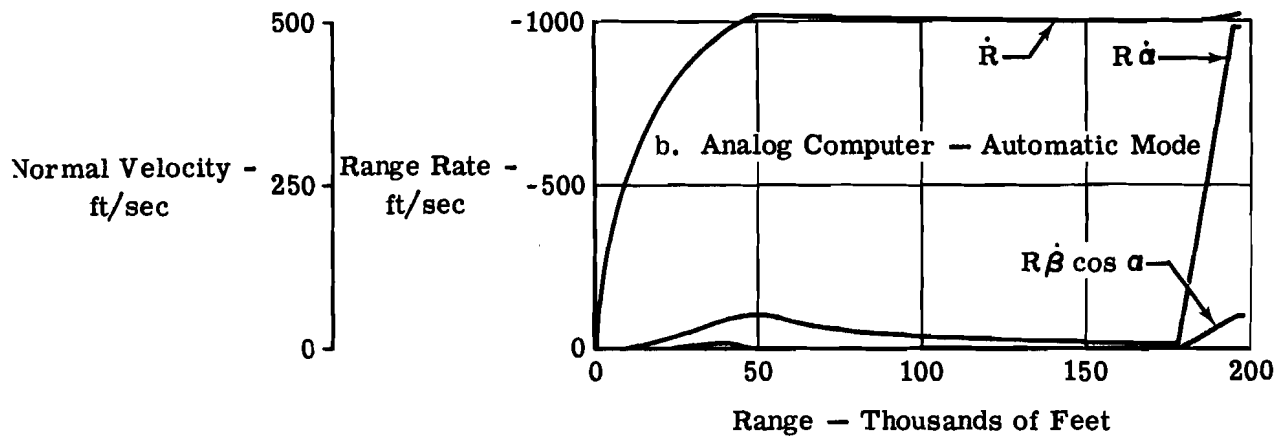
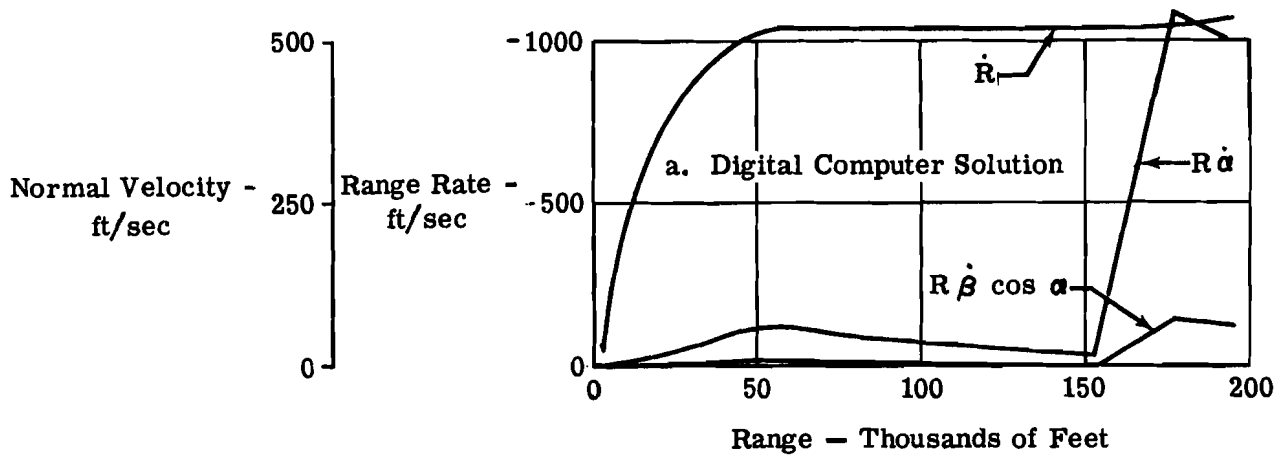
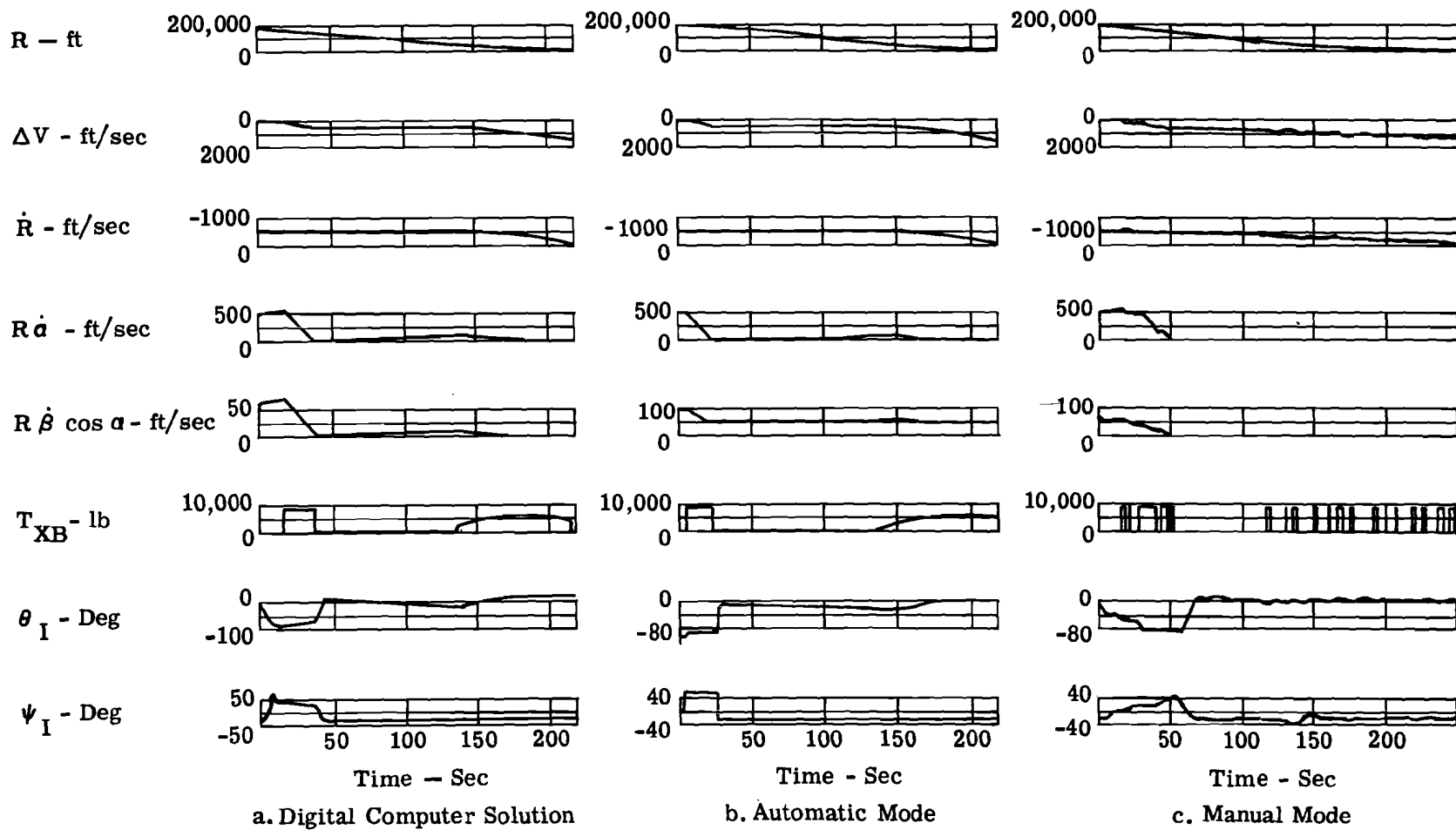


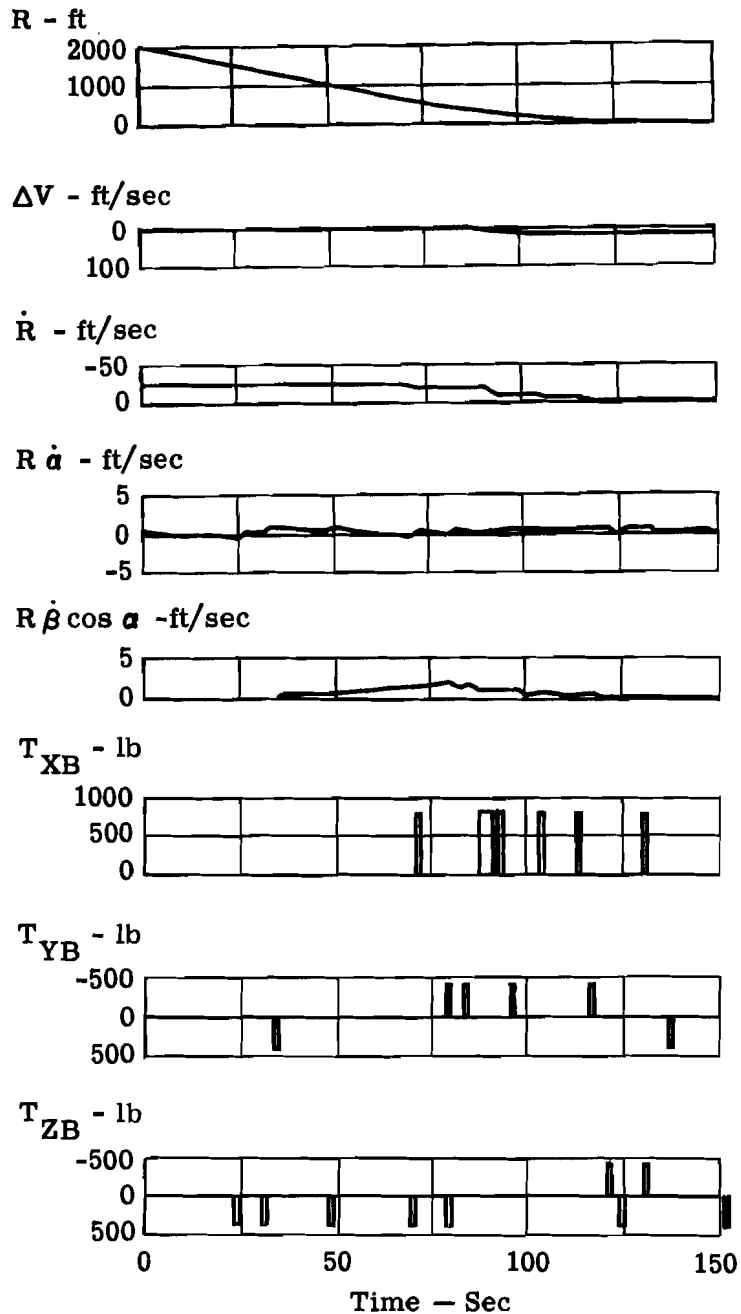
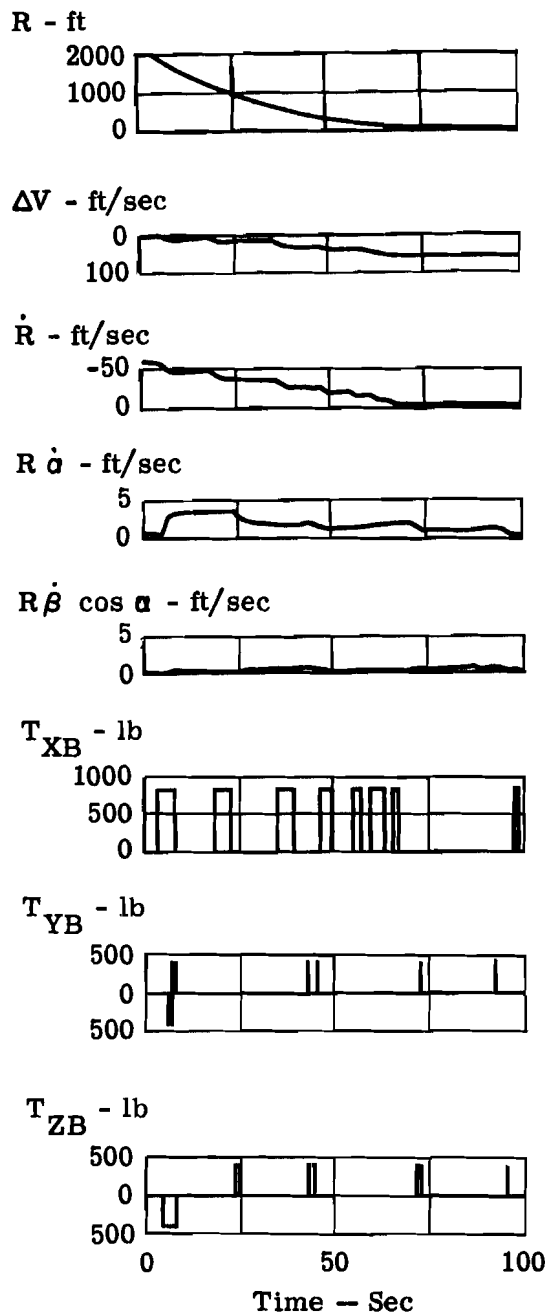
Figure 88. Velocity Trajectories of Mission Run No. 8



Initial Conditions: $R_o = 195,424 \text{ ft}$
 $\dot{R}_o = -1060 \text{ ft/sec}$
 $(R \dot{\alpha})_o = 500 \text{ ft/sec}$
 $(R \dot{\beta} \cos \alpha)_o = 61 \text{ ft/sec}$

$\alpha_o = 0$
 $\beta_o = -22.9^\circ$

Figure 89 Time Histories of Mission Run No. 8



(a) Pilot had Full Use of all Displays.

(b) The Pilot Controlled on the Basis of the Visual Scene Only.

Figure 90. Time Histories of a Manually Controlled Docking Maneuver

Figure 90b, on the other hand, presents a typical docking maneuver, where all displays were eliminated, and the pilot was controlling attitude and the firing of his maneuvering thrusters manually. It can be seen, that he did a satisfactory job in bringing his interceptor vehicle to a condition which would permit latching, if that were his mission.

As a result of the runs described in the preceding, the following was concluded:

- (a) The analog simulation performed satisfactorily in all modes; alignment, braking and docking.
- (b) The pilot, if given suitable displays, and reasonable initial conditions, is capable of controlling rendezvous with ease, without excess use of fuel. In most docking cases, the displays could be eliminated, as the target was approached, with the pilot using only the visual scene to determine how to control the vehicle.

3. Pilot Capabilities

To determine pilot capabilities in the rendezvous phase, a series of tests were conducted varying the initial conditions of closing speed (\dot{R}), range (R), and velocity normal to the line of sight ($V_N = \sqrt{(R \dot{\alpha})^2 + (R \dot{\beta} \cos \alpha)^2}$). In tests of this type, it was felt that control of the normal velocity should be of the same degree of difficulty, regardless of how it was divided between its components $R \dot{\alpha}$ and $R \dot{\beta} \cos \alpha$. Therefore, variation of the normal velocity was obtained by changing $R \dot{\alpha}$, however, small components of $R \dot{\beta} \cos \alpha$ were present in most cases. In each run, the pilot had full use of his situation displays, but was required to control the attitude of his vehicle manually by his sidearm controller and rudder pedals. He was also required to determine, for himself, when to apply thrust, and to do so through the switches available in the cockpit.

Initial conditions were varied in successive runs so as to progressively tax the pilot in performing the mission. When he failed, these initial conditions were recorded. Figure 91 presents the results of this experiment. It can be seen that the pilot does have a capability of performing a satisfactory rendezvous over a reasonable range of initial conditions.

4. Computational Task for the Analog Computer

As demonstrated by the analog computer simulation program of rendezvous and docking which is described in the preceding sections, a moderately complex analog program can be developed to perform many worthwhile studies. If a complete simulation is required, however, such as the digital simulation described in Section V, then the difficulty of the analog simulation is appreciably increased. In the following tabulation, the equipment used in the analog simulation is listed along with an estimate of the equipment requirements for a complete mission simulation. To perform the complete simulation on analog equipment, re-scalings of the problem variables must be made at two or three points in the mission. Provisions for this have been included in the following equipment estimate:

	<u>Present Simulation</u>	<u>Complete Mission Simulation</u>
Amplifiers	140	250
Pots	100	150
Multipliers	8	43
Resolvers	7	24
Comparators	13	15

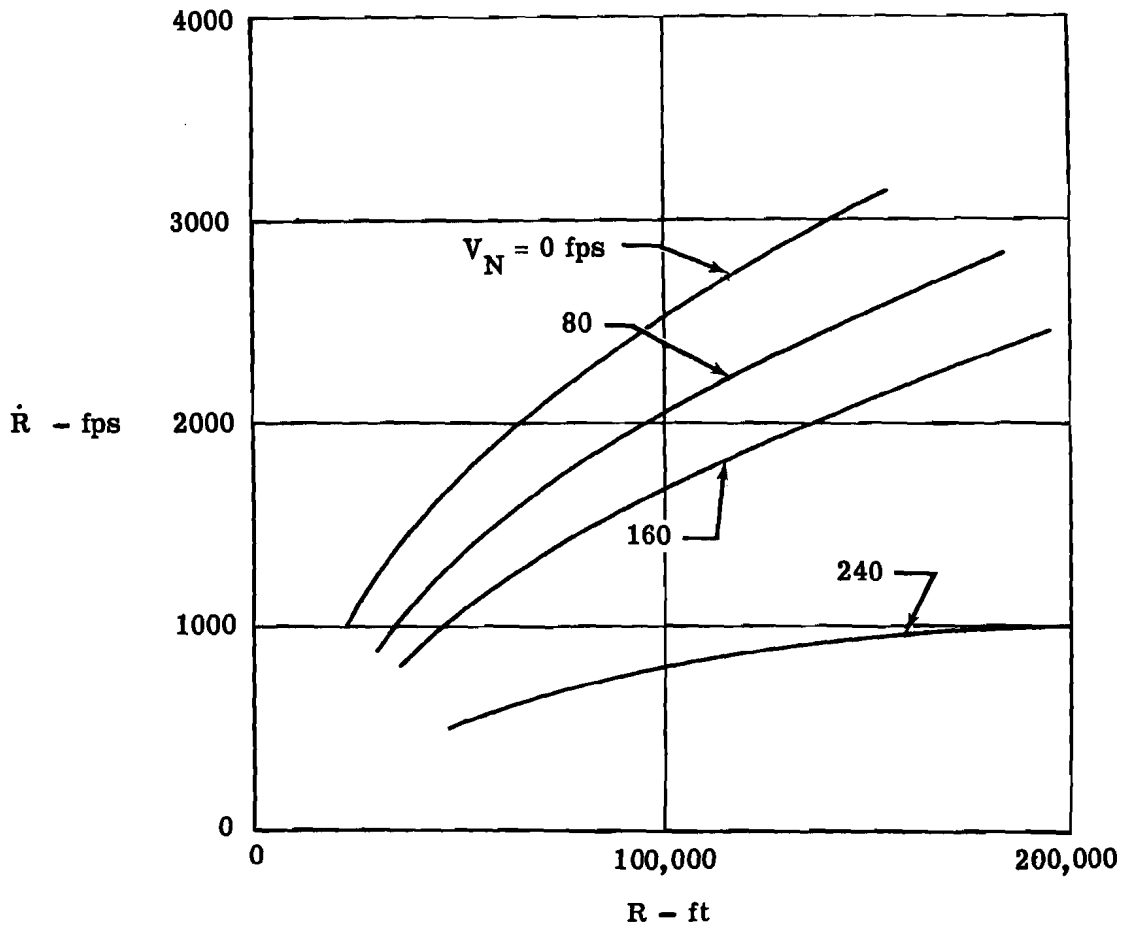


Figure 91. Initial Conditions within the Pilot's Capability

If investigations which are required of a simulation can be satisfactorily accomplished by an analog simulation such as developed on the subject program, then a choice of analog equipment for this purpose is not an unreasonable one. If the type of investigations to be made require the complete form of the rendezvous and docking simulation, then a choice of digital computing equipment is more reasonable in most cases. This latter choice is suggested largely because of the standard problems in accuracy, reliability and flexibility which result when large programs are mechanized on analog computers, and because of the significant advances which have been taken recently in the area of digital computer speed, cost, programming ease, etc. Of course, in any given application the availability of existing equipment will play a large role in the choice of computing technique.

VII. SUMMARY AND CONCLUSIONS

1. The many types of rendezvous and docking techniques proposed and studied in the literature can be classified into two types: (1) "Orbital Mechanics Techniques" which are based on exact, special cases, or simplified equations of orbital mechanics; and (2) "Proportional Navigation Techniques" which involve simplified equations and command rules based upon relative motion between the two vehicles.

2. In general, the range at which orbital mechanics effects can be neglected is a function of the speed at which the interceptor is approaching the target vehicle and the separation distance. The higher the closing speed, and shorter the separation range, the sooner proportional navigation techniques can be validly employed.

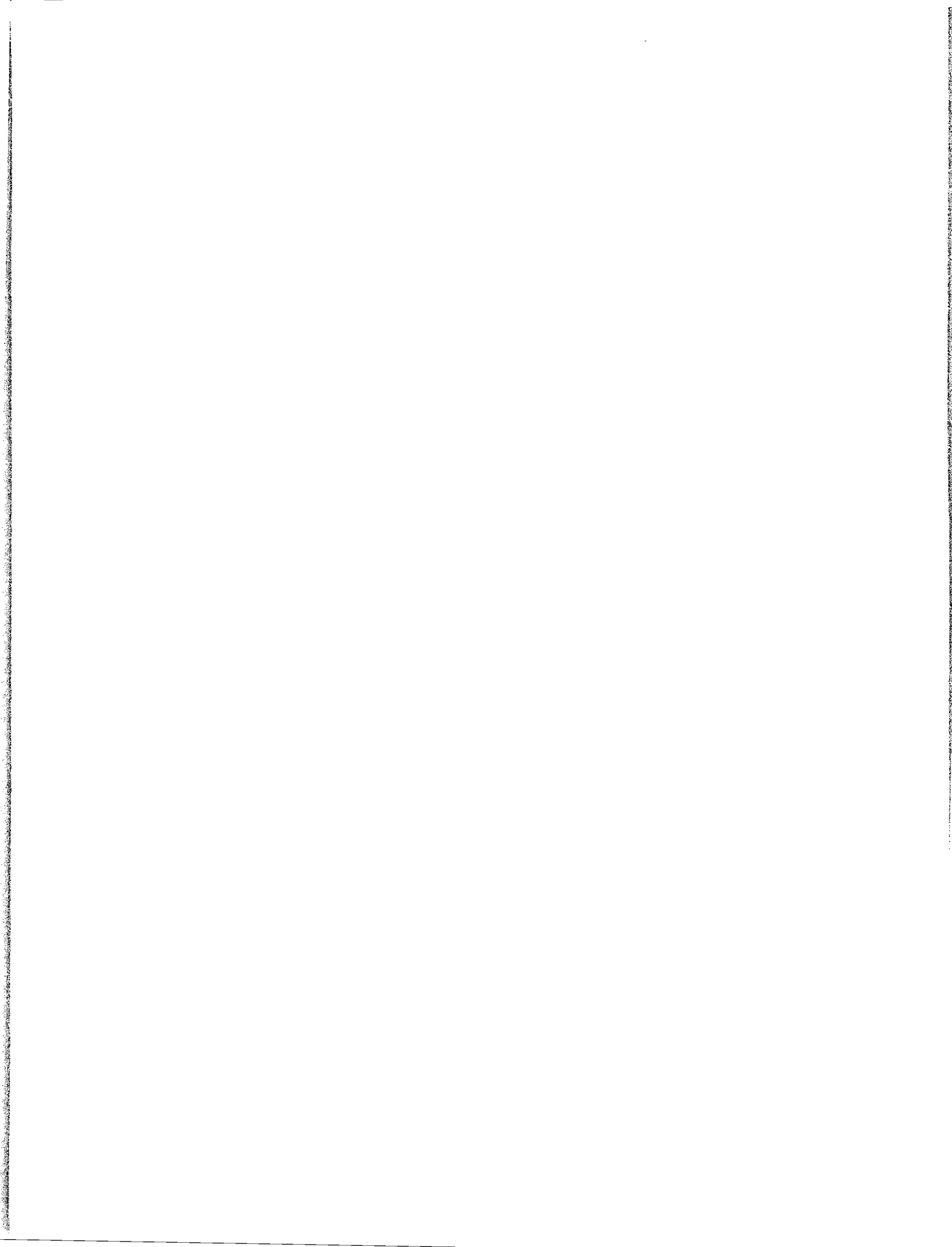
3. For a digital simulation of the rendezvous, docking, departure and deorbit missions, the computer should have a 7500 word memory, of which 500 are needed for data storage. Its average add and multiplication times should be 60 to 70 microseconds, and a minimum word length of 18 binary digits appears desirable.

4. An analog simulation of the complete rendezvous mission results in a rather elaborate program requiring an extensive amount of equipment and two or three re-scalings of the problem variables during the mission. If the type of investigations which are required permit the problem to be limited to one or two phases of the complete rendezvous mission (as was done in the present study), analog equipment can be conveniently employed.

5. With modest information and an attitude rate command system, the pilot will be able to perform rendezvous over a large range of initial conditions, both in the terminal guidance and docking phases.

6. The simulation of the complete rendezvous mission can be conveniently accomplished by using a digital computer. However, a hybrid computer, mainly digital, but employing analog computing with analog-digital conversion capability is also a practical arrangement. In this case, computations involving high accuracy can be best done digitally, while computations requiring high speed solutions, such as the attitude control loop and inputs to the visual display, can be best accomplished on analog equipment.

7. The portion of the simulation used for guidance and control computations has little in common with the energy management portion of deorbit and flight within the atmosphere. Therefore, there appears to be little reason to combine these two operations other than for computational convenience. However, the equations of motion relating a vehicle in space to the earth appear in both mission operations. Therefore, in an overall mission simulator, the combining of these equations warrants further investigation to determine the possible computational savings which could result.



REFERENCES

1. Emerson, J. E., Birkemeier, J. R., and Ryken, J. M., (Unclassified Title) Simulation of Energy Management Systems for Hypersonic Glide and Reentry Vehicles, (Confidential Report) Technical Documentary Report No. MRL-TDR 62-6, 6570th Aerospace Medical Research Laboratories, Aerospace Medical Division, Wright-Patterson Air Force Base, Ohio, February 1962.
2. Miller, B., "Radar, Infrared Studied for Rendezvous," Aviation Week, Vol. 77, pp 54-63, July 16, 1962.
3. Griffin, J. B., A Study of a Self-Maneuvering Unit for Orbital Maintenance Workers, ASD-TDR-62-278, Aeronautical Systems Division, Wright Patterson Air Force Base, Ohio, August 1962.
4. Thompson, H. B. and Stapleford, R. L., A Study of Manual and Automatic Control Systems for the Terminal Phase of Orbital Rendezvous, Part 1, Basic Guidance and Control Information, ASD-TR-61-344, Part I, Aeronautical Systems Division, Wright-Patterson Air Force Base, Ohio, June 1962.
5. Houbolt, J. C., "Problems and Potentialities of Space Rendezvous," Astronautica Acta, Volume VII, 1961, Fasc. 5-6, pp 406-429.
6. Astronautics, Vol. 7, April 1962.
7. Romaine, O., "Gemini," Space/Astronautics, Vol. 38, No. 5, October 1962, pp 54-59.
8. Eggleston, J. M. and Beck, H. D., A Study of the Positions and Velocities of a Space Station and a Ferry Vehicle During Rendezvous and Return, NASA TR R-87, National Aeronautics and Space Administration, Langley Research Center, Langley Field, Va., 1960.
9. Eggleston, J. M. and Dunning, R. S., Analytical Evaluation of a Method of Midcourse Guidance for Rendezvous with Earth Satellites, NASA TN D-883, National Aeronautics and Space Administration, Langley Research Center, Langley Field, Va., June 1961.
10. Soule, P. W. and Kidd, A. T., Terminal Maneuvers for Satellite Ascent Rendezvous Institute of the Aerospace Sciences - American Rocket Society Paper 61-206-1900, Los Angeles, June 13-16, 1961.
11. Eggleston, J. M., A Study of the Optimum Velocity Change to Intercept and Rendezvous, NASA TN D-1029, National Aeronautics and Space Administration, Langley Research Center, Langley Field, Va., February 1962.
12. Shapiro, M., An Attenuated Intercept Satellite Rendezvous System, Institute of the Aerospace Sciences - American Rocket Society Paper 61-155-1849, Los Angeles, Calif., June 13-16, 1961.
13. Lineberry, Jr., E. C. and Foudriat, E. C., Study of an Automatic System for Control of the Terminal Phase of Satellite Rendezvous, NASA TR R-128, National Aeronautics and Space Administration, Langley Research Center, Langley Field, Va., 1962.

14. Stapleford, R. L., An Automatic Flight Path Control System for the Terminal Phase of Orbital Rendezvous, American Astronautical Society Preprint 62-10, Washington, January 16-18, 1962.
15. Brissenden, R. F., Burton, B. B., Foudriat, E. C., and Whitten, J. B., Analog Simulation of a Pilot-Controlled Rendezvous, NASA TN D-747, National Aeronautics and Space Administration, Langley Research Center, Langley Field, Va., April 1961.
16. Clohessy, W. H., and Wiltshire, R. S., "Terminal Guidance System for Satellite Rendezvous" Journal of the Aerospace Sciences, Vol. 27, No. 9, September 1960 pp 653-658, 674.
17. Spradlin, L. W., "The Long-Time Satellite Rendezvous," Aero/Space Engineering Vol. 19, pp 32-37, June 1960.
18. Hord, R. A., Relative Motion in the Terminal Phase of Interception of a Satellite or a Ballistic Missile, NACA TN 4399, National Advisory Committee for Aeronautics, Langley Aeronautical Laboratory, Langley Field, Va., September 1958.
19. Ward, J. W. and Williams, H. M., Orbital Docking Dynamics, ARS Paper 1953-61, Stanford, Calif. August 7-9, 1961.
20. Bailey, W., Chipchak, J., Powe, W. E., and Seale, L. M., Study of Space Maintenance Techniques, ASD-TDR-62-931, Aeronautical Systems Division, Wright-Patterson Air Force Base, Ohio, May 1963.
21. Fogarty, L. E. and Howe, R. M., Flight Simulation of Orbital and Reentry Vehicles Part II - A Modified Flight Path Axis System for Solving the Six-Degree-of-Freedom Flight Equations, ASD Technical Report 61-171 (II), Aeronautical Systems Division, Wright-Patterson Air Force Base, Ohio, October 1961.
22. Austin, R. W. and Ryken, J. M., (Unclassified title) Study and Preliminary Design of an Energy Management Computer for Winged Vehicles, (Confidential Report) WADD Technical Documentary Report No. ASD-TDR-62-51, Aeronautical Systems Division, Wright-Patterson Air Force Base, Ohio, March 1962.
23. Computer Equations for a Visual Space Simulator for Rendezvous Missions, Bell Aerosystems Company Report No. 60009-185, P. O. Box 1, Buffalo 5, N. Y., November 1962.
24. Isakson, G., Flight Simulation of Orbital and Reentry Vehicles, Part I - Development of Equations of Motion in Six Degree of Freedom, ASD Technical Report 61-171 (I), Aeronautical Systems Division, Wright-Patterson Air Force Base, Ohio, October 1961.
25. Proposal for a Visual Simulator for Space Rendezvous Missions, Bell Aerosystems Company Report No. 60002-253, P. O. Box 1, Buffalo 5, N. Y., March 1962.
26. Design Study of a Device to Simulate the Effects of Reduced or Zero Gravity, Bell Aerosystems Company Report No. D7172-953001, P. O. Box 1, Buffalo 5, N. Y., April 1962.